Universidade do Minho
Escola de Engenharia

José Torcato Vaz de Matos Ribeiro de Almeida

Textile Hybrid Kinetic Adaptive Structures: A Case Study

May, 2018

UMinho | 2018

José Torcato Vaz de Matos Ribeiro de Almeida

Textile Hybrid Kinetic Adaptive Structures: A Case Study

Universidade do Minho
Escola de Engenharia

José Torcato Vaz de Matos Ribeiro de Almeida

Textile Hybrid Kinetic Adaptive Structures: A Case Study

Dissertação de Mestrado
Ciclo de Estudos Integrados Conducentes ao
Grau de Mestre em Engenharia Civil

Trabalho efectuado sob a orientação de
Professor Doutor José Luís Ramos
Professor Doutor Miguel Ângelo Dias Azenha
Engenheiro José Carlos Lino

May, 2018

Acknowledgments

First of all, my advisor, professor José Luís Ramos, deserves a huge thank you for all the knowledge, availability and patience provided during the development of this project, especially in the beginning stages were my knowledge about these concepts was irrelevant and also for always proposing harder challenges and providing the information needed to overcome them. In the same way, my co-advisor, professor Miguel Azenha, who represented a huge role, not only in the development of this work, but during my entire academic growing experience, for being the best critic that any student could have but also, for sharing his experience and knowledge, for the availability and patience, and for the right amount of small praises in the precisely right time that they were needed, for that reasons I am eternally grateful to him. As well, a huge thank you goes to the engineer José Carlos Lino, for the sureness provided and the always being receptive to help and support this project.

To my family, for the support provided during all my life. For being my life advisors and counselors and for the monetary support provided, that made possible the concretization of this work. In particularly to my mother and father, for being patient and for providing me with everything, even in the hardest periods.

To all my friends and colleagues, for always showing support and encouragement when it was most needed. In particularly to my dear friends Rafael Silva and Diogo Santos, for the companionship that they provided during this whole academic experience.

Last but not least, to my girlfriend Carolina Torres, for being the kindest caring person during this entire process. For always giving me the support and reassurance I needed, for always being there when I needed and for all the time spent listening to my gibberish.

Abstract

This thesis has the main objective to study three distinct typologies of structures. These structures are, form-active structures, in particular membrane structures, bending-active structures and the integration of both concepts with a kinetic principle, therefore adaptive hybrid structures. Both membrane and bending-active are structures that require form finding, since the form of these structures is dependent on the loading and boundary conditions, thus only known *a posteriori*. These structures are subject to large deformations and thus, geometric nonlinearities must be considered during the calculation. Additionally, the flexibility of membrane structures conjugated with the elastic behaviour of bending-active structures creates the perfect conditions for the development of hybrid kinetic structures that adapt according to the external loading conditions present. This study intends to elaborate an exploratory approach on these concepts, thus bringing forward the main problems that originate when analysing a structure of this type. Therefore, firstly a study on membrane, bending-active, hybrid and kinetic structures is presented, containing the most relevant knowledge that currently exists regarding these topics. Then, the structural aspects that are inherent to these structures are exposed. Three routines are developed in Sofistik® in order form find and calculate the above-mentioned structures. Validations are made on these routines and software analysis. The structural feasibility of an architectural concept proposed by Costa (2017) of a hybrid adaptive concept is studied by applying these routines, and the kinetic hybrid concept is simulated in Sofistik®. The adaptive principle is also extended to function structurally, by taking advantage of the bending prestress implied by the bending-active elements. Finally, external wind loads are applied to this structure, in order to test the effectiveness of the structural adaptive concept. It was concluded that there is significant importance of the bending adaptive movement in the loadbearing capacity of the overall system. Additionally, the choice of the initial shape of the structure defines a crucial step on the definition of the structure, since it affects the process of form finding, that latter affects the structural performance.

KEY-WORDS: membrane structures, bending-active structures, textile hybrid, adaptive structures, form finding.

Resumo

A presente dissertação tem como objetivo principal estudar três tipologias distintas de estruturas. Estas estruturas são as estruturas de forma ativa, particularmente as estruturas em membrana, as estruturas de flexão ativa e a integração de ambos os conceitos com um princípio cinético, ou seja, estruturas hibridas adaptativas. Tanto as estruturas de membranas como as estruturas de flexão ativa são estruturas que requerem determinação da forma pois, como a forma destas estruturas é dependente das condições de tensão e de fronteira, apenas é conhecida *a posteriori*. Estas estruturas estão sujeitas a grandes deformações e, portanto, as não linearidades geométricas devem ser consideradas durante o cálculo. Para além disto, a flexibilidade das estruturas de membrana conjugada com o comportamento elástico das estruturas de flexão ativa geram condições perfeitas para o desenvolvimento de estruturas cinéticas hibridas que se adaptam de acordo com as condições de carregamento presentes. Este estudo pretende elaborar uma aproximação exploratória a estes conceitos, trazendo para primeiro plano os principais problemas originários da análise deste tipo de estruturas. Desta forma, primeiramente é apresentado um estudo sobre estruturas de membrana, flexão ativa, hibridas e cinéticas, contendo a informação mais relevante que existe atualmente sobre estes assuntos. De seguida, os aspetos estruturais inerentes a estas estruturas são expostos. Três rotinas são desenvolvidas no Sofistik® de forma a determinar a forma e calcular as estruturas anteriormente mencionadas. São realizadas validações destas rotinas e da análise preconizada pelo software. A viabilidade estrutural de um conceito de arquitetura proposto por Costa (2017) sobre uma estrutura hibrida adaptativa é estudada através da aplicação destas rotinas, e o princípio cinético hibrido é simulado através do Sofistik®. O princípio adaptativo é alargado de modo a funcionar estruturalmente, tirando partido da pretensão implícita pelos elementos de flexão ativa. Finalmente, são aplicadas cargas externas de vento à estrutura, de forma a testar a eficácia do principio adaptativo estrutural. Foi concluído que o movimento adaptativo de flexão tem uma importante significância ao nível da carga admissível na estrutura. Adicionalmente, a escolha da geometria inicial da estrutura define uma etapa fundamental na definição da estrutura, pois afeta o processo de *form finding*, que mais tarde afeta o desempenho estrutural.

PALAVRAS-CHAVE: estruturas de membrana, flexão ativa, estruturas hibridas, estruturas cinéticas, estruturas adaptativas, textile hybrid, form finding, curva elástica.

Table of contents

List of abbreviations and symbols

CAD – Computer-aided design

CDB – Central database

CFRP – Carbon fibre reinforced polymer

CPU – Central processing unit

DRM – Dynamic relaxation method

EC1 – Eurocode 1

EN – European standard

FDM – Force density method

FEM – Finite element method

FRP – Fibre reinforced polymer

GFRP – Glass fibre reinforced polymer

PET - Polyethylene terephthalate

PTFE – Polytetrafluoroethylene

PVC - Polyvinyl chloride

SLS – Serviceability limit state

THV – Tetrahydrocannabivarin

TH2 – 2nd second order problem (in Sofistik®)

TH3 – 3rd third order problem (in Sofistik®)

ULS – Ultimate limit state

VBA – Visual basic for application

$\sigma_{M,Rk}$ – Flexural strength

E – Young modulus

K – Stiffness matrix

δ – Displacement

$\dot{\delta}$ – Velocity

$\ddot{\delta}$ – Acceleration

M – Mass

C – Viscous damping coefficient

Δt – time interval

Table of figures

Table of tables

1. INTRODUCTION

1.1. Scope and motivation

The categorisation of basic structural systems has played an important part in developing analytical calculation techniques that help analyse structures on the basis of abstract static systems (Lienhard 2014). This categorisation has been made in several ways, however, the definition of the structural typologies according to structural action is commonly the most used one. This particular typology defines abstract 'families' of structural action, each of which is subdivided into 'types', and finally 'structure singles' (Lienhard 2014). Structural action describes the process of receiving, transferring and transmitting a load. Figure 1 shows an overview on the structural typology suggested by Lienhard (2014). Here, one can delineate several structural families, however, the scope of this work is focused particularly in:

- Form-active structures (specifically membrane structures);
- Bending-active structures;
- Hybrid structures.

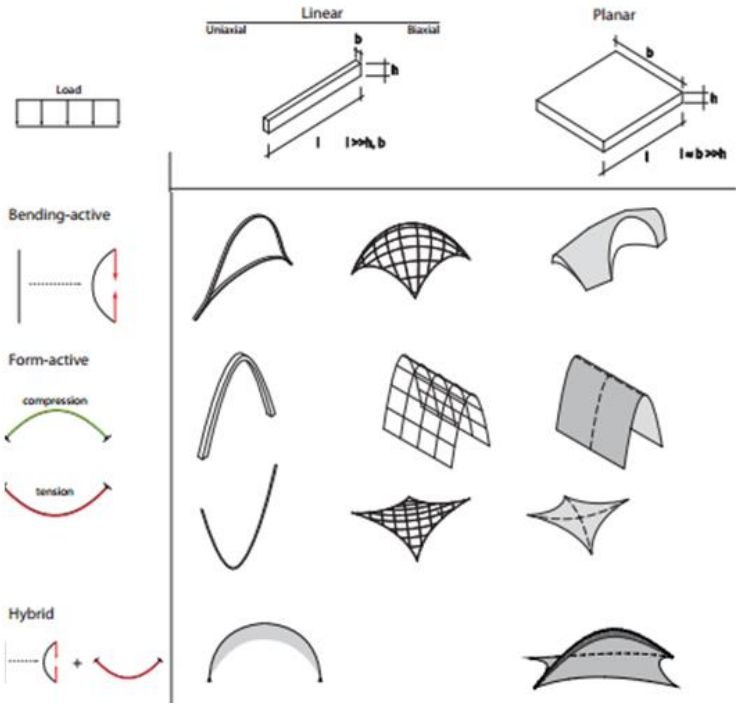

Figure 1 - Different types of load bearing structures categorised according to structural action.

(Knippers, Cremers et al. 2011) apud (Lienhard 2014)

Form active structures

Form active are structures that carry forces solely by tension or compression forces, like cables and membranes or arches, without shear forces or bending moments. For purpose of this work, membrane structures are the only studied example. Wide-span and light surface structures made of materials, which serve both structural purposes and provide protection against environmental influences, are normally called membrane construction. This description (lat. *membrana* = skin) implies on the one hand a function and on the other a dimension, and thus signifies a skin-like thin material (Seidel 2009).

To Forster and Mollaert (2004), tents have a long history the origins of our contemporary fabric structure technology are to be found in the 19th century, for instance, the mechanical spinning of yarn and weaving of cloth enabled large portable tents to be created for the travelling circuses that abounded in the latter part of that century. From an engineering point of view fabric structures are thin membranes of constant thickness which, by virtue of their surface shape and inherent large deflection behaviour, are able to support the imposed loads required by Building Codes. These membranes are then prestressed in order to improve their stiffness. The thrive of membrane structures in the simplicity modern forms was very noticeable during the last century, which lead to many developments in this area. Also, the adaptability of membrane structures, the easiness to cover large spans and the appetizing variety of forms created a powerful desire within architects for these types of structures. Figure 2 shows two examples of membrane structures applied in modern construction and covering of wide spaces. However, the limitations inherent to a structure that defines its form according to boundary conditions and prestress, like it is the case for membrane structures, generate difficulties in its calculation as well as with modern design rules and norms. Also, for the same reason, structural engineering general purpose software is not usually able to calculate the complexity characteristic to membrane structures.

Figure 2 - Majlis Tent, Thowal, Saudi Arabia, 1991, SL Rasch (left), Diplomatic Club Riyadh, 1998 (right). (Forster and Mollaert 2004)

Introduction

Bending-active structures

According to Gengnagel, Alpermann et al. (2013), a bending-active structure relies on the utilisation of elastic deformation as a shaping process for straight linear elements or planar elemental surfaces. To Lienhard (2014), bending-active structures are structural systems that include curved beam or shell elements which base their geometry on the elastic deformation from an initially straight or planar configuration. Bending-active, in structural terms, can be described as constrained statically indeterminate structures with residual bending stress (Lienhard 2014). Figure 3 shows two simple examples of the bending-active principle.

Bending-active structures are arguably a distinct approach, rather than a new structure category. For Lienhard (2014), since the load bearing includes a combination of bending and normal forces, bending-active structures can be understood as a sub category of section-active structures. However, in the load transfer of bending-active structures, the residual bending stresses play an important role, which makes them unique from the other families of structural action.

Figure 3 - Basic bending-active components. (Lienhard 2014)

The pre-stressing of bending-active structures is generated through large nodal displacements in statically indeterminate structures which results in individual building elements being largely deformed and therefore exposed to a constant bending stress (prestress) (GARTI, Tutor et al.). Similarly, to membrane structures, the geometry must be form found, in this case simulating, the elastic bending deformation, however, in contrast to membrane structures the form finding result does not automatically define a structurally optimised geometry (Lienhard 2014). Thus, the research on bending-active structures focuses

on imposed force and form interaction, which is an inseparable relationship where the disciplines of architecture and structural engineering are equally addressed. The advantages of bending-active structures lie, not only in the possibility of generating complex curved geometries for static structures, but also in the shape adaptation possibilities, and furthermore, in kinetics, which are entirely based on reversible elastic deformation (Brancart, De Laet et al. 2016). However, the research is yet considerably new and a wide amount of work is still needed in this topic. In addition, the majority of FEM software that is commonly used for calculation of concrete and metallic structures is not ready to deal with the complexities of bending-active structures.

Hybrid Structures

For Lienhard (2014), the intentional combination of load transfer mechanisms is referred to as a hybrid structure. Therefore, a hybrid structure results from the linkage of two parental systems of dissimilar internal load transmission into a coupled system. Many types of hybrid structures can be created from distinct combinations of materials however, in this work, only textile hybrids are taken into consideration. A particular combination of these parent systems is one that integrates membrane structures and bending-active elements as the internal flexible spine of the system. According to Lienhard, La Magna et al. (2014), this interdependence of form and force of mechanically prestressed textile membranes and bending-active FRP is suggested to be classified as a Textile Hybrid. Thus, this nomenclature will be considered further on during this document. An example of a Textile Hybrid is shown in Figure 4.

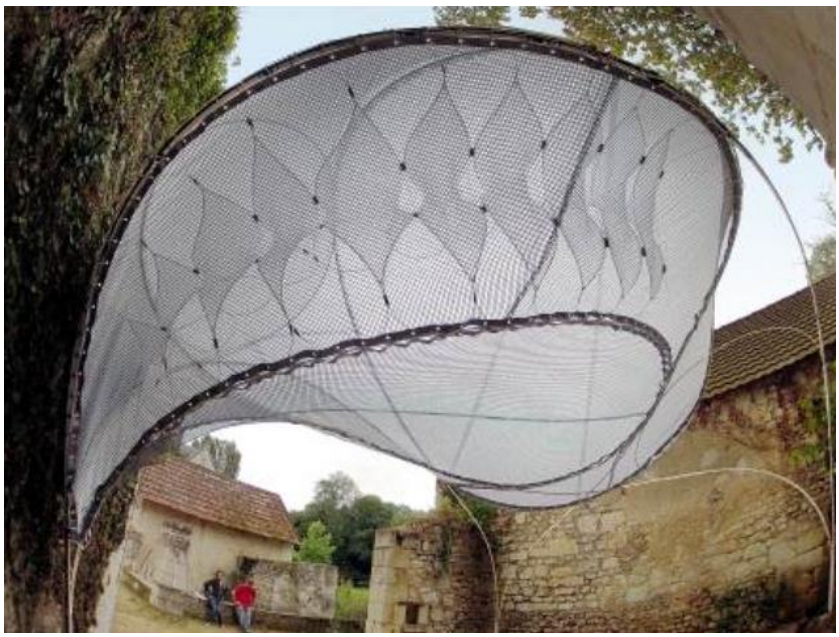

Figure 4 - The textile hybrid M1. (Lienhard, Ahlquist et al. 2013)

Kinetic and adaptive structures are not, by any means, a recent trend. The use of movable parts in building and construction has been with it since its dawn. From the simple concept of a door to a wider and more recent variety of kinetic roofs and facades, the need to adapt to different circumstances has been present in the construction of buildings during centuries. Yet, all these existing adaptive systems serve a function that is not structural, they all serve a practical or architectural function to the building. The examples of structures that adapt to serve structural purpose are few. Thus, the flexibility of membrane structures linked with the elasticity and transformability of bending-active structure creates optimal conditions for the construction of adaptive kinetic structures. With the right choice of materials, highly sustainable structures can be erected using this principle.

However, the current investigation in this field is relevant but few. Norms and codes that provide a basis for the calculation of such structures are also absent. Consequently, the application of this principle in construction is currently not common. Methodologies to calculate these structures are also few. These research gaps allied to a growing interest in sustainable options for structural engineering, make bending-active adaptive membrane structures a viable research field.

1.2. Objectives and methodology

Taking into account the research gaps identified in the previous section, the objectives of this work are to identify the numerous typologies of structures as well as retain the most important knowledge about materials, case studies and design procedures that currently exists both for membrane structures, bending-active structures and adaptive structures that correlate the preceding structural typologies. Another objective of this work consists in identify and explore the structural aspects behind all these typologies of structures, as well as explore the existing software capable of handling the calculation of membrane structures and bending-active structures. Finally, a case study of an adaptive structures that contemplates these two typologies is to be chosen and an analysis of this case study is to be implemented.

However, considering that this work is only a master thesis and that the time for completing it is limited, several simplifications are to be made during the work. Concerning the external actions on the structure, only a brief analysis is to be made. Therefore, the analysis made cannot, by any means, be considering a full analysis to the kinetic structure.

1.3. Thesis outline

The objectives discussed in the previous section are to be exposed in several chapters. Therefore, this document is to be divided in, besides chapter 1, five additional chapters, being:

- Chapter 2: A state of the art on membrane, active-bending, hybrid and kinetic structures. This chapter consists on exposition of the current developments in these topics. Also, material properties for the more common materials used for each structure are slightly discussed here. Several case studies are introduced on hybrid and kinetic structures are introduced.
- Chapter 3: The exposition of the structural aspects regarding membrane and bending-active structures. During this chapter the structural aspects are to be presented and discussed. Also, a software is to be chosen, based on the needs exposed in the structural aspects. This choice is then validated by means of three case studies, one for membrane structures and two for the elastica curve of bending-active structures.
- Chapter 4: Analysis of a case study of an adaptive hybrid structure. During this chapter the analysis of a hybrid adaptive structure is to be made. The case study is to be analysed from a structural point of view and several structural aspects are to be discussed.
- Chapter 5: Conclusions of the work. This chapter is to be a brief overview on the conclusions that can be taken from the work done during this project.

2. MEMBRANE, BENDING-ACTIVE, HYBRID AND ADAPTIVE KINETIC STRUCTURES

2.1. Introduction

During the present chapter an introduction to the concepts of membrane structures, bending-active structures and finally hybrid adaptive structures is made. Thus, the chapter is subdivided in three distinct subchapters, one for each structural typology. For each structural typology the most relevant aspects are introduced. Firstly, membrane structures are introduced, followed by bending-active structures, and lastly the hybrid and adaptive concept which is composed by the previous two. Figure 5 shows an overview of the present chapter, including the subchapters and the main sections for each chapter.

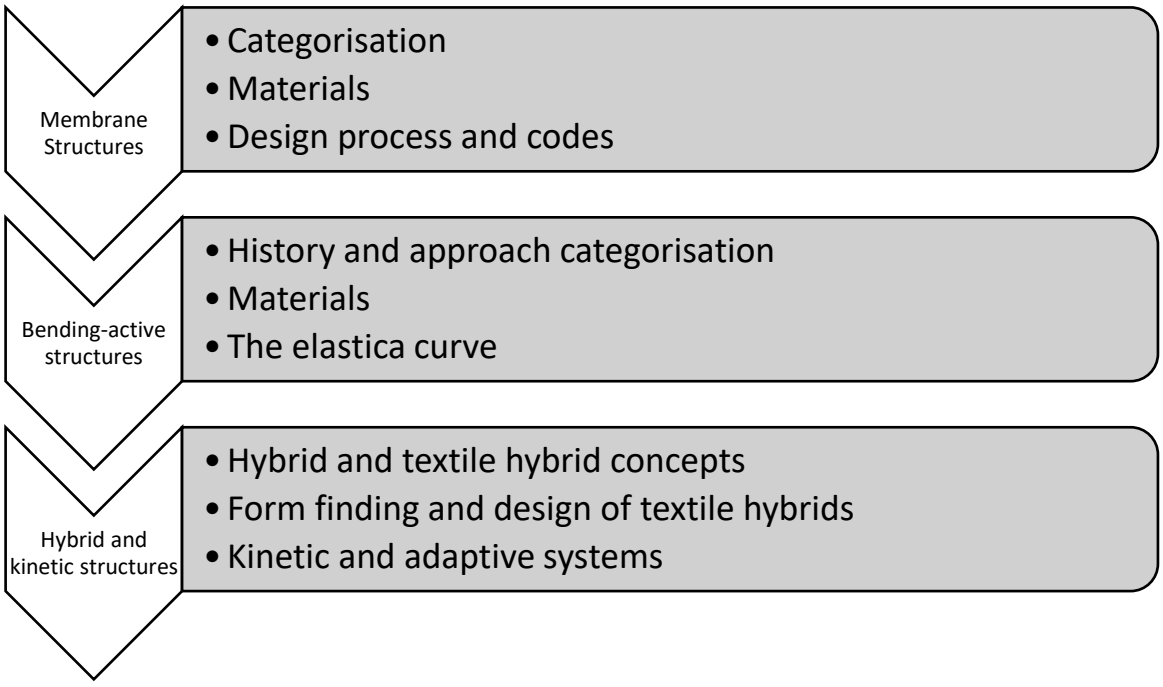

Figure 5 - Overview of the chapter.

The framework used for the subchapter of membrane and bending-active structures is comparable, firstly by categorising the structure, followed by a definition of the materials commonly used for these types of structures and lastly a specific section for each typology, referring the design process for membrane structures and introducing the concept of the elastica curve for bending-active structures. The subchapter of hybrid and kinetic structures is subdivided in the introduction of the hybrid and textile hybrid concept,

followed by the form finding approaches and design of these structures and lastly the introduction of the kinetic and adaptive principle applied to these systems.

2.2. Membrane structures

2.2.1. Categorisation

The essential elements of a membrane structure are, according to Lewis (2003): a highly flexible fabric held under tension to generate stiffness in the surface; one-dimensional flexible elements, for example ties or cables, to create ridges, valleys and edge boundaries; rigid support members sustaining compression or bending. There are two main ways to generate the tension in the fabric, thus creating two main types of membrane structures (Figure 6):

- Boundary tensioned membranes – Membranes that are stressed by stretching the surface to meet the boundaries made of flexible, tension cables, or a rigid frame/beam;
- Pneumatic structures – Membranes that are stabilized by increasing the inner pressure, thus generating a pressure difference between the interior and exterior of the enclosure.

Figure 6 - Boundary tensioned membrane (left) and pneumatic structure (right).

Membrane structures are light in weight, because their structural stability results from their prestressed shape rather than the mass of the materials used, consequently being much lighter than conventional building structures yet offering high stability (Forster and Mollaert 2004). Tensioned membrane structures are not rigid, changing their form under the influence of wind and snow. The principal response of membrane structures to external loading is by the occurrence of large deformations, thus changing their form during the loading. The degree of change and response depend on the elasticity of the material and the prestress level used for the structure (Forster and Mollaert 2004).

2.2.2. Materials

In membrane structures, three main types of materials are generally used:

- Foils;
- Open mesh fabrics;
- Coated mesh fabrics.

A foil consists in a thin layer of material which are currently used in many tension structures canopies, providing satisfactory shading conditions while being water tight. Also, according to Beccarelli (2015), architectural foils are widely used for pneumatic application thanks to their level of air tightness. However, foils lack a fibre structure, thus being generally weaker than other membrane material configurations. The reduced mechanical properties limit their use for large cushions and single skin envelopes. In recent projects, this limit has been partially addressed by adding reinforcing steel cables as a support in case of heavy loads (Beccarelli 2015).

Mesh fabrics (both open and coated) form a system from woven yarns, which are arranged orthogonally when unstressed and consist of single threads, parallel or twisted together. They have been used in many fields for hundreds of years and enjoyed a renaissance in the construction industry during the last century among committed architects and engineers, particularly the architect Frei Otto (Seidel 2009). Thus, the fibre structure, or fabric, can be understood as the structure generated by this system of woven yarns.

Open mesh fabrics are made by the same fibres used for coated fabrics but they are designed with a specific level of permeability to light, wind and rain. According to Beccarelli (2015), for applications which do not require weather tightness, the use of open mesh fabrics is recently becoming quite popular. Knitted high density polyethylene shade fabrics are probably one of the most promising materials due to the extremely reduced cost, the relatively high life span and the extraordinary elasticity (Beccarelli 2015).

On the other hand, coated fabrics are the result of the combination of the fabric and one or more coatings. The composition of a generic coated fabric is shown in Figure 7. According to Beccarelli (2015), the coating is generally applied on both sides and can be the result of several layers and materials. Large spans, resistance against the effects of load, time and temperature require technical membranes with the appropriate composition for the purpose, if this composition is to be achieved through the arrangement of single elements or layers, then this is called bonded construction or composite materials

(Seidel 2009). Coated mesh fabrics are such a composite material. Figure 7 illustrates the general composition of a coated mesh fabric.

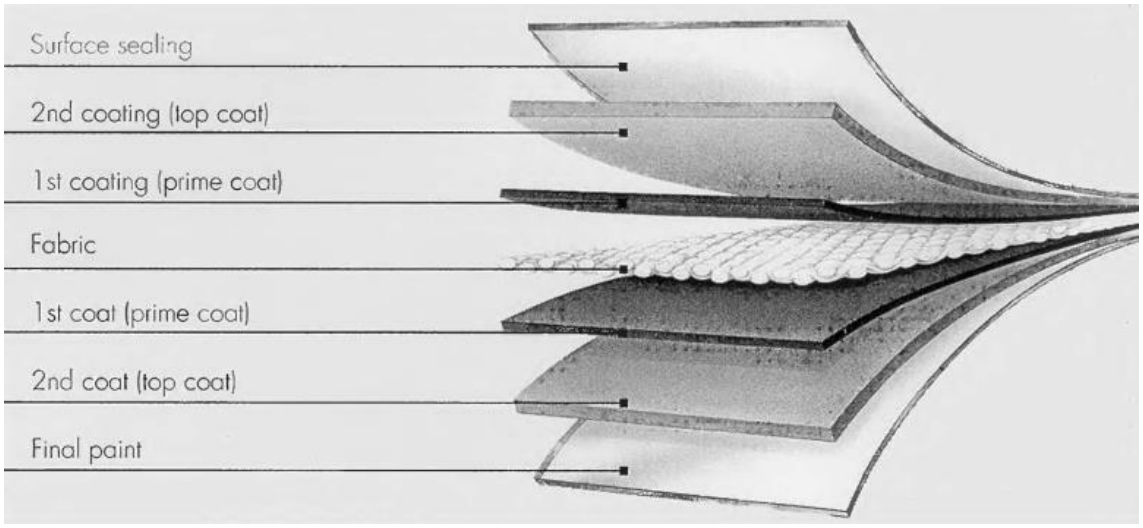

Figure 7 – Example of the composition of a coated mesh fabric. (Forster and Mollaert 2004)

2.2.2.1. Fibres

The term "technical fabric" is used to indicate the wide class of fabrics in which the technical aspects are more significant than the aesthetic ones (Beccarelli 2015). As beforehand explained, the basic composition of a coated or open mesh membrane is the technical fabric, which is composed a woven system of yarns or fibres. In practical terms, there are two main aspects that can influence the strength of the fabric, being the material of the fibres and the sewing pattern used in the fabrication of the technical fabric. The material of the fibres, which can be natural or artificial, is one of the most important factors which contribute to the final performance of the fabric, especially from the mechanical point of view (Beccarelli 2015). Table 1 shows a list of the common types of material used to produce fibres for fabrication of technical fabrics. The natural fibres have the considerable advantage of a reduced environmental impact, however, their properties cannot be significantly altered in order to meet particular requirements and this reduces considerably their application. On the contrary, artificial fibres can be obtained by using a wide range of bulk materials and processes which satisfy a wide range of requirements such as the mechanical and chemical properties (Beccarelli 2015).

Table 1 - Commonly used materials for fibres in technical fabrics.

Fibres	Polyester
	Polyethylene
	Fiberglass
	Expanded PTFE
	Nylon
	Aramids
	Acrylic
	Polyurethane
	Cotton

The polyester fibre is the most used fibre for architectural fabrics since the early 1960s due to the reduced price, good mechanical performance and expected lifespan (Beccarelli 2015). The progressive degradation due to UV rays and the behaviour in case of fire can be easily improved with an adequate coating, and also, the fibres are quite flexible and are very common for temporary and seasonal structures. Houtman and Orpana (2000) say that these fibres have a good tensile strength and elasticity, because of its considerable elongation before yield, the material is "forgiving". Furthermore, thanks to new technologies, coated fabrics, based on polyester fibres, are now recyclable, says Beccarelli (2015).

Fibreglass is generally used for permanent heavy-duty applications due to the high modulus of elasticity and the tensile strength, and because of its intrinsic high resistance to fire and UV degradation it does not require additional additives (Beccarelli 2015). Also, according to Houtman and Orpana (2000), the fibreglass has a high tensile strength, but remains brittle and has low elastic strain. Ageing exerts little influence on the material what has a tremendous impact on the expected lifetime of the structure, but the tensile strength of the material decreases when it is subjected to moisture (Houtman and Orpana 2000). However, Beccarelli (2015) says that glass fibres are quite brittle and can crack easily and for this reason the panels of fabric should be folded and handled with care avoiding repeated flexing and low radius of curvature.

Materials like polyethylene, nylon, acrylic, polyurethane and cotton are usually less expensive when compared with the rest of the materials used for the composition of the fibres. According to Beccarelli (2015), polyethylene fabrics are generally woven from high-density polyethylene slit tape and coated on both sides, being generally used for low-budget applications despite the shorter life span compared to

polyester. Nylon fibres are generally used for projects which require lightweight and stretchable fabrics with relatively low mechanical properties (Beccarelli 2015). Therefore, they are frequently applied in indoor or outdoor small temporary and deployable structures. However, according to Houtman and Orpana (2000), the nylon fibre has a bad resistance against UV light, swells in length direction when it gets wet and is herewith of little importance for textile architecture. Acrylic fibres, due to the reduced mechanical performance, are commonly used for small deployable tents and umbrellas due to their flexibility and good resistance to oils, chemicals, and to deterioration from sunlight exposure (Beccarelli 2015). Polyurethane, or elastane, is a polyurethane-polyurea copolymer, which is exclusively used for indoor applications that require exceptional elasticity (Beccarelli 2015). This highly reduces the risk of wrinkles in the fabric, yet, the fabric produced from this material is not suitable for snow or wind loads. Finally, pure cotton is characterised by a poor tensile strength, a relatively high elasticity and a high vulnerability to microbial attack and the consequent biological degradation. Frei Otto used it for his early garden show structures and nowadays it still is applied in some rental tents, but when used permanently it has an expected lifetime of about 4 years (Houtman and Orpana 2000).

Expanded PTFE and aramids materials have a high cost when compared to the rest of the materials used for producing technical fabrics. According to Beccarelli (2015), expanded PTFE has high translucency, strength, flexibility, long life-span, high chemical resistance and very good soiling behaviour. However, due to the high cost this material it is generally used for specific projects which require, and highlight, its unique luminosity. Aramid fibres are very popular for nautical applications due to the extremely high modulus of elasticity and breaking strength. According to Houtman and Orpana (2000), the material has a high tensile strength and is chemically resistant, yet the low elastic strain and the bad resistance against high temperature and UV-light. They are non-combustible but need to be protected against UV light. Due to the relative high price, their use is generally related to special applications which require their unique mechanical performance (Beccarelli 2015).

2.2.2.2. Sewing patterns

The process of fabrication of the fibres, as well as the specific polymer used for the fabrication of the fibres, can highly influence the final properties of the technical fabric. For example, according to Seidel (2009), for PVC-coated polyester fabrics, synthetic polymer fibres (Polyethylene terephthalate or PET) are the most commonly used. The major advantage of PET fibres is their dimensional stability against the effect of chemical and physical influences and that they do not rot. Figure 8 shows a general view on the

processes of production of these fibres. The decisive factors determining the strength of fibres are the orientation and bonding of the chains of molecules with each other and their degree of polymerisation (chain length), being PET fibre polymer chains are arranged in triclinic symmetry, as shown in Figure 8 (right) (Seidel 2009). Thus, to improve the mechanical properties of the fibres, further processing is necessary to produce an elongated, nearly parallel arrangement of the molecules. To achieve this, the monomers are polymerised, the resulting granulate is spun to fibres and then evenly stretched in a stretching process. After the production of the starting material, the granulate is melted in a melting and spinning process, filtered and led to a heated spinning manifold. Then the spinning mass is pressed through jets into a spinning shaft, and transformed into filaments, being later fixed by uniform blowing of air. In this condition, the macromolecules of the fibre are pre-oriented, being the orientation parallel to the fibre axis produced in the stretching process, where the raw, already solid fibre is fed through a variable-speed roller system and elongated to many times the original length, as shown in Figure 8 (Seidel 2009). Finally, the fibres are twisted together and the sum of the fibres spun out of the jets and twisted is called yarn.

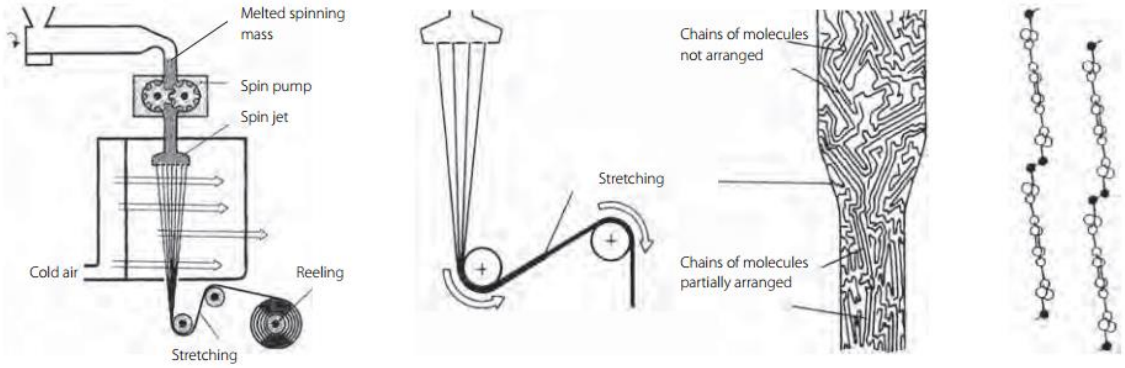

Figure 8 - Diagram - left: Spinning process; middle: Stretching; right: Crystalline structure of PET polymer chains. (Seidel 2009)

The technical fabric properties will also be influenced by the sewing pattern used during the production of the fabric. According to Seidel (2009), a raw fabric is made by the interlacing of the warp and the weft threads, and the thread density gives the number of threads in warp and weft. The yarns can be combined according to different geometries which lead to different properties, depending on the final use (Beccarelli 2015). Thus, according to the principle used they can be divided into:

- Woven fabrics;
- Knitted fabrics;

- Non-woven fabrics.

Woven fabrics are generally the most common types of fabrics used to produce open or coated mesh fabrics. However, according to Seidel (2009), various methods of crossing the warp and weft threads lead to the characteristic waviness (crimp) of the three-dimensional fabric. The weaving process can follow different patterns, leading to distinct aspects and properties, being the most common the plain weave, the satin weave and the twill weave (Beccarelli 2015). Figure 9 shows an overview on these weaving processes as well as the visual distinct properties obtained from each one. During the weaving process the yarns undergo different levels of curvature, depending on the pattern adopted, with a consequent reduction in their tensile resistance.

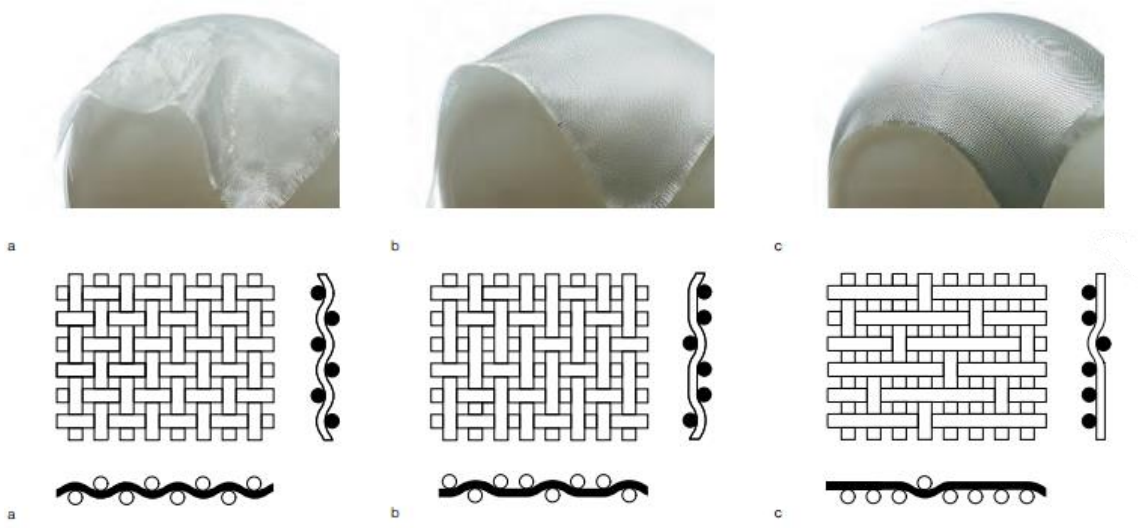

Figure 9 – Drapability of woven fabrics. a - Plain weave; b - Twill weave; c - Satin weave. (Knippers, Cremers et al. 2011)

According to Beccarelli (2015), knitted fabrics, divided into warp-knit and weft-knit, include several types of fabrics obtained through the interlocking of loops of yarn rather than interlacing two sets of yarn, as in weaving. This geometry leads to a fabric that is more elastic and form-fitting than counterparts made from a woven fabric, a characteristic much appreciated when the fabric is used to reinforce a complex three-dimensional surface (Beccarelli 2015). However, the high level of curvature leads to a stress concentration in the yarns, with a consequent reduction in the maximum tensile strength.

Non-woven fabrics present a structure obtained by putting small fibres together in the form of a sheet and then binding them either with an adhesive or by interlocking them with serrated needles in such a way that the inter-fibre friction results in a strong fabric (Beccarelli 2015). Also, their production is generally

less expensive than woven and knitted fabrics and the overall behaviour is characterised by a low level of stretch and a higher tensile resistance.

2.2.2.3. Coatings

While the structural function is mainly provided by the yarns, the protection from chemical and biological influences, fire-retardant behaviour, weld ability, waterproof qualities and UV ray resistance depend on the coating layer (Beccarelli 2015). However, depending on the coating and fibre used, this may not be the case. Figure 10 shows an example were the fire destroyed the coating but the fibre remained intact, thus ensuring the structural stability of the structure. Albeit, in generally terms, the final properties of a coated fabric, with the only exception of the mechanical performance, are mainly related to the materials used for the top coatings (Houtman and Orpana 2000).

Figure 10 - PVC coated Polyester structure in the Netherlands after local fire a hole occurs in the membrane, but the fabric itself is not destroyed. (Houtman and Orpana 2000)

The basic composition of a coated mesh fabric can be seen in Figure 11. Apart from the fabric, composed by the warp and weft system of yarns, there is usually an inside and outside coating, as well as a topcoat or finish. This composition generates a coated mesh fabric that cumulates all the properties of its constituents. This type of fabrication permits a great variation of functionality, depending on the required application for the coated mesh fabric.

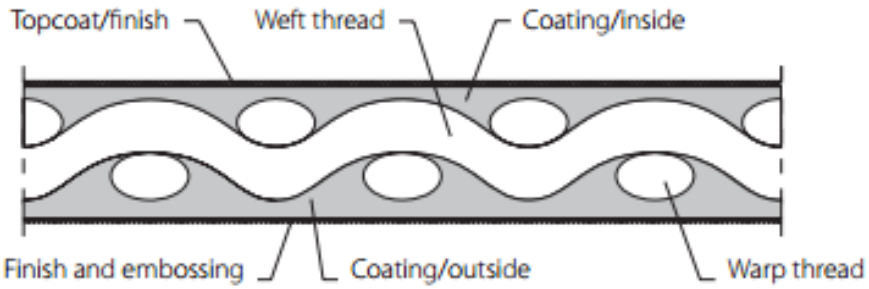

Figure 11 - Internal construction of a polyester fabric coated on both sides and with top coating. (Seidel 2009)

According to Houtman and Orpana (2000), to create durable and water tight cloths most of the fibres need a coating on both sides. The most common ones are PVC coatings, Teflon coatings and silicone coatings, but sometimes a coating is not applied, but a foil is laminated upon the fabric (Beccarelli 2015). Table 2 shows an overview on the commonly used coats in coated mesh fabrics.

Table 2 - Commonly used materials for coating of technical fabrics.

Coatings	PVC
	Fluoropolymer coatings
	Silicone
	Polyurethane
	Polyethylene
	Synthetic rubbers
	Low E coatings

PVC coating is generally used in combination with polyester fabrics. Additional additives and top-coatings are generally used to improve the fire behaviour, the expected lifespan, the self-cleaning properties and the colour stability (Beccarelli 2015). It can also be used to coat aramid fibres. Despite the higher price, fluoropolymer is the most common material for coatings when there are requirements for particularly high resistance to UV radiation and to chemical and biological corrosion. Polytetrafluoroethylene (PTFE) is the strongest bond in organic chemistry and the most used fluoropolymer coatings (Houtman and Orpana 2000). Silicone is mainly used in combination with woven glass fabrics due to the high flexibility and light transmission, being relatively cost effective and has excellent characteristics of UV and flame resistance (Beccarelli 2015). Silicone coatings are considered the most environmentally sustainable

coating in the market. The principal drawback of silicon coating is that it tends to pick up airborne particles and dirt and the main technical limit is represented by the seaming process which requires PTFE threads or silicone adhesive tapes.

The polyurethane coatings, when compared with PVC coatings, have better properties in terms of elasticity, transparency, and resistance to oil, grease and abrasion. However, due to the relatively high cost and the progressive yellowing, its use is restricted to special applications such as biogas plants and flexible tanks (Beccarelli 2015). Also, the use of coatings based on synthetic rubbers for architectural fabrics is relatively restricted due to the cost, but neoprene is one of the most common rubber coatings for architectural uses thanks to its flexibility over a wide temperature and the resistance to corrosion, degradation and abrasion (Houtman and Orpana 2000). On the other hand, polyethylene coatings are used for cost effective alternative to more durable coated fabrics when a shorter lifespan is acceptable such as temporary shelters and ground sheets (Beccarelli 2015). Finally, and due to the increasing demand of coated fabrics with better thermal performance, the so called low-E (low emissivity) coatings are becoming more popular for architectural fabrics. They are mainly based on the same technology used for insulating glass and consist of an ultra-thin metallic coating based on fluorinated tin oxide or thin silver layers (Houtman and Orpana 2000).

Methods of coating

The methods used to apply the coating to the fabric can affect the properties or even the lifetime of the coated mesh fabric. According to Beccarelli (2015), the doctor blade (PVC), or air knife system, and the dip coating (PTFE), are the most common coating methods however, the coatings can be applied to the fabric also by laminating, rolling or brushing on the basis of the chemical compatibility with the fibres. These methods are respectively shown in Figure 12 and Figure 13.

Seidel (2009) says that PVC-coated polyester fabrics are mostly coated using a knife coating system in Europe. Additionally, Knippers, Cremers et al. (2011) say that this method is generally used for PVC and silicone coatings. The process is illustrated in Figure 12, where the premixed, viscous coating paste (plastisol) for PVC-coated polyester membranes (polyester-PVC), consisting of PVC powder dispersed in a plasticiser. Additives such as heat and light stabilisers, fungicides, bactericides and pigments are mixed in as required and this paste-like compound is then spread over the woven fabric and the excess scraped off with fixed doctor blades (Knippers, Cremers et al. 2011).

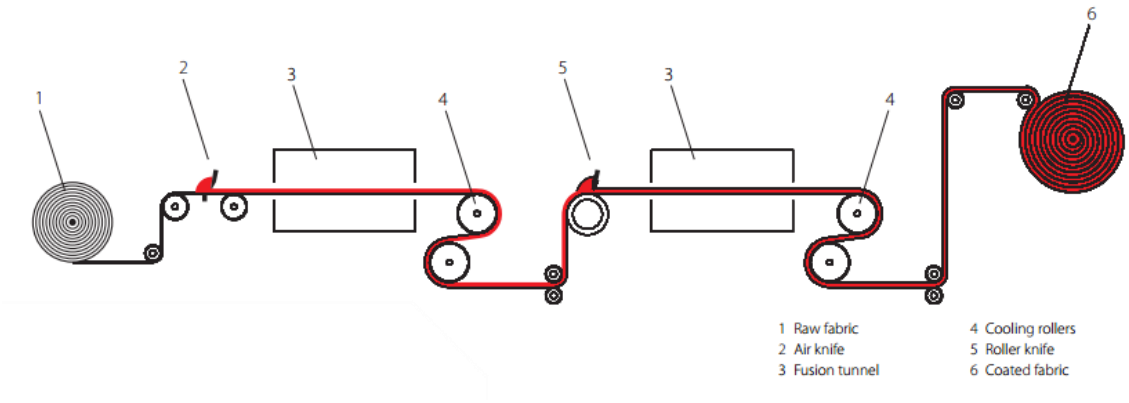

Figure 12 - Coating process using the air knife system. (Seidel 2009)

On the other hand, the dip coating method is used primarily for PTFE coatings, but in some instances also for PVC coatings on wide-mesh fabrics. The method of dip coating is illustrated in Figure 13. To coat glass-fibre materials with PTFE (PTFE/ glass), the fabric is immersed in a dispersion of PTFE particles and thus coated on both sides, then raising the temperature incrementally during the drying and sintering stages causes the water to evaporate, the wetting agent for reducing the interfacial surface tension to decompose and, finally, the PTFE particles to sinter at approximately 330 °C and the process is then repeated several times in order to achieve the coating thicknesses necessary (Knippers, Cremers et al. 2011). PTFE coatings can only be applied to woven fabrics with a very high melting point because of the high sintering temperatures so, coating a polyester fabric with PTFE is therefore impossible.

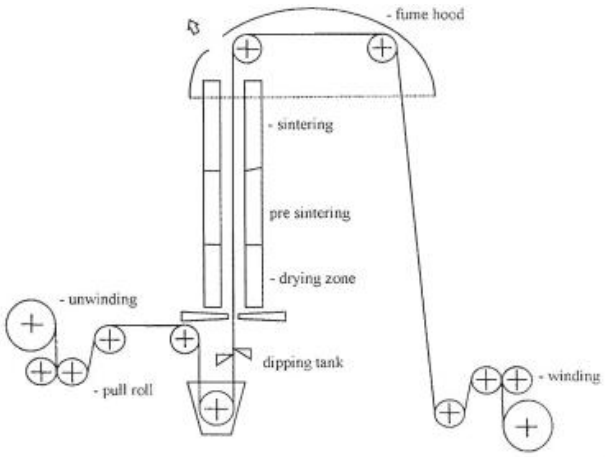

Figure 13 – Dip coating. Processing of PTFE membrane coating. (Forster and Mollaert 2004)

Common coated mesh fabrics

Membrane, bending-active, hybrid and adaptive kinetic structures

There are two types of material mostly used for coated mesh fabrics in construction, being polyester fabrics with a PVC coating and glass fibre fabric with PTFE coating. Silicone-coated glass fibre fabrics are also in use (Seidel 2009). However, fluoropolymers and polyolefin coated polyester fabrics, coated fluoropolymer fabrics and PVC-coated aramid fabrics are less commonly used. Table 3 displays some of the common combinations between coatings and fabrics. Between these coated mesh fabrics, the more common are PVC-coated polyester, PTFE-coated glass fibre and the silicone-coated glass fibre.

Table 3 - Common combinations of fabric and coatings.

Coated mesh fabrics	PVC-coated polyester
	THV-coated polyester
	PTFE-coated glass fibre
	Silicone-coated glass fibre
	Polyurethane-coated nylon

PVC-coated polyester is one of the most used type of textile membrane in the building industry due to the good compromise of price and performance (Houtman and Orpana 2000). The five types (type I to type V) of polyester woven fabrics cover a wide range of tensile strengths suitable for all the main structural applications (Beccarelli 2015). In addition, thanks to a relatively good flex cracking resistance, this type of fabric is also successfully used for deployable structures. Also, the use of THV coatings as a replacement for PVC is quite recent in the building industry with little data and examples regarding their use.

On the other hand, glass-fibre fabric coated with PTFE, considered one of the most durable membrane materials, is the most recommended material for permanent projects with an expected service life over 25 years (Houtman and Orpana 2000). However, the relatively high cost of the material, especially compared with PVC-coated polyester, combined with the additional manufacturing and installation costs due to its low flex cracking resistance, has reduced its use for temporary and low budget projects and for geometries with a high level of curvature (Beccarelli 2015). The disadvantage of PTFE-coated fabrics, which are susceptible to wrinkling, is overcome by using clear or opaque silicone treated with additives. However, one disadvantage is that its surface charges up statically and attracts dirt and, in addition, the high cost of the raw material and the relatively complex and expensive manufacturing process reduces its use in architecture. Also, polyurethane-coated nylon fabrics are characterised by and extreme flexibility

and light transmittance (Houtman and Orpana 2000). Yet their use is reduced due to the relatively low mechanical performance of the nylon fabrics. Figure 14 shows a comparison of the mechanical strength, flex cracking resistance, long-term stability, light transmittance and cost between the three more common combinations of coated mesh fabric.

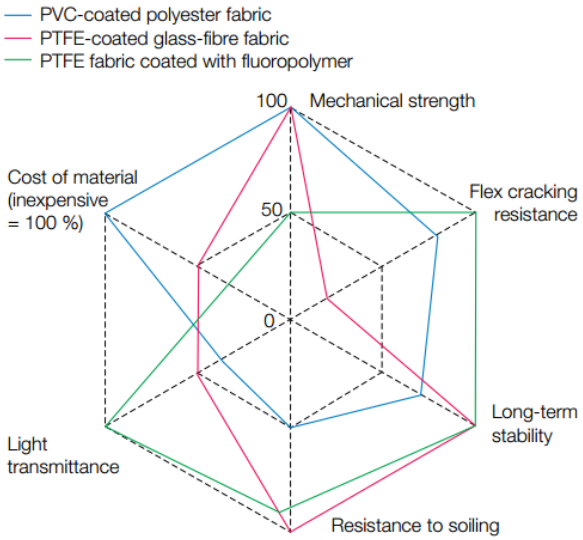

Figure 14 - Comparison of three typical membrane materials. (Knippers, Cremers et al. 2011)

2.2.2.4. Mechanical Properties

As beforehand explained, the mechanical properties of membrane structures materials depend on several aspects, being the one of outmost importance the material and the sewing pattern of the fabric. Because of the chemical composition and physical structure of polymers, deformations arising under loading, depending on temperature range, are partly of an elastic (reversible) and partly of a viscous-plastic (irreversible) nature (Seidel 2009). This has the result that important mechanical properties not only depend on the type of loading and the temperature, but above all on the time, the duration of the loading and the speed of loading. Most of conventional building materials are commonly known by their linear elastic and isotropic behaviour, where only when the elastic limit is reached and yield area starts, different rules need to be applied. Materials used in textile architecture have a completely different behaviour and act as following (Houtman and Orpana 2000):

- Nonlinear, that means that the stress-strain behaviour of the material cannot be modelled with a linearization of the curve;
- Inelastic, that means that the behaviour of the material is dependent on the added loading;

- Anisotropic, that means that the material itself has two dominant head directions, which makes all the important mechanical properties direction-dependent.

Nonlinear and inelastic behaviour of membrane fabrics

The deformation of a synthetic fabric under load can be defined as of nonlinear nature, since it cannot be described with Hooke's law of elasticity. If a uniaxial test is performed on a fabric strip, it can be established that the resistance of the material to deformation grows with increasing action of force and that the relaxation curve differs from the loading curve (Seidel 2009). If this test is repeated, then it can be recognised that all subsequent loading and unloading curves are different from all previous loading and unloading curves, as it is shown by Figure 15, right side (Seidel 2009). Moreover, after loading and unloading there are permanent strains in the material, the extent of which depends on the loading history, therefore the fabric behaviour is dependent on the extent, speed, duration and number of load cycles. With increasing duration of loading or extent of loading, the resistance against deformation increases. Additionally, Seidel (2009) says that when tension stress is applied, a clear time-dependant development of strain can also be observed. If an applied stress leads to an immediate instantaneous strain (without time delay), which however does not lead to a permanent strain, then this is called inelastic behaviour. If a purely elastic and inelastic deformation component is followed by a plastic (irreversible) component, then this is called visco-elastic deformation.

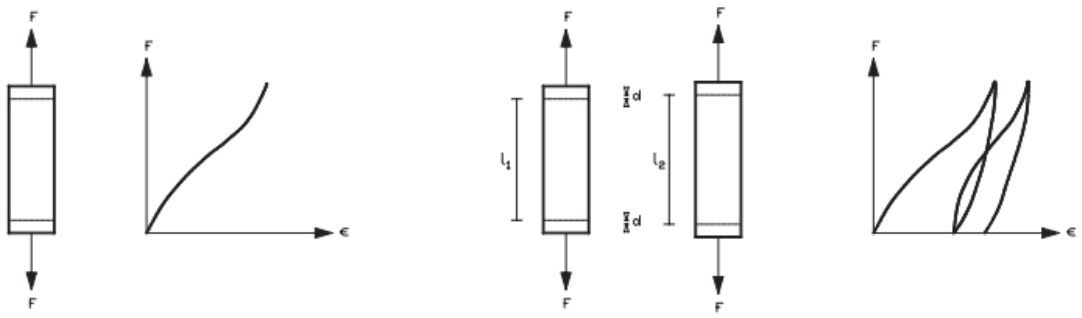

Figure 15 - Geometrical nonlinearity (left); Strains under repeated loading (middle); Loading and unloading curves (right). (Seidel 2009)

Anisotropic behaviour and influence of thread geometry

Anisotropic mechanical behaviour can be defined when distinct mechanical values are recorded with the changing alignment of a test piece relative to a coordinate system. The dependence of the stress-strain relationship resulting from a force applied to a fabric strip on the orientation of the strip to its axis

substantially influences the stiffness distribution of an equilibrium area (Seidel 2009). The geometric differences between warp and weft threads generate a different response depending on the direction of loading. The considerably greater thread curvature of the weft thread is the reason for the lower strain stiffness of the fabric in the weft direction thus, in the axial direction of the fabric, the material has higher tensile strength than in weft direction, the stiffer warp direction therefore stretches less under loading than the weft direction (Seidel 2009). This effect is illustrated in Figure 16.

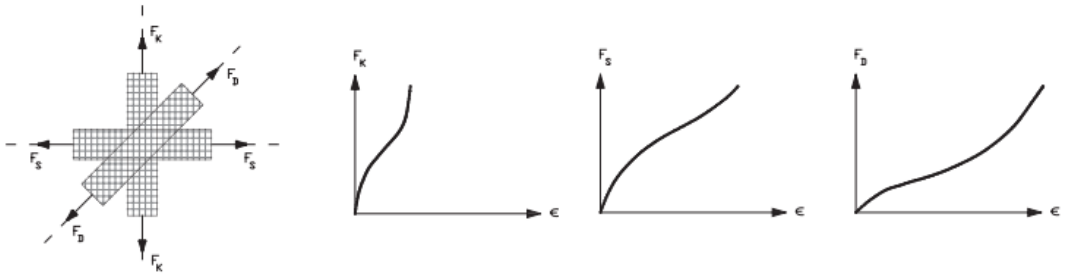

Figure 16 - Dependence of fabric behaviour on strip orientation. (Seidel 2009)

Additionally, because of the interaction between weft and warp threads at the crossing points and the course of the thread line, the curvature of the warp thread also alters with extension in the weft direction, and the additional curvature experienced by the warp thread causes a shortening (see Figure 17) of the fabric in the warp direction (Seidel 2009). If the warp direction is also under tension loading, it exerts a resistance when the weft thread is stretched. This shows that the alteration of the thread curvature in the fabric is not only dependent on the extent of the load but also from the load relationship between warp and weft.

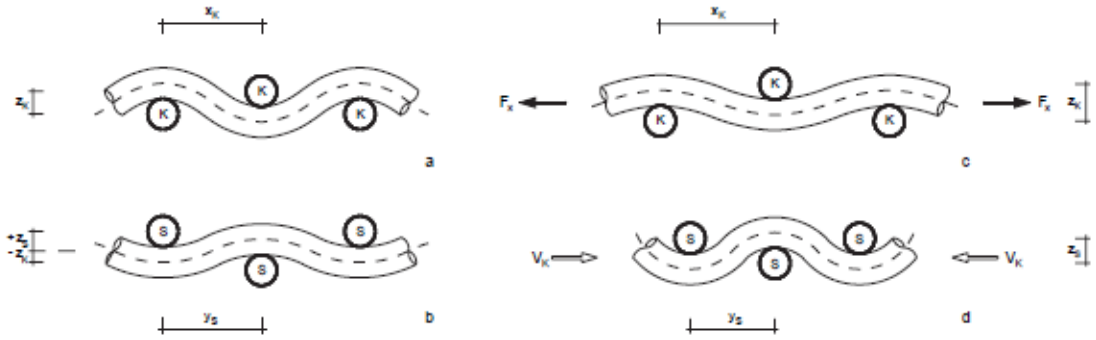

Figure 17 - Layout model of the fabric threads under no tension (left) vs uniaxial tension (right). (Seidel 2009)

2.2.3. Design process and codes

The design of traditional rigid structures follows a linear sequence in which the initial architectural shape is transmitted to the engineering office in charge of the structural design; subsequently, the definitive project is transmitted to the builder for construction (Beccarelli 2015). In contrast, the design of lightweight tension structures requires full integration of both engineering and architectural skills, which is dictated by the need to understand the interaction between the shape of the structure and load patterns that may develop (Lewis 2003). Whereas, the initial shape of membrane structures is the result of a preliminary structural analysis called "form finding", which assures that each point of the surface is in equilibrium, given the tension ratio in warp and fill direction and the boundary conditions (Beccarelli 2015). The design process of tension membranes can be summarised in three main steps: the form finding, the static analysis and the patterning, with the possible addition of dynamic analysis when required (Beccarelli 2015). This process is represented in the flowchart shown in Figure 18.

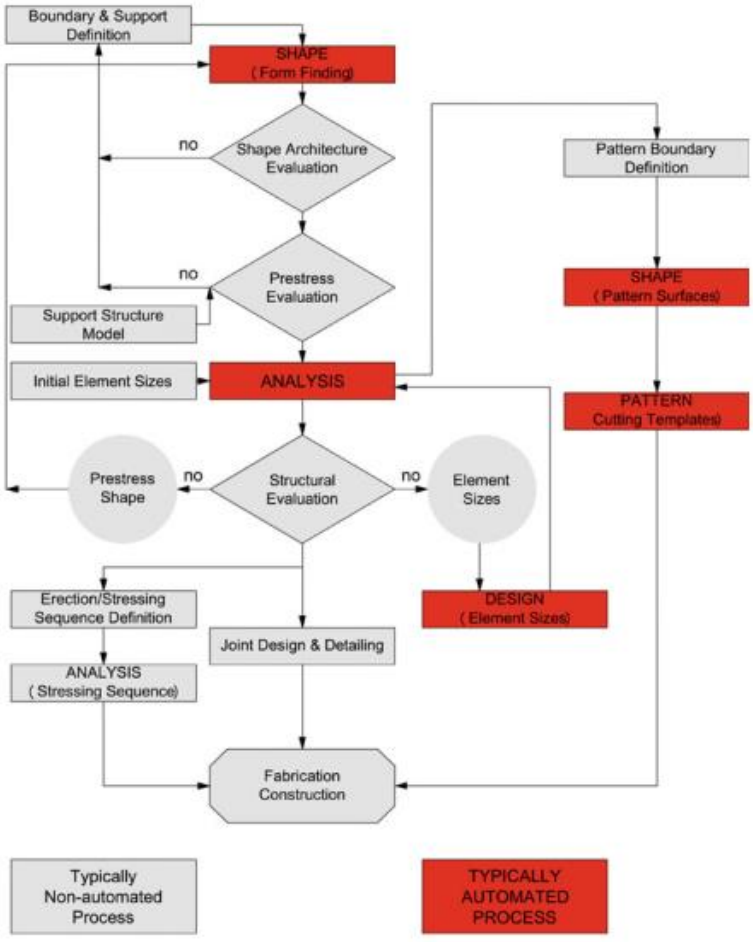

Figure 18 - Flowchart illustrating the general approach to tensile membrane structures design and engineering. (Campbell 1991) apud (Beccarelli 2015)

2.2.3.1. Surface shape and usual membrane structures

According to Forster and Mollaert (2004), the form and physical behaviour of fabric structures are very different to those of conventionally stiff “linear-elastic" framed structures used in most buildings. When compared with conventional rigid structures, membrane structures define their own contour on the basis of the boundary conditions, the material properties and the level of prestress into the surface (Beccarelli 2015). Thus, this level of prestress defines the shape of the structure, along with the boundary conditions. The level of prestress may also be set so as to avoid loss of stress in both directions in a particular zone of the surface under applied load. The setting of such values is generally made in combination with the selection of shape. Prestress contributes significantly to a the membrane stiffness due to its opposing curvature components interacting to constrain what would otherwise be severe deformations typical of flat or singly curved surfaces (Forster and Mollaert 2004).

However, in membrane structures, any discontinuity or lack of tension will be fully exposed and will lead to wrinkling, deformation and a reduced life expectancy (Forster and Mollaert 2004). On the other hand, structural membranes provide minimal use of material combined with an attractive and impressive language of shapes, being these shapes directly mechanically motivated: based on the boundary conditions and the prescribed prestress field, form finding analysis is used to determine the shape of equilibrium which allows the membrane to act in pure tension (Philipp, Wüchner et al. 2016). This mechanical background usually leads to an iterative design procedure, where the mechanical form finding and the modification of boundary conditions and prestress conditions as design handles mutually interact until a solution that is desirable from a structural as well as from an aesthetical point of view is found (Philipp, Wüchner et al. 2016). Although, there are commonly defined membrane shapes that are generally used. These shapes are predefined to work with the double curvatures to transfer forces efficiently. Figure 19 shows the usual shapes used for membrane structures. The most common shapes are the hypar, the saddle and the cone, since they are simple point supported structures. Edge supported structures and air supported (pneumatic) shapes are also common, presenting a wider variety of forms.

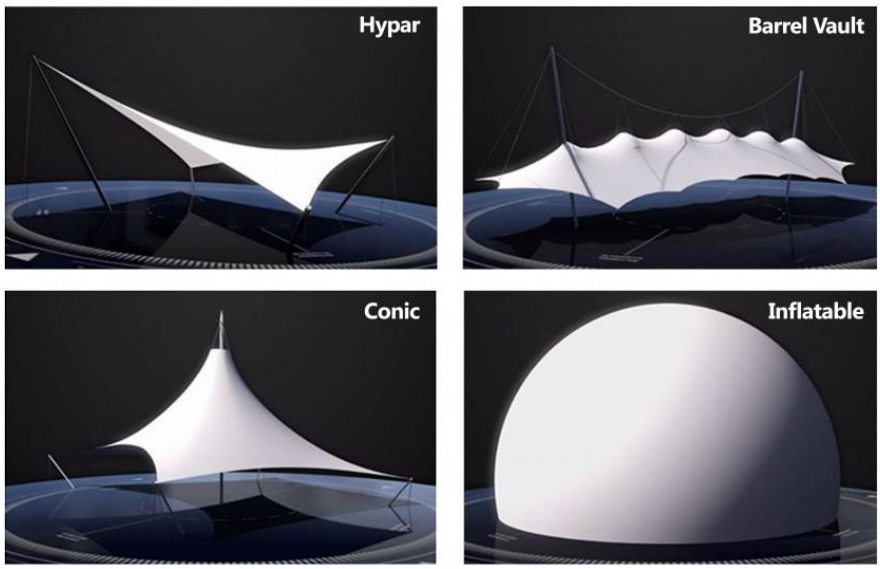

Figure 19 – Basic types of membrane structural shapes.

2.2.3.2. Form Finding and structural behaviour

The definition of shape in common linear-elastic structures is practicable because these constructions are characterised by small deformation, thus there are no considerable consequences on the geometrical shape, which is generally chosen at priori with limited attention to the structural problems. However, this methodology is totally inadequate for tension membranes, the aesthetic issues go hand in hand with the structural aspects because the overall shape of the structure depends on its equilibrium thus, the membrane shape cannot be imposed, but it has to be found by working on the boundary conditions and the internal stress distribution due to pre-stress (Beccarelli 2015). According to Forster and Mollaert (2004), this process of determining the shape and form of the structure is commonly referred to as "form finding". The process of form finding should yield optimal structural shapes: shapes that would satisfy the functional requirements and attendant durability and strength at a minimum cost (Lewis 2003).

The process of form finding of surface stressed membranes involves: the construction of small-scale physical models using soap film, fabric, or paper and/or the development of computational models using a variety of numerical techniques (Lewis 2003). The production of physical models to determine the final shape of the structure is very common in membrane structures, mainly the use of soap films, which was largely used by the architect Frei Otto during the 20th century. Forster and Mollaert (2004) say that the geometry of a soap film's surface is unique to its given boundary and so changing the boundary, in whole or part, changes the film's surface geometry. This is useful because each surface is the product of a specific set of boundary conditions, therefore simulating the form finding process. On the word of Lewis

(2003), soap films serve as examples of ideal lightweight tension membranes, since they are laminae that adopt a configuration consistent with a (local) minimum potential energy arising from surface tension. Because the potential energy is a minimum, the configuration is stable and can be realized by a soap film, therefore such a configuration is characterized by a minimum surface area (Lewis 2003). Figure 20 shows an example of the use of soap films to find the minimal surfaces inherent to a specific set of boundary conditions.

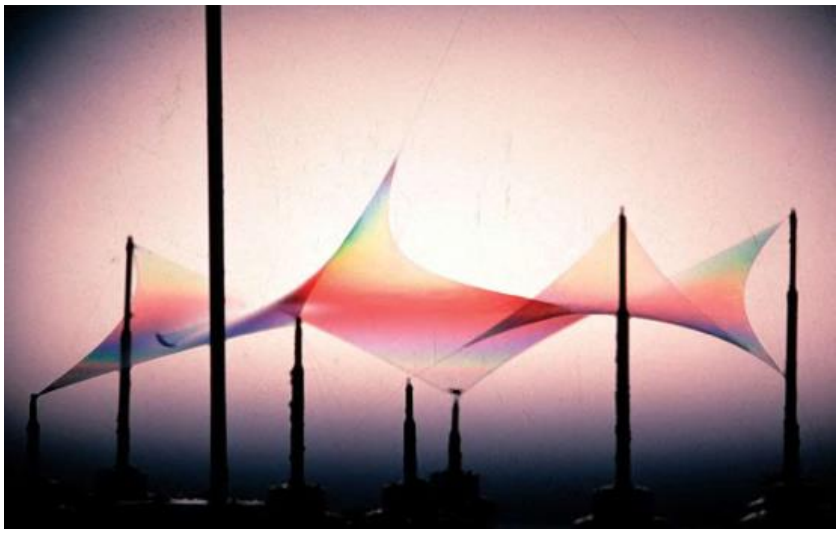

Figure 20 - Free shaped soap film model as study for "Minimal Surfaces", studies at IL by Frei Otto. (Forster and Mollaert 2004)

In mathematical language, a soap film is referred to as a *stable minimal surface*. Mathematicians have discovered many properties of minimal surfaces, together with two well-known classes of solutions, which are the catenoids and the right helicoids. Figure 21 shows an example of both these classes of solutions. Lewis (2003) says that at each point, a surface of minimum area must have a mean curvature of zero. However, this feature of zero mean curvature is not unique to minimum area surfaces, such as soap films, it is instead a feature of minimal surfaces. Soap films can be considered minimal surfaces that are stable and also have a minimum area. Lewis (2003) summarizes it by saying that every soap film is a minimal surface, but not every minimal surface is a soap film, thus defining a soap film with the term “stable minimum surface”, rather than “minimal surface”.

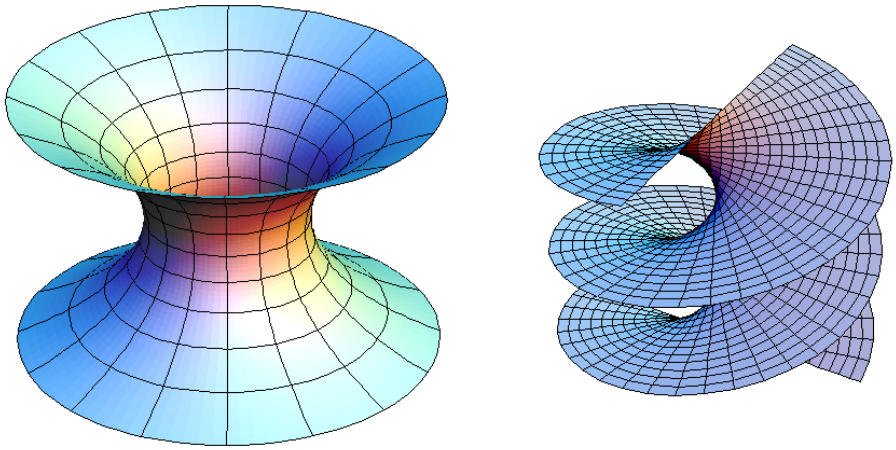

Figure 21 - Example of minimal surfaces, catenoid (left) and helicoid (right).

It is now clear that the shape of a membrane structure is obtained by the form finding process. Thus, the initial shape of a membrane structure is a function of the stress ratio in a warp and fill direction and the boundary conditions; external loads are not considered at this stage (Beccarelli 2015). It is possible to stabilise an element in space using only tension forces, provided that it is held by a minimum of 4 tensile force vectors that are not acting in a single plane and are in equilibrium. This structural principle allows the stable configuration of tensile surface structures (Forster and Mollaert 2004). Therefore, all the structural components that define the boundary conditions of the membrane should also be designed to follow the principles of minimal configurations. Form follows function, and as the membrane itself finds its shape under tension equilibrium so each boundary support should be of a minimal configuration according to the flow of forces and should clearly express its structural function (Forster and Mollaert 2004).

Lightweight tensioned structures are safe structures designed and dimensioned according to such national codes and guidance notes as exist, being particularly stable in horizontal loads like earthquakes (Forster and Mollaert 2004). Also, in the case of an unexpected failure, lightweight structures are usually less dangerous than common rigid type structures because they have much lower mass. The risks are even smaller when the layout of the tensioned structure guarantees that stiff supporting elements, like masts and beams, will not collapse should the membrane tear. In order to protect them from rain and snow, the form of the structure should be one that allows for easy drainage of water and snow, thus avoiding ponding of rainwater or large accumulations of snow. To keep rainwater out, the membrane material and its joints have to be closed and tight and the edge has to be detailed very carefully to prevent water getting inside the envelope (Forster and Mollaert 2004). In addition, a static analysis is made in

order to assure that the membrane does not fail under these types of loads. According to Beccarelli (2015), the static analysis is performed assuming as initial configuration the one determined in the form finding stage. Through the static analysis it is possible to predict the stress and the displacements which arise in the tensioned surface due to the presence of these external loads.

Dynamic analysis can also be performed for membrane structures. Beccarelli (2015) says that the scope of dynamic analyses is the evaluation of the interaction between a fluctuating external load and the structure and, for membrane structures, this issue is generally related with the fluctuation of wind pressure. However, for projects with particular relevance or for the validation of simplified models for standard applications, the expected data should be confirmed through tests performed in a wind tunnel (Forster and Mollaert 2004).

2.2.3.3. Erection and patterning

The erection of membrane structures is a process that requires precise dimensions in order to obtain the required forms and prestress levels. Accurate fabrication dimensions are essential to the successful construction of fabric structures, which requires membrane cutting patterns to be taken out of the "at prestress" model of the structure (Forster and Mollaert 2004). These dimensions are defined in the so-called patterning stage. According to Lewis (2003), the patterning stage allows a three-dimensional shape of a tensioned surface to be translated and relaxed into a two-dimensional cutting pattern, to enable the manufacture of the membrane. This operation is generally based on mathematical studies carried out for several applications, such as the determination of the surface area of solids or the topographic issues related to the realisation of accurate bi-dimensional maps of the globe (Beccarelli 2015). According to Lewis (2003), the pattern must be made out of strips of fabric of 2 to 3m wide, with minimum waste of material and distortions of the fabric. Figure 22 shows an example of the patterning process, starting with the form found geometry, passing into the relaxed 2d pattern and, finally, the drawings for production.

Figure 22 - Digital cutting patterns layout, stripes and cutting patterns: Tent for Mercedes Benz Magdeburg, SL Rasch, Germany, 1994. (Forster and Mollaert 2004)

The strips of fabric are cut off from a roll that generally has a maximum width between 1,80m and 3,00m. They are then joined together in order to obtain the biggest panel of fabric transportable and mountable, reducing the use of welding machines or other high precision processes on the building site (Beccarelli 2015). The initial shape should always be adequately compensated and provided with extra material necessary for the joint realisation. There are several ways of materializing the joint, namely:

- Welding;
- Gluing;
- Mechanical stitching;
- Clamping;
- Lacing.

The seams between the panels of fabric are generally based on heat or high-frequency welding which provide a higher level of water-and airtightness. However, glued or mechanical stitching, clamping or lacing are also possible according to the specific requirements (Beccarelli 2015). Figure 23 shows an overview on some process of joining, namely welding and mechanical stitching.

Figure 23 – Jointing processes. Manual welding device (left), industrial sewing machine (right). (Knippers, Cremers et al. 2011)

On the word of Forster and Mollaert (2004), welding is the most widely used technique for membrane constructions, conferring some practical advantages such as fabric water tightness. Knippers, Cremers et al. (2011) say that welding consists in the fusion of thermoplastic coatings through a combination of heat and pressure. The heat required for this is provided by high-frequency radiation, heating elements or electric impulses, once the weld seam has cooled sufficiently while applying constant pressure, it can reach about 90% of the strength of the parent material depending on the specific material and the welding process also, the strength depends on the contact pressure, the shape of the contact elements (smooth, serrated), the welding temperature and the pressure application time and that the typical seam widths lie between 50 and 100 mm. One advantage to membrane structure erection is that, once on site, the assembly process is relatively fast and efficient due to the high level of accuracy of manufacture (Beccarelli 2015).

2.2.3.4. Design codes, norms and guides

The geometrically non-linear behaviour of membrane structures gives rise to an action effect which is not proportional to the increase of the action (Pyl, Wang et al. 2016), therefore super position of load effects is not applicable to membrane structures (Beccarelli 2015). Also, the fact that membrane structures behave completely different from typical structures creates a lack of applicable design codes to this type of structures.

According to Beccarelli (2015), in the United States, the activity of the American Society of Civil Engineers (ASCE) and the Structural Engineering Institute (SEI) contributed to the development of several standards and manuals of practice, being the most relevant the ASCE Standard 55-10 “Tensile Membrane

Structures", on the other hand, the only European Standard currently available about membrane structures is the EN 13782:2005 "Temporary structures-Tents-Safety". Also, the characteristics, the requirements and the test methods for coated fabrics intended for temporary structure and tents are summarised in the European Standard EN 15619:2008+A1:2010 "Rubber or plastic coated fabrics—Safety of temporary structures (tents)—Specification for coated fabrics intended for tents and related structures" (Beccarelli 2015). From this, it becomes obvious that it exists an absence of applicable and validated code for designing membrane structures.

It was for this reason that the European Network for Membrane Structures (TensiNet) developed the TensiNet Design Guide (Forster and Mollaert 2004) which represent the most complete and updated state of the art in this field realised by means of the contribute of several groups of research, designers, material producers, software developers and fabricators operating in Europe. The set of guidelines represents the starting point for the development of an assignment for the European Committee for Standardization (CEN TC250 Working Group 5), of the future Eurocode 10 (Beccarelli 2015).

Nevertheless, for the remaining structural typologies yet to be discussed, official rules and norms do not exist or are not coherent enough to be applied. Usually, adaptations are made of existing rules to these other structural typologies (bending-active and hybrid structures).

2.3. Bending-active structures

2.3.1. History and approach categorisation

Active bending techniques were utilised in remote areas with no access to more traditional building techniques, thus there are many examples of the utilization of bending-active elements in vernacular architecture around the world, as shown in Figure 24 with two examples of tents constructed with bending-active elements. To Lienhard (2014), in order to guarantee sufficient load bearing capacity of a structure that includes considerable self-equilibrating bending stress, materials of high breaking strain must be chosen. Since building materials like bamboo and reed offer such characteristics, an extensive use of active bending in the constructions of vernacular architecture across cultures and continents. Then, as the industrial revolution took place also brought with it steel as a new construction material as well as a new organization in the construction process, splitting the distinct tasks between the many specialists, therefore limiting the construction geometries. To Gengnagel, Alpermann et al. (2013), building what was designed by others systematically limits the highly integrated concept of bending-active structures. After

that, during the 20th century architecture the use of elastic deformation was mainly utilised as an economic construction method for double curved shell structures. Only recent developments in simulation techniques have formed the basis for new exploration in bending-active structures that include new types of surface.

Figure 24 - Oca, Amazonian Basin, Brazil (left). Dorze tribe house, Ethiopia (right).

A large variety and combination of structural systems can be generated by means of elastic deformation. As is shown in Figure 25, three main approaches can be mentioned, namely the behaviour based approach, the geometry based approach and the integral approach which is a combination of the previous two. For Lienhard (2014), these can be defined as follows:

- In a behaviour based approach bending is initially used intuitively and the system's geometry and structural behaviour are studied empirically. Material limitations are tested physically.
- In a geometry based approach the system's geometry is predefined based on analytical geometry or experimental form finding methods, both of which are used as a controlled means to approximate the actual bending geometry. Material limitations are considered analytically based on moment curvature relation.
- In an integral approach the elastic bending deformation is analysed through numerical form finding, which enables full control of material behaviour based geometry. Material characteristics and limitations are included in the numerical analysis model.

Membrane, bending-active, hybrid and adaptive kinetic structures

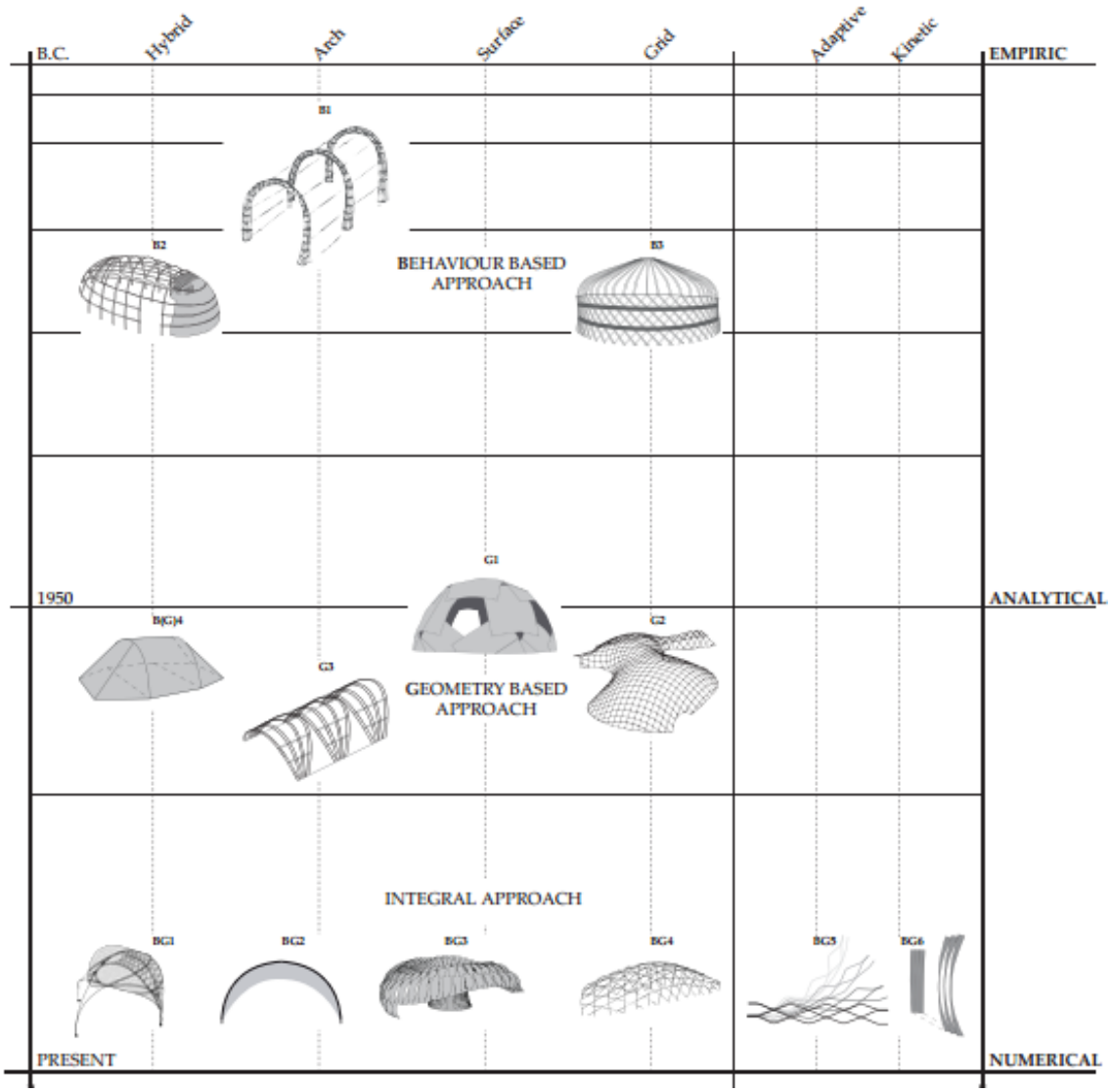

Figure 25 - Development of bending-active structures. (Lienhard 2014)

When looking at the historical development, starting with the behaviour based approach, it becomes apparent that this approach leads to the most realised projects and is a recognised construction type which is still used today. It took until the 20th century for an analytical, geometry based approach to appear (Lienhard 2014). Throughout the 19th and 20th centuries, several form finding strategies based on material and force were developed, which led to a wide expansion of the interest for lightweight construction. Enabled by the powerful simulation methods we are equipped with today, the two approaches may be combined by simulating the large bending deformations of the erection or shape adaptation themselves and thereby fully tap the potential of active bending (Lienhard 2014).

The behaviour based approach is the oldest approach and, since it bases the whole procedure of elaborating bending-active structures in the behaviour of the material and the structure itself, it was widely

used during all stages of civilization. One example of this are the Mudhif houses, which construction procedure is shown in Figure 26. They are permanent structures using reed bundles that are first vertically fixed into bucket foundations and later connected at the top to form elastically bent arcs (Lienhard 2014). Although, still today there are various examples of bending-active structures that are predicated on the behaviour based approach (Brancart, De Laet et al. 2016).

Then, during the 20th century development of lightweight structures, many double curved surfaces and grid shells start to emerge. An example of this approach is the Water and Wind Café, shown in Figure 26. However, the simulation techniques which are starting to be developed were not yet able to simulate large elastic deformations, since the most common form finding method of the time was the hanging model, which could be handled both experimentally and analytically (Lienhard 2014). Recent developments in simulation techniques now allow form finding and analysis of structures that derive their complex curved geometry, like the GFRP and membrane pavilion shown in Figure 26, solely through the erection process in which they are elastically deformed (Lienhard 2014). Figure 26 shows a clear differentiation and evolution between the three approaches mentioned.

Figure 26 – Mudhif houses, Madan people (left); Water and Wind Café, Bamboo Bar, Binh Duong, Vietnam, 2008 (middle); GFRP and membrane pavilion, Stuttgart, 2004 (right). (Lienhard 2014)

2.3.2. Materials

The existence of materials of high breaking strain is a precondition for the work with bending-active structures whose form and performance is entirely based on material behaviour. Figure 29 shows a range of common materials apt for bending-active structures, as well as the materials apt for elastic kinetic structures, based on the ratio between flexural strength and stiffness. To Lienhard (2014), adequate materials for bending-active structures offer a ratio of $\sigma_{\mathrm{M,Rk}}(MPa)/E(GPa) > 2.5$. Also, some traditional building materials, such as timber, already offer an appropriate elastic range. Although, according to Lienhard (2014), owing to their low density and high strength combined with low bending

stiffness, Fibre Reinforced Polymers (FRP) embody the potential for exploring further light weight bending-active structures.

Accordingly, generally tree types of materials are used as bending-active elements, wood (usually plywood or bamboo), metals (aluminium or spring steel) and FRP (GFRP or CFRP). Three distinct examples of bending-active structures are shown in Figure 27 and Figure 28, one for each material mentioned. Selecting a material for a bending-active element is typically a process that requires a compromise between the material strength and the flexural modulus. Lienhard (2014) gives the example that steel is stiff and rubber is compliant, however, steel may be more adequate for bending active structures since it also offers high strength, consequentially, the combinations of properties are more important than a singular aspect of mechanical behaviour for finding appropriate materials.

It is also important to separate the concept of active bending from the elastic kinetic concept. A material that is appropriate to be used as a bending-active element may not be appropriate to be used as a kinetic element, but usually the opposite is not true. A bending-active element is one that would be bent and remain in the position that it was bent to. On the other hand, a kinetic element may use the elastic energy stored from the bending induced prestress in order to retract to a slightly less prestressed state, or even to the initial relaxed state. Additionally, for Lienhard (2014), in static bending-active structures, creep deformation and consequential loss of prestress may be of little consequence to the system's integrity, thus if the prestress is not playing a decisive role in the system stiffness, materials such as timber may be chosen.

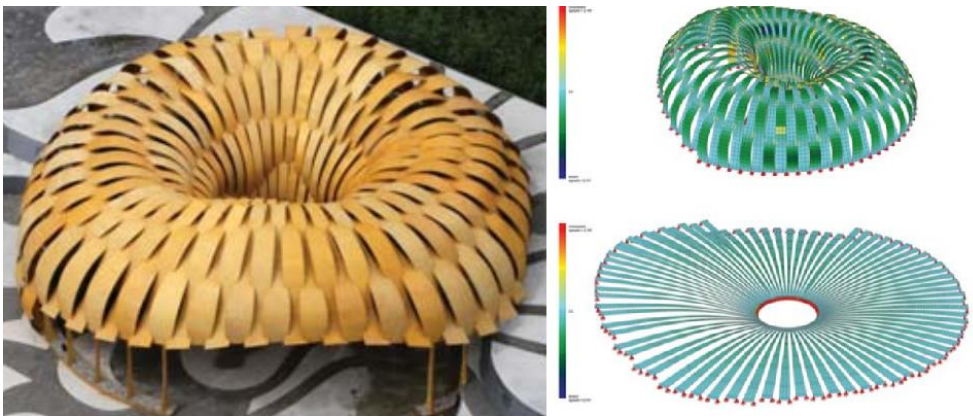

Figure 27 - Outside view of the ICD/ITKE Research Pavilion, 2010 (left); FEM form finding model of the pavilion structure (right). (Lienhard 2014)

Figure 28 - Strut and cable braced cantilever, Munich, UK, 2002 (left); LOOP, New York, 2006 (right).

(Lienhard 2014)

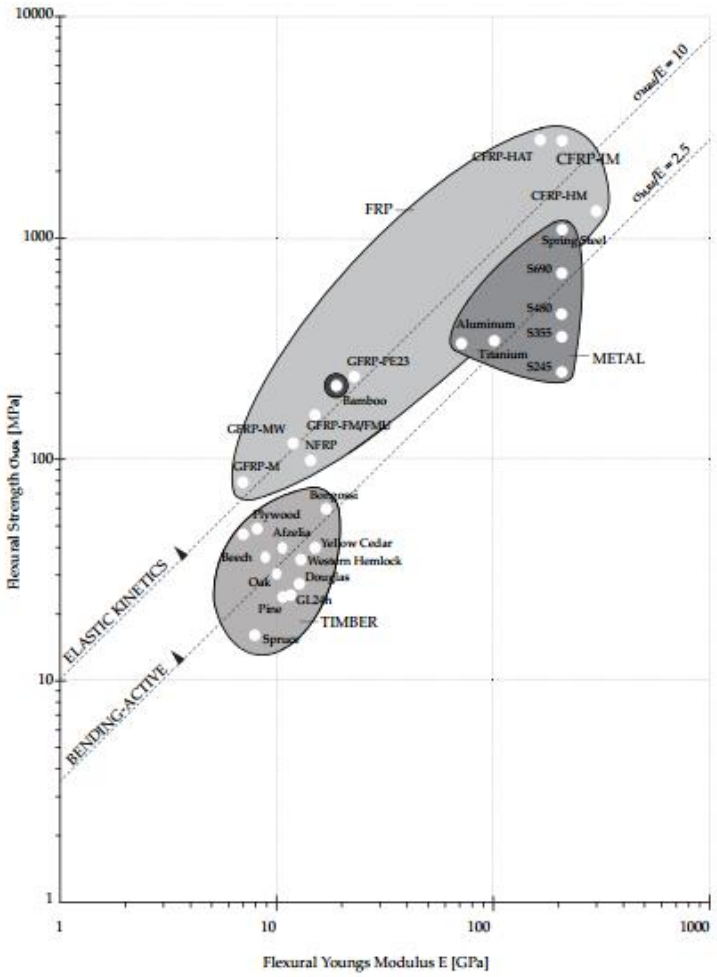

Figure 29 - Common building materials with ratio of strength $\sigma_{M,Rk}$ [MPA] to stiffness E [GPA].

(Lienhard 2014)

Fibre Reinforced Polymers

Since, as explained above, FRP are the material that can unveil the full potential behind this principle, a simple introduction about the constitution of Fibre Reinforced Polymers is given here, also, the mechanical properties of FRP materials are slightly addressed. According to Knippers, Cremers et al. (2011), the optical and mechanical properties of fibre reinforced polymers are determined by the inter action of their constituents. The fibres increase the load-carrying capacity and stiffness of the polymer and hence are essentially responsible for those properties in the finished composite material while the polymer, on the other hand, does not perform any loadbearing functions as such, but rather stabilises and protects the fibres. Figure 30 shows an overview on the process of manual lamination GFRP. Firstly, a layer of pure resin is applied (gelcoat) on a mould previously treated with a release agent, then the fibres are compressed into place, and lastly the liquid fibre is applied.

Figure 30 - Process of manual lamination of GFRP. (Knippers, Cremers et al. 2011)

The main function of the polymer matrix is to define the shape of the composite component and to protect the fibres against UV radiation and aggressive agents, such as moisture and chemicals. At the same time, the polymer forms the surface and therefore determines the degree of transparency, the colour and feel of the fibre composite. Also, as Knippers, Cremers et al. (2011) say, various additives and fillers are added to the fibre composite material to control or adjust the properties of the final material, for example flame retardants are added to comply with fire protection requirements. On the other hand, the strength of the composite component depends on the interaction between the fibres and the polymer matrix, since the fractures in the component are generally caused by an excess strain. Thus, using a polymer with a high maximum permissible strain therefore increases the strength of the entire composite component. Therefore, the adhesion between the fibres and the polymer is also crucial for the load-carrying capacity of the component, since flaws reduce the adhesion between the fibres and the matrix and this means the

strength is always lower than that of the un reinforced polymer (Knippers, Cremers et al. 2011). Figure 31 shows an example of the glass and carbon fibres used in GFRP and CFRP, respectively.

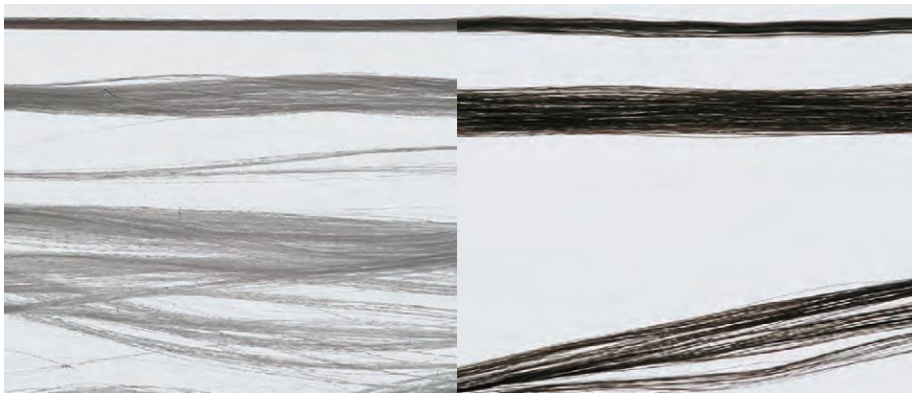

Figure 31 – Glass fibres (left); Carbon fibres (right). (Knippers, Cremers et al. 2011)

Although machine-made GFRP components can achieve the strength of structural steel, their elastic modulus is at best only one-tenth that of steel but CFRP, on the other hand, has a similar elastic modulus to that of steel and at the same time a much higher strength (Knippers, Cremers et al. 2011). An overview of the mechanical properties of FRP compared with other common materials is shown in Figure 32. It is visible that CFRP behaves more like a rigid type material, withstanding high stresses with very small strains. On the other hand, GFRP has a more elastic behaviour, while comprising also reasonably high strains.

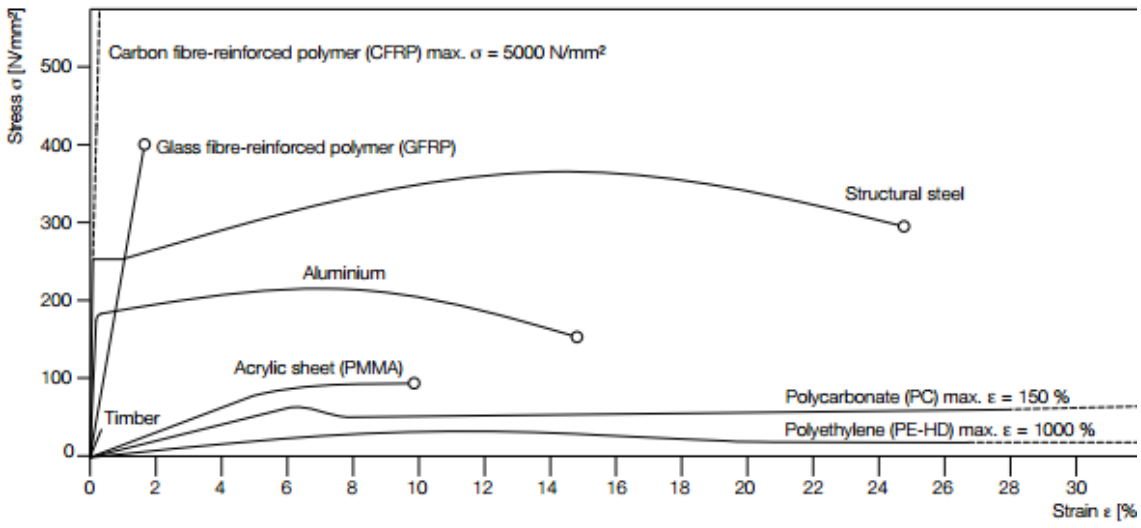

Figure 32 - Mechanical properties of polymers compared with traditional building materials. (Knippers, Cremers et al. 2011)

2.3.3. The elastica curve

The basis of the geometry of a bending active structure lies in the shape of the elastica curve. According to Lienhard, La Magna et al. (2014), the geometry of curves described by a beam's elastic deformation in its post buckled shape has fascinated scientists for centuries. According to Levien (2008), in the recorded literature, the problem of the elastica was first posed in *De Ratione Ponderis* by *Jordanus de Nemore* (Jordan of the Forest), a 13th century mathematician. After that, the elastica caught the attention of many of the brightest minds in the history of mathematics, including Galileo, the Bernoullis, Euler, and others (Levien 2008).

Galileo, in 1638, posed a fundamental problem, founding the mathematical study of elasticity: "Given a prismatic beam set into a wall at one end, and loaded by a weight at the other, how much weight is required to break the beam?". Here, the consideration of large deformation was still not addressed. However, the complete solution for the elastica curve is most commonly attributed to Euler in 1744 because of his compelling mathematical treatment and illustrations, but in fact James Bernoulli had arrived at the correct equation a half-century earlier (Levien 2008). Figure 33 shows the problem proposed by Galileo and the solution to the elastica curve proposed by Bernoulli.

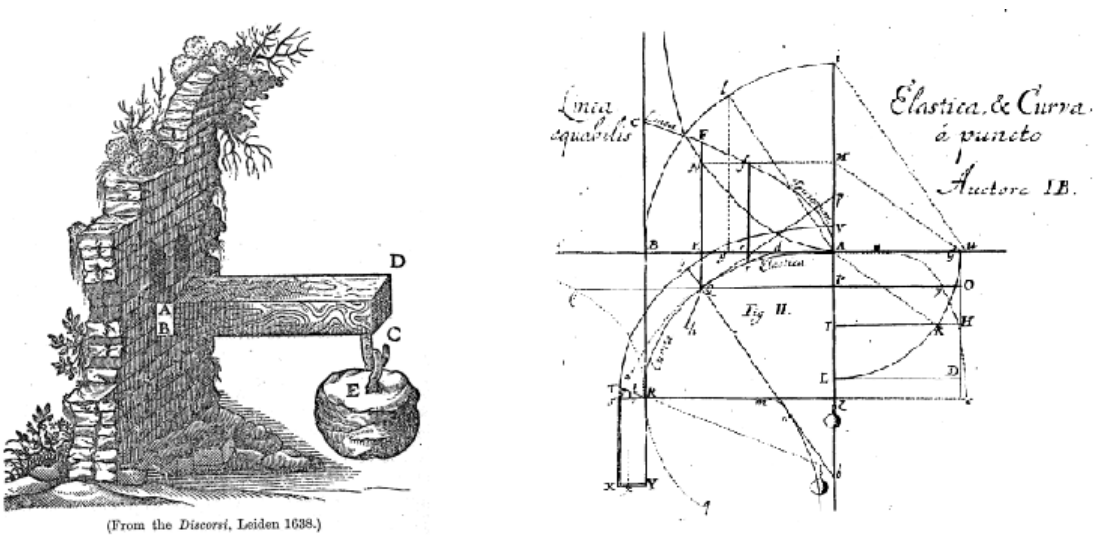

Figure 33 - Galileo's 1638 problem (left); Bernoulli's 1964 publication of the elastica (right). (Levien 2008)

According to Levien (2008), the elastica can be understood from a number of different aspects, including as a mechanical equilibrium, a problem of the calculus of variations, and the solution to elliptic integrals.

For Lienhard (2014), based on the understanding of structural mechanics, the Elastica may be described as:

- Post-buckling curve states after passing a critical point on the load deflection;
- Moment progression in a static system curve that generates a minimum of potential bending energy in the overall system;
- Equilibrium of forces in a static system (FEM approach).

The understanding that the elastica is a curve that generates a minimum of potential bending energy in a constrained system describes best the inseparable interdependency of mechanical behaviour and form present in all bending-active structures. Elastic bending of the beam produces potential energy in the system (Lienhard 2014). The total amount of the potential energy of a beam is described by equation (1):

$$\tilde{E}[\kappa(x0)] = \frac{1}{2}\int_0^l EI \cdot \kappa(x0)^2 dx_0 \qquad (1)$$

Where $\kappa(x0)$ represents the local curvature, $\tilde{E}$ the total amount of bending energy in Joules, E the Youngs modulus in Megapascal and l the length of the deformed beam in meters. When completely unconstrained, the Elastica will assume the shape of a straight line, in which the curvature everywhere is zero, and thus, the total bending energy is also zero (Lienhard 2014). The typical geometry of an elastica curve is shown in Figure 34. This evolution of the geometry of an elastica curve is independent of its mechanical properties (Lienhard 2014).

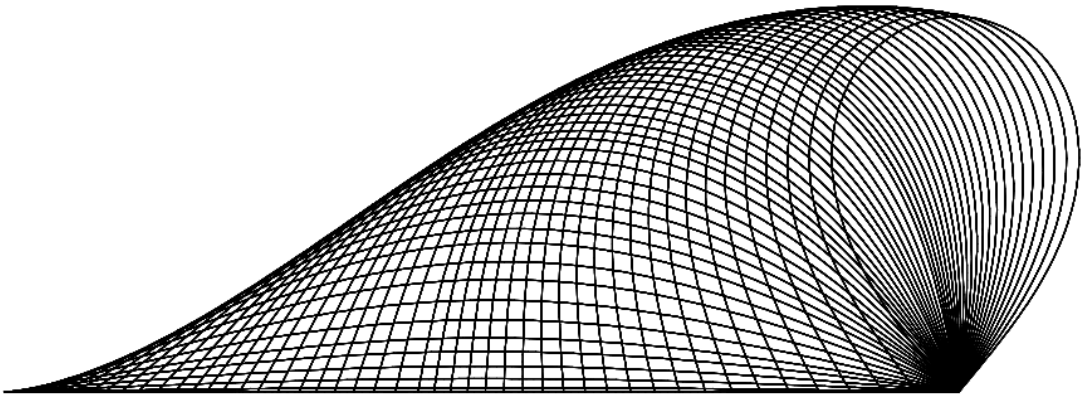

Figure 34 - Evolution of the elastica curve simulated for a single span beam from straight to maximum deformed configuration. (Lienhard 2014)

2.4. Hybrid and kinetic structures

During this subchapter, the concept of hybrid and kinetic structures is discussed. Additionally, the existing form finding procedures for hybrid structures are slightly addressed. For each type, some case studies are presented, as well as the biomimicry concept, which is highly connected with these two concepts.

2.4.1. Hybrid and textile hybrid concepts

Regarding membrane structures, the simple shapes discussed in section 2.2.3.1 are not the only possibilities. Indeed, hybrid versions and combinations thereof increase the choice of forms considerably (Forster and Mollaert 2004). One of these variations, and the one considered for the present work, is the textile hybrid which was suggested by Lienhard (2014) as the interdependence of form and force of mechanically prestressed textile membranes and bending-active elements, and that was already introduced in section 1.1.

According to Lienhard (2014), the flexibility and lightness inherent to bending-active structures integrates well with the prestressed membrane structures that are themselves flexible and adjust to applied loads. Functionally, the integration of elastic beams within a prestressed membrane surface offers the possibility of short-cutting tension forces and creating free corner points, thus the system is stabilised solely by the elastic beams which, in turn, are restrained by the membrane surface (Lienhard 2014). As the stiffness of a hybrid system is much higher than the stiffness of the bent element itself, very small cross-sections are feasible. Also, investigations have been made in order to apply this principle to columns. A membrane restrained column is shown in Figure 35. According to Gengnagel, Alpermann et al. (2013), the motivation to use elastically-bent elements for membrane restrained columns is their small package volume and easy transport, since straight elements also offer the possibility to use interlocking elements.

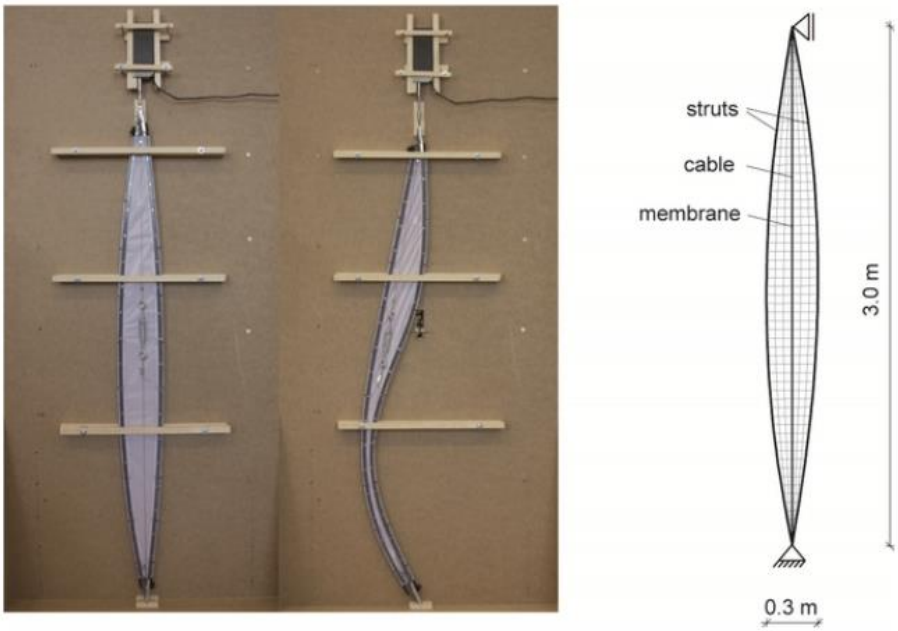

Figure 35 - Prototype of a 2D membrane restrained column with elastically bent struts (left). Buckling failure (middle). Numerical model (right). (Gengnagel, Alpermann et al. 2013)

2.4.2. Form finding and design of textile hybrids

According to Lienhard (2014), the integration of elastic beams in a form-active surface for extremely light and integrated primary structures in mechanically prestressed membranes has been a challenge for numerical form finding methods. The particular situation of form finding a textile hybrid needs a combined form finding of the membrane and the bending-active elements. According to Lienhard (2014), there are three principal approaches that can be followed to achieve such a combined equilibrium system:

- Additive, where the form finding of the bending-active and form-active structure are separated, then the two systems are coupled together once the separate entities are form-found;
- Successive, where the process is separated into first, the form finding of an elastically bent beam structure and second, the form finding of the membrane attached to the beams;
- Simultaneous, since some scenarios also allow the simultaneous form finding of the bending-active beam elements and pre-stressed membrane elements.

Therefore, to Lienhard (2014), the necessity and advantage of FEM in the development of Textile Hybrids in particular lies in the possibility of a complete mechanical description of the system. Figure 36 shows an example of the whole design process for the textile hybrid M1 project. This includes the form finding, the static analysis, the CAD model and the patterning process. According to Lienhard (2014), among

architects Particle Spring Based Methods have become popular in computational design. This means that in a project like situation, where there is direct interaction between the architect and the engineer, a connection between these models is recommended. Thus, and quoting Lienhard (2014), for civil engineering purposes, the FEM software packages offer expedient means for subsequent structural analysis with the use of a large variety predefined sub-routines. This shows that the FEM model promises to be able to handle the form finding problem, without the need for Particle Spring Based Methods.

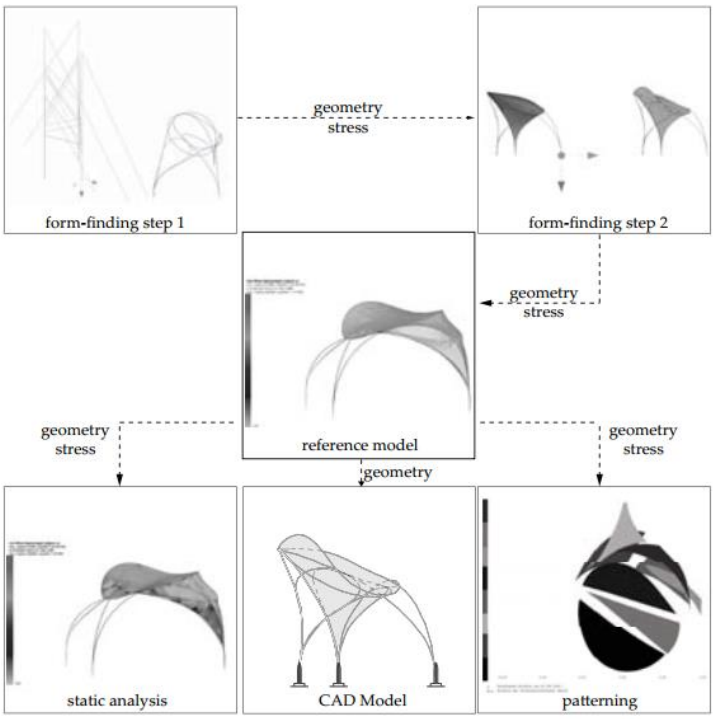

Figure 36 - Continuous mechanical description of the structural FEM model from form finding to patterning on the example of the M1 project. (Lienhard 2014)

2.4.3. Kinetic and adaptive systems

2.4.3.1. Kinetic structures

According to Lienhard, La Magna et al. (2014), it may be concluded that, providing the right material properties and a reversible erection process, bending-active structures can become adaptive and even kinetic without a change of topology or degree of static determinacy, leading to the hypothesis that bending-active structures and elastic kinetics are comparable on a structural level. Therefore, using the intrinsic elastic behaviour of flexible bending-active elements in the design of transformable or deployable structures leads to a wide range of kinetic concepts (Brancart, De Laet et al. 2016). Incorporating

transformability in the design and construction of temporary structures, can greatly improve their reusability and reconfigurability and reduce their assembly time, thus not only avoiding excessive waste production, but also bettering their efficiency in responding to short-term or critical needs (Brancart, De Laet et al. 2016). This principle has been used in construction for a long time, on example is given in Figure 37, a folding bridge that adapts to the traffic conditions. According to Knippers and Speck (2012), the bridge is moved through a complex cable system of numerous ropes, winches and rollers, and simultaneously each change to the construction's position had to be stabilized to counteract wind loads from all directions. The architectural intent was to incorporate not only the mechanics but also the aesthetics of the surrounding harbour cranes and transfer it to the bridge construction (Knippers and Speck 2012).

Figure 37 - Folding Bridge, Kiel, 1998. (Knippers and Speck 2012)

Accordingly, to what has been explained in section 2.3.2, about the material for bending-active structures, a similar condition is imposed when selecting materials for elastic kinetic systems using active bending principles. On the word of Lienhard (2014), for elastic kinetic systems, the additional requirements for fatigue control further limit the permissible permanent elastic stress, therefore, ratios of $\sigma_{\mathrm{M,Rk}}(MPa)/E(GPa) > 10$ are needed, which is a ratio 4 times greater than the one required for bending-active static systems. Adaptive and kinetic structures rely, next to a high materials yield strength and low bending stiffness, also on advantageous long-term behaviour, allowing for cyclic exposure to large elastic deformation, although, the resetting effect can only be utilised if no long term permanent creep deformation occurs, thus FRPs may provide the required material behaviour (Lienhard 2014).

2.4.3.2. Textile hybrid adaptive structures

According to Rao (2014), sustainable development is moving to a new level where buildings are integral to nature, supporting nature's work rather than interfering with life-sustaining ecosystems. Biomimicry is a science that can help tackle the problem of sustainability. According to Aziz (2016), biomimicry is the

study of emulating and mimicking nature, where it has been used by designers to help in solving human problems. On the word of Rao (2014), one of the most effective ways to cut down the ecological footprint of buildings is to follow the lead of nature through biomimicry. According to Knippers and Speck (2012), architectural design and biological evolution are nondeterministic processes. Therefore, the same problem can have several solutions.

One example of the concept of biomimicry applied to hybrid structures is the investigation project Flectofin®, shown in Figure 38. According to Lienhard (2014), the Flectofin® is based on the sophisticated pollination mechanism of *Strelitzia reginae*. The plant uses a system in which when the bird lands on this structure to reach the nectar at the base of the flower, its weight causes the perch to bend downwards (Lienhard 2014). This bending triggers a sideways flapping of the petal laminae, and the previously enclosed anthers are exposed so the pollen can be attached to the bird's feet and chest and then, when the bird flies away, the open perch resets to the protective closed state again due to its elastic properties (Lienhard 2014). Flectofin® mimics this principle with the objective to develop a smart module for shading facades. Also shown in Figure 38 is the investigation of the eucalyptus leaf, during the development of the Flectofin® project, to minimize the stresses during the transition from the semi-elastic shell element to the beam element.

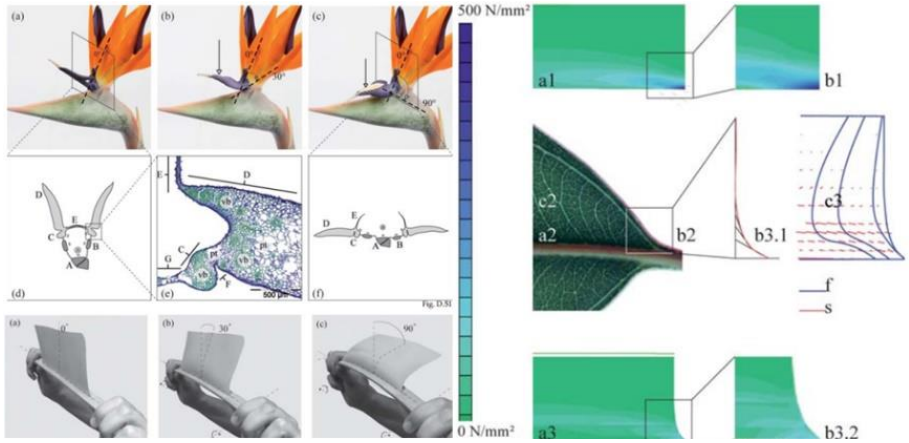

Figure 38 - Flectofin project (left); Reduction of stress concentrations using contour geometry of a Eucalyptus spec. leaf. (Lienhard 2014)

The need to adapt has been within the human nature for many centuries. This is also true in construction and architecture, since structures, has well as humans, need to adapt to distinct environmental circumstances, such as temperature, wind or loading configurations. For Forster and Mollaert (2004), convertible structures can be seen as manmade adaptive systems, which, like many natural organisms,

change according to necessity. They are flexible and adaptable in their spatial arrangement and response to climatic variations (Forster and Mollaert 2004). Bridges are usually perfect examples of adaptive systems. One of the first examples of kinetic architecture is a drawbridge, like the one shown in Figure 39, that can be retracted and thus selection can be made on who crosses it. Also, another perfect yet simple example of an adaptive system is a structural hinge, like the one shown in Figure 39. The hinge allows the structure to make small, yet important, adaptations, thus allowing a dissipation of resistance through displacement.

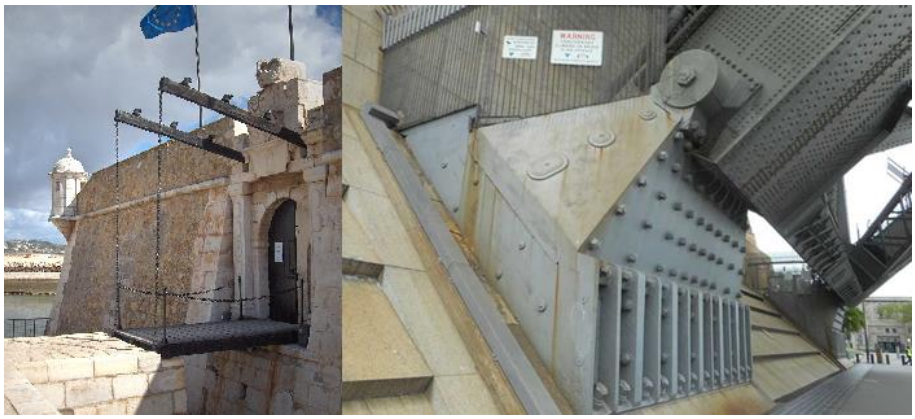

Figure 39 – Drawbridge at the fort of Ponta da Bandeira, Lagos, Portugal (left); Hinge detail, Sidney Harbour Bridge (right).

The approach of adapting a structure through kinetic enhancement can also be used in roofs and other type of structures. According to Forster and Mollaert (2004), this design approach leads automatically to the possibility of energy saving, through the control of natural light and internal temperature. The concept of textile hybrid structures, introduced in section 2.4.1, clearly defines a standpoint in the adaptive concept. The flexibility of membranes allied with the elastic reversible properties of bending-active structures provides a sturdy foundation for developing the kinetic adaptive principle. This can deliver several benefits, as Forster and Mollaert (2004) say, the flexibility of convertible structures makes it possible to change the architectonic space, as the space can be experienced in a more open or sheltered way. Also, thermic advantages appear from adaptive structures, since it is possible to control the internal environment through the movement of the structure.

In the recent studies developed by University of Minho, membrane structures have been having a significant importance, materialised by the concretization of some master thesis and research projects. Though, few projects exist that develop this particular adaptive hybrid concept. Yet, there is one master thesis, developed by Costa (2017), that develops an architectural conceptual project of an adaptive textile

hybrid structure for a roof and shading system. According to Costa (2017), the project proposes the conceptual development of an architectural intelligent structure, corresponding to a module. This module is based on distinct properties of leaves, like composition and adaptation, which can then be added with similar modules to create massive canopies or roof systems. The concept, which is illustrated in Figure 40, is to design a module capable of adapting, which is also lightweight and sustainable. This adaptation is introduced by the means of intentionally introducing large displacements in the structure, taking advantage of the elastic properties of some materials, to achieve an adaptation that resembles a leaf moving.

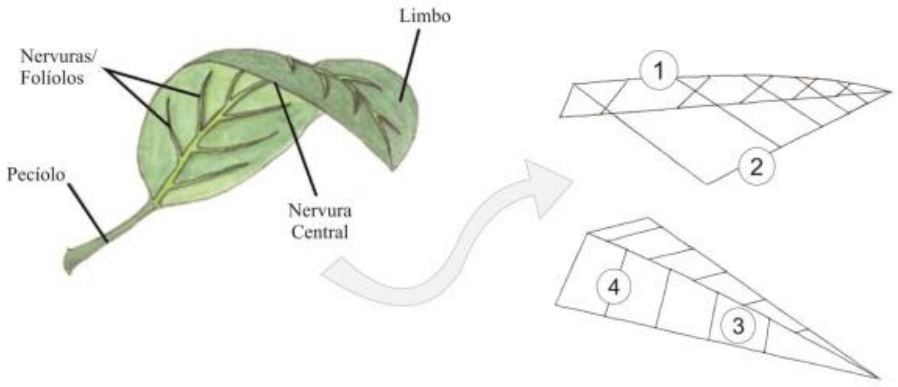

Figure 40 - Conceptual scheme of the structure. (Costa 2017)

This idea was based on leaves, which also adapt according to the sunlight and temperature, and a lot of other factors depending on the type of leaf. According to Costa (2017), in a general way, the idea of the leaf applied to the module structure leads to general concepts of change, movement, flexibility and adaptation, bringing a rereading of the form and mechanical behaviour of a nature found element to the reality of the architecture and engineering. If the conceptual architectural project suggested is structurally viable, then there is a wide range of possible applications and advantages that can be achieved. The adaptive module can contribute for the control of the optimization of the internal environment, where ventilation, light and even temperature can be controlled by direct movement of the right specific modules. One of the possible modular arrangements concepts is illustrated in Figure 41.

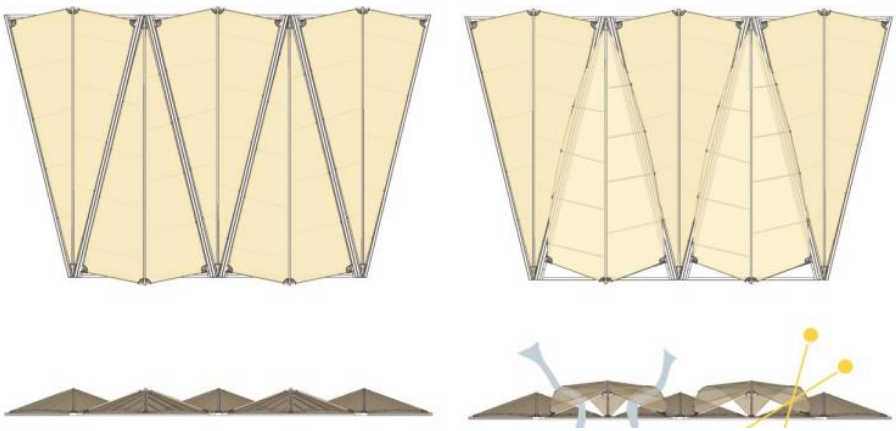

Figure 41 - Example of a 5 modules configuration. (Costa 2017)

From a structural engineering point of view, certain failure modes are of major importance, thus pointing these failure modes is essential for the development of this project. Naming possible types of failure:

- Profiles and connections
  - Failure by surpassing the mechanical resistances (axial, shear, flexural, torsion) of the material;
  - Localized failure of the specific rigid and hinged connections between the profiles;
  - Localized failure of the connection between the membrane and the profiles;
  - Support connection failure;
  - Fatigue.
- Membrane
  - Failure by surpassing the mechanical resistances (axial and shear) of the membrane;
  - Plasticisation;
  - Wrinkling of the membrane;
  - Failure by puncture of the membrane.
- Local
  - Local buckling in the profiles, due to high localized tensions.
- Global
  - Instability failure;
  - ULS failure;
  - SLS failure.

Besides the possible failures of the materials and the connections by surpassing their mechanical resistances simply by inducing bending in the structure, since this bending is recursive, fatigue and connection problems may also occur. The mechanical behaviour of the membrane is also a very important aspect, since membrane structures are only able to carry tension forces, they will wrinkle when subject to compression forces, which may cause not only aesthetic problems but also change the load path, which may lead to additional unexpected problems. According to Lienhard (2014), using the elastic behaviour of a material to shape a curved geometry will always raise the question of deformation and stability under external loads. Controlling this by increasing elastic stiffness is not an option if the elements are to be bent into a significantly curved geometry with sufficient load bearing reserves (Lienhard 2014). Therefore, the membrane needs to play a key role stabilizing the whole structure. An analysis of this case study is presented in chapter 4.

3. STRUCTURAL ASPECTS AND SOFTWARE VALIDATION

3.1. Introduction

As explained in section 1.1, different typologies of structures exist. During this chapter, the structural aspects behind bending-active and form-active (membrane structures) and bending-active structures are exposed. The existence of large deformations in these structures, subjects them to a special structural analysis, considering the nonlinearities inherent to the system. Therefore, special considerations when calculating these types of structures must be taken. The software utilized for this purpose must be carefully chosen in order to do a proper calculation considering all the above enunciated aspects.

Then, the objectives of this chapter are, besides exposing the structural aspects about these types of structures, to define and provide solutions in order to surpass the structural difficulties adjacent inherent to the use of this structures. As well, the validation of these proposed solutions is exposed during this chapter, by means of analysing and comparing the results obtained through these techniques with other experimental or documented case studies. This being, the chapter is subdivided in two subchapters, namely the structural aspects and the software choice and validations.

3.2. Structural aspects

In the present subchapter several structural aspects concerning bending-active and form-active structures are presented. Considering that both types of structures are subjected to large-deformations inducing a geometric nonlinear behaviour in the structure. Considering membrane structures, besides the geometric nonlinear behaviour also material nonlinearities exist. The stiffness matrix and the aspects regarding the changes to the stiffness matrix during large deformations are presented. Additionally, the form finding strategies concerning both membrane and bending-active structures are exposed.

3.2.1. Nonlinearity

A system of equations is considered nonlinear when system equations cannot be written as a linear combination of system variables (Lienhard 2014). In Figure 42 it is graphically shown the difference between linear and nonlinear behaviour. Generally, rigid-type structures follow a linear equilibrium path, since no large deformations occur, the proportion between the displacements is linear in accordance to

the force applied. On the contrary, in structures that follow a nonlinear equilibrium path, like bending-active or membrane structures, due to the inherent large deformations, this relation is not linear.

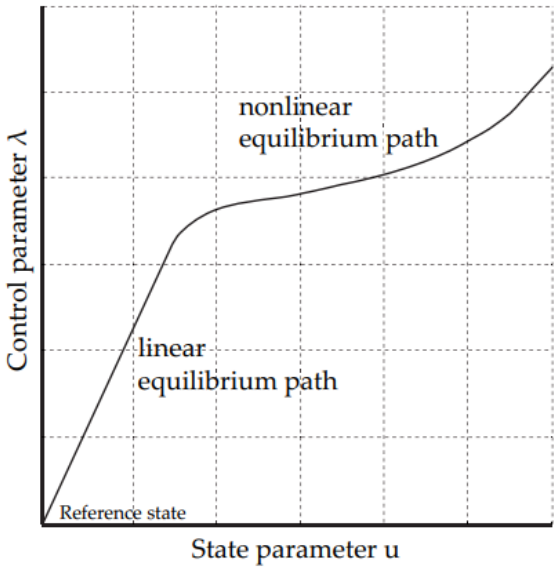

Figure 42 - General load deflection diagram. (Lienhard 2014)

Therefore, it is crucial to denote that distinct types of nonlinear behaviour may appear in a certain system. More particularly, and according to Lienhard (2014), in the analysis of structural systems, several aspects of nonlinearity can be differentiated:

- Nonlinear boundary conditions: change of supporting condition under deformation (may be considered in bending-active structures, where large deflections lead to additional supporting points and contact between initially separate elements);
- Nonlinear material behaviour: plastic deformation (not considered in bending-active structures);
- Geometric nonlinearity: nonlinear relationship of external forces and deflection (must be considered in all bending active strictures).

It is important to understand that for a textile hybrid system, since large deformations are present in both the form-active and bending-active structure, all the problems are of nonlinear nature. In addition, the fabric of the membrane has a nonlinear material behaviour, adding more complexity to this problem. However, the form finding approach to form-active and bending-active structures is of different nature. Next, the above-mentioned nonlinearities are explained in more detail. However, since for the purpose of this work nonlinear boundary conditions are not considered, this topic will not be addressed.

Structural aspects and software validation

As above-mentioned, in textile hybrid structures, nonlinear material behaviour is present due to the membrane material properties. According to Seidel (2009), because coated fabrics are plastic composites constructed for a purpose, their mechanical behaviour cannot easily be compared with the mechanical behaviour of traditional materials. Fabric threads and coating have differing stiffness as individual elements and are subject to differing stresses causing differing deformations. Altogether, they form a statically indeterminate system (Seidel 2009). Thus, membrane structures, by being composed by this kind of composite material, present a nonlinear material behaviour. The deformation behaviour of a synthetic fabric can basically be described as non-linear, because it cannot be described using Hooke's law of elasticity (Seidel 2009). Consequently, there is not a linear relation between the load applied to the fabric and the respective strains.

In contrast to geometric linear theory, geometric nonlinear theory considers the static equilibrium on the deformed system (Lienhard 2014). Both form-active structures as well as bending-active structures are susceptible to geometric nonlinear behaviour. This occurs due to the existence of large deformations in the system. These large deformations imply an update of the system stiffness matrix, making it variable with the geometric deformations. Thus, since the stiffness matrix is not considered constant like in linear systems, the relation between the displacement and the load applied is also not constant. A detailed explanation on the geometric nonlinear behaviour is given by Lewis (2003). Here, a few important mentions are given about this behaviour.

The sample is based on a two-bar system, shown in Figure 43, hinged on the sides and at the centre. The bars are elastic and have a length L_m. The elongation of each bar is defined as e_m, and the current length of the bar is then $L_m + e_m$. The system is loaded at the centre joint with a force P.

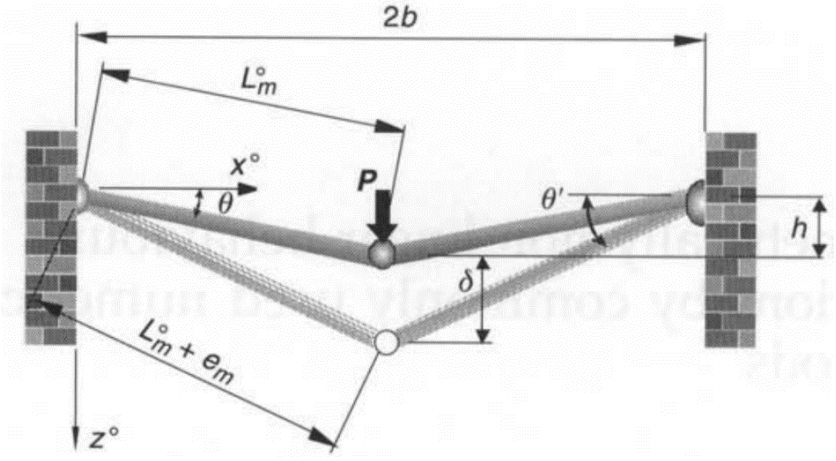

Figure 43 - Two-element structure. Vertical load. (Lewis 2003)

For this system, considering the large displacements, and after the deductions explained by Lewis (2003), the force P is given by equation (2):

$$P = 2\mathrm{K}\left(\delta + \mathrm{h} - \frac{L_m(\delta + h)}{\sqrt{(\delta + \mathrm{h})^2 + b^2}}\right) \quad (2)$$

From equation (2) it becomes clear that only for small displacements the relation of P and δ is of linear nature. When large displacements are present in the system, the second order part of the problem cannot be ignored. This shows that the relation of load P and displacement δ is of nonlinear nature. Thus, to solve a geometric nonlinear system, some solutions to this nonlinear problem must be found. By further manipulation of equation (2), one gets equation (3). For small deformations, the value of $h^2/(L_m^o)^2$ is a constant (see Figure 43), thus the relation between the displacement (δ) and the force P is linear.

$$P = \frac{2Kh^2}{(L_m)^2}\delta \quad (3)$$

Therefore, for a nonlinear system behaviour, equilibrium is only fulfilled in the deformed configuration where the stiffness matrix is no longer constant and updated based on the actual deflections (Lienhard 2014). Thus, an n times larger force vector results in an m times larger deflection the value of n is different and disproportionate to the value of m.

Regarding the solutions, there are many ways to solve this type of problem, and a couple of distinct approaches. From this diverse field of approaches, for this work, two of them stand out in the application to membrane structures and to bending-active structures. The first is the Dynamic Relaxation Method (DRM), which uses dynamic equations to solve a static problem. Then, there is the Force Density Method (FDM), which uses the force densities to surpass the nonlinear problem. Both methods are explained in sections 3.2.3.1 and 3.2.3.2, respectively.

3.2.2. System stiffness

According to Lienhard (2014), in geometric nonlinear analysis, the stiffness matrix is generally referred to as Tangent Stiffness Matrix, defined by K_t, which can be split into the Elastic Stiffness Matrix, defined by K_e, the Initial Displacement Stiffness Matrix, defined by K_u, and the Geometric Stiffness Matrix,

defined by K_g, which is computed based on the stress state of the previous equilibrium iteration. Therefore, for a geometric nonlinear problem, the tangent stiffness matrix is decomposed in three distinct child stiffness matrices, depending on distinct aspects of the system. In equation (8) it is shown that the tangent stiffness matrix multiplied by the displacement vector equals the force vector for a geometric nonlinear system. Also, equation (9) shows in mathematical language the above explained principle, discretizing the tangent stiffness matrix.

$$\underline{\underline{K_t}} \times \underline{u} = \underline{F} \tag{4}$$

$$\underline{\underline{K_t}} = \underline{\underline{K_e}} + \underline{\underline{K_u}} + \underline{\underline{K_g}} \tag{5}$$

Figure 44 shows the evolution of the three discretized stiffness components for the buckling problem of a three-hinged triangular frame. In general, a tensile normal force causes an increase of stiffness in a building structure (Lienhard 2014). The geometric stiffness directly depends on the actions applied in the system thus, if the system is in tension, a gain of geometric stiffness occurs. On the other hand, if there is compression in the system, a decrease of geometric stiffness occurs. The imposed stresses which are existent in the deformed state of the structure lead to the formulation of geometric stiffness, also known as initial stress-stiffness (Lienhard 2014). Thus, the effect of normal tension forces in the structure leads to an increment of the geometric stiffness and, consequently, the tangent stiffness matrix, this effect is known as stress-stiffening effect. As this stiffening effect is only visible for systems with low elastic stiffness, it is usually only considered for slender structures with small bending stiffness compared to axial stiffness, such as cables, thin beams and shells (Lienhard 2014).

The introduction of tension in textile hybrids is made through the effect of applying prestress to the membrane. Therefore, the interaction between membrane structures and bending-active elements generally leads to the existence of the stress-stiffening effect, which in most of the cases increases the geometric stiffness of the structure. The geometric nonlinearities that are inherent to bending-active structures may lead to stress stiffening effects that work in favour of the structural performance (Lienhard 2014).

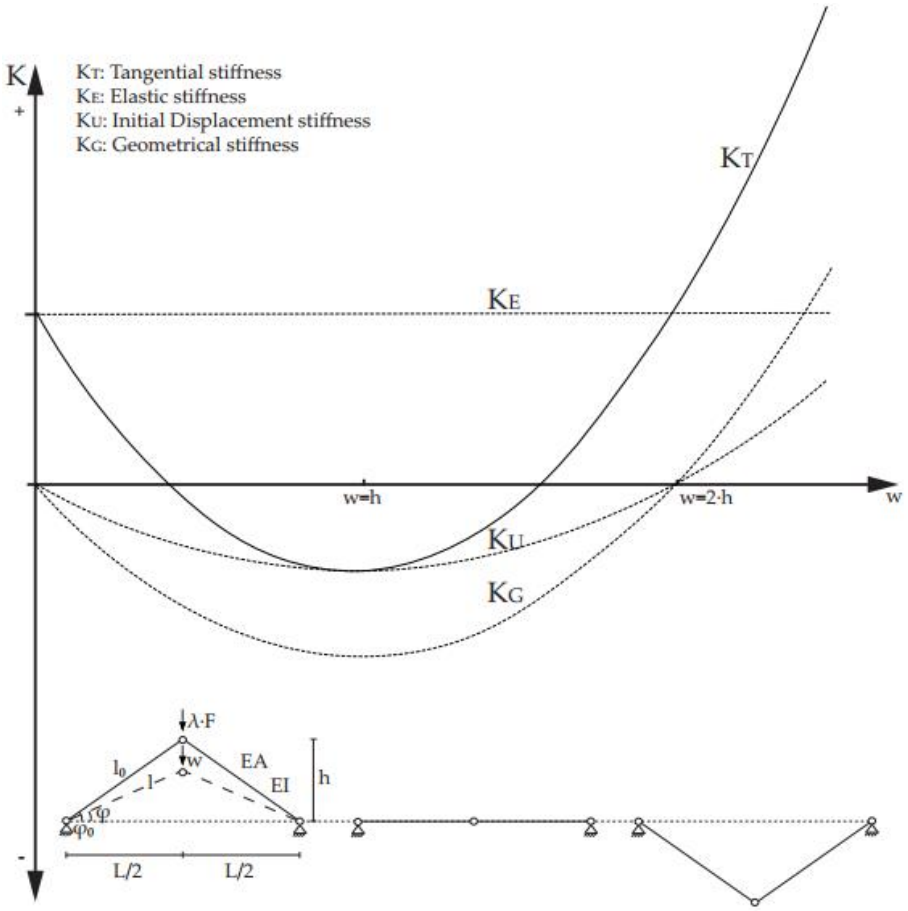

Figure 44 - Development of the three stiffness components for the snap-through buckling problem of a three-hinged triangular frame. (Lienhard 2014)

3.2.3. Form finding methodologies

On the word of Lewis (2003), the term form finding, used in relation to computational modelling, can mean one of the following:

- The finding an optimal shape of a tension membrane, like a stable minimal surface.
- Finding a shape of a tension membrane that is in static equilibrium, but does not necessarily have constant surface stress;
- Finding a shape, which approximates the state of full static equilibrium (common in some design methodologies combining form finding and patterning).

Table 4 shows a comparison between the type of inputs and outputs in the form finding process of both bending-active structures and form-active structures. Regarding the geometric aspects, in both process the boundary conditions are inputs. This geometric aspect is totally defined by the user, and this is one

of the main aspects in defining the output surface or element curvature, which is an output in both form finding processes. However, the length of the bending-active element is pre-defined as an input, since the length of a rod for example cannot change during the form finding. On the opposite, for form-active structures, the surface dimension totally depends on the form finding process. For example, the surface length of a membrane totally depends on the prestress applied in the form finding process. Also, the sectional dimensions are only an input in the bending-active elements, since the form finding process of form-active structures does not consider this aspect.

Concerning the material aspects, while the material stiffness is an input in the bending-active structure, and the form finding process possible depends on this, in the form-active structure the material stiffness is not considered and is often reduced to almost zero. Then again, the stress is an input in the form-active structure, in this specific case the membrane prestress is an input, whilst the stress of the bending-active structure or element depends on the amount of bending applied.

Table 4 - Comparison between the form finding of bending-active and form-active structures. Adapted from Lienhard (2014).

		Bending-active	**Form-active**
GEOMETRIC	Boundary points and edges	INPUT	INPUT
	Length and surface dimension	INPUT	OUTPUT
	Sectional dimensions	INPUT	-
	Surface/element curvature	OUTPUT	OUTPUT
MECHANIC	Material Stiffness	INPUT	-
	Stress	OUTPUT	INPUT

It is possible to affirm that the process of shaping elastic elements through the means of bending can also be considered a process of form finding, with slightly variations. Since the process of form finding of bending-active elements involves more inputs than the form finding of form-active structures, and since the aspect of structural optimisation is not automatically included, Lienhard (2014) suggests that may be more precise to speak of a “form developing” process. Yet, Lienhard (2014) quickly states back, affirming that however, despite having more variables of physical boundary conditions, it is still a deterministic process, objectively based on mechanical behaviour, and shall therefore generally be referred to as “form finding”.

However, regarding the form finding of textile hybrid structures, additional attention is required. According to Brancart, De Laet et al. (2016), the large interdependency of the form and material behaviour of bending-active structures, contrary to conventional form-active structures, requires a specific modelling approach. Thus, the form finding of membrane structures with bending-active support systems necessitates a simultaneous form finding of the form- and bending-active elements (Lienhard, Ahlquist et al. 2013):

1. The process can be separated into first the form finding of an elastically bent beam structure and second form finding of the membrane attached to the beams. Here the second form finding step serves to generate an intricate equilibrium system which is based on further deformations in the beam structure.
2. Some scenarios also allow the simultaneous form finding of the bending-active beam elements and pre-stressed membrane elements. For numerical form finding the bending of beam elements requires out of plane forces on the beam; this may be achieved by eccentricities and/or three-dimensional input of the membrane-mesh.

As above-mentioned, solutions to the nonlinear problem must be discussed. In the last decades several methods of form finding have been developed, being the first of these methods typically applied to discrete cable-net structures and then extended to surface elements for membrane structures. According to Veenendaal and Block (2012), it is possible to categorize these in three main families:

- Stiffness matrix methods – These methods are based on using the standard elastic and geometric stiffness matrices. These methods are among the oldest form finding methods, and are adapted from structural analysis;
- Geometric stiffness methods – These methods are material independent, with only a geometric stiffness. In several cases, starting with the force density method, the ratio of force to length is a central unit in the mathematics;
- Dynamic equilibrium methods – These methods solve the problem of dynamic equilibrium to arrive at a steady-state solution, equivalent to the static solution of static equilibrium.

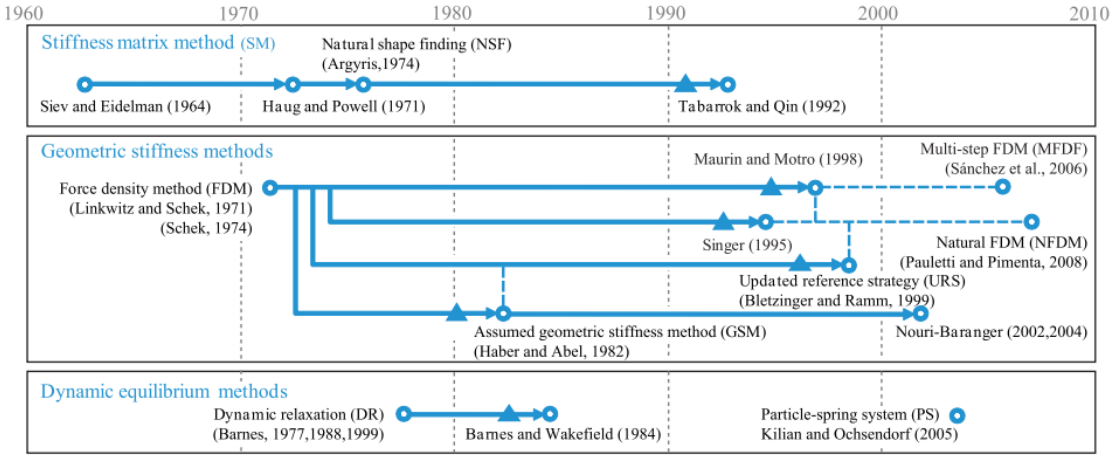

Figure 45 - Development and categorization of form finding methods with key references. Arrows denote offspring, dotted lines denote independent but related methods and triangles a first formulation using surface elements.(Veenendaal and Block 2012)

For this work, only a two of these methods are explained. Firstly, representing the dynamic equilibrium methods there is the DRM (Dynamic Relaxation Method). Then, representing the geometric stiffness methods, the FDM (Force Density Method). Both methods are explained bellow. Finally, and since according to Lienhard (2014), a typical numerical method for simulating large deformations and nonlinear behaviour in civil engineering is the Finite Element Method (FEM), a FEM approach is suggested.

3.2.3.1. Dynamic Relaxation Method

The DRM relies on a discretized continuum in which the mass of the structure is assumed to be concentrated (lumped) at given points (nodes) on the surface (Lewis 2003). The method is based on the principle that these nodal masses will oscillate, while being damped due to a damping factor, until the equilibrium position is reached in that node. The system of lumped masses oscillates about the equilibrium position under the influence of out of balance forces. With time, it comes to rest under the influence of damping (Lewis 2003). Contrary to other methods, the method of dynamic relaxation does not rely on matrix manipulations for the solution of the system of non-linear equilibrium equations (Lewis 2003). The numerical model is built on the assumption that the state of static equilibrium is a consequence of a pseudo-dynamic state (Lewis 2003).

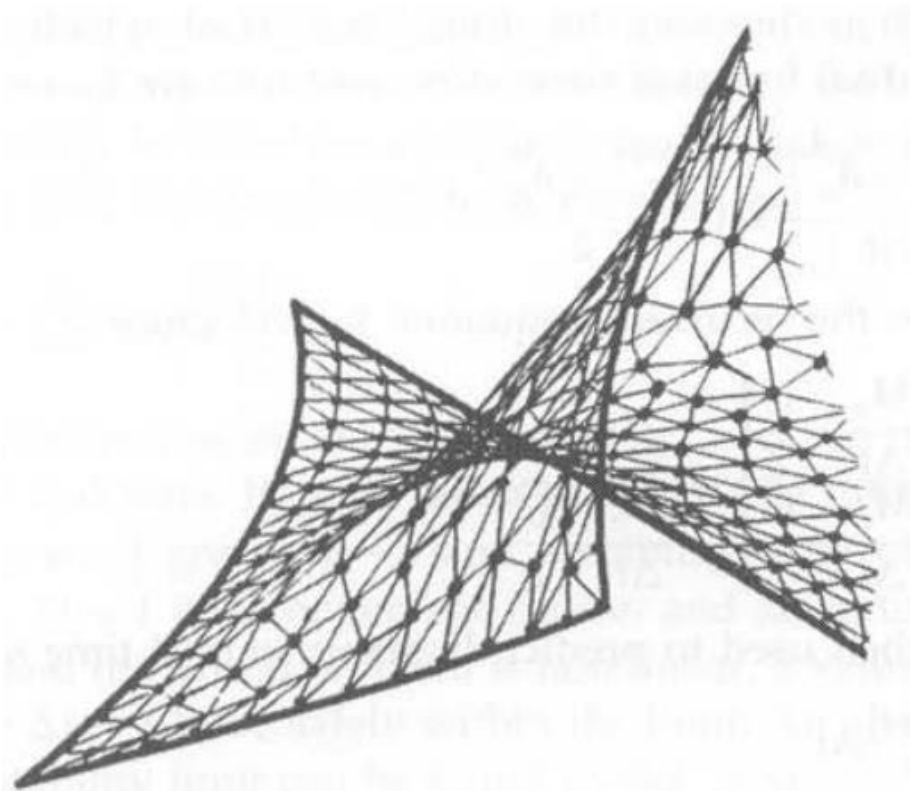

Figure 46 - Discretized continuum. (Lewis 2003)

There are many variations of the DRM, being generally the damping process the changing aspect between the methods. There are two main different methods of the DRM, known as the DRM with viscous damping and the DRM with kinetic damping. Lewis (2003) says that in its original form, the method makes use of viscous damping.

3.2.3.1.1. Dynamic relaxation method with viscous damping

The DRM with viscous damping is based on the equation of motion. It states that the node will move around the equilibrium position, being that movement caused by the difference between the external and internal forces, the residual forces. An iteration process begins, with the objective to reduce these residual forces to zero. While these residual forces are not zero, or very close to zero, the iteration process continues moving the nodes of the structure until the position of equilibrium is found.

According to Van Asselt (2007), the equation of motion is given by equation (6):

$$P_{ji} = \left[\sum K \cdot \delta\right]_{ji} + M_{ji} \cdot \ddot{\delta}_{ji} + C_{ji} \cdot \dot{\delta}_{ji} \qquad (6)$$

In equation (10), the j stands for each node number and i is each direction in a discretized system. P is the external applied load and the component $[\sum K \cdot \delta]_{ji}$ is the internal load, being K the stiffness matrix and δ is the nodal displacement vector. If this external load differs from the internal load a residual force appears. To reach the static equilibrium, this residual force must become zero. In the beginning of the process there is not an equilibrium position, thus the node oscillates until it reaches this equilibrium position. In practical terms, this means that a nodal acceleration ($\ddot{\delta}$) and a nodal velocity ($\dot{\delta}$) are introduced to the system, which on their behalf cause the residual forces. The displacement (δ) for which the residual forces becames zero must be found in order to find equilibrium. This is done with an iterative process. When rewriting the equation of residual forces in terms of velocity, one gets equation (7):

$$\dot{\delta}_{ji}^{n+\frac{1}{2}} = \left\{ \dot{\delta}_{ji}^{n-\frac{1}{2}} \frac{\frac{M_{ji}}{\Delta t} - \frac{C}{2}}{\frac{M_{ji}}{\Delta t} + \frac{C}{2}} \right\} + \frac{R_{ji}^{n}}{\frac{M_{ji}}{\Delta t} + \frac{C}{2}} \tag{7}$$

Next, equation (8) is used to predict the displacements at time $n+1$:

$$\dot{\delta}_{ji}^{n+\frac{1}{2}} = \delta_{ji}^{n} + \dot{\delta}_{ji}^{n+\frac{1}{2}} \Delta t \tag{8}$$

The process becomes iterative because the use of these last equations is repeated until the residual forces reach almost zero. Residual forces are calculated by the form of equation (9):

$$R_{ji}^{n} = P_{ji} - \left[\sum K \cdot \delta \right]_{ji}^{n-1} = P_{ji} - [\tilde{P}_{ji}]^{n-1} \tag{9}$$

As a matter of using the above explained method, it is necessary to assume the values of the masses, damping coefficients and the time increment. Figure 47 shows the difference of the DRM with and without damping introduced in the system. Since the main objective of this method is not to follow the exact path of the structure to equilibrium, but to find the final equilibrium position, it is not of crucial importance the path of the dynamic process but only the final position, therefore these assumptions can be assumed more and less freely, always considering the values of the masses (M) and the damping value (C) should be such that ensure the iterations do converge to static equilibrium.

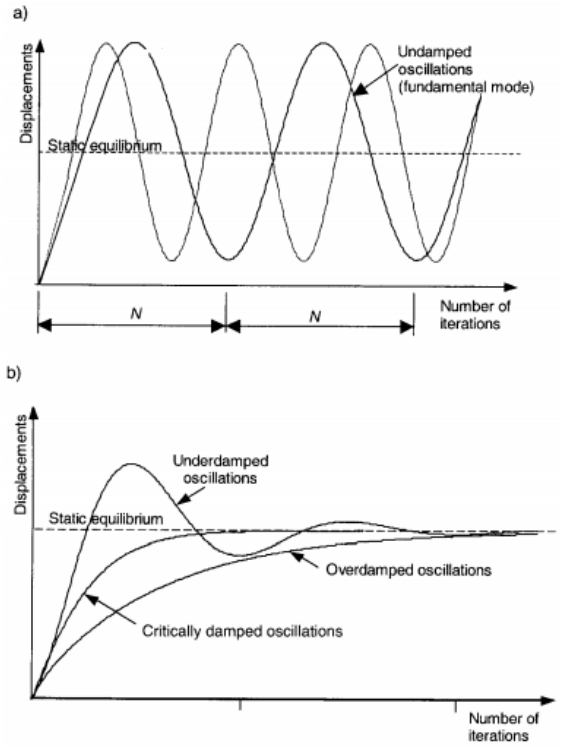

Figure 47 - Oscillations of displacements in dynamic relaxation algorithm (viscous damping). a) undamped, b) damped. (Lewis 2003)

3.2.3.1.2. Dynamic relaxation method with kinetic damping

The DRM can also be performed with kinetic damping. The process is based on the previous explained one, but not considering the viscous damping coefficient. During the iterations, the velocities and the displacements get smaller, as the residual forces became smaller over a period of time (Lewis 2003). Hence, the peaks in kinetic energy gradually becomes less pronounced and eventually the whole system settles down to static equilibrium, at which the residual forces are (almost) zero (Lewis 2003). Figure 48 shows the displacements in relation to the kinetic energy of a given system where DRM with kinetic damping is applied.

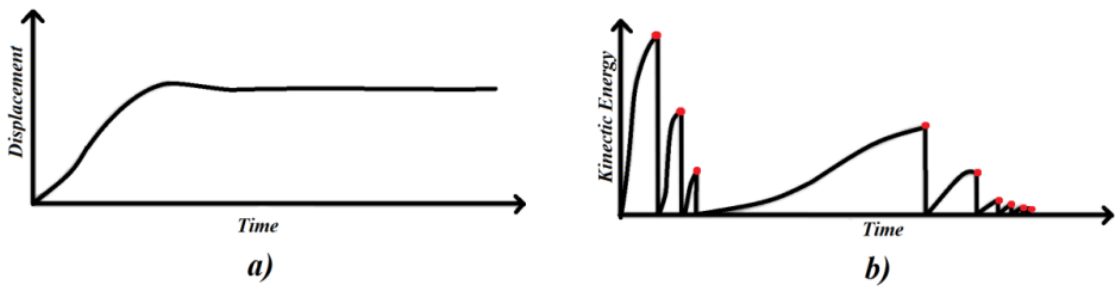

Figure 48 - Expected graph for: a) displacement, b) kinetic energy. (Gomes 2014)

On the words of Lewis (2003), the method of damping described above relies on the observation that, in simple harmonic motion, maximum kinetic energy is achieved in a configuration that corresponds to minimum potential energy. One example of this principle is the motion of a pendulum, where a position of maximum kinetic energy corresponds to a position of minimum potential energy. Thus, this principle can be applied to a more complex structure, modelled as a system of nodal masses. Under the influence of loading, the nodes oscillate about their positions of equilibrium (Lewis 2003). By stopping the movement for the position where the kinetic energy peaks, the stable equilibrium position of the entire system can be approximated.

Implementing the numerical stability criterion shown in equation (10), and by defining $\Delta t = 1$ for matters of simplicity, one gets the velocities and the displacements by equation (11) and (12), correspondingly:

$$\Delta t < \frac{2}{\sqrt{\mu_1}} \tag{10}$$

$$\dot{\delta}_{ji}^{n+\frac{1}{2}} = \left\{\dot{\delta}_{ji}^{n-\frac{1}{2}}\right\} + \frac{R_{ji}^{n}}{\frac{1}{2}K_{ji}} \tag{11}$$

$$\delta_{ji}^{n+1} = \delta_{ji}^{n} + \dot{\delta}_{ji}^{n+\frac{1}{2}} \cdot 1 \tag{12}$$

These equations generate the iterative loop of the DRM with kinetic damping. It can be deduced that the kinetic energy peak has occurred when the current value of the kinetic energy is smaller than in a previous iteration (Lewis 2003). At a kinetic energy peak, velocities are set to zero and the whole system is restarted from the current configuration (Lewis 2003). As it is shown by Figure 49, being the iterative process punctuated by discrete time intervals Δt, the precise location of the point at which a maximum value of kinetic energy has occurred is not known, but it can be estimated (Lewis 2003). It is important to do so, in order to correct the displacements, as these would have been calculated after a kinetic energy peak has occurred (Lewis 2003).

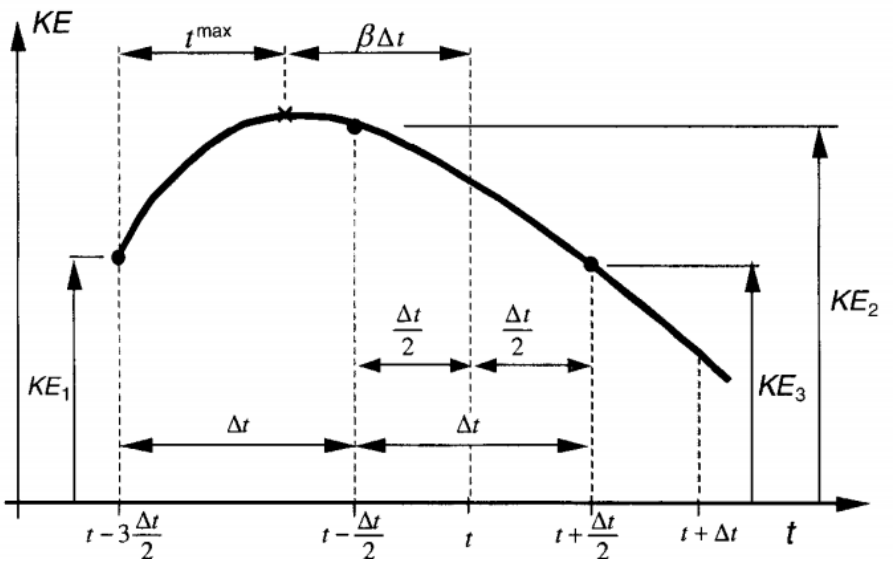

Figure 49 - Location of the point of maximum kinetic energy in dynamic relaxation algorithm. (Lewis 2003)

3.2.3.2. Force density method

According to Lewis (2003), the method of force density was developed in response to the need for computational modelling of structures for the Munich Olympic complex. Yet, the initial methods proposed by Siev (1963) had the form finding solutions dependent on a number of simplifying assumptions, such as a constant value for the horizontal component of the prestress. Thus, the resulting shapes were also restricted by these assumptions. The method originally purposed by Linkwitz and Schek (1972) is less restrictive than the previous method. It relies on an ingenious mathematical assumption that the ratio of tension force to length of each cable can be constant (Lewis 2003). This transforms a system of nonlinear equations to a set of linear equations that, in principle, could be solved directly (Lewis 2003). Lewis (2003) says that the form finding process modelled by the force density method does not equate with finding shapes of stable minimal surface membranes, it simply allows one to generate shapes of tension structures that are in static equilibrium. Yet, the method has the potential to be developed into a numerical tool for finding stable minimal surfaces (Lewis 2003).

The principles of the force density method are illustrated with the help of the following example based on the work of Lewis (2003). Figure 50 shows a simple structure that can be understood as a set of cables from a larger network. The equation of equilibrium of forces at node 5 can be obtained by resolving the tension forces T_m of the connecting members into the x^0, y^0 and z^0 global components (Lewis 2003).

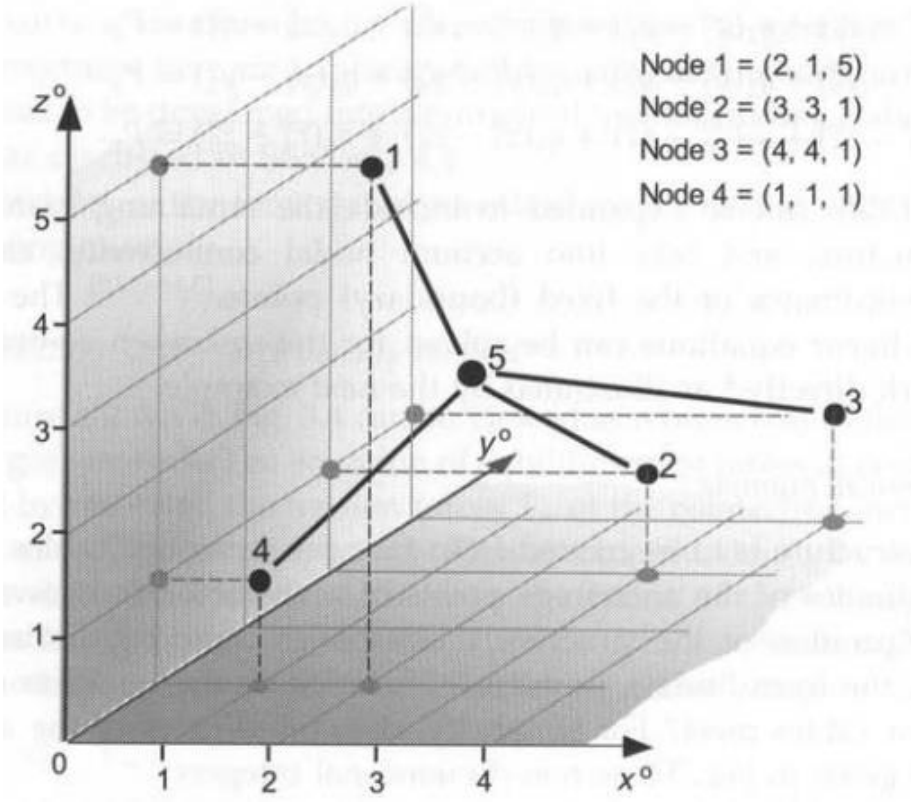

Figure 50 - A simple form of cable structure. (Lewis 2003)

This is accomplished by multiplying T_m by the direction cosines[1]. For the present example, the value of m takes the values $1, 2, 3$ and 4. Thus, the equilibrium forces at node 5 are given by equation (13), where $\{P_{x^0};\ P_{y^0};\ P_{z^0}\}$ are the values of the components of the external load vector acting on node 5. By introducing constant values of tension coefficients, also known as force densities (q_m), defined as the ratio of member force to member length, namely $q_m = T_m/L_m$ the system of equations becomes linear. The system of equations (13) can be expanded to include the remaining branches of a larger structure, and take into account nodal connectivity, as well as known coordinates of the boundary points (Lewis 2003).

$$P_{x^0} = q_1(x_1^0 - x_5^0) + q_2(x_2^0 - x_5^0) + q_3(x_3^0 - x_5^0) + q_4(x_4^0 - x_5^0) \qquad (13)$$

[1] **Direction Cosines:** For a given vector V defined by $ax + by + cz$, with the length $D = \sqrt{a^2 + b^2 + c^2}$, the direction cosines of the vector V are given by $\{\cos\alpha\,;\cos\beta\,;\cos\Upsilon\} = \{\frac{a}{D};\frac{b}{D};\frac{c}{D}\}$.

$$P_{y^0} = q_1(y_1^0 - y_5^0) + q_2(y_2^0 - y_5^0) + q_3(y_3^0 - y_5^0) + q_4(y_4^0 - y_5^0)$$

$$P_{z^0} = q_1(z_1^0 - z_5^0) + q_2(z_2^0 - z_5^0) + q_3(z_3^0 - z_5^0) + q_4(z_4^0 - z_5^0)$$

On the word of Gomes (2014), a generalized cycle of calculations for the FDM can be summarized as follows:

1. Define the boundary conditions.
2. Define the support conditions.
3. Define the fixed force density.
4. Input or calculate the loads.
5. Determine the equilibrium state.

Also, and according to the explanation of the FDM given above, the final shape can be influenced and adjusted by varying the value of the force density load, the boundary conditions and the support conditions (Gomes 2014).

3.3. Software choice and validations

It is the purpose of this subchapter to select a software that can handle the structural aspects referred above, thus able to handle the form finding and further calculation of membrane and bending-active structures. Also, validations of this software are demonstrated and conclusions are taken on the results obtained.

Firstly, form-active structures are validated by a simple hypar membrane case study. The results are then compared with the ones obtained by Henrysson (2012). Next, the results regarding the form finding of bending-active elements in Sofistik® is validated by means of two additional case studies. The second case study consists in a practical experiment, using a small spring and tracing the evolution of the elastica curve, and then comparing the obtained geometry with the geometry obtained through Sofistik®. The third case study involves a similar comparison of the elastica curve geometry, but the basis of comparison is the curve and length ratios of the elastica curve. For this third validation, the basis of comparison are the results obtained by Adriaenssens and Barnes (2001) in the same subject.

3.3.1. Computing with Sofistik®

It has become clear by now that form finding a form-active, a bending-active structure or both, it is a matter of solving a nonlinear problem. Solving this problems by means of analytical methods can be considered near to impossible. Thus, a specific software is needed to solve this type of problems. There is a variety of structural FEM software available today, but not many that can solve nonlinear problems, or simulate the bending process.

For the matter of the present work, since hybrid and kinetic principles were to be analysed as well as bending-active and form-active membrane structures, the following list of characteristics were required from the software:

1. Capable of solving geometric nonlinear problems;
2. Capable of considering material nonlinearity;
3. The software should have parametric properties or a custom programming platform;
4. Ability to use import the previous load to the next iteration;
5. Feasible geometric interface, like CAD;
6. Preferably, membrane or bending-active oriented, or both.

Along the process of choosing the software, a couple of options were considered. Rhinoceros 3D® Grasshopper was one of them due to the great geometric capabilities and the wide variety of custom plugins developed to it. However, no plugin could satisfy the complete set of required characteristics. Yet, according to the work of Melville, Brandt-Olsen et al. (2017), this is a viable option for hybrid structures, though the point 4 was not yet consolidated and it was preferable to explore other options. A membrane specific software, ixCube®, was also explored, it had been used during the work of Marques (2015), yet the lack capabilities to deal with bending-active elements were very limiting.

According to Lienhard (2014), the necessity for simulation of large elastic deformations in order to form-find bending-active structures poses no problem to modern nonlinear finite element analysis. Advanced structural design software, like Sofistik® and Ansys, indeed show great capabilities to deal with the form finding procedure. Also, Lienhard (2014) says that these Finite Element Modelling software offer the full consideration of stress stiffening in nonlinear analysis of truss, beam and shell elements. Additionally, using computational mechanics for the form finding of bending-active structures offers a direct integration of the form finding result into the subsequent structural analysis and computer-assisted design and fabrication processes (Lienhard 2014), which could also represent an important aspect for the further

development of this work. Therefore, both options were tested. Here, Sofistik® has shown all the required specifications defined above, since it already had a proper function to deal with the point 4 of the previous mentioned list of required characteristics. Also, a custom programming interface is available, TEDDY which is a powerful control centre as well as an editor, which fully supports and utilises the CADINP language (SOFiSTiK 2011). For these reasons, Sofistik® was the software used during this work. Sofistik® is divided in modules that all interact in a common database called (CDB). A general view of the structure of this software can be seen in Figure 51.

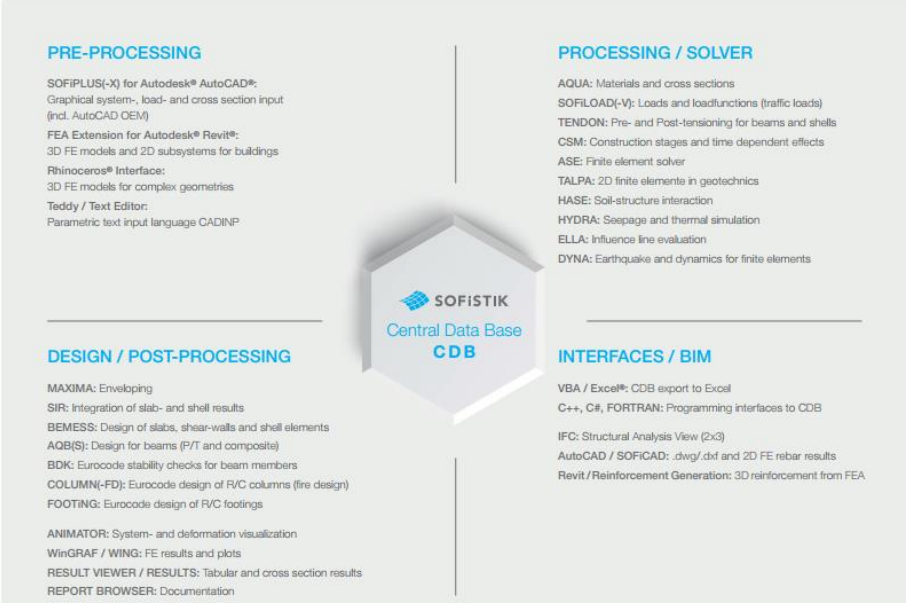

Figure 51 – Sofistik® program structure.(SOFiSTiK 2011)

For the purpose of validating the results obtained by means of calculation with this software, two sets of problems should initially be solved. These problems are fully discussed in section 3.3. Firstly, a membrane structure solving approach should be achieved. Then, a simple bending-active problem should also be considered for means of validation. Sofistik® has already implemented a method for solving membrane structures. According to the information in SOFiSTiK (2014), the membrane element implemented in ASE (the static solution engine) can be calculated considering large deformations using what it calls a 3rd order problem (TH3).

This 3rd nonlinear problem (TH3) differs from another nonlinear 2nd order theory (TH2). Figure 52 shows the main differences between TH2 and TH3 by applying each problem to a simple column, respectively. Solving this column using TH2, causes a stiffness reduction in the column due to the compression normal force (geometric stiffness) (SOFiSTiK 2014). This effect is explained in section 3.2.2 as the stress

stiffening effect. For TH2, this creates an additional deflection in the x direction, but not in the z direction, thus the beam can get longer than in the original shape (SOFiSTiK 2014). The bottom bending moment increases due to the displacement of the vertical load (SOFiSTiK 2014). This is also known as the P-delta effect. On the other hand, for the same column, a TH3 problem follows the physically correct path, thus equilibrium is iterated on the real deformed shape (SOFiSTiK 2014). This can be considered a complete geometric nonlinear analysis.

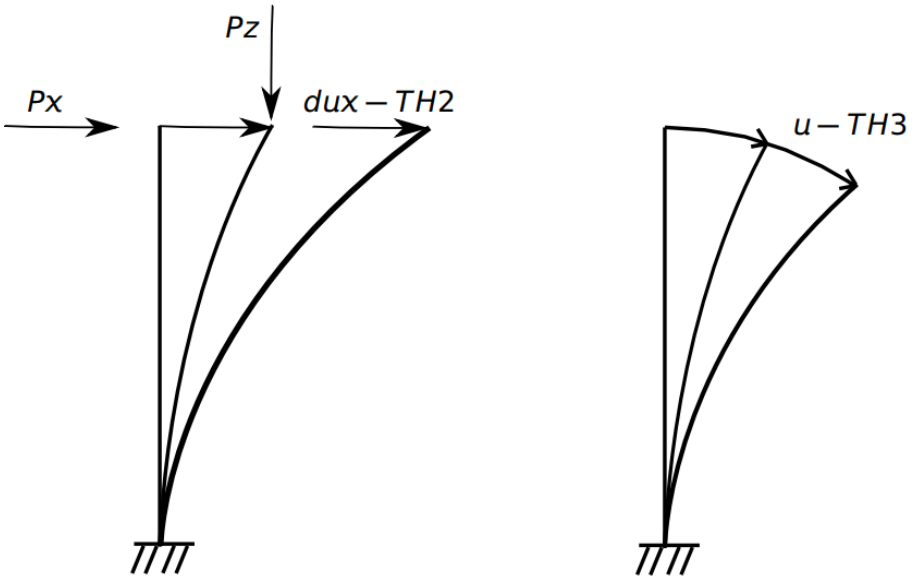

Figure 52 - Difference between 2nd (left) and 3rd (right) order nonlinear theories. (SOFiSTiK 2014)

As shown in Figure 53, for the TH2 problem there is no consideration for the residual normal force in the beam. In contrast, for the complete geometric nonlinear analysis with the TH3 the created normal force (N) carries a part of the load, thus reducing the vertical deformation (SOFiSTiK 2014). This happens because in TH3 the forces are always related to the deformed beam coordinate system (SOFiSTiK 2014). According to SOFiSTiK (2014), for a geometric nonlinear analysis a Line Search technique with an update of the stiffness matrix is used to solve the nonlinear problem.

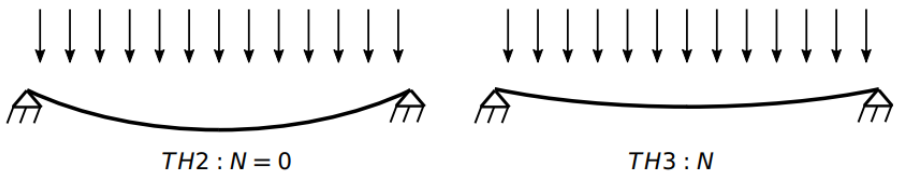

Figure 53 - Consideration of normal force, 2nd (left) vs 3rd (right) order theories. (SOFiSTiK 2014)

Regarding the material behaviour, bending active elements are simple treated with simple elastic linear behaviour. On the other hand, the membrane material needs a nonlinear module, in order to obtain reliable results, because of the reasons enunciated in section 2.2.2.4. In ASE a nonlinear yarn-parallel warp-fill behaviour is implemented (SOFiSTiK 2014). This behaviour is based on the nonlinear model proposed model by Galliot and Luchsinger (2009). The nonlinear behaviour is expressed as a stress-strain relation, where for a given warp stress (σ_w) and weft stress (σ_f), it is obtained a given value for the nonlinear strain (ϵ_w, ϵ_f), given by the equation (14):

$$\begin{bmatrix}\epsilon_w \\ \epsilon_f\end{bmatrix} = \begin{bmatrix}\frac{1}{E_w(\gamma_w)} & \frac{-\nu_{wf}}{E_w(\gamma_w)} \\ \frac{-\nu_{wf}}{E_w(\gamma_w)} & \frac{1}{E_f(\gamma_f)}\end{bmatrix} \cdot \begin{bmatrix}\Delta\sigma_w \\ \Delta\sigma_f\end{bmatrix} \tag{14}$$

Where the values of the normalized load ratios are given by equation (15):

$$\begin{Bmatrix}\gamma_w = \frac{\sigma_w}{\sqrt{\sigma_w^2+\sigma_f^2}} \\ \gamma_f = \frac{\sigma_f}{\sqrt{\sigma_w^2+\sigma_f^2}}\end{Bmatrix} \tag{15}$$

And the elastic moduli are given by equation (16):

$$\begin{Bmatrix}E_w(\gamma_w) = \Delta E_w \cdot \left(\gamma_w - \frac{1}{\sqrt{2}}\right) + E_w^{1:1} \\ E_f(\gamma_f) = \Delta E_f \cdot \left(\gamma_f - \frac{1}{\sqrt{2}}\right) + E_f^{1:1}\end{Bmatrix} \tag{16}$$

The routine used to solve membrane structural form finding is based on this TH3 problem and the raw algorithm inputted in TEDDY can be consulted inthe Appendix.

For the bending-active elements the solution is a bit more elaborated, however it is still based in the same TH3 problem. According to Lienhard, La Magna et al. (2014), the large deformations that beam elements undergo during the form finding of bending-active structures cannot be simulated in a single load step. Therefore, an iterative process must be implemented where the bending is slightly increased, but taking

into consideration the stresses implemented in the beam from the previous load case. Sofistik® has a function built into CADINP (the programming language of TEDDY) that can achieve this procedure, called the PLC (previous load case). Here, the deformations and strains of an already solved load case may be referred to by defining it as a primary load case for the calculation of a current load step (Lienhard, La Magna et al. 2014). Therefore, deformations and stresses from a prior load step may be linked to another load case, thus reducing the calculation time (Lienhard, La Magna et al. 2014).

As it was included in the scope of this work, two distinct custom routines were programmed in TEDDY in order to simulate the bending process. These routines are shown in Figure 54 and Figure 55. The two routines are very similar, the main difference being the use of linear or adaptive increments to the displacement that induces bending. The raw code for both approaches can be consulted in the Appendix. The basic procedure consists in looping a TH3 problem, where a displacement is induced taking into account the previous load case obtained through the use of the PLC function. The displacement is incremented for each step by a linear manner (Figure 54) or by an adaptive manner (Figure 55). The former effectively reduces the computation time, without compromising the feasibility of the results.

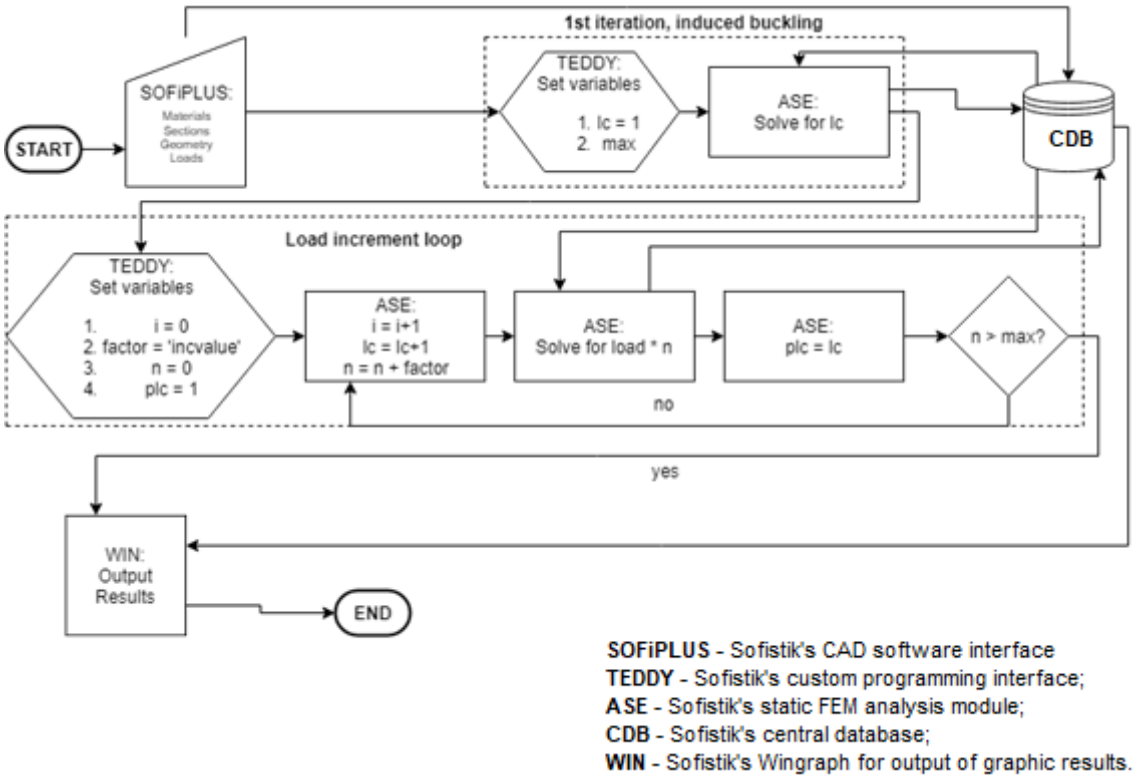

Figure 54 - General workflow of the solving process implemented in the Sofistik® using linear increments.

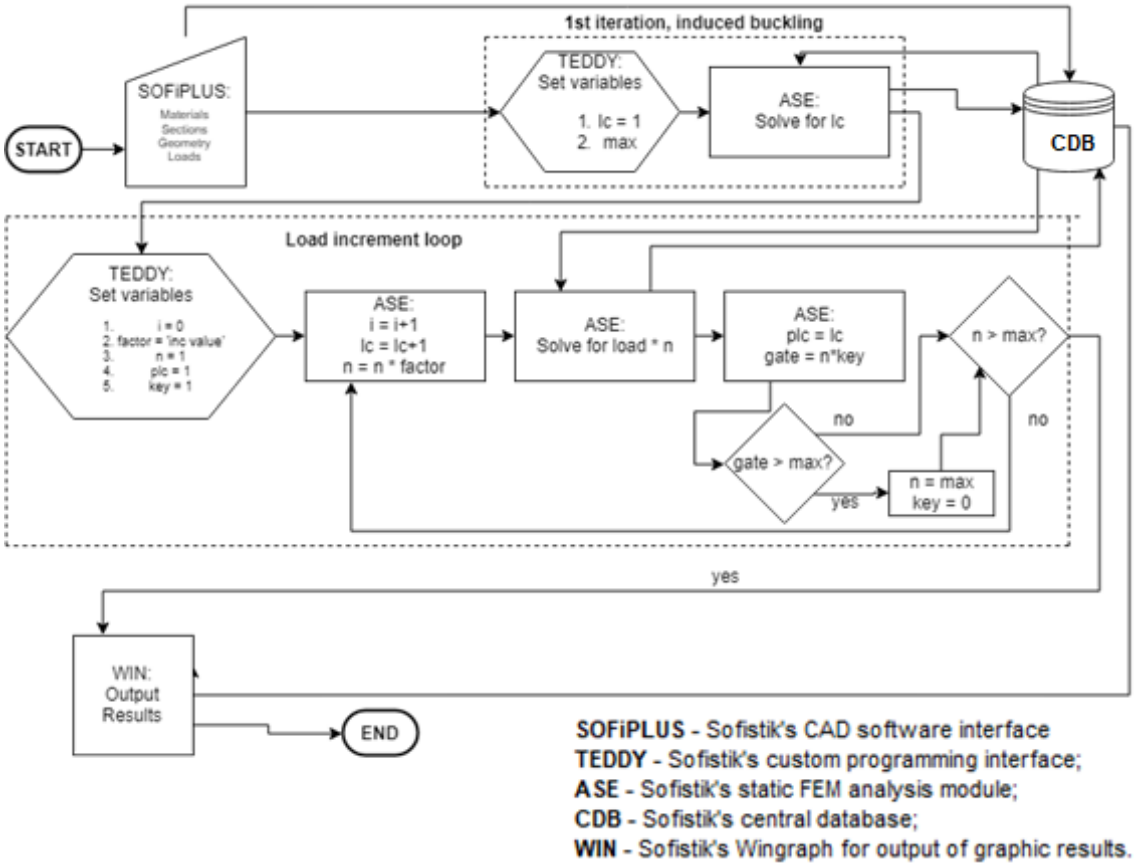

Figure 55 - General workflow of the solving process implemented in the Sofistik® using adaptive increments.

Complementarily, a distinct method was developed by Lienhard, La Magna et al. (2014), which uses the same principle above mentioned, but instead of displacements it applies increasing pretension to an elastic cable. Figure 56 shows a side a side view of the different methods applied to a planar element. This method basically consists applying and incrementing the prestress of cable which the stiffness has been reduced to almost zero. Thus, the cable will contract and, when fixed to the specific nodes, move the whole structure along. This method was also used in the case study presented in chapter 4.

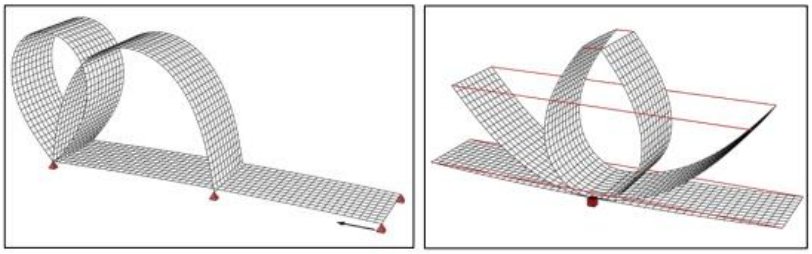

Figure 56 - Example of a bending-active component form-found via support displacement (left) and elastic cable approach (right). (Lienhard, La Magna et al. 2014)

3.3.2. Membrane validation

As a matter of validating the results of the membrane form finding done in Sofistik®, the analysis done by Henrysson (2012) of a simple hypar structural form finding was chosen as a case study. Figure 57 shows the geometry of the case study structure, including its dimensions.

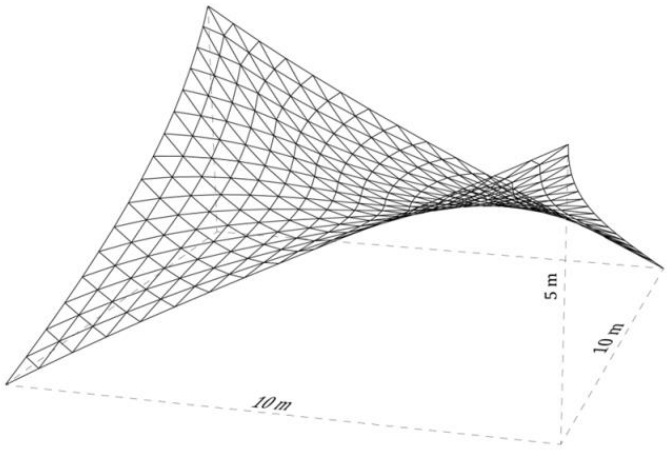

Figure 57 - Geometry of the analysed hypar, showing the form found shape. (Henrysson 2012)

Henrysson (2012) starts with the geometry shown in the left side of Figure 58, and form finds it, obtaining the form found shape shown in Figure 57. Then a simple loading is applied in the form found structure. In his work, he uses a triangular mesh to model the hypar. Additionally, the mechanical system is represented by a particle system with a set of discrete masses. Henrysson (2012) says that this method has shown to be deficient in the presence of large strains and in the presence of shear stress. Therefore, some differences between the results may appear, since Sofistik® uses a more complex and complete procedure to calculate the membrane. Figure 58 shows the initial geometry and the final shape with the applied load in the form found shape in Henrysson (2012) work.

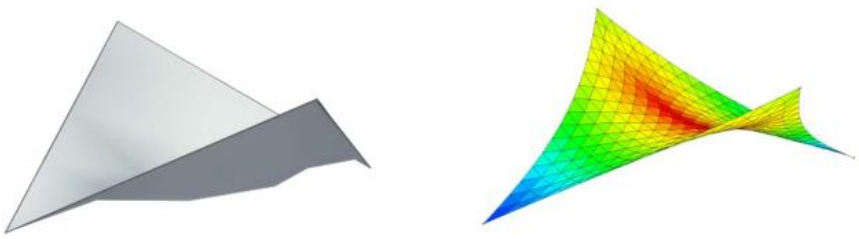

Figure 58 – Starting geometry (left), and the structure analysed under load applied (right). (colours indicate the wrap stress). Adapted from Henrysson (2012).

Although according to Veenendaal and Block (2012), the problem of form finding membranes is in principle a geometric one, and thus material independent, since the current case study also uses an area load, in order to later be able to compare those stresses, the membrane and cable properties were carefully loaded into Sofistik®.

However, the value of the Young modulus of steel for the cables was not given in the work of Henrysson (2012). Table 5 shows the results input values for the material properties in Sofistik®, both for the cables and for the membrane. These values match the ones used by Henrysson (2012), with the exception of the Young modulus of steel, as above mentioned. Thus, any fluctuation in the final stress results may be partially due to an assumption of a higher or lower steel Young modulus that can affect the overall form found geometry, as well as the stiffness matrix of the entire system.

Table 5 - Material properties input in Sofistik® for the hypar model.

Material	**Membrane**		**Cables**
	Weft	Warp	
E	670 N/mm^2	400 N/mm^2	195000 N/mm^2
Poisson Ratio	0	0	0.3
Weight	10.3 kN/m^3		81.7 kN/m^3
Thickness/Diameter	1 mm		10.1 mm
FEM element	Quadrangular mesh 70mm element length		Cable element

The first method for validation of the Sofistik® approach to the membrane calculation is the visual aspect of the form finding geometry of the hypar. The form finding is calculated by applying a prestress of $2kN/m^2$ in both warp and weft directions. Figure 59 shows a comparison between the geometries of both the Henrysson (2012) approach and the Sofistik® approach. The form found geometry by Henrysson (2012) has an identical appearance to the one obtained through Sofistik®, as it is shown by Figure 59. Therefore, it can be concluded that the results of the form finding procedure implemented in Sofistik® seem to be rather accurate.

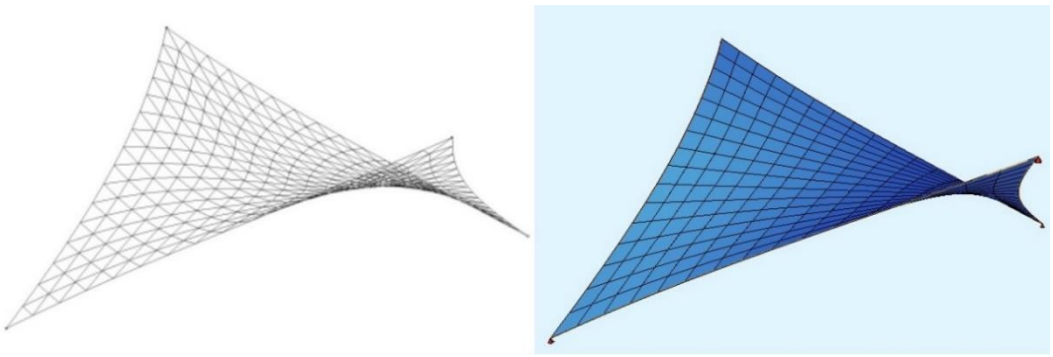

Figure 59 - Hypar form finding geometry. Henrysson (2012) approach (left) versus the Sofistik® approach (right).

Next, the results of the stresses can be compared for each solution. In order to obtain the stresses, a $1kN/m^2$ area load is applied to the membrane in the local z direction, thus pointing down locally on each node. Figure 60 shows a graphical comparison on the results obtained by Henrysson (2012) and the results obtained by Sofistik®. It is visible that slight differences can be noticed. The approach by Henrysson (2012) seems to result in smaller shear stresses. This confirms the above explained considerations made by Henrysson (2012).

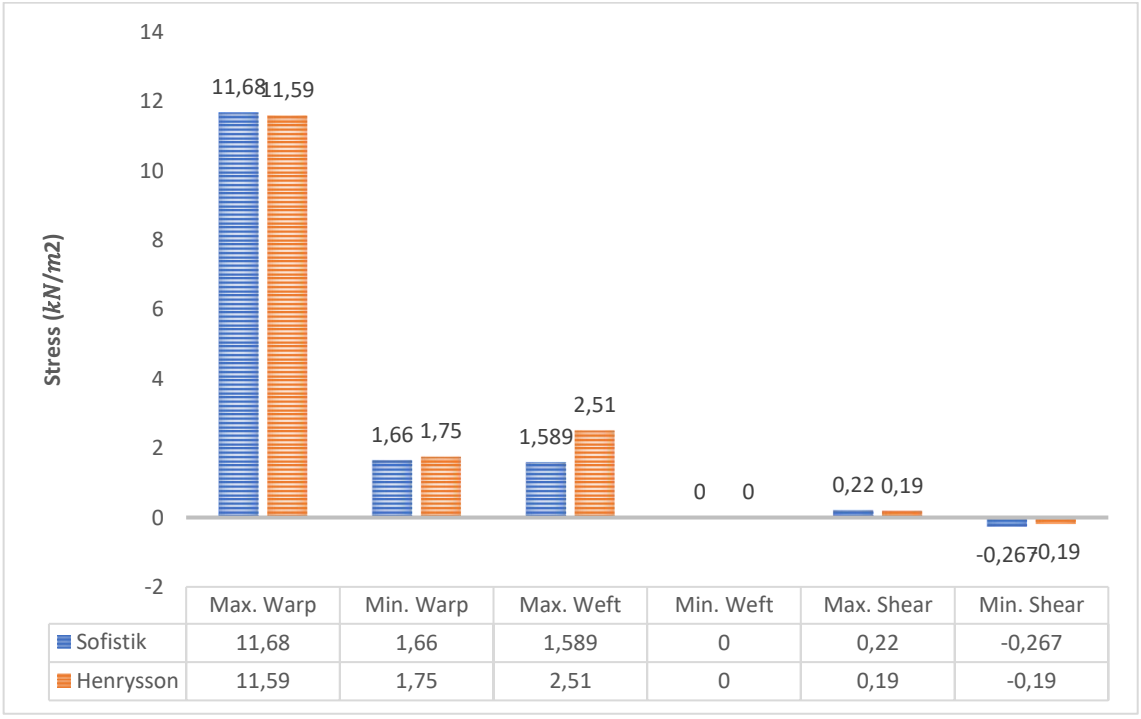

	Max. Warp	Min. Warp	Max. Weft	Min. Weft	Max. Shear	Min. Shear
Sofistik	11,68	1,66	1,589	0	0,22	-0,267
Henrysson	11,59	1,75	2,51	0	0,19	-0,19

Figure 60 - Graphical comparison of the stress results.

However, the small differences obtained can be considered acceptable, since the methods of calculations used in Sofistik are not the same as the ones employed by Henrysson (2012). The method adopted by Henrysson (2012), and quoting, "considers significant simplifications that enable a quick calculation and generates accurate values as long as the shape is reasonable". Also, the methods that Henrysson (2012) used for consideration of the orthotopic behaviour differ from those that Sofistik® uses. These aspects, in conjunction with the fact that the Young modulus assumed may not be the one that Henrysson (2012) actually used can justify these small discrepancies. In addition, it is visible when analysing Figure 61, Figure 62 and Figure 63 that the stress patterns are rather similar. In all these images the red values represent the highest values shown in Figure 60, while the blue values represent the lowest values. Therefore, since the values from both approaches are similar, the scale can be considered the same for both pictures, thus showing that Sofistik is indeed able to form find and calculate loads in membrane structures.

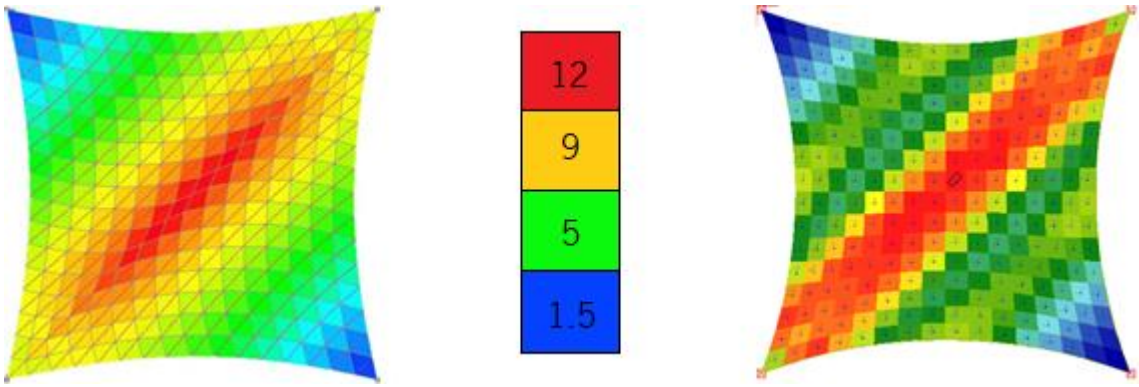

Figure 61 – Warp stresses for the hypar structure. The Henrysson (2012) approach (left) vs the Sofistik® approach (right).

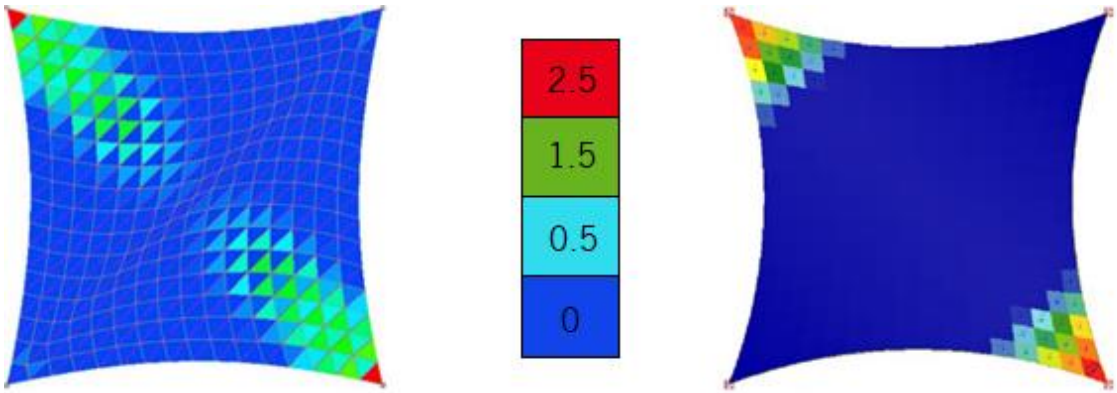

Figure 62 - Weft stresses for the hypar structure. The Henrysson (2012) approach (left) vs the Sofistik® approach (right).

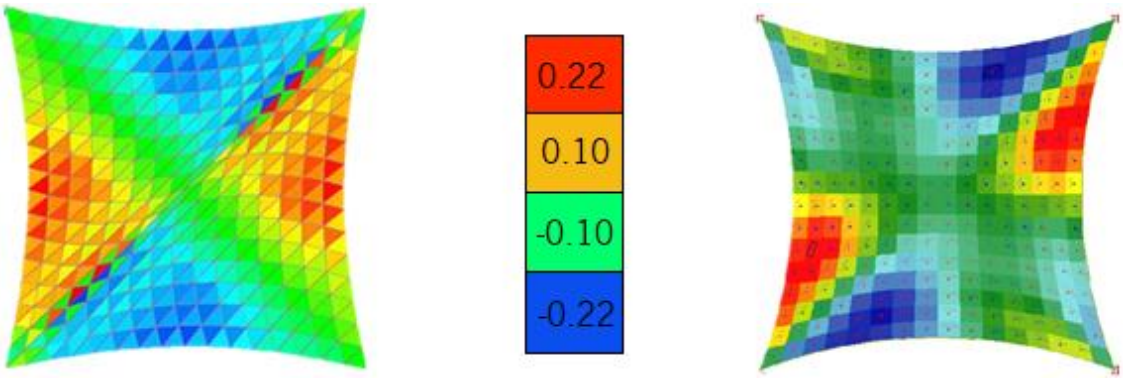

Figure 63 - Shear stresses for the hypar structure. The Henrysson (2012) approach (left) vs the Sofistik® approach (right).

3.3.3. Elastica curve validation

Since the form finding of bending-active elements is a considerably low explored topic and since the suggested approach for the form finding of this type of elements was developed during this work an extensive validation was also needed. Therefore, two case studies were chosen for validating bending-active form finding with Sofistik®. Also, two different load cases were needed, thus, an experimental case study was developed. For the second case study, tabled results were extracted from the work of Adriaenssens and Barnes (2001) and compared with the results obtained by the Sofistik® approach.

Additionally, the validation of bending-active form finding was essentially focused on the geometry of the elastica curve and not on the stresses. This because validating the stresses of an elastic bending would require a considerable amount of time and, since the method used in Sofistik® to form find bending-active elements is the same as the one used for membrane structures, a TH3 problem, and assuming the properties used are correctly introduced, the results should also be exact as it was confirmed in section 3.3.1.

Experimental case study

Firstly, an experimental case study was developed. This case study consists in tracing the geometry of the process of bending a small spring. Thus, tracing what can be called an experimental elastica. The tracing of the curves was done with millimetric paper and then the data was introduced in a spreadsheet and computed. Two small pins were used to simulate the pinned supports, were one has its position fixed and the other is placed in various positions to simulate the elastica curve. An overview of the experimental process is shown in Figure 64. The spring used should simulate with accuracy the process of bending,

yet since this is a small experimental process done solely by hand, and since the centre line of the spring could not be traced, some error may be present in the data of this experimental process.

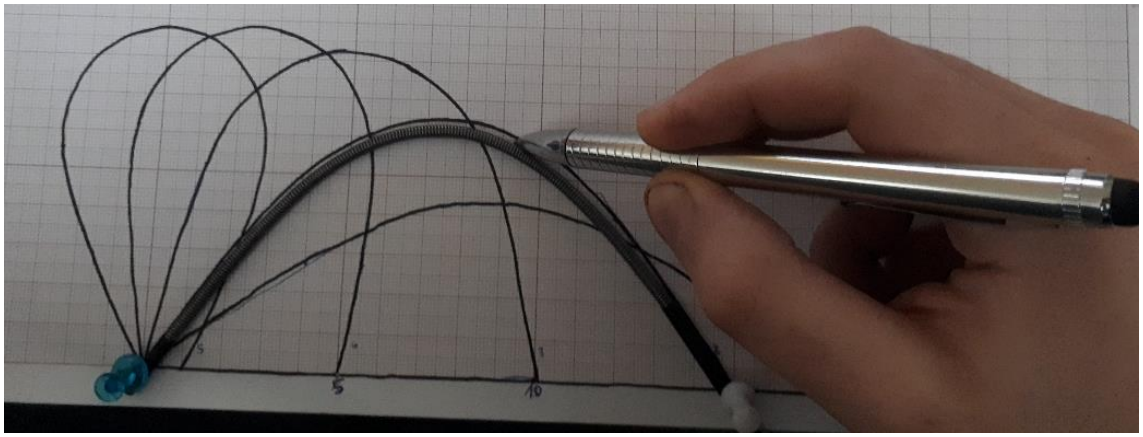

Figure 64 – Overview of the development of the experimental case study.

Figure 65 shows the resulting elastica curve for this small experiment. The spring has a total length of 200mm. The displacement is applied along the bottom axis with 50mm increments, except for the first and the last ones, which are made with 25mm and 40mm increments, respectively. The reason for this is that the first increments are of higher importance, since a great amount of bending occurs with the initial displacements. In the last displacement it was impossible to put both ends of the spring in the same place, thus the need for a 10mm spacing between them. This geometrical data is then exported to a spreadsheet and converted to a graphic.

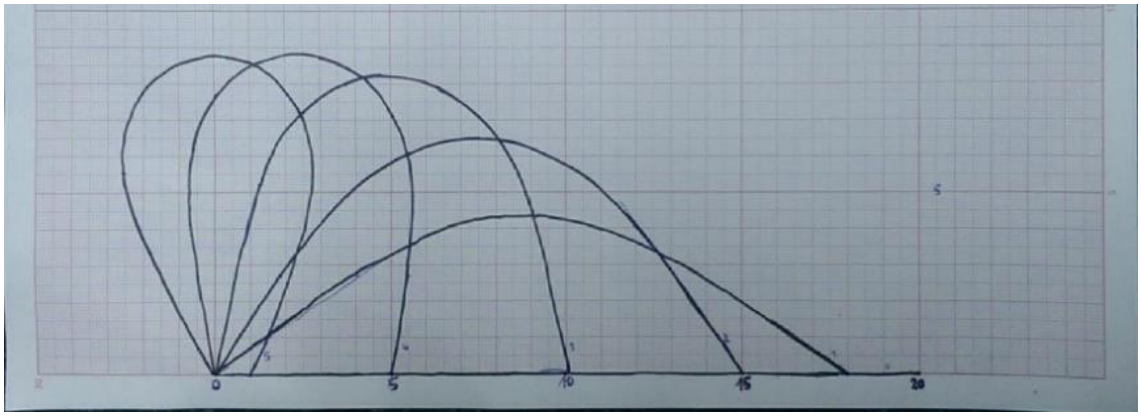

Figure 65 – Author's small spring elastica experiment, traced on millimetric paper.

As it was before explained in section 2.3.3, the geometry of a simple elastica curve is material and size independent, thus material properties and cross-sections are not relevant for the purpose of this case study. Therefore, a simple case study was developed in Sofistik® with a span of 3m and then reduced to

the size of the experimental case study. Figure 66 shows an overview on the process of bending the spring in Sofistik® with the implemented procedure.

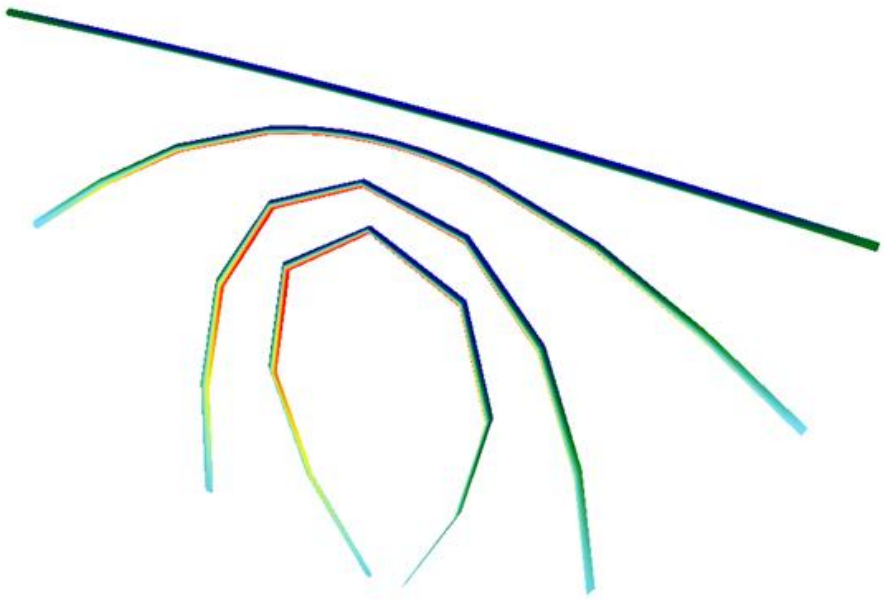

Figure 66 – Bending simulation from the Sofistik® Animator.

Two different problems are solved. Firstly, the routine exemplified by Figure 54 is applied, incrementing the displacement applied to the spring by steps of just 5mm. Then the adaptive increments routine, previously defined in Figure 55 is applied, defining the factor with a value of $1{,}4$. After calculation of both routines, the values of the nodal positions for every iteration are exported to a spreadsheet. In order to create a graphical representation of the elastica curve, the nodal positions should define a curve, and each iteration should represent a set of data. Since this would be a very dilatory process to be completed manually, a VBA routine was established to generate the graphics automatically, based on the number of nodes and the arrangement of the data in the spreadsheet. The VBA code for this routine can be seen in the Appendix.

The graphical representations of the elastica curve obtained with Sofistik® are shown in Figure 67 and Figure 68, respectively representing the linear increment approach and the adaptive increment approach.

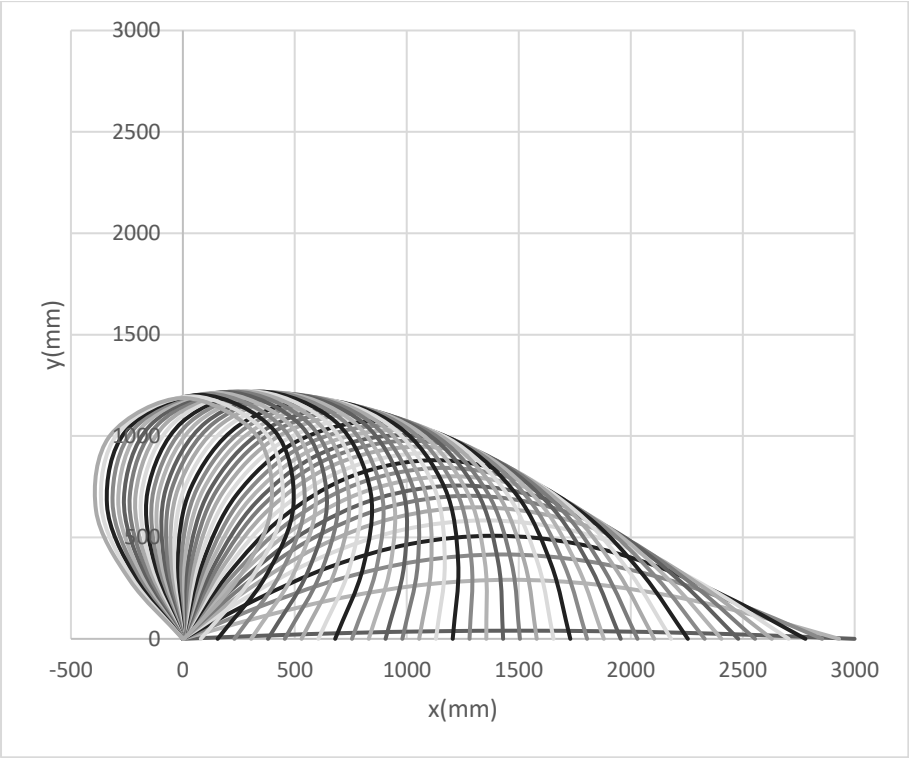

Figure 67 - Elastica curve obtained in Sofistik® with the linear increment routine.

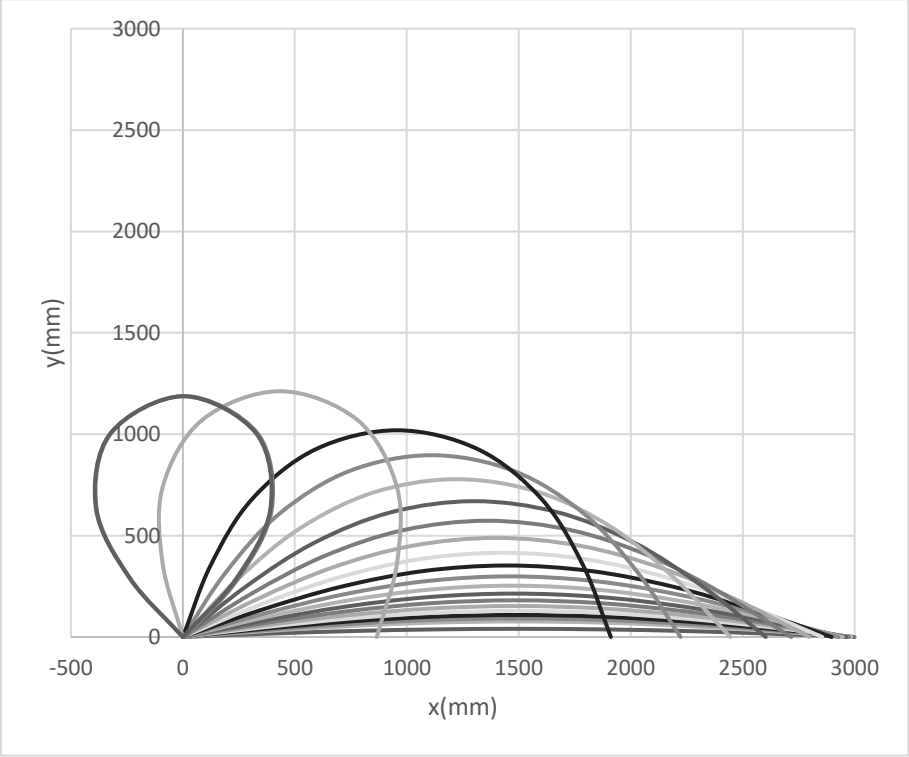

Figure 68 - Elastica curve obtained in Sofistik® with the adaptive increment routine.

Figure 69 shows a decal of the elastica curve obtained experimentally and the scaled model obtained with linear increments in Sofistik®. This graphic shows that the results are not exact, especially for the last iterations of the elastica curve. However, for the first iterations the results are rather accurate. The inaccuracy of the results may be due to the fact that in the experimental procedure it was hard to place the spring in the right positions in order to trace the curve, particularly for the last iterations.

Nevertheless, this results alone are not enough to validate the bending-active form finding process through the proposed approach in Sofistik®. Yet, they represent a key step in the validation, since for small increments the results revealed to be rather satisfactory. Concluding, another method for validation is required to confirm the capacity of the form finding routine established in Sofistik®.

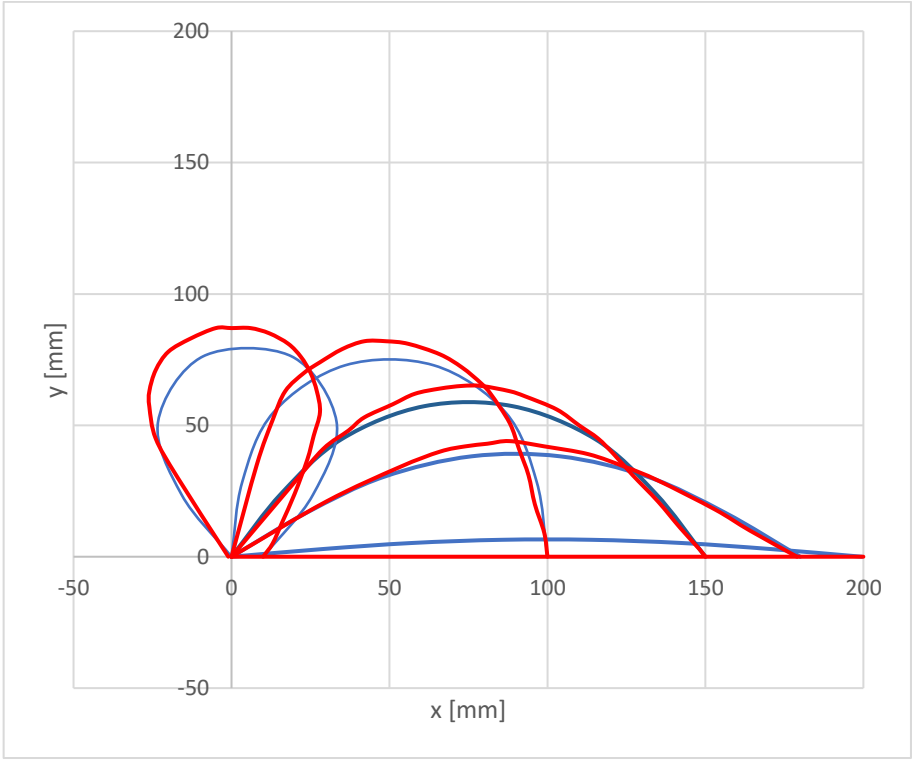

Figure 69 – Overlap of the elastica curve obtained from the spring experiment (red) against the Sofistik® approach (blue).

Tabled results

The third case study consists in a study and comparison of the ratios of the elastica curve. As a matter of comparison, the work of Adriaenssens and Barnes (2001) is employed. In this work a study of the ratios between the highest y position and the highest x position with the overall length of the element is performed. The process is actually based on the work of Timoshenko and Gere (1961). Figure 70 shows

an overall view of the procedure and also shows the referential used. Basically, it consists in applying a given force at the ends of the rod, thus obtaining the elastica curve. Then the results are recorded and compared.

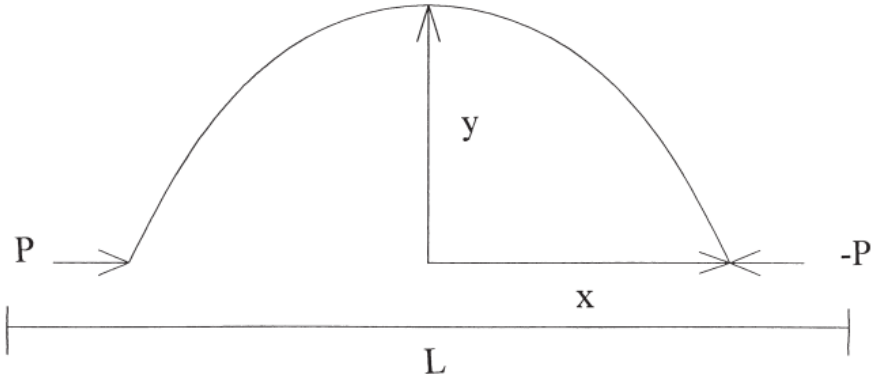

Figure 70 - Diagram showing the relations used by (Adriaenssens and Barnes 2001)

The numerical test example is a tubular strut with a length of 10m, which is supported on end rollers and restrained to lie in the XY plane, and subject to increasing pairs of end axial loads, all above the Euler load (Adriaenssens and Barnes 2001). Several methods are used to solve the problem, however, for simplicity, only the analytical method and the method using 64 segments is used for comparison. Table 6 shows the results obtained by Adriaenssens and Barnes (2001), comparing the x/L and y/L ratios for every buckled stage shown in Figure 71.

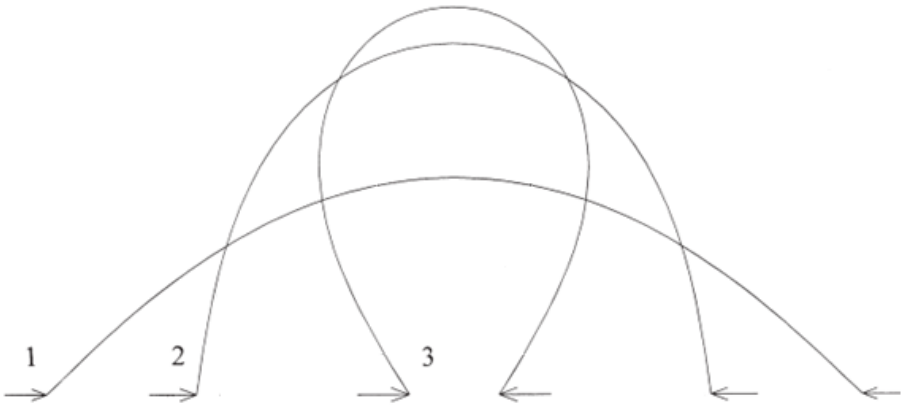

Figure 71 - The four buckled states analysed in the paper. (Adriaenssens and Barnes 2001)

Table 6 - Analytical and numerical values of displacement for central node of beam under four buckled states. (Adriaenssens and Barnes 2001)

Buckled States	**1**		**2**		**3**	
Central Node	x/L	y/L	x/L	y/L	x/L	y/L
Analytical	0,4405	0,2110	0,2800	0,3595	0,0615	0,4015
Numerical 64 segments	0,4413	0,2099	0,2848	0,3572	0,0614	0,4019

As it is shown by Figure 67 and Figure 68, the results of the elastica curve obtained through the linear increment method (Figure 54) and the adaptive increment method (Figure 55), are almost exactly the same. The adaptive increment approach (Figure 55) represents a reliable way to obtain the same results with much less computation cost, since reaching the final position requires much less iterations. Therefore, for matters of simplification, only the results from the linear increment method (Figure 67) are compared with the results from Adriaenssens and Barnes (2001), shown in Table 6. Therefore, the values obtained through the linear increments approach (Figure 67) are reduced to the format of the x/L and y/L ratios. Also, since the referential used in the work of Adriaenssens and Barnes (2001) is not the same as the one used in Sofistik®, this was also taken into consideration during the translation of the results. The full range of values translated are shown in Figure 72. Each value of the x/L ratio is corresponded by another y/L ratio. It is visible, through Figure 72 that with the reduction of the x/L ratio, the y/L ratio increases, as it was expected, since the y point increases with the increasing of deformation, as it is shown in Figure 71. These relations can be better understood by analysing the referential in Figure 70.

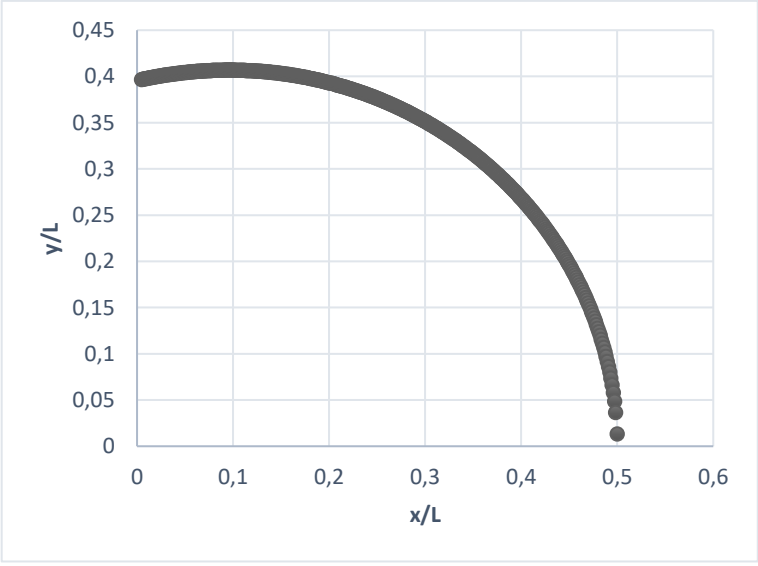

Figure 72 – Set of all the ratios obtained through linear increment approach in Sofistik®.

The specific values of Table 6 can now be compared by the corresponding translated nearest values shown in Figure 72. The results of this comparison are shown graphically in Figure 73 and Figure 74. From this graphic it is visible that almost all the results are very similar, except for the stage 2 x/L ratio of the 64 segments numerical method. However, the result obtained through Sofistik® are very similar to the analytical ones. Then, using this comparison data, the relative error is calculated for each y/L ratio, by reducing it to the x/L ratio, both for the analytical approach and for the 64 segments numerical method. The values of these relative errors are shown in Table 7. From these values it is visible that Sofistik® clearly does a clear approximation of the geometry of an elastica curve. Thus, it can be concluded that this validation has proven successful, since the error percentage is very small and the obtained results seam coherent.

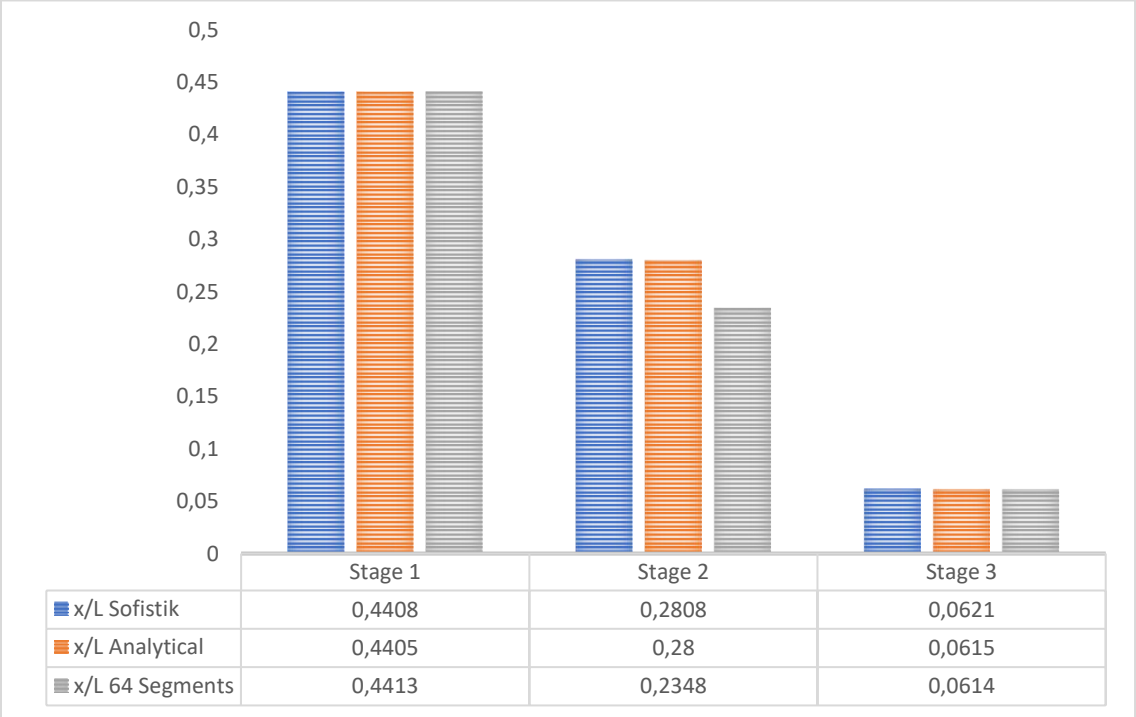

	Stage 1	Stage 2	Stage 3
x/L Sofistik	0,4408	0,2808	0,0621
x/L Analytical	0,4405	0,28	0,0615
x/L 64 Segments	0,4413	0,2348	0,0614

Figure 73 - Comparison of the x/L ratio between the Adriaenssens and Barnes (2001) results and the results obtained in Sofistik®.

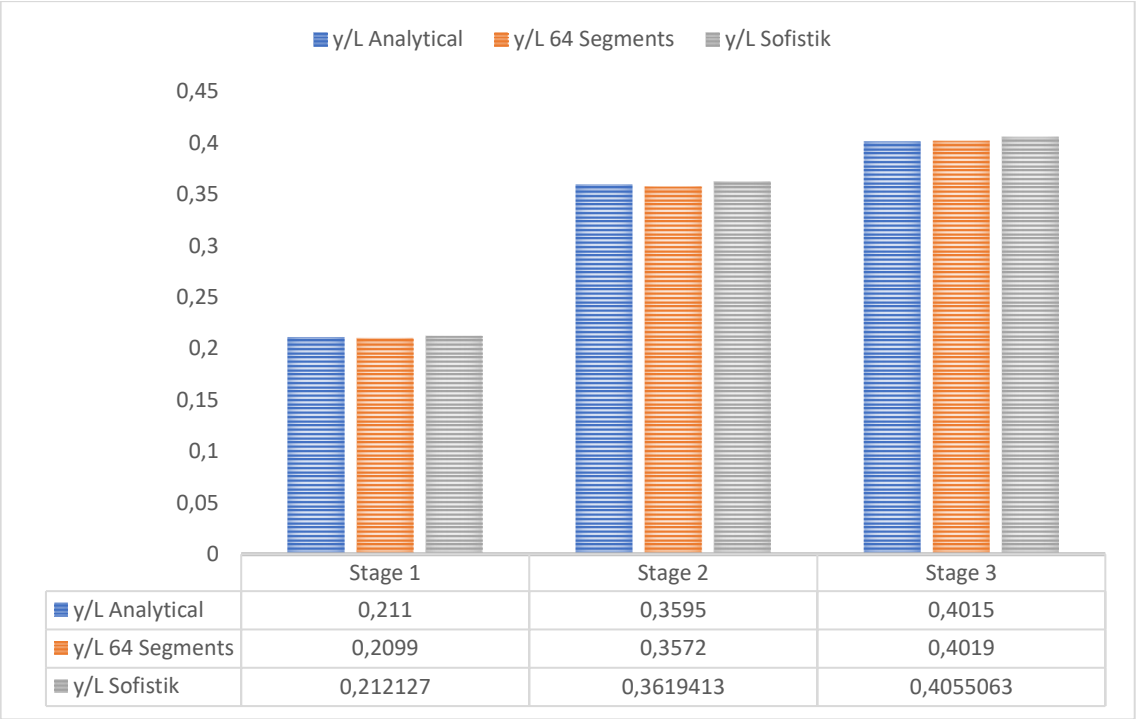

	Stage 1	Stage 2	Stage 3
y/L Analytical	0,211	0,3595	0,4015
y/L 64 Segments	0,2099	0,3572	0,4019
y/L Sofistik	0,212127	0,3619413	0,4055063

Figure 74 - Comparison of the x/L ratio between the Adriaenssens and Barnes (2001) results and the results obtained in Sofistik®.

Table 7 - Relative error of the y/L ratio.

	Stage 1	**Stage 2**	**Stage 3**
Analytical	0,46%	0,38%	0,05%
64 Segments	1,15%	0,85%	0,21%

4. ADAPTIVE HYBRID CASE STUDY

4.1. Introduction

With the purpose of the structural study of the hybrid principle explained in chapter 2, a case study was to be chosen. Therefore, an architectural conceptual project needed to be selected to be structurally analysed. With that purpose in mind, one of the concepts already introduced in section 2.4.3.2 is chosen. The structure chosen was the architectural concept introduced by Costa (2017), that can be visualised in Figure 40. Thus, it is the main objective of this chapter to bring forward and analyse this particular case study making the necessary alterations to improve it in structural means. Although consideration must be made to the impossibility of reaching the optimal structural shape due to various restrictions, mainly time and Software ones.

4.1.1. The structural challenges

With the architectural originality of the concept above-mentioned, obvious new structural challenges come with it. This unorthodox approach generates some structural difficulties, contradicting the usual defined approach to analyse structures. The main principle of the structure is to be adaptive, thus introducing movement and large deformations to the system. This can only be achieved by using slender profiles of an elastic material for the main frame, henceforth designated skeleton, in conjunction with a light material, such as PVC or PTFE textile membranes, henceforth designated membrane, covering the span created by these profiles.

Based on the failure criteria introduced in section 2.4.3.2, this chapter is more focused on the global instability aspects of the structure, as in the membrane failures and profile failures. The global instability problem is of constant presence on this structure. Since slender profiles must be used to be possible to bend the structure, structural instability may occur if the profile sections and materials are not carefully combined. Also, since a planar geometry is present any compression stresses will cause wrinkling to the membrane. On the other hand, high tension stresses may cause plasticization, which is also not sought, due to the need of the elastic properties in the system to be able to adapt the system.

4.1.2. Global overview

The present chapter is subdivided is steps accordingly to the approach taken to deal with the case study. The overview of the chapter is shown in Figure 75. As it can be seen, the chapter is subdivided in 5 steps, a predesign stage, 2 intermediate steps and the structural analysis.

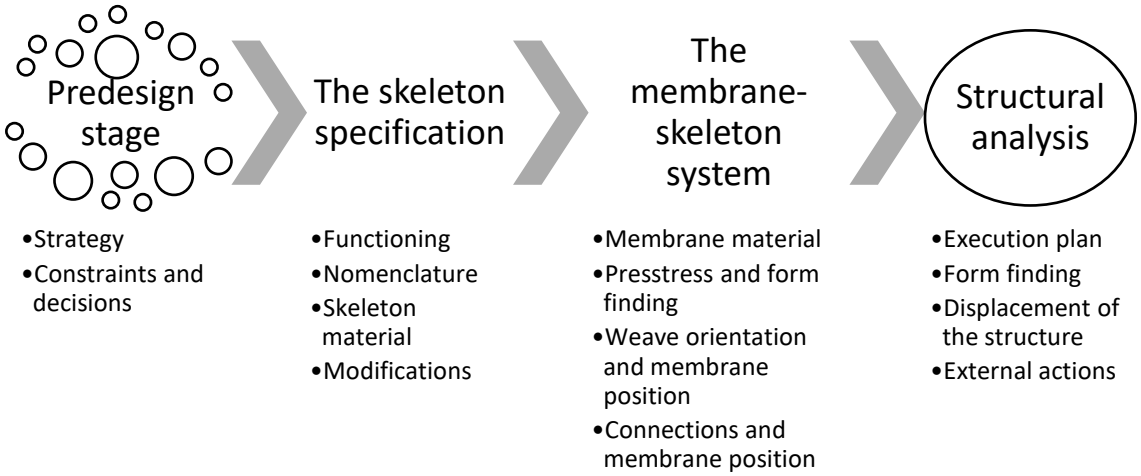

Figure 75 - Overview of the chapter.

The predesign stage consists in a definition of the strategy used to choose the materials for the structure, as well as the cross-sections. Also, the constraints that appeared from these choices are pointed. These constraints created the need to make some decisions about the factors previously defined in the strategy. Thus, these decisions are also pointed in this subchapter.

Before the structural analysis is made, a structural overhaul of the structure was required, thus there are two intermediate steps before this analysis. Firstly, the skeleton is optimized in the skeleton specification. In this subchapter the skeleton is analysed as a standalone system, without the interaction of the membrane. Also, the function of the skeleton is explained, as well as a nomenclature to its members.

The next intermediate step is a verification of the effects of introducing the membrane into the system. The definition of the prestress levels, as well as its interaction with the form finding are explained. Also,

the membrane position and local coordinates are defined. These aspects are fundamental to the form finding step of the overall system.

It is important to mention that these two intermediate steps were mostly based on a trial error process that culminated in the arrival of better solutions that cannot be considered optimal ones. In order to achieve optimal solutions, the process of defining these aspects needed to be a lot more complex and it was not the main purpose of this chapter.

The last subchapter consists on the realization of a primitive structural analysis of the system. This subchapter starts by defining the general execution plan of the analysis which defines the path taken to obtain the results. Then, the form finding process is fully explained and the stress results are exposed and commented. Next, the kinetic part of the structure is solved two different exploratory solutions. The results for this process are also exposed and commented on. Finally, a very primitive approach on the external actions is done and some considerations are made.

4.2. Predesign stage

In the present subchapter the starting principles are defined. Initially, a strategy of approach was carefully considered. Consequently, some difficulties originated by external constraints were pointed. These difficulties were sensibly explained and exposed, thus originating the need to make some decisions that considerably defined the path and approach taken to solve this task. Therefore, these decisions henceforth taken restrain some aspects of the entire project.

4.2.1. Strategy

The first aspect that should be taken into consideration is that a general approach strategy must be underdrawn in order to tackle such complex geometry and structural non-linear principles. In the beginning, a considerable amount of starting points must be taken into consideration to obtain satisfactory results. Therefore, the following principles were considered:

1. It is possible that the initial arrangement suggested by Costa (2017) is not the best structural approach, therefore, slight changes to this structural arrangement are probable. Since direct communication between the structural engineer and the architect was not available during the development of this work, the structural engineer can do the changes with only structural performance in mind. Nevertheless, the original architectural idea must be maintained.

2. The same goes for original material choices and cross-sections, although, a wider range of choices and modification are to be considered in this field, as long as it does not affect the general aesthetics of the project.
3. This being a less conceptual approach, economical aspects must also be taken into consideration which can highly limits the material and cross-section range.
4. A step by step approach was used, since this topic is a lightly explored and very complex one, doing the complete integration on the first step would only lead to misleading errors. Consequently, in a first step only the skeleton is to be analysed, later the membrane is introduced and the integration between the both, as well as the form finding, are approached. Lastly the introduction of movement of the complete structure is dealt with. This allows for a more explanatory and complete process, instead of undertaking the full process in the beginning.
5. It is intended to avoid starting with an imperfect geometry, as well as additional loads to achieve the desired form.

Considering these principles, the strategy of approach shown in Figure 76 was created.

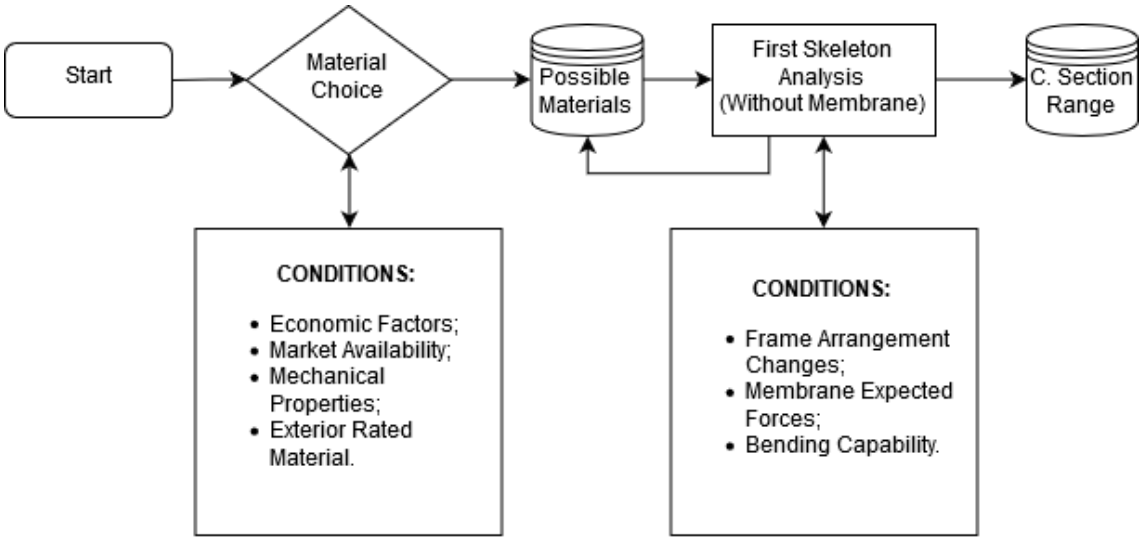

Figure 76 - General flowchart of the adopted strategy.

The first process is to choose the possible materials to be used, according the conditions represented in Figure 76. After that, a possible material range is selected. This material range affects the consequent step, which is the cross-section range selection. Then, a very primitive skeleton FEM model is created and a first analysis is done. This first skeleton analysis decreases the possible materials, since the result of this analysis can eliminate the viability of some of these materials.

4.2.2. Constraints and decisions

Naturally, to the initially defined strategy some constraints appeared that made the process not to flow as expected. Some problems during the material choice process appeared.

Firstly, the profile's material could only be chosen from a specific selection of materials, the reason for that is mentioned in section 2.3.2. This limited our choosing to only a couple of materials, since the basic requirements set for elastic kinetics are only fulfilled by FRPs and interestingly, bamboo (Lienhard 2014). Being a natural material, bamboo stalks are susceptible to humidity and temperature changes. Also, it is not a very smooth material and, since the profiles would be coupled by custom connections as well as with the membrane, this could reveal a problem. Therefore, FRP materials, either GFRP or CFRP, were the main consideration for the profiles.

In the same subject, some challenges arise when trying to get exact material properties for FRP these materials. Doing laboratory test, to obtain the exact properties, was out of this thesis initial plan and, since, in this stage, cross-section range was completely unknown, and regarding the profile constitution, the matrix used in the production of hollow profiles is not always the same as the one used in solid profiles, even if it has been initial planned for, laboratory tests were out of the picture.

Regarding textile membrane materials, another similar problem appeared. As small membrane structures are usually double curvature common shapes, as explained in 2.2.2.1, the catalogues are usually lacking some information about their exact properties. According to Stimpfle and Günther (2016), the experts on the field apply often material properties based on experience. Only for major projects individual biaxial tests are made to determine the material properties (Stimpfle and Günther 2016). Biaxial tests are used to determine compensation factors for membranes, and mechanical properties of the used membranes (Stimpfle and Günther 2016).

Again, since laboratory tests were initially out of this thesis initial plan, and as the idea was to test a wide amount of membrane properties and check for which was the best fit, another solution to obtain the membrane material properties should be obtained. Therefore, the solutions found to tackle these constraints are reached for by starting with a set of decisions that limit the effects of these constraints.

Regarding materials, at least two types of materials had to be chosen one elastic material for the skeleton and a membrane material. The main aspect considered when choosing the materials for the module was the criteria shown in Figure 76, naming:

- Economic factors;
- Market availability;
- Mechanical properties;
- Exterior rated material.

Economically, the materials chosen must be relatively affordable. Since this is a modular project, the cost of each module must not be very expensive and must be possible with common cross-sections and materials that are currently available on the market. Also, the mechanical properties of these materials must be acceptable, with low fatigue constraints. All the materials chosen must be usable outdoors, factor that also imposes some barriers to the available options.

These constraints will be taken into consideration when making the material choice for the skeleton in section 4.3.3 and for the membrane in section 4.4.1.

4.3. The skeleton specification

This subchapter explains in detail the structural function of the profiles arrangement, henceforth called skeleton. A nomenclature based on the structural functioning of each group was proposed. The skeleton material is chosen based on the principles before defined. The cross-section selection process is explained and significant changes are made in order to improve structural performance.

The membrane interaction is only explained in the next subchapter, therefore, in the present subchapter, all the analyses was done without the membrane, albeit the membrane interaction was thought off and was be slightly addressed.

4.3.1. Functioning

Besides the approach by Costa (2017) to the architectural principle is based on biomimicry, these concepts must be analysed by structural means to attain some conclusions. To understand the principle behind the function of a leaf structure, a similar leaf should be analysed. In an optimal situation, a double supported leaf would be taken into consideration, since this is the proposed support arrangement for the skeleton, although, this type of leaves does not exist or are very hard to find. As an alternative, the leaf in Figure 77 was analysed, also, the denomination of the parts that compose the leaf are illustrated in the picture. These parts are the midrib, the veins and the blades.

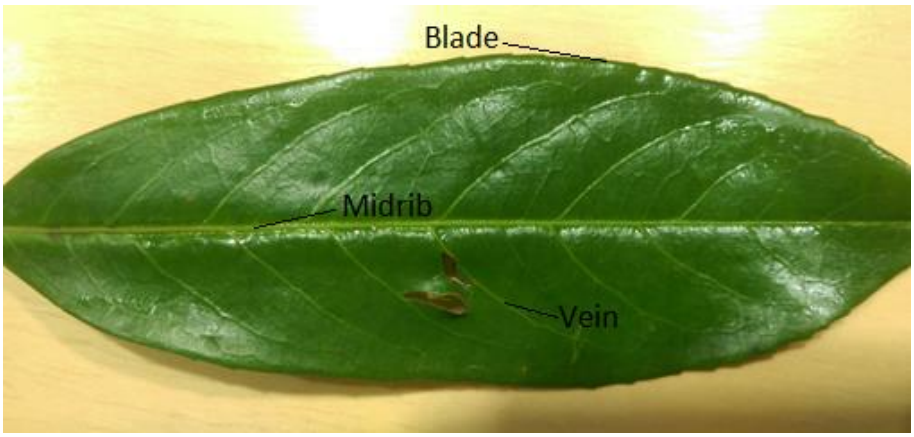

Figure 77 - Example of a pointed leaf.

There are two main types of net-veins in leaves, *pinnate* and *palmate*. *Pinnate* leaves have a featherlike composition, while *palmate* leaves have an organization like the palm of a hand. The leaf in Figure 77 has a *pinnate* net-vein pattern, therefore, has a midrib, which is the large central vein, extending from the base of the blade to its tip. The remaining ribs are simply called veins. The leaf in question is also a pointed leaf, which was chosen to be so due to the resemblance to the original suggested structure by Costa (2017).

Firstly, it is noticeable that almost all the veins meet in the same point in the midrib. In this case, it probably happens due to the symmetry of the leaf, genetics, or easiness on the process of making nutrients reach the leaf. Albeit, this concept will be imported to this project to eliminate some residual bending stresses. Secondly, due to the lack of support in the point of the structure, the veins tend to go forward. This allows to compensate the lack of support on the end of the blade by adding rigidity to the leaf.

It is worth noting that, structurally speaking, there are perceptible differences between the leaf in Figure 77 and the project suggested by Costa (2017) visible in Figure 40, naming:

1. The leaf is not subject to a pretension load, like the skeleton is by the membrane;
2. The existence of supports is completely different. This is illustrated in Figure 78;
3. The blades on the natural leaf do not have the same composition as the midrib. The opposite happens for the skeleton.
4. The geometry arrangement is not completely similar.
5. The geometric biological scale is not the same, since a natural leaf only has, at best, a few dozens of centimetres and the original skeleton proposal would extend for a span of 10 meters.

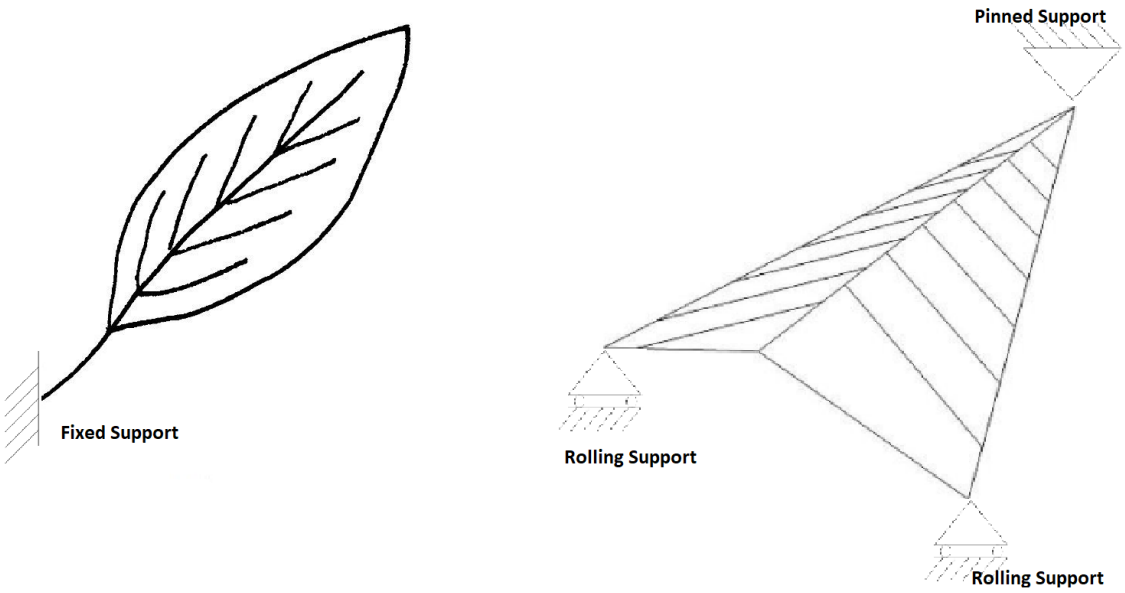

Figure 78 - Comparison of the support systems. The natural leaf support system (left) and the skeleton support system (right).

The above exposed differences have a high impact in the structural performance of the system, since support and geometry principles represent a key role in structural performance of any structure, in the case of a highly non-linear structure these aspects have even more impact.

Therefore, in the next section, some modifications are suggested in interest of pursuing satisfactory structural performance. Without these modifications, hereinafter suggested, the stability of the structure may not be even possible.

4.3.2. Nomenclature

There is a need to establish a structural nomenclature for the system, with the objective of achieving coherence in the upcoming explanations. Therefore, a simple structural division was made by dividing the elements based on their function.

Due to the structural function similarities of the elements in the same group, this nomenclature is also used in the software to be able to apply different cross-sections. The nomenclature suggested is expressed by consulting the Figure 79 in conjunction with the Table 8.

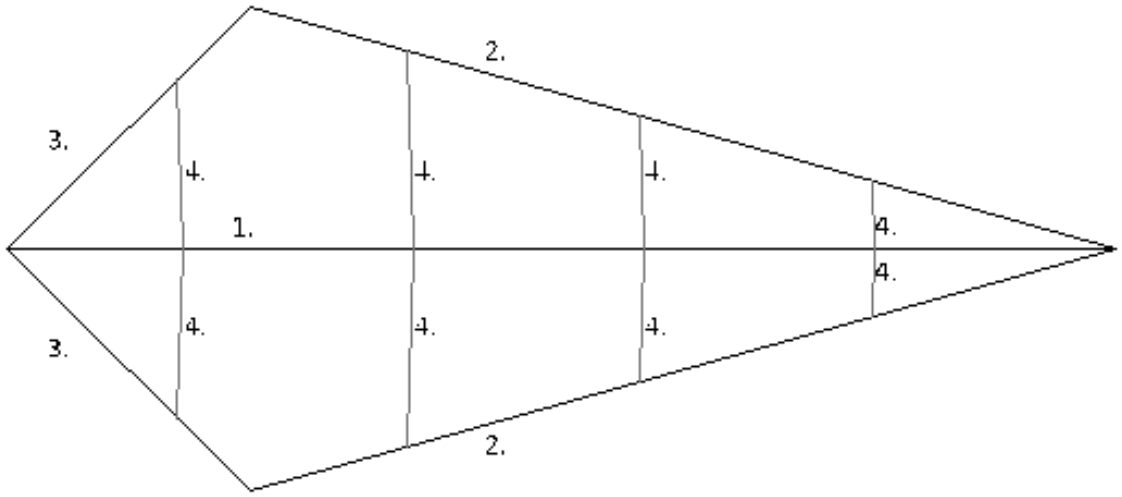

Figure 79 - Basic nomenclature of the skeleton.

Table 8 - Nomenclature legend.

1.	Main Spine	3.	Oars
2.	Side Spines	4.	Veins (90° angle with main spine)

With the purpose of being able to control the various parts of the structure, in Sofistik® software, according to their structural function, the elements were also divided in groups. This division is discretized in Table 9, giving the nomenclature previously explained in Table 8. This nomenclature is used in the remaining document.

Table 9 - Grouping of the elements in Sofistik®.

Group 1:	All Spines (1, 2)	Group 14:	The Membrane
Group 2:	The Oars (3)	Group 23:	All the veins (4)

4.3.3. Skeleton material

Notwithstanding that for Costa (2017), to the main spine, the choice of aluminium, is obvious, due to the weight-resistance relation, durability, corrosion resistance and material flexibility. However, aluminium is a material very susceptible to fatigue problems, due to the lack of an endurance limit. The endurance limit is a property that indicates the stress which a material can be used for an infinity number of cycles. Since aluminium does not have an endurance limit, it can fail even for small stress values, after a defined number of cycles. Also, for this reason, according to Figure 29, aluminium is only considered for bending-

active structures and not for kinetic structures. Thus, a new solution for material choice must be taken into consideration.

As beforehand explained, FRP materials are the best option, since ambient changes can affect bamboo and, also, the rough surface of bamboo can cause tearing when interacting with membrane and combability problems with the connections. Also, since bamboo is not an artificial material, finding uniform cross-sections also present a challenge. Thus, the choosing was limited between GFRP or CFRP. This being, economically, the aspects about inducing movement to the structure must also be taken into consideration. Therefore, if CFRP was too be chosen, due to its relatively higher flexural Young's modulus, higher torque motors would be needed in order to be able to move the structure. Besides that, CFRP by itself is much more expensive than GFRP. Therefore, GFRP seems to be the best option for all the spines. Also, Costa (2017) says that the veins need to behave rigidly, in order not to change their shape in all the stages of the formal change of the structure, suggesting the use of 2cm CFRP profiles for these smaller inner elements. This can be easily achieved by slightly increasing the cross-section of a GFRP profile. These bars are not very long, and as the direction of the stresses is not such to easily bend the nerves, thus the use of GFRP for the nerves can be considered feasible. Thus, the use of GFRP profiles is considered for the whole skeleton.

Regarding the endurance limit, GFRP behaves differently from aluminium. Figure 80 shows a comparison of the normalized S-N curves of a set of GFRP profiles and joints. According to Keller, Tirelli et al. (2005), the corresponding linear representation shows a high drop in fatigue resistance down to approximately 40% of the UTS within the first million cycles. Subsequently, the values stabilize and a fatigue limit of approximately 25% of the UTS can be seen at ten million cycles (Keller, Tirelli et al. 2005). Besides this, the material research in the field of FRPs is always improving these materials. For example, the fatigue life of GFRP composite with 9% rubber microparticle in a modified epoxy matrix is about three times higher than that of GFRPs with neat matrix (Lienhard 2014).

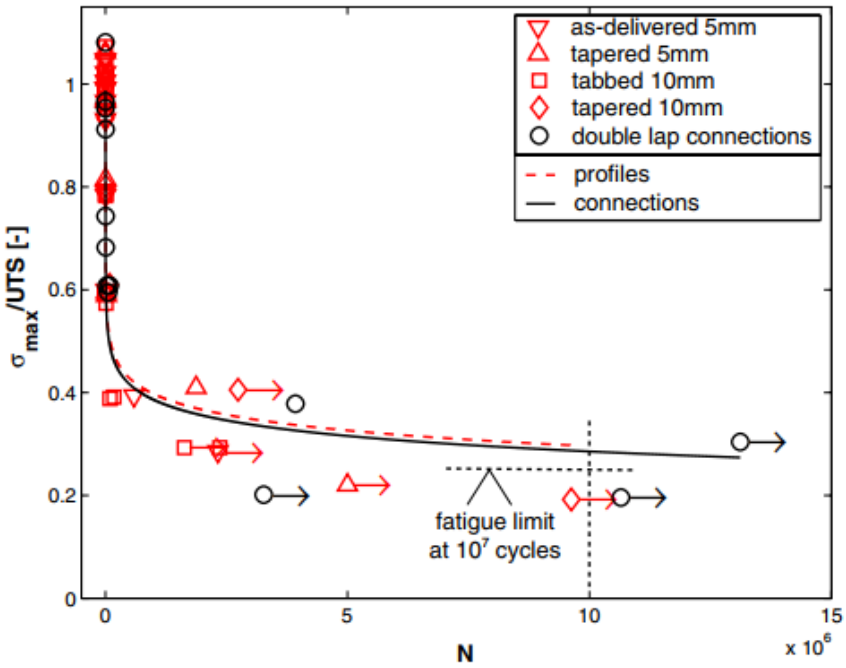

Figure 80 – Comparison of the normalized S-N curves of profiles and adhesive joints, linear representation, fatigue limits. (Keller, Tirelli et al. 2005)

As beforehand mentioned, the criteria for selection of the material were economic factors, market availability, mechanical properties and exterior rated material. The economic factors and mechanical properties were addressed above. The market availability and the exterior rated material are factors with lesser complexity, thus with a quicker and easier response.

Nowadays, the variety of the market for GFRP extruded profiles is very extensive. The possibility of custom profiles to meet the needs of the structure is also a reality, therefore, this would not represent a problem. During the development of this project, several brands of GFRP profiles were contacted, providing valid confirmation about their ability of producing a wide range of profiles.

Regarding the resistance of GFRP to the conditions of an external environment, as Knippers, Cremers et al. (2011) say, the polymer matrix defines the shape of the composite component and protects the fibres against UV radiation and aggressive media such as moisture and chemicals. Therefore, the ability for the GFRP to handle exterior conditions it is easily accomplished by picking the correct matrix component to protect the fibres.

Considering the above elucidated aspects, it is possible to confirm that GFRP conforms to the characteristics defined in the strategy defined in section 4.2.1 about the choice of material. This decision

reflects the need to get information about the mechanical properties of GFRP profiles. As explained in section 4.2.2, during this process problems appeared when obtaining exact mechanical properties. In Europe, GFRP properties are generally provided by stating that the material respects a certain class defined in the European Standard EN 13706, either class E23 or class E17. Although, it is likely that that the actual mechanical properties of the GFRP are much higher than these minimal requirements. On the word of Lienhard (2014), while the geometry of a single and homogenous elastica curve is independent of size and material, the structurally necessary coupling of several bending-active components results in a material dependent geometry. Thus, for the purpose of this case study, exact properties of the GFRP would be ideal, yet obtaining these exact properties was not possible.

As an alternative, the solution found was to define a set of properties based on the values used in the work of GARTI, Tutor et al. (in conjunction with the minimum values defined by the class E17 of the European Standard EN 13706. These properties are represented in Table 10.

Table 10 - GFRP material properties suggested.

$E = 20000\ N/mm^2$	$E_{90} = 1000\ N/mm^2$
$\upsilon = 0$	$\upsilon_{90} = 0$
$G = 3500\ N/mm^2$	$K = 333\ N/mm^2$
$\gamma = 17\ kN/m^3$	$\rho = 1733\ kG/m^3$

4.3.4. Modifications and cross-sections definition

As before explained, some changes must be made to improve structural performance. These changes tend to have the architectural principle in consideration, thus always avoiding opposing to it.

Having a triangular external shape, created by the side spines, already works in favour of the structure, by being this a very structurally stable geometric shape. Ergo, there is no need to change the external geometry of the skeleton, since these changes would apply small structural benefits, but would highly change the general aesthetics of the overall structure. In Figure 81 it is visible the original conceptual proposal by Costa (2017). The only problem that can appear relatively to the external geometry of the spines is a scaling one, since 10 meters is a huge span for a structure like this. Apart from that, the modifications will focus on the internal geometry of the skeleton, mainly the veins arrangement and also in a proper definition of the cross-sections of the GFRP profiles.

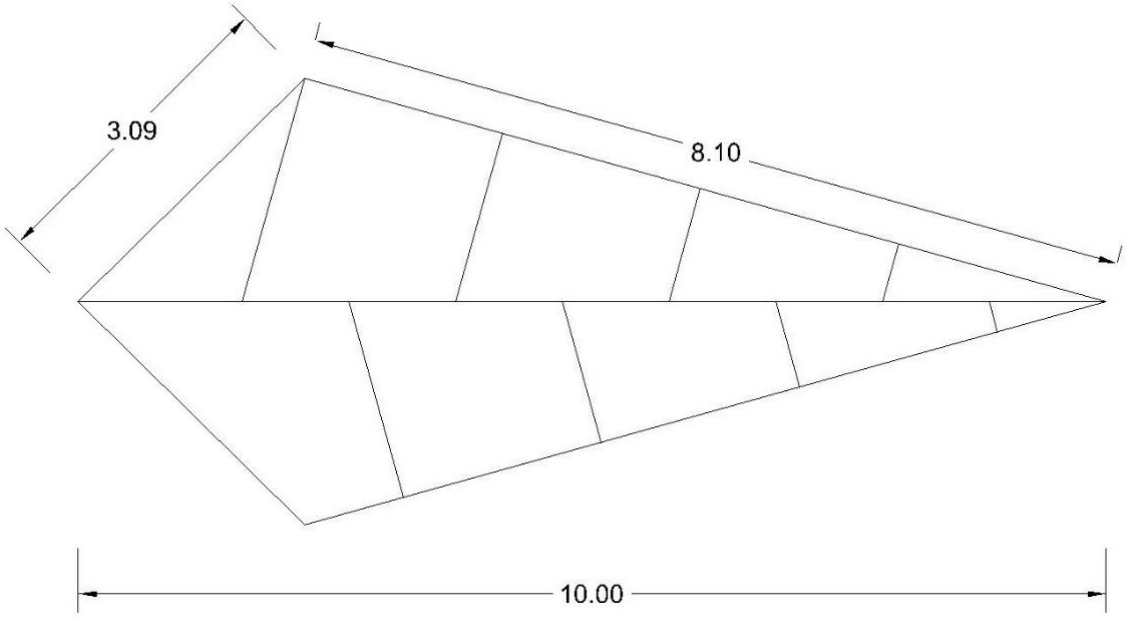

Figure 81 - Original suggestion by the architect. Dimensions in meters.

Following the strategy described in section 4.2.1, the cross-sections of the structure should be defined. The process of defining the cross-sections of the skeleton was essentially based on a process of trial and error that culminated in the best compromise between elastic stiffness and slenderness. The first aspect was to define the cross-section geometry. It was obvious that the spine cross-section should be slender enough to bend, but also stiff enough to sustain the loads and the bending stresses. Additionally, a homogenous geometry for the profiles was a better option since by doing this, the bending plane would not be conditioned by the cross-section geometry. Thus, the skeleton profiles are defined to be composed with only circular profiles.

Now that the profiles were defined to have a circular geometry, their dimensions should be defined. This was a very sensitive process that was optimized by means of trial and error. The right dimensions had to be chosen in order to sustain the correct behaviour for the structure. To simplify the process two distinct cross-sections were designated to appear, the cross-section for the external members (spines and oars) and the cross-section for the internal elements (veins). A correct balancing between these two distinct cross-sections should be attained. Based on the material properties defined in Table 10, the first models based on the architectural solution shown in Figure 81 were calculated. Table 11 shows an evolution of the cross-section selection process. The first models, based on the architectural proposal with 10m span could only be stabilized by using huge cross-sections, which massively increased the structure weight.

After several attempts with the initial 10m models the use of smaller cross-sections was not feasible, as shown in Table 11, for the first attempt with a solid 50mm diameter cross-section, the effective length of 8m gives a slenderness ratio of 640, which is excessively high for the intended functioning of the spines. Then the section was increased to the double, a solid 100mm cross-section. This effectively reduced the slenderness ratio but the buckling tensions are too high thus the structure would not bend. At this point it was obvious that something was wrong with the structure itself.

Therefore, and as expected, a reduction on the scale of the structure was needed in order to make this project feasible. Although the project developed by Costa (2017) is a great architectural achievement, structurally speaking it misses on a crucial point. Leaves tend to be small flexible surfaces, that don't need to support much weight. The adaptive movement of a leaf is also feasible because it deals with smaller stresses. Also, the structures of leaves in general were improved by years of evolution to resist only these smaller stresses. Despite all the structural differences mentioned before in section 4.3.1, the scaling of the structure of a leaf to 10m is unfeasible due to the allometric grown of a leaf.

According to Galilei (1914), one can plainly see the impossibility of increasing the size of structures to vast dimensions either in art or in nature; likewise the impossibility of building ships, palaces, or temples of enormous size in such a way that their oars, yards, beams, iron-bolts, and, in short, all their other parts will hold together; nor can nature produce trees of extraordinary size because the branches would break down under their own weight; so also it would be impossible to build up the bony structures of men, horses, or other animals so as to hold together and perform their normal functions if these animals were to be increased enormously in height; for this increase in height can be accomplished only by employing a material which is harder and stronger than usual, or by enlarging the size of the bones, thus changing their shape until the form and appearance of the animals suggest a monstrosity.

Therefore, only by changing the overall shape of the structure the 10m span of the module could be maintained. Since changing the overall architectural principle of the structure was not intended, as that would defeat the whole purpose of this project, it was decided to scale the modules to be smaller. As it is shown in Table 11, the third attempt reduces the span to 3, giving a spine effective length of 2,43 meters. This way, the cross-sections could be decreased in such a way that the slenderness ratio could be maintained more and less at the present levels of 300, but drastically reducing the Euler Load.

Table 11 -Evolution of the cross-section finding attempts. First attempt (top) to final solution (bottom).

Attempt	**Length**	**Spines**				**Veins**	
	(m)	Ext. Diam. (mm)	Int. Diam. (mm)	λ	Euler Load (kN)	Ext. Diam. (mm)	Int. Diam. (mm)
#1	8	50	0	640,0	0,9462	10	0
#2	8	100	0	320,0	15,1398	20	0
#3	2,43	16	0	607,5	0,1075	8	0
#4	2,43	20	0	486,0	0,2625	10	0
#5	2,43	50	40	151,8	6,0550	20	16
#6	2,43	30	20	269,6	1,0666	20	16
#7	2,43	20	15	388,8	0,1795	16	12
#8	2,43	25	23	286,1	0,1818	18	14

Since the overall objective of this project is to use the elastic capabilities to bend the structure to distinct positions, a correct balance of stiffness and slenderness must be attained. During the process of finding a better solution for the cross-section, illustrated by Figure 82, increasing the cross-section of the spines or veins was not always the solution because, when these cross-sections were increased in an uncontrolled manner, the slenderness would drastically decrease and thus increasing the Euler load and creating weight problems, which made the structure fall in its own weight. Therefore, an iterative process between reducing and increasing the cross-sections was made until a stable solution was found.

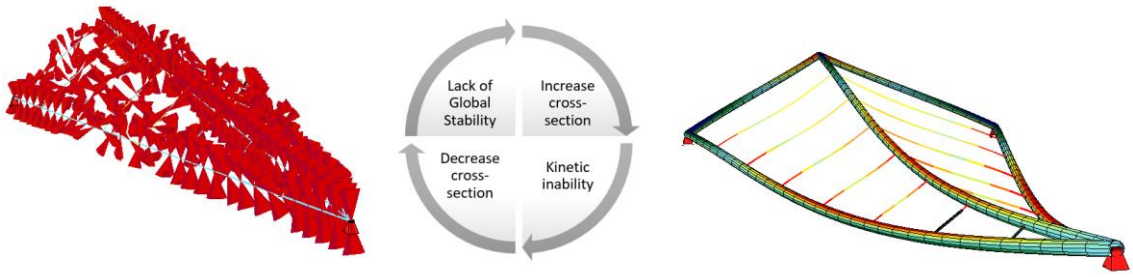

Figure 82 - Process of refining the cross-section. Instability problems (left) and weight and kinetic problems (right).

Based on the material properties defined in Table 10 and the last cross-section defined in Table 11 and considering the global scaling from 10m to 3m span, the first primitive model of the skeleton without the membrane is calculated. This model is shown in Figure 83 where it is visible that the main spine does

not bend as much as desired. This is due to the lack of a rigid compression connection between the oars and the main spine, and due to the lack of the stress stiffening effect of the membrane prestress. The connection between the veins and the spines is kept as suggested by Costa (2017), realising the bending in the y direction, as this will prevent undesirable bending of the veins.

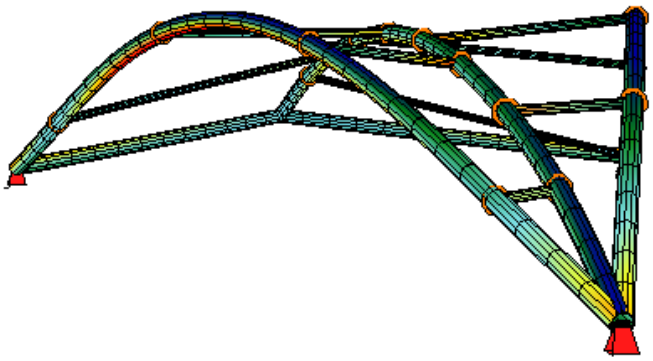

Figure 83 - Analysis of the first skeleton models without membrane.

According to what was already mentioned in 4.3.1, the veins internal vertexes don't meet in the same place. This aspect has a significant importance structurally, as the veins will resist, mostly, at compression stresses due to the membrane prestress, the existence of this missing space would generate residual bending stresses in the main spine, which can be avoided if the internal vertexes match. Therefore, the veins are rearranged in such a way so that their vertexes meet in the same place. By doing this these residual bending stresses around the z axis are eliminated.

As referred above, regarding Figure 83, the absence of a physical connection between the oars and the main spine generates a situation of lack global stiffness. This situation can be corrected. Since there is an important amount of load being transmitted by the oars to the main spine when moving the structure, the absence of a compression connection between these three elements would limit their connection to be a merely traction one, apart from the rigid connection element at the internal vertex of the oars. The receding of a vein to connect the oar with the main spine allows the efficient load transfer needed to the movement of the structure, increasing the global stiffness of the skeleton and improving the load path for the stress stiffening effect. Figure 84 illustrates the final suggested structural arrangement, with the beforehand mentioned alterations.

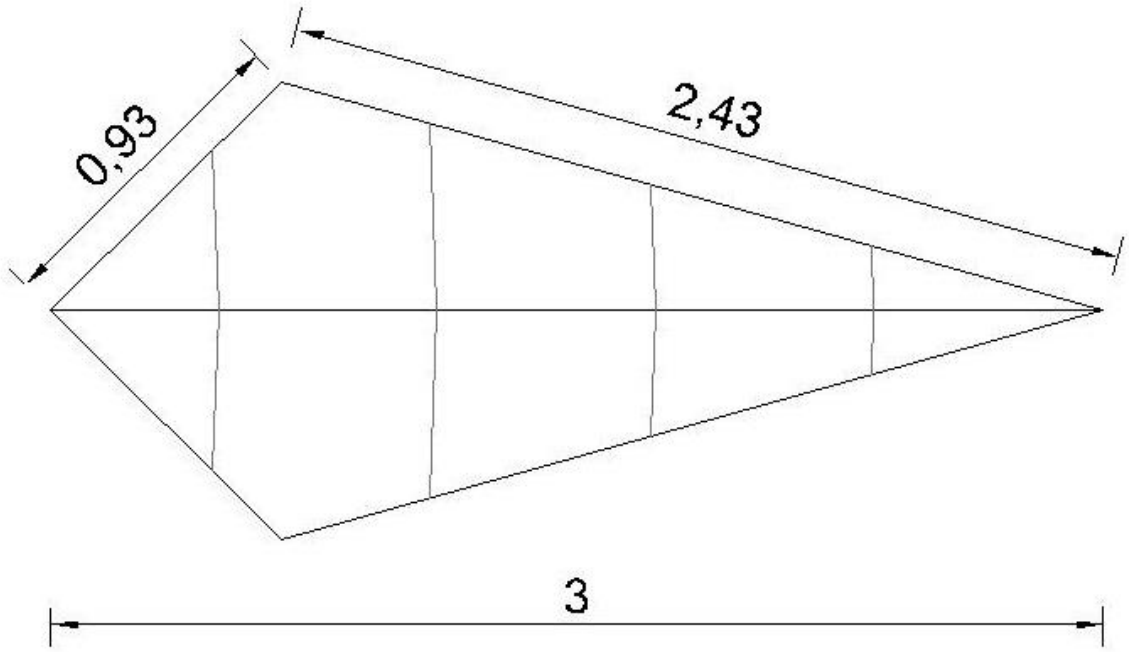

Figure 84 – Suggested modifications to the skeleton. Dimensions in meters.

Summing up, the following significant changes were made:

1. Scaling the model from 10 meters span to 3 meters span;
2. Defining a stable set of cross-sections;
3. Changing the number of internal members;
4. Changing the orientation of the internal members;
5. Adding a connection between the oars and the main spine.

4.4. The membrane-skeleton system

In this subchapter the membrane is introduced on the previously suggested skeleton arrangement, in subchapter 4.3. The material for the membrane is selected and the interaction principle between the skeleton and the membrane is explained in detail, namely the prestress and its impact in the form finding process, as well as the fibre weave orientation choice and the reasons for this choice.

Introducing the membrane on the skeleton, represented in Figure 84, is a meticulous process that requires attention to detail. To quote Forster and Mollaert (2004), designers of fabric structures concern themselves with three primary structural factors – choice of surface shape, levels of prestress and surface deformability.

Firstly, the membrane needs to be prestressed. The prestress value needs to be carefully selected. Higher prestress than needed and global instabilities appear, making it impossible to perform further calculations on the system. If the prestress is too low then the stress stiffening effect is not availed at an optimal level, which may cause in the latter stages a wrinkling of the membrane or even the inability to carry external loads. Secondly, the weave orientation is of foremost importance. As the prestress, in Sofistik®, is applied according to the weave pattern. These two concepts are explained in detail in the following topics. Lastly, the connections between the elements and the membrane are suggested by technical drawings.

4.4.1. Membrane Material

The textile membrane material is a very sensitive subject since the choosing of the material will affect the whole structural behaviour. A detailed explanation of the composition of textile membranes and their distinct types can be consulted in section 2.2.2. The principles applied to the choosing of the membrane material are described in section 4.2.1.

Since the module leaf will constantly be changing position, the need for slightly smaller Young's modulus in the membrane is present, otherwise plasticization may occur. This practically eliminates the fiberglass fibre option, that despite having high tensile strength, remains brittle and has low elastic strain. The best material for this type of structure, considering the materials presented in 2.2.1.4 is a composition of polyester fibre coated with PVC. According to Beccarelli (2015), PVC is the most used coating for architectural fabrics due to the reduced cost, the easy weld ability and the range of colours available, in addition, it can be easily painted or printed. In order to obtain a non-stick, self-cleaning surface resistance to UV rays, PVC is generally combined with a top-coating based on acryl, polyurethane, polyvinyl fluoride or polyvinylidene fluoride (Beccarelli 2015). All these facts combined, make for the Polyester fibre coated with PVC the best choice for this project.

However, problems obtaining exact properties for the membrane material appeared. The main problem was not to have a precise Young's modulus to use, since all the other resistance properties can be obtained. This aspect is not relevant for the form finding procedure since, according to Lienhard (2014), the actual mechanical material properties of the membrane are not considered since the form finding is purely based on the equilibrium of tension forces and only geometrical stiffness is considered. Yet, the rigidity of the membrane is an important aspect for the movement of the structure. Therefore, a more exploratory approach was taken, assuming a Young's modulus that resembles the obtainable spectre for this type of membranes. This was possible by analysing the work previously made by Uhlemann (2016)

about the mechanical properties of membranes. During this process type II membranes were considered. Taking this in consideration, the suggested membrane properties can be consulted in Table 12.

Table 12 - Suggested polyester coated with PVC membrane properties.

$E = 400\ N/m^2$	$E_{90} = 300\ N/m^2$
$\mu = 0.2$	$\mu_{90} = 0.2$
$G = 4\ N/mm^2$	$K = 222\ N/mm^2$
$\gamma = 12\ kN/m^2$	$\gamma_a = 2\ kN/m^2$

4.4.2. Prestress and form finding

According to Forster and Mollaert (2004), the prestress of membrane structures is a fundamental part of the shape and structural behaviour. After all, the membrane prestress and the initial geometry of the skeleton, including the cross-sections and materials, are the only input variables that are available for user control. Everything else is generated depending to these inputs. Therefore, and since all geometry aspects have been discussed and defined in section 4.3, the membrane prestress remains the only control variable.

Likewise, the membrane prestress was fixed at the value of $1\ kN/m$ in both directions, since according to Forster and Mollaert (2004), for many structures the same quantity of prestress is applied to both directions of the textile's weave. As Forster and Mollaert (2004) say, for PVC coated Polyester membrane structures, a "rule of thumb" is that the prestress should not be less than 1.3% of the average tensile strip capacity of the material in both the warp and weft directions. To satisfy this rule, the following table is provided:

Table 13 - Minimum prestress levels for PVC coated Polyester membrane structures. (Forster and Mollaert 2004)

Type I	$0.70\ kN/m^2$
Type II	$0.90\ kN/m^2$
Type III	$1.30\ kN/m^2$
Type IV	$1.60\ kN/m^2$
Type V	$2\ kN/m^2$

The use of $1\ kN/m^2$ can be considered plausible, since the dimensions of the structure have been reduced to a 3 meters span. Therefore, a thinner membrane like the Type I or Type II of PVC coated Polyester is totally acceptable.

The whole idea behind textile hybrid structures is that the pretension of the membrane defines the form finding of the structure, in conjunction with the boundary conditions. This allows to limit construction errors and form found imperfections. On the other hand, introducing pre-camber to the system could change the obtained geometry through the form finding process. These changes in geometry can result in different load response of the structure. In addition, Lewis (2003) said, dictating the shape of a tension structure beyond what is known to be its optimal form, i.e. an anticlastic shape, may have unforeseen consequences and, long term, may prove to be futile; over a period of time, the structure will creep towards its minimum energy form, in an attempt to equalize stresses. Thus, starting with a planar geometry and let the prestress influence the form finding is the ideal path to take for textile hybrids. Also, besides the initial geometry and the material and cross-section choice, the membrane prestress is the only input controlled by the user. Thus, letting the membrane prestress define the form finding was the choice taken, as exemplified in Figure 85.

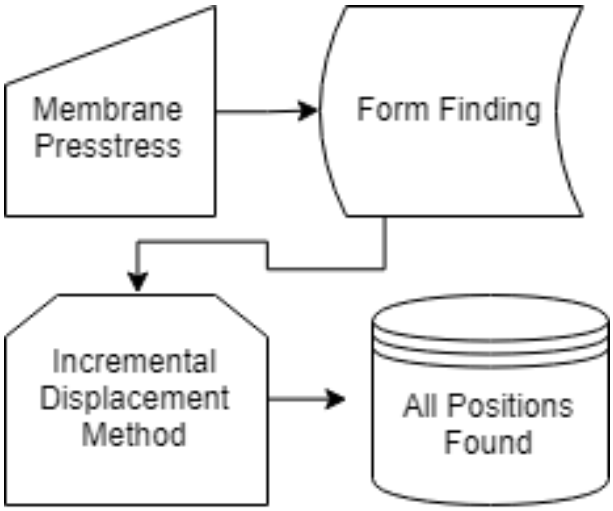

Figure 85 - General workflow of the structural form finding and kinetic process.

By applying prestress to the membrane, small bending is being introduced in the GFRP profiles, and the overall skeleton form is found. Therefore, the final stressed shape of the overall structure must be defined initially, by the skeleton geometry and the weave orientation. The membrane prestress, depending on the weave orientation defined, will generate different initial shapes.

According to Forster and Mollaert (2004), the chosen level of prestress will normally be a compromise – low enough to reduce the work done during the installation whilst sufficiently high to maintain a sufficient prestress after losses due to "creep" of the membrane material over time. Although, for this structure, the prestress must also be high enough to compensate for the structure movement of adaptation, therefore avoiding the emergence of wrinkling in the membrane.

Therefore, it is desirable to achieve the purest form possible, without any influential initial imperfection on the skeleton to achieve the desired curvature. This way, the overall structure curvature desired must be explicitly created by the membrane prestress and implicitly defined by the geometry of the skeleton. The interaction between the two is what commands the global shape of the structure.

4.4.3. Weave orientation

The weave orientation plays a leading role in the before explained process, and furthermore, in the general structure loading and performance. The direction of the weave can control several aspects of the structure, not only the initial shape by interacting with the skeleton.

Quoting Forster and Mollaert (2004), unlike in more conventional forms of building construction deformability is seen as a useful and important characteristic of a fabric structure. Indeed due to its relatively low surface stiffness (both in-plane and out-plane), changes in geometry/surface are a fabric structure's primary response to externally applied load coupled with changes in stress distribution throughout its surface (Forster and Mollaert 2004). Therefore, if more global elasticity is desired, then the weave must be orientated in a 45° with the loading pattern, but this highly decreases the loading capacity, since the displacements will be bigger. On the other hand, if more global geometric stiffness is desired, then the weave should be orientated along the loading pattern of the structure.

In Sofistik®, the weave orientation translates by the local coordinates of the FEM area mesh element, simulating the membrane. Figure 86 shows the used local coordinate system for the membrane mesh. The XY plane is parallel to the membrane. Firstly, it is defined the direction that the skeleton force reactions to the membrane prestress must take. As explained before, the main objective is that, by applying prestress to the membrane, the GFRP profiles bend into the desirable shape. Therefore, it is the process of applying prestress to the membrane that is introducing small and barely noticeable imperfections to the global structure. These imperfections are then exploited to achieve the desirable shape further on.

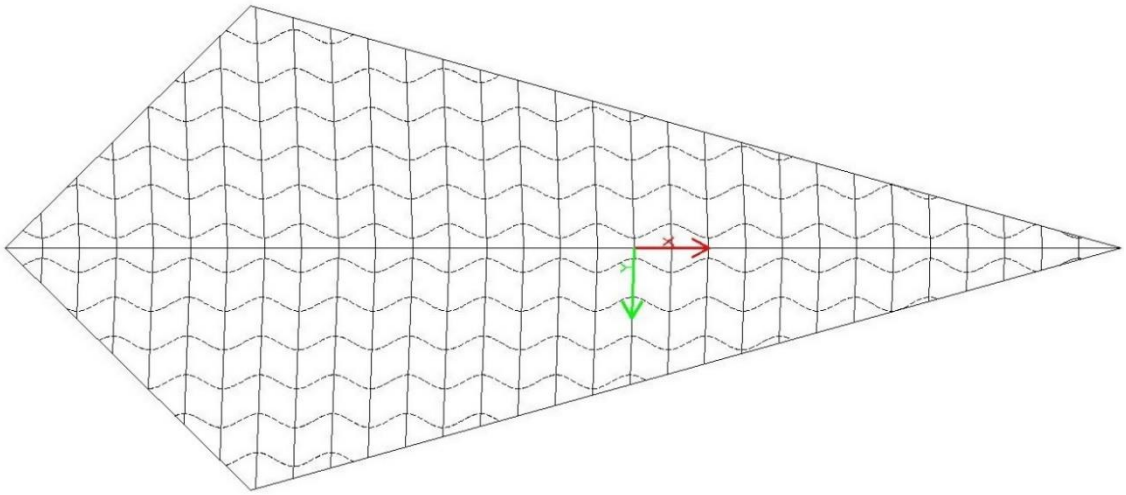

Figure 86 – Local coordinate system of the membrane mesh. Weft (undulated) is defined by the x direction and warp (straight) is defined by the y direction.

There is prestress applied to the weft (x) and to the warp (y) of the membrane fabric. Defining the local coordinate system for the membrane mesh as it shown in Figure 86 also defines the direction in which the prestress will be applied further on. This prestress will then be transmitted to the skeleton through tension forces. Thus, the skeleton profiles will be bent by these tensions and deform to find a new equilibrium position. Apart from the GFRP Young modulus, this equilibrium position depends solely on the boundary conditions, the geometry of the skeleton and the direction of the reaction forces from the pretension of the membrane. Therefore, the direction of the weft and warp of the membrane, represented by the local mesh coordinates shown in Figure 86, in relation to the skeleton plays significant importance to the final shape of the structure.

For this structure, it was found that the orientation that works better for the weave was having the weft parallel to the main spine. This implies a better distribution of the external actions along the spines and provides a little flexibility along the longitudinal direction of the structure, which is desirable for the kinetic adaptation. Also, by orientating the weave this way the geometric stiffness increases without losing the elasticity desired for being able to move along the adaptation. Figure 87 illustrates the decomposition of the reaction forces from the prestress, both for warp and weft directions.

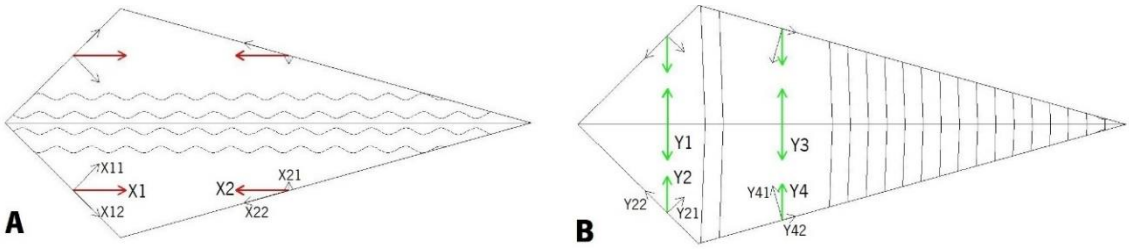

Figure 87 – Discretized force reactions on the skeleton by the weft (A) and warp (B) prestresses.

Regarding the main spine, it is desirable that no out of plane reaction occurs, since the location of the main spine is already the desired one and the bending direction is assured by the geometry of the skeleton, since the veins can transmit the bending motion, in conjunction with the oars, from the side spines to the main spine. Thus, as a way of avoiding indirect forces in the main spine, the weft direction is defined parallel to it, as illustrated in Figure 86. This way, there are only reactions in the warp direction, represented in Figure 87 as Y1 and Y3 forces, but these forces are balanced due to the symmetry of the structure.

On the other hand, the side spines need to bend slightly upwards. If there was no initial bending, after the form finding, when applying the displacement method to move the structure, these side spines could bend downwards or sideways, which is not sought for this structure. By analysing the forces X2 and Y4 shown in Figure 87, it is visible that the resulting reaction on the side spine forces the side spine to bend upwards ($X21 + Y41$) and the remaining force acts along the direction of the side spine ($X22 - Y42$). This effect generates the desired bending to the side spines.

The oars are the backbone of the entire process. It is visible in Figure 87 that the direction of the reaction points to the spine. By introducing a vein between these two elements, as explained in section 4.3.4, it allows to create a compression connection, avoiding the undesirable bending of the oars, as well as providing a more efficient way of transmitting the bending motion to the main spine.

4.4.4. Connections and membrane positioning

The connections of the system must be carefully analysed and possible restrictions that these may cause to the kinetic system must be studied with advanced 3D models or prototyping. Nevertheless, here a simple sketch is given on all the connections of the system. In order to do that, a simple nomenclature for the connections is shown in Figure 88. Then, the connections are presented and commented bellow.

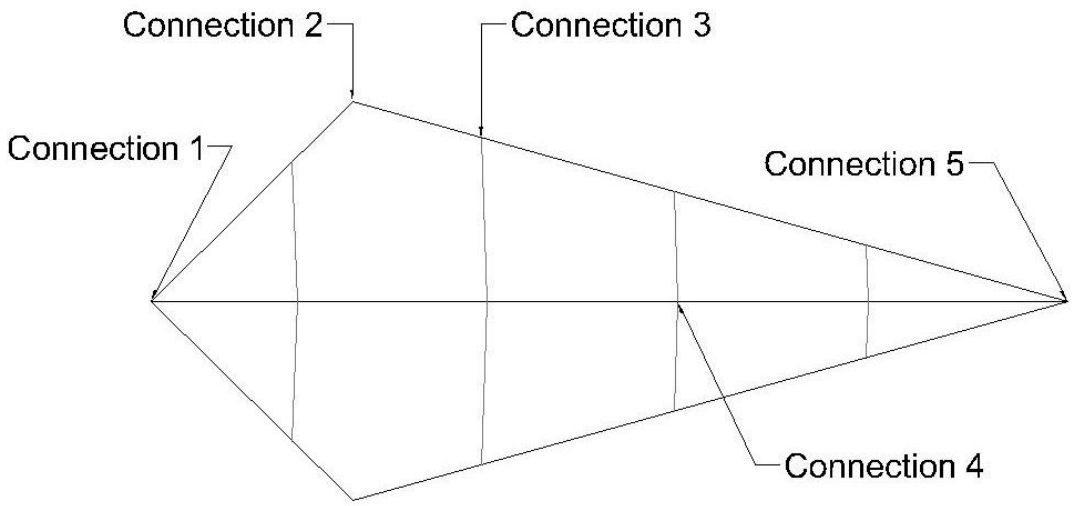

Figure 88 - Connection nomenclature and position.

A suggestion for the connection 1, being the connection between the oars and the main spine, is shown Figure 89. The connection is made with tubular steel fittings, where the GFRP profiles connect to. The membrane connects to the GFRP profiles with a fold followed by a welded seam, and it connects to the connection element by a steel plate and screws. The connection detail A is shown in Figure 94.

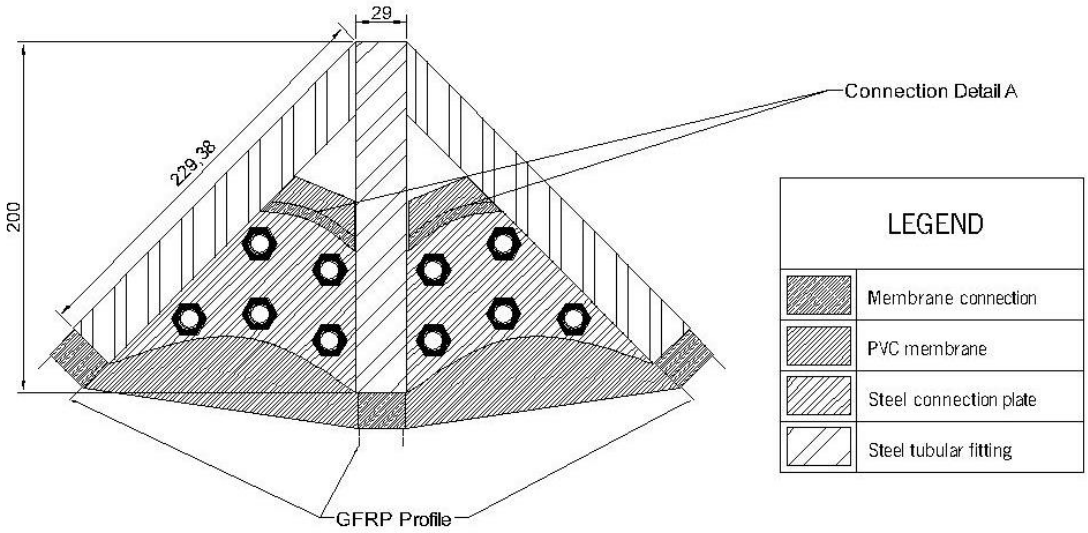

Figure 89 - Connection 1. Oars and main spine.

Following, the suggested connection 2, between the oar and the side spine, is shown in Figure 90. The principle is the same as in connection 1.

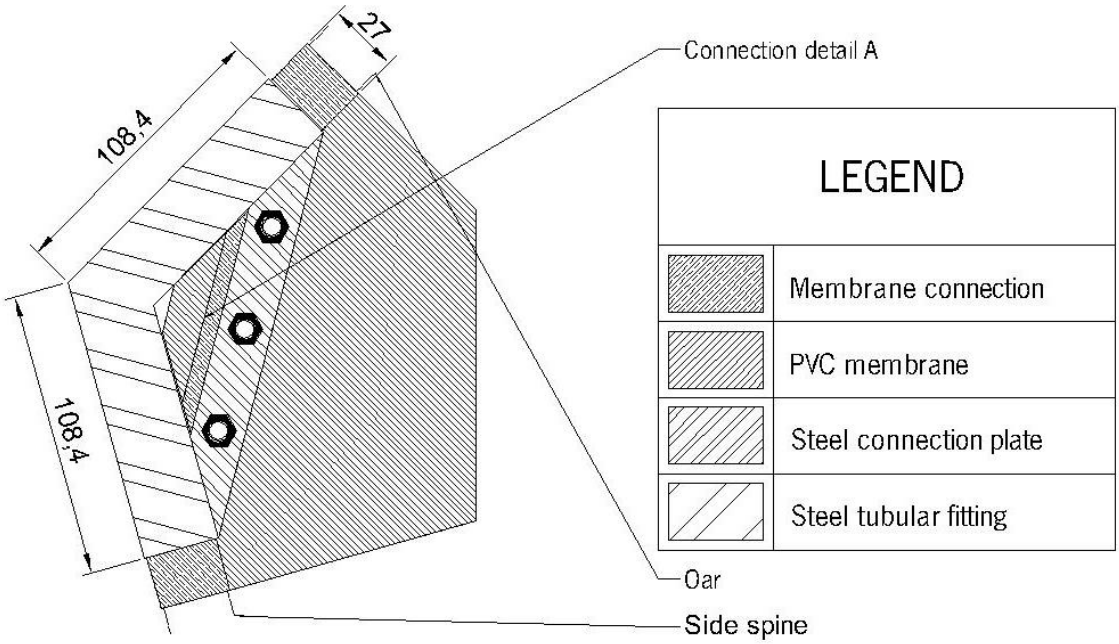

Figure 90 - Connection 2. Oar and side spine.

The connection between the veins and the side spine, is shown in Figure 91, as well as the connection between the vein and the main spine, is shown in Figure 92, respectively being connections 3 and 4. The views from these connections are bottom views. These connections use a bending release system, to allow the spine to rotate upwards or downwards while the spines bend. The connection between the two profiles is accomplished by a special connector. A small hole in the membrane fold is made, on the bottom part, in order to be able to connect the special connector to the spine. The membrane is connected to the profile by means of the same type of fold used in the other connections, followed by a welded seam. The detail of the welded seam is shown in Figure 95.

Here, a fundamental aspect must be discussed. As it is visible in the section A-A in Figure 91, the membrane is not positioned in the plane formed by the centreline of the main and side spines, and is placed above, may cause additional torsion stresses to the profiles that were not accounted for in the FEM model. Also, the points of the connections may also cause additional stiffness to the spines, compromising the bending as it was obtained in the FEM model. These aspects must be further studied in more detail.

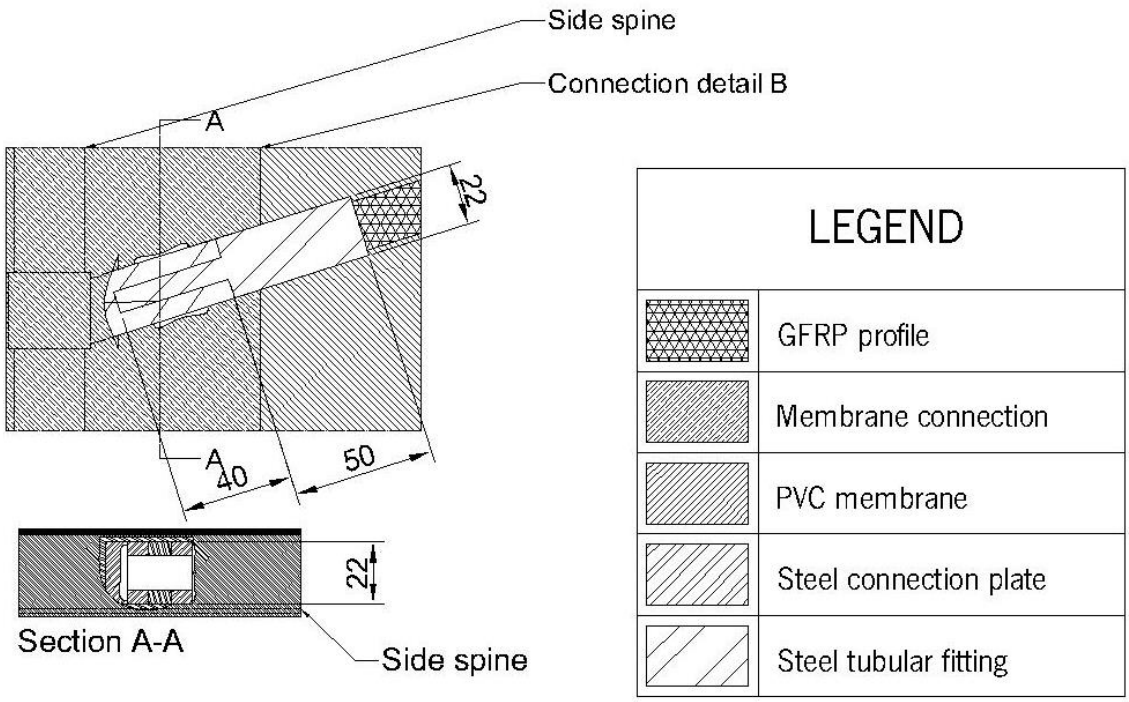

Figure 91 - Connection 3. Vein and side spine. Down view.

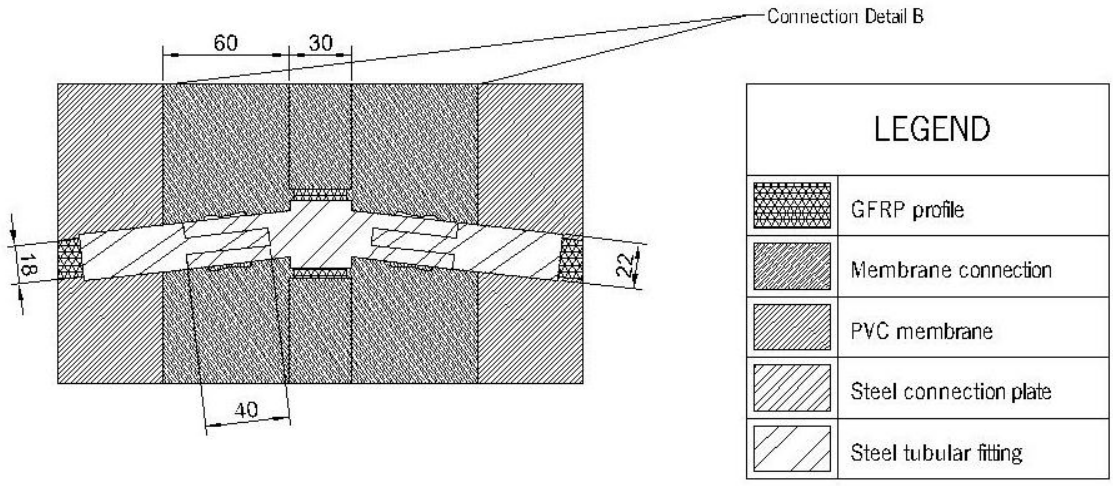

Figure 92 - Connection 4. Veins and main spine. Down view.

Lastly, connection 5, or the connection between all the spines, is shown in Figure 93. This connection is based on the same principle explained for the remaining connections. The connection details A and B used in the drawing are shown in Figure 94 and Figure 95, respectively.

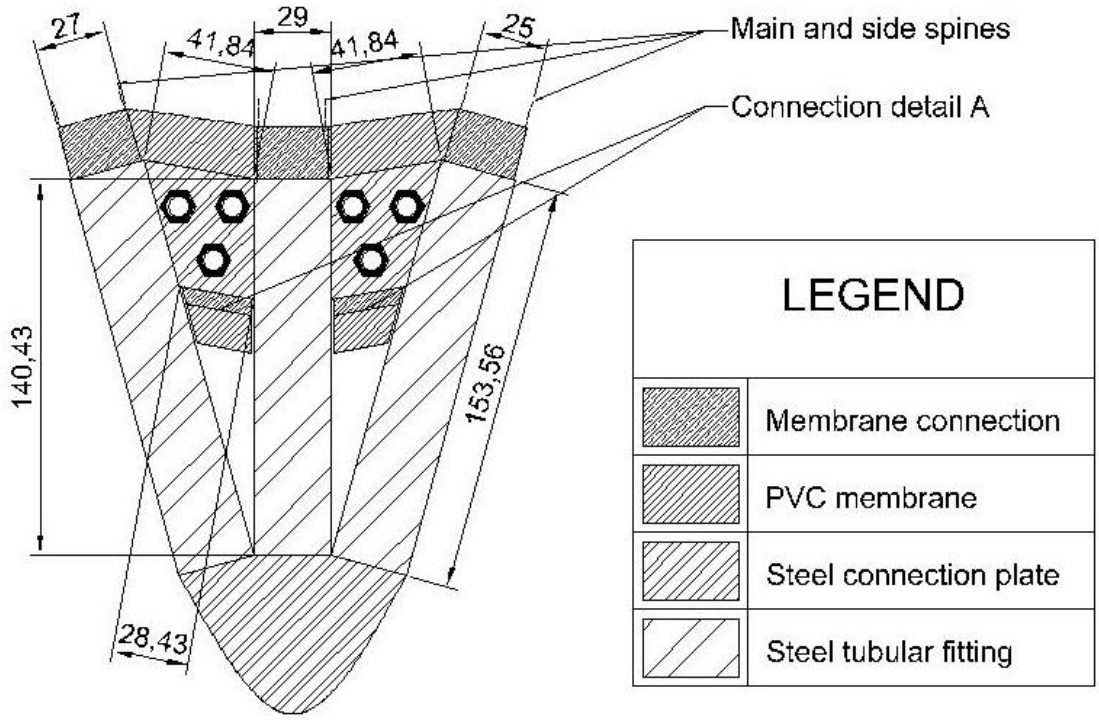

Figure 93 - Connection 5. Main and side spines.

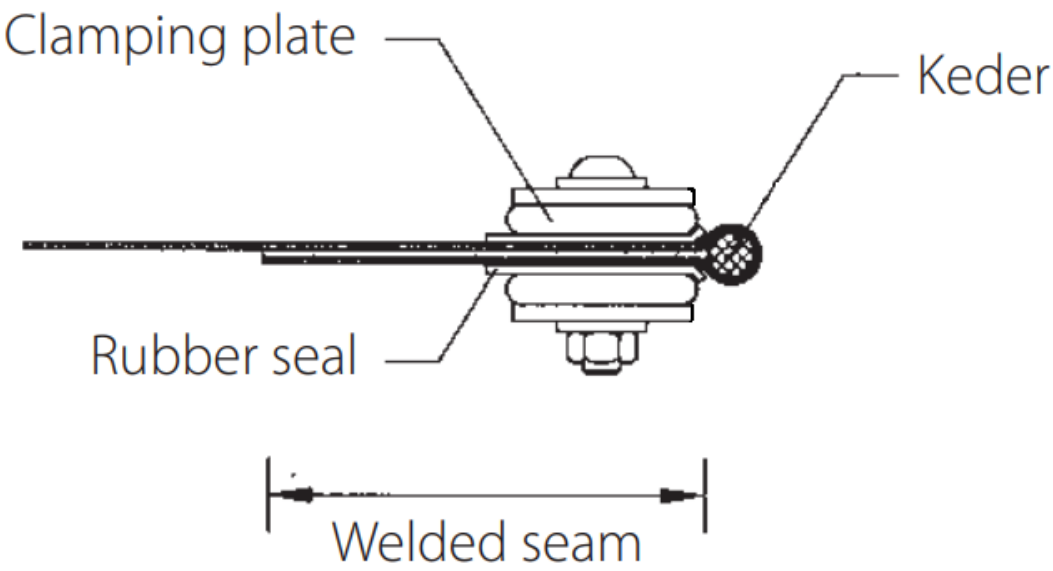

Figure 94 - Connection detail A. Edge joint, adapted from Seidel (2009).

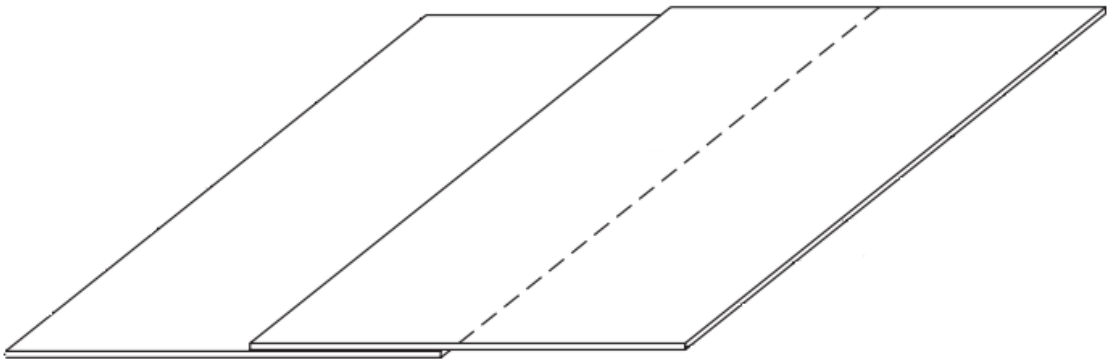

Figure 95 - Connection detail B. Surface joint, plain welded seam adapted from Seidel (2009).

4.5. Structural analysis

Now, that all structures presentations, modifications and general analysis basis were set, the analysis itself can be addressed. In this subchapter, the process of analysis was carefully explained. The processes adopted for applying large displacements to the structure were described. Finally, the results were analysed and conclusions were taken. Finally, some drawings were shown.

4.5.1. Execution plan

Apart from the strategy previously defined in 4.2.1, an execution plan is defined to represent the interaction between the CDB of Sofistik® and the user. Firstly, all the tasks in processes are identified, namely:

1. Input of the initial geometry system;
2. Exporting the geometry to the CDB;
3. Form finding;
4. Displacement loop of the structure;
5. System update;
6. Wind Loading;
7. Patterning;
8. Exporting the results.

The above-mentioned tasks are simplified and are explained in more detail along the present subchapter. Figure 96 illustrates the execution plan.

Adaptive hybrid case study

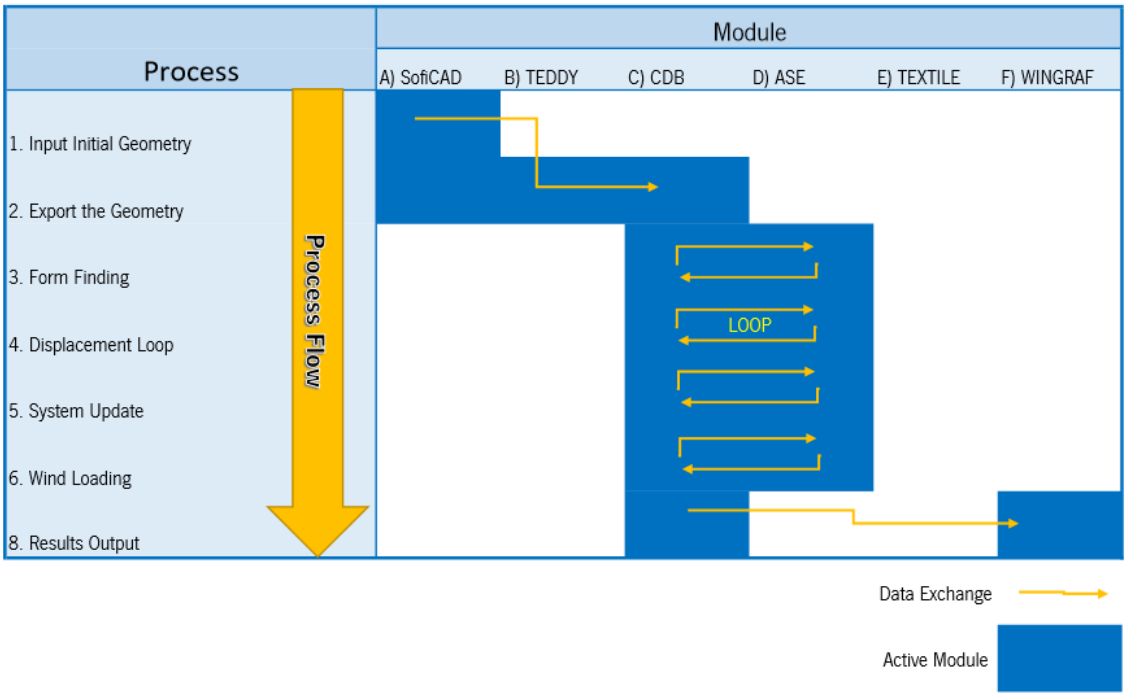

Figure 96 - Execution plan of the structural analysis process.

4.5.2. Form finding

As explained beforehand, the process of calculation for this type of structure must always start by finding form. In this particular case, the membrane prestress is applied and the form of the structure is achieved. Also, as explained in section 4.4.2, the geometry is manipulated in order to achieve the desired structure. This geometry is defined in the software by the process 1A defined in Figure 96. The values used for the material properties as well as the dimensions of the cross-sections used for each group element of the structure are summarized in Table 14.

Table 14 - Material properties and cross-sections used in the FEM model.

Skeleton GFRP material		**PVC coated polyester membrane material**	
$\boldsymbol{E = 20000\ N/mm^2}$	$E_{90} = 1000\ N/mm^2$	$E = 400\ N/m^2$	$E_{90} = 300\ N/m^2$
$\boldsymbol{\upsilon = 0}$	$\upsilon_{90} = 0$	$\mu = 0.2$	$\mu_{90} = 0.2$
$\boldsymbol{G = 3500\ N/mm^2}$	$K = 333\ N/mm^2$	$G = 4\ N/mm^2$	$K = 222\ N/mm^2$
$\boldsymbol{\gamma = 17\ kN/m^3}$	$\rho = 1733\ kG/m^3$	$\gamma = 12\ kN/m^2$	$\gamma_a = 2\ kN/m^2$
Cross-Sections	External Diameter (mm)	Internal Diameter (mm)	
Spines and Oars	25	23	
Veins	18	1	

The form finding process is done as an adaptation of the membrane form finding. Using the third order theory (TH3) problem, as explained in section 3.3.1, but introducing beams to the problem. The routine for solving this problem is defined by the process 3C defined in Figure 96. As before, by controlling group 14, the membrane's stiffness is reduced to almost 0 in order to be able to proceed with the form finding process. Then the prestress of $1\ kN/m$ is applied, both in the warp and weft directions. This process is stored in a disposable load case. After that, the TH3 problem is repeated, in order to compensate for any residual stresses. This second load case is stored as load case number 1 and is defined as the found form of the structure, after applying prestress to the membrane. Figure 97 illustrates the initial geometry and form found geometry for the structure.

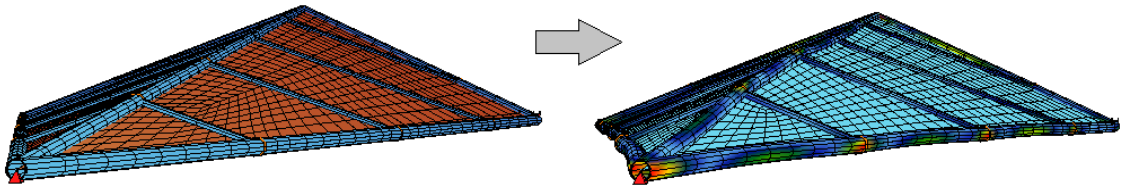

Figure 97 - Input geometry (left) to form found geometry (right).

Upon applying the prestress to the membrane and finding the form the results can be analysed graphically using the module WINGRAF. These results can be visualized in the Appendix. The results are subdivided in two groups, membrane related and skeleton related.

In general, the results turned out to be satisfactory. In Figure 98 maximum and minimum results for the various stress values of the membrane can be visualized. As shown, the local x and y stresses resemble much like the prestress input of $1\ kN/m$ in both warp and weft directions. Also, principal stresses are analogous to the local x and y stresses, since the shear stress is zero.

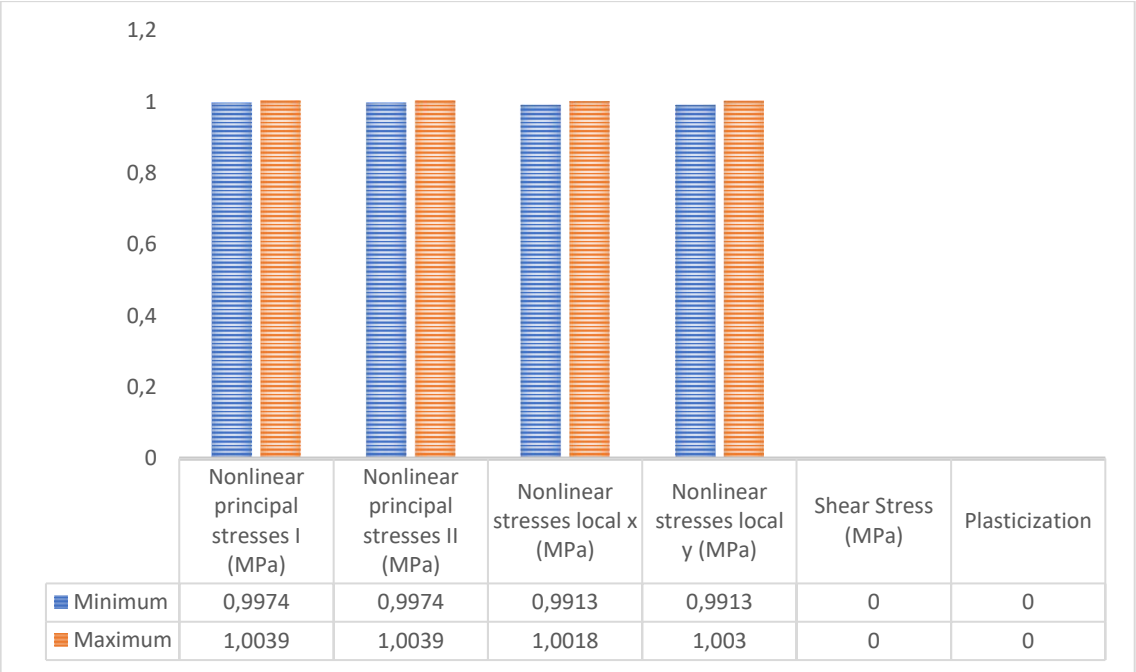

	Nonlinear principal stresses I (MPa)	Nonlinear principal stresses II (MPa)	Nonlinear stresses local x (MPa)	Nonlinear stresses local y (MPa)	Shear Stress (MPa)	Plasticization
Minimum	0,9974	0,9974	0,9913	0,9913	0	0
Maximum	1,0039	1,0039	1,0018	1,003	0	0

Figure 98 – Minimum and maximum results for the membrane mesh at the form finding load case.

The above-mentioned results are satisfactory, since the membrane mesh has been set to the value of $1\ kN/m$ in both directions. In this step, the shear stress does not exist because the structure has not yet experienced any significant movement from the skeleton or from external loads. The small deviations are acceptable. Also, there is no occurrence of plasticization of the membrane, which is likewise satisfactory.

Regarding the skeleton, also satisfactory results were achieved. The maximum compression and tension forces are shown in Table 15 and can be consulted in the Appendix. The values are generally very low for this load case, since the prestress applied is not very high and the geometry of the structure has been changed to receive this kind of stress. Yet, since the cross-sections are very small, the cross-section stresses tend to be greater. The results for the stresses are summarized in Table 16 and can be consulted in a report form in the Appendix. The values are satisfactory, since GFRP can usually get to much higher stress levels than these.

Table 15 - Skeleton's maximum compression and tension forces for the form finding load case.

GFRP Forces	Main Spine		Side Spines		Oars		Veins	
	Minimum Negative	Maximum Positive	Minimum Negative	Maximum Positive	Minimum Negative	Maximum Positive	Minimum Negative	Maximum Positive
N (kN)	-0,596	-	-0,338	0,0633	-0,381	-	-0,677	-
Vy (kN)	-	-	-0,291	0,29	-0,355	0,355	-0,0528	0,269
Vz (kN)	-0,229	0,250	-0,113	0,185	-0,044	0,0575	-	-
My (kNm)	-	-	-0,0087	0,0128	-0,008	-	-	-
Mz (kNm)	-0,0393	0,0143	-0,0389	0,0389	-0,0448	0,0449	-	-
Mt (kNm)	-	-	-0,0012	0,0012	-	-	-	-

Table 16 - Cross-sections with the highest tension stresses for the form finding load case.

Group	Section Code	Compression (MPa)	Tension (MPa)
Main Spine	10047; 0.000m	-95.99	81.64
Side Spine	10030; 0.111m	-90.19	91.84
Oars	10099; 0.000m	-102.48	102.18
Veins	230008; 0.121m	-44,98	33,92

4.5.3. Displacement of the structure

Now that the form of the structure was found, it must be moved through all the positions with very small increments to simulate the kinetic principle. Since this is an exploratory topic, two distinct approaches were taken. First the incremental displacement approach with linear increments. Then the elastic cable approach was done. Both these methods are explained in section 3.3.1. The nodes simulating both connections 2 (see Figure 88) are considered rolling supports that can translate in the x direction, and the node simulating the connection 5 (see Figure 88) is considered a pinned support.

4.5.3.1. Incremental displacement approach

Since in the form finding process the membrane's stiffness had been reduced to almost zero, in order to apply the initial prestress, in this step, the stiffness must be restored to its original value. This implies that the membrane is now a stretched mesh linking the skeleton together by means of tension. The loop applies a small and incremented displacement to the rolling supports. This process bends the elastic spines into form. Figure 99 shows an overview of the process. Each stage represents an iteration of the

displacement loop. For example, in this particular case, a total of 24 stages are calculated, displacing a total of 12cm. This means that for each iteration, a displacement of 5mm is applied to the structure in both supports.

Also, as Figure 100 shows, it was possible to use the same process but only apply the displacement in one of the supports of the structure. This way, a single sided bend is achievable. Global instabilities did not occur, but further confirmation on the plasticization shows that this process is only viable for a small number of steps. Larger steps imply the plasticization of the membrane. The overall process can be further improved to allow this movement, but this was out of this project main objective. Therefore, only the double-sided movement, shown in Figure 99, is analysed.

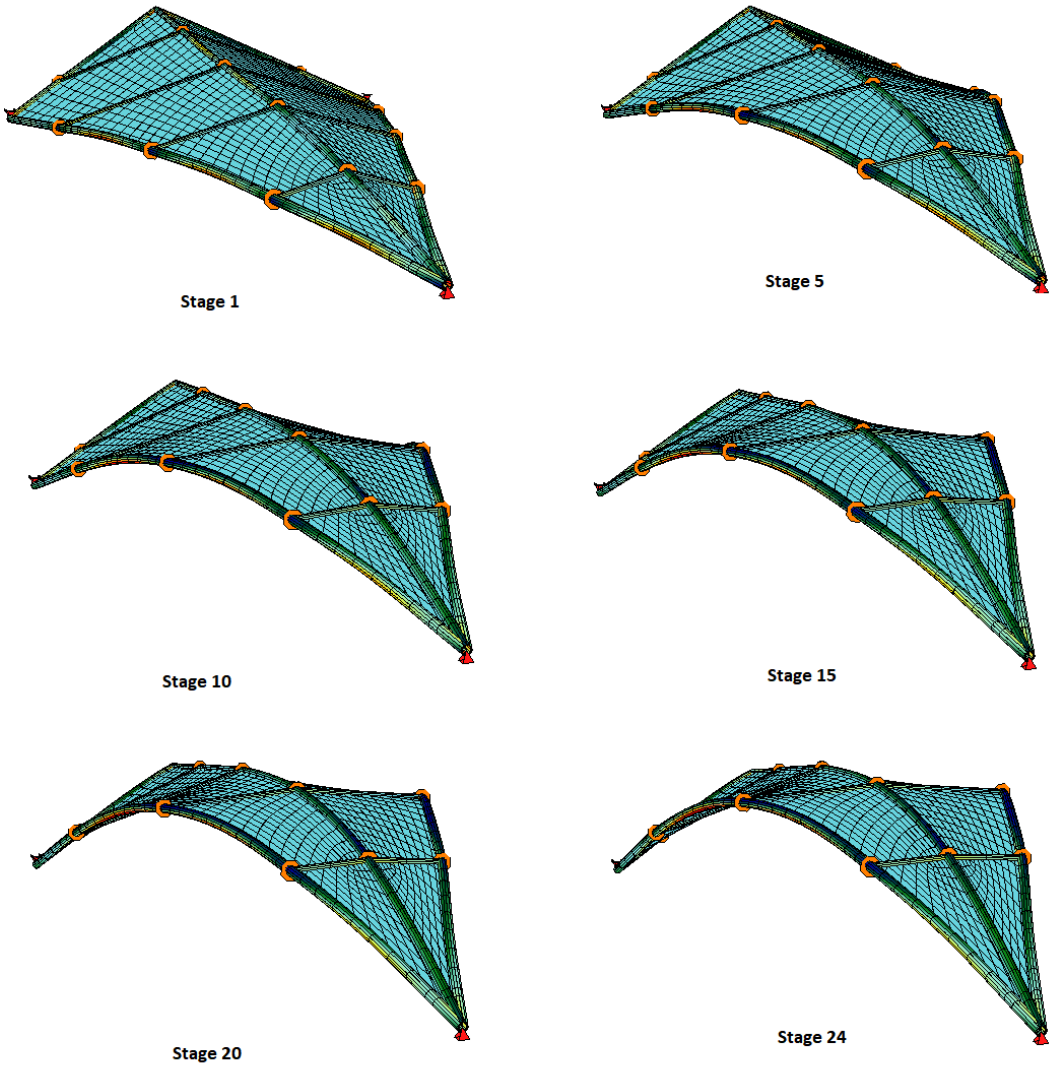

Figure 99 - Distinct stages of the structure.

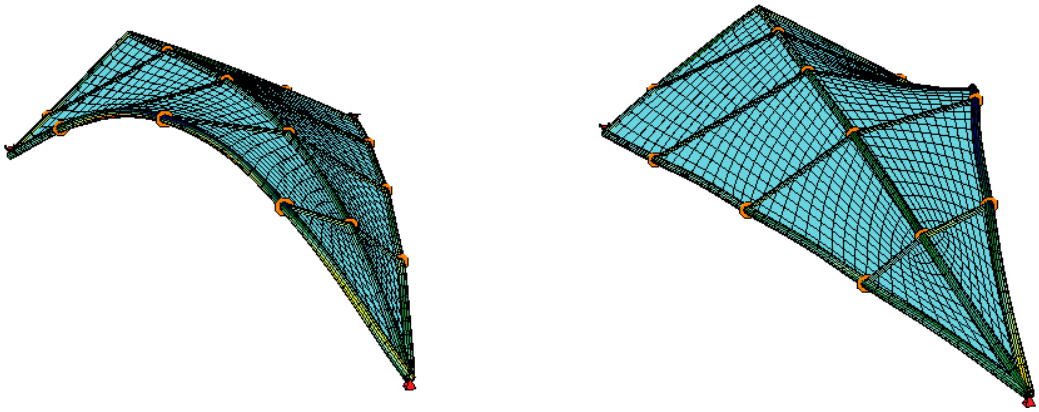

Figure 100 - Single side movement.

For matters of simplicity, only one of the stages is exposed, since the results are very extensive exposing the full results would generate a rather complex document. Therefore, stage 24 is chosen, since this is the stage more prone to plasticization and wrinkles, being the displacement stage with further movement. The graphic results for this load case can be consulted in the Appendix.

The maximum results relating the membrane are summarised in Figure 101. The results are not as satisfactory as during the form finding, but acceptable. Comparing to the form finding results, the principal stress has now decreased, since a great modification affected the overall geometry of the structure. This means that some shear stress is now present, which can be accepted since it has very low values. Also, there is a big loss of tension in the y direction located in the connection between the oars and the side spines. This loss of tension could be optimized, for example, by allocating another vein to this part of the structure. Also, some plasticization occurs, but this plasticization is very small and localized, and FEM meshes are known to present this problem, therefore this is likewise acceptable.

Adaptive hybrid case study

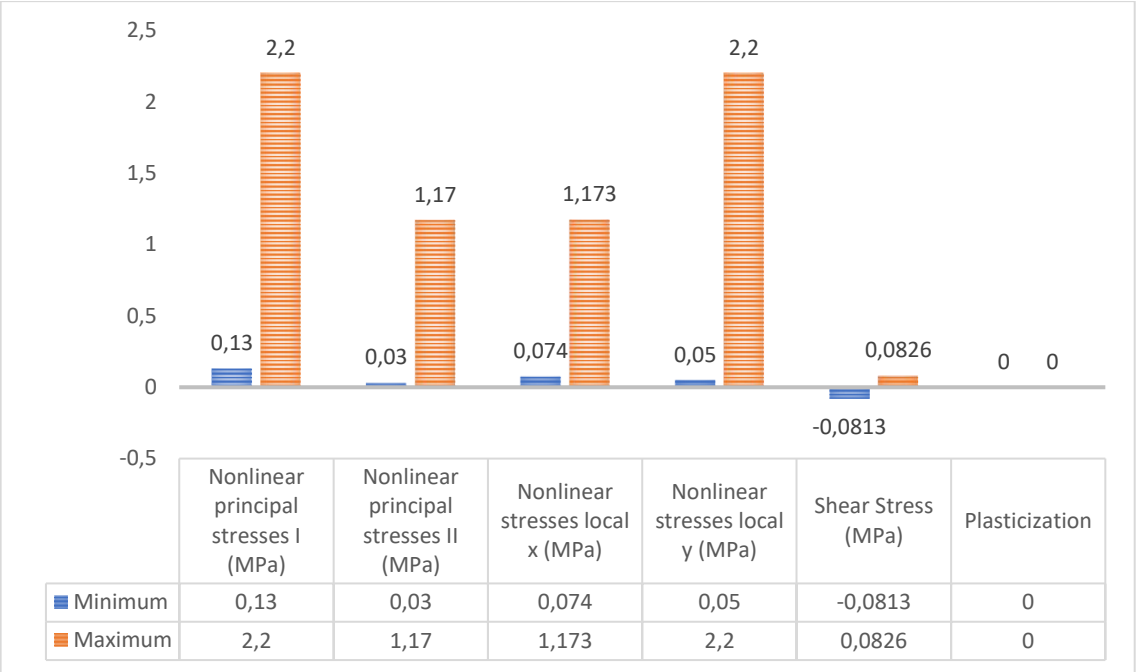

Figure 101 – Minimum and maximum results for the membrane mesh for load case 24.

Regarding the skeleton, the results of the forces are summarized in Table 17. It's is noticeable that the main spine has a loss of positive bending force in the span between the veins. This can be explained by the membrane tension, which is pulling on the main and side spine, therefore reducing this force. Also, the veins are generally more loaded in the front which, in conjunction with the loss of tension in the back of the structure, suggests that a possible optimization could be increasing the angle of the veins of the back of the structure.

Table 17 - Skeleton's maximum positive and negative forces for the stage 24.

GFRP Forces	**Main Spine**		**Side Spines**		**Oars**		**Veins**	
	Minimum Negative	Maximum Positive	Minimum Negative	Maximum Positive	Minimum Negative	Maximum Positive	Minimum Negative	Maximum Positive
N (kN)	-0,488	-	-0,471	-	-0,242	0,0538	-0,889	-
Vy (kN)	-	-	-0,413	-0,413	-0,323	0,323	-0,141	0,142
Vz (kN)	-0,155	0,207	-0,147	0,159	-0,02	0,0552	-0,0022	0,0022
My (kNm)	-0,0646	0,0161	-0,0754	0,0238	-0,0255	0,0129	-	-
Mz (kNm)	-	-	-0,0467	0,0467	-0,0507	0,0507	-	-
Mt (kNm)	-	-	-0,0027	0,0027	-0,0151	0,0151	-0,0108	0,0108

Table 18 shows the cross-sections with highest stresses. It is visible that most of the cross-sections are not the same as for the form finding load case. This occurs because there is a distribution of stresses along the movement of the structure. Also, the stress stiffening effect obtained by applying prestress to the membrane, also prestresses the skeleton. In some areas this prestress is beneficial, being annulated by the movement of the structure, thus balancing some initial high stresses. Albeit the high tensions presented in the side spines, this tension falls within the admissible tension stresses of GFRP. A report of this cross-section stresses can be consulted in the Appendix.

In short, the stage 24 seems to be feasible, but the need for further optimization is still present. Although, the main problem when optimizing this type of structure is that the changes always must be made in the initial geometry, which can cause form finding instabilities. Therefore, one should never have in mind optimizing the structure just for one specific stage, but with all the stages in mind.

Table 18 - Cross-sections with the highest tension stresses for the stage 24, displacement approach.

Group	Section Code	Compression (MPa)	Tension (MPa)
Main Spine	10047; 0,000m	-151,15	145,94
Side Spine	10016; 0,052m	-199,66	186,96
Oars	10099; 0,000m	-144,85	136,47
Veins	230024; 0,000m	-51,13	35,03

4.5.3.2. Elastic Cable Approach

As explained above, since this is just an exploratory approach, an alternative method for displacing the structure had to be used. This method is an adaptation of the method initially suggested by Lienhard, La Magna et al. (2014). According to Lienhard, La Magna et al. (2014), the proposed approach greatly simplifies the setup of the simulation model, freeing the analyst from the difficult and in some cases impossible task of precisely defining the paths of the nodal displacement needed to perform the form finding of the bending active structures.

The employed cable elements work with a temporary reduction of elastic stiffness which enables large deformations under constant pre-stress. The cable element thereby becomes a free load defined by the magnitude of pre-tension and the rigidity of the elements in between which it is contracting (Lienhard 2014). Figure 102 shows the elastic cable approach applied to the structure. In this example a simple

elastic cable is incrementally prestressed, thus pulling on the rolling supports and thereby bending the structure.

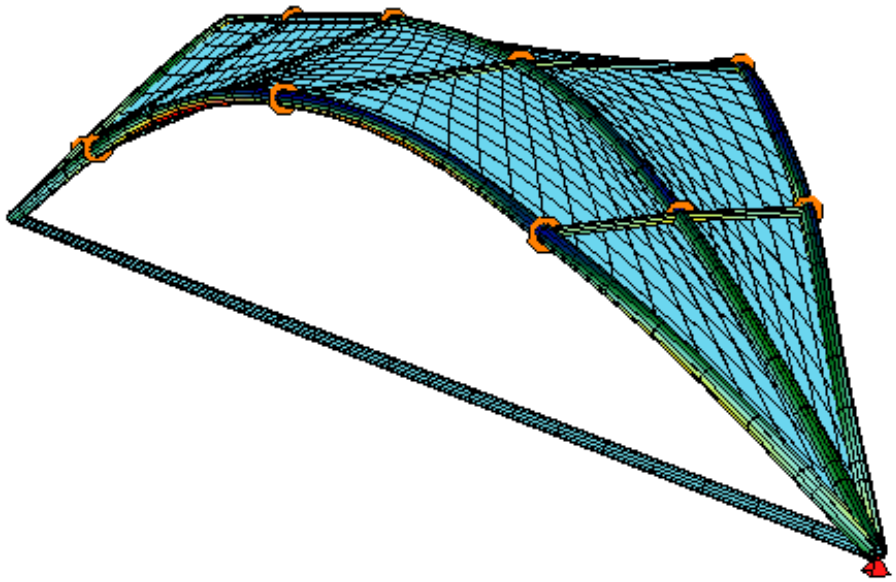

Figure 102 - Example of the elastic cable approach applied to the structure.

Table 19 shows the representation of the cross-sections with highest stresses for each type of element. It is visible, when comparing it with Table 18, that small deviations occur. This is due to a different approach being used. The elastic cable approach is a faster solution but increments the displacements exponentially, by using the prestress in the cable to bend the whole structure. This is fine when form finding a simple bending element, but when using it with larger structures minor differences may occur. Also, the majority of the results don't vary much, but the maximum occurs slightly ahead or before, which may also be a signal that the results obtained by an incremental displacement approach are more reliable than the ones obtained by the elastic cable approach.

Also, for this specific case, the linear incremented displacement simulates better all the possible positions of the structure, thus it is a better method for simulating the kinetic process. Notwithstanding, both results present viable results, yet further study on the comparison of both methods when applied for entire structure is required.

The graphical results obtained by this method can be accessed in the Appendix.

Table 19 - Cross-sections with the highest tension stresses for the stage 24, elastic cable approach.

Group	Section Code	Compression (MPa)	Tension (MPa)
Main Spine	1039; 0,000m	-147,58	140,40
Side Spine	10014; 0,017m	-201,36	188,88
Oars	10099; 0,000m	-130,47	125,96
Veins	230027; 0,000m	-64,22	46,12

4.5.4. External actions

4.5.4.1. Adaptive principle

Analysing external loads in an adaptive structure is a task of great complexity. A particular stage may not be the best position for that specific load, meaning that the structure needs to adapt. This adaptation principle consists in moving, by means of an automated motor driven system, the side spines thus modifying the overall geometry. By doing this, the structure can adapt to different load scenarios, increasing the performance of the overall system. A small study is done to demonstrate the effect of the geometry change in the overall response of the structure. Next, a very brief study of the effect of the wind in each stage is presented.

4.5.4.2. Wind

The wind is the action that represents more importance in the structure also, it is a highly variable load, which can imply dynamic effects. Ideally the structure would be studied in wind tunnels, this would allow for a more elaborated study, including a very perceptive study of the adaptive principle. However, this was not possible. According to Forster and Mollaert (2004) in membrane structures, wind is generally considered as a static load case, defined by a dynamic pressure multiplied by a pressure coefficient C_p. This coefficient depends on the form of the structure, since different geometries lead to different wind reactions. Also, the C_p value is usually obtained by wind tunnel tests or from previous work done on similar geometry. however, the present geometry is unique and has not been studied regarding this aspect yet.

As an alternative, a small static study is done. The study here presented only aims to learn, on a very basic level, how the structure reacts to an external applied load, and not to do a fully safety calculation of the wind in the structure. For that purpose, wind tunnel tests are recommended to study in more detail

the C_p values. As said before, the form of the structure is of greater importance for load response. Firstly, the overall geometry changes, which implies that the response must also be of different nature. Secondly, the spring effect of the skeleton GFRP prestresses the spines, making them more agile to certain actions.

Two upwards and downwards loads are applied, representing wind positive and negative pressures in the structure, in 6 distinct stages of the structure. These chosen stages are stage 0, 5, 10, 15, 20 and 26. This way, a wider insight about the structure response to the distinct stages is obtained. As matter of comparison, the displacement of the global z coordinate was chosen. Also, the maximum values possible without getting global instabilities were applied, which doesn't mean that the structure isn't failing in matters of wrinkling or plasticization of the membrane. The results only show the limits of global stability of the structure.

Figure 103 shows a graphic representing the maximum pressure load applied upwards and downwards in the structure. It is clearly visible that for higher deformation stages a higher pressure can be applied. Also, a smaller range of upwards pressure is applied, without causing instabilities. This may relate to the fact that upwards wind can move the rolling supports, therefore increasing the bending. The software probably considers this movement as an instability. This does not happen for the downwards load because the structure is restrained to move backwards by the rigidity of the cable, which has been set to normal during this analysis.

Low stages of the structure have a very small wind load capability. Although, this model does not consider that the GFRP profiles are supported by the gutters, as originally suggested by Costa (2017). Albeit, the bending of the GFRP clearly is necessary for supporting higher loads.

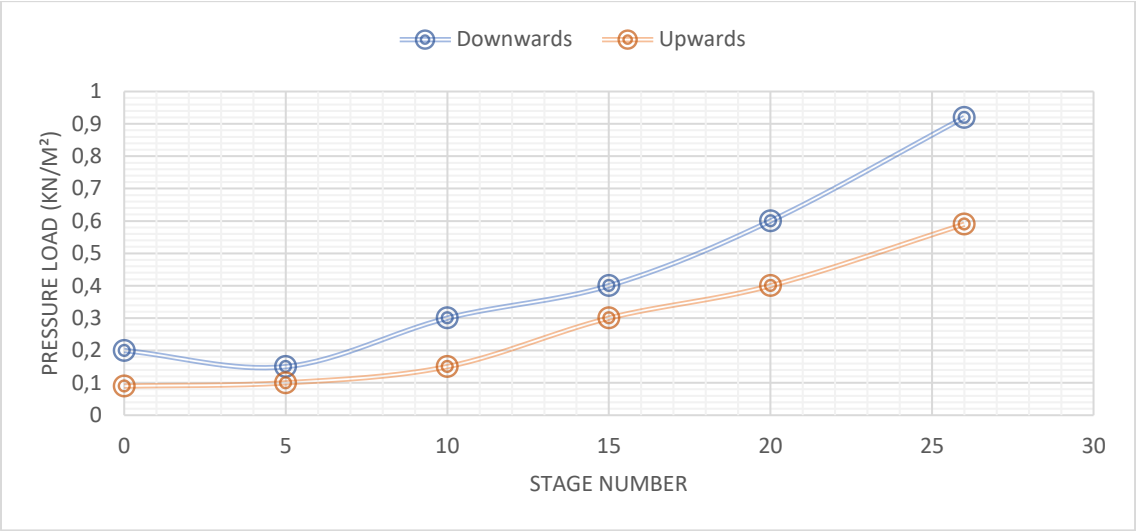

Figure 103 - Maximum pressure load per stage without global instability.

Figure 104 shows that increasing the structure stage, by incrementing the global X position of the rolling supports, increases both the maximum and minimum global Z displacement of the structure. At first glance, this implies that the tangent stiffness is not increased by the bending of the profiles. Thus, as the stage of the structure increases, the applied load also increases, meaning that it is natural to obtain also larger displacements.

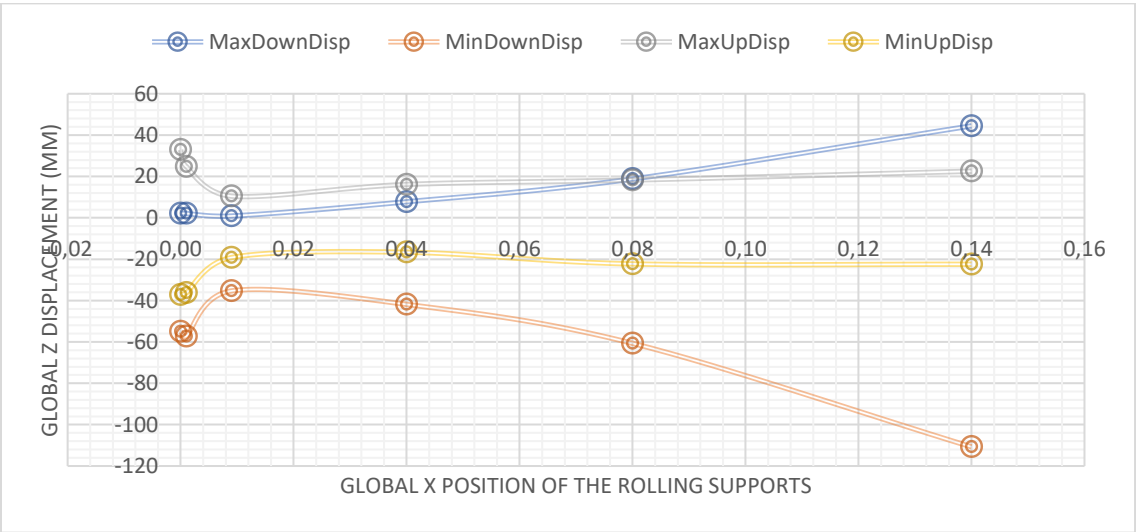

Figure 104 – Maximum and minimum global Z displacement along the adaptation of the structure.

On the other hand, Figure 105 shows an easier understanding of the evolution of the global Z displacement along the adaptation of the structure. In this graphic the displacement has been reduced based on the applied load in each stage. In this example, it is clear that the exponential gains on adapting

the structure stabilize at the 4cm stage. Further movement only adds linear gains. Thus, structurally speaking, most of the adaptive movement should occur after the 4cm. For say, if it is a windy day with medium pressures the structure should automatically be taken to, for example, stage 10, and only be adapted from there.

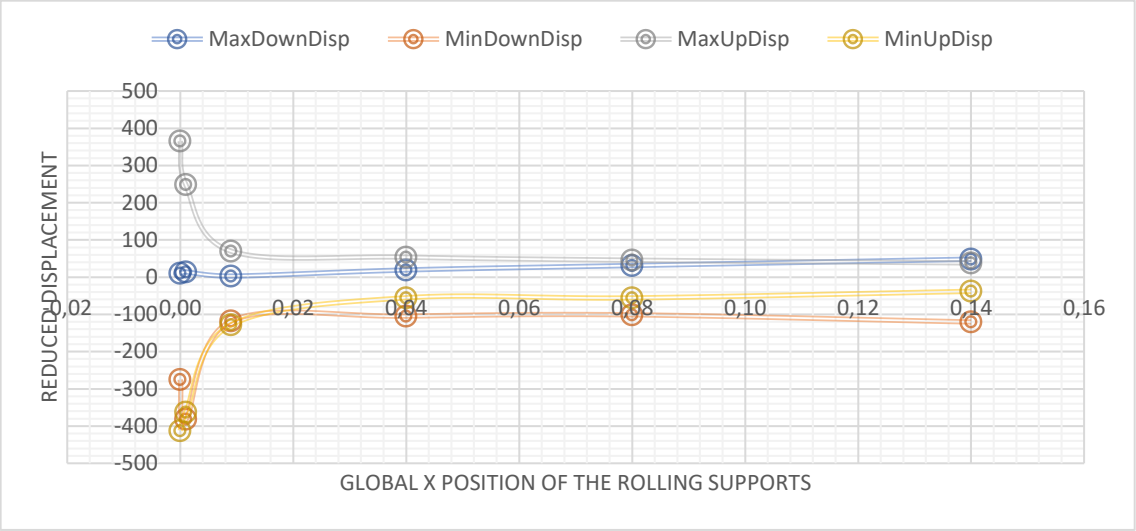

Figure 105 - Reduced global Z maximum and minimum displacement along the adaptation of the structure.

4.5.4.2.1. Wind pressure by Eurocode 1

According to Forster and Mollaert (2004), the site wind speed and dynamic pressure can be derived as described in EC1, part 2.4. For that matter, the wind pressure is calculated according to Eurocode 1. This value is then compared to the values obtained above.

According to En (1991), the wind pressures are obtained in the following manner:

1. By the national appendix, chart $NA.I$, considering A zone:

$$v_{b,0} = 27\ m/s \tag{17}$$

2. Then, the base velocity of the wind is calculated:

$$v_b = c_{dir} \times c_{season} \times v_{b,0} = 27\ m/s \tag{18}$$

3. According to the national appendix, chart $NA - 4.1$, assuming class IV:

$$z_0 = 1 \tag{19}$$

$$z_{min} = 15 \tag{20}$$

4. The value of k_r is obtained by:

$$k_r = 0{,}19 \times \left(\frac{z_0}{z_{0,II}}\right)^{0{,}07} = 0{,}19 \times \left(\frac{1}{0{,}05}\right)^{0{,}07} = 0{,}234329 \tag{21}$$

5. The roughness coefficient, assuming $z = 15$, is calculated by:

$$c_r(z_{min}) = k_r \times \ln\left(\frac{z}{z_0}\right) = 0{,}234329 \times \ln\left(\frac{15}{1}\right) = 0{,}634574 \tag{22}$$

6. Then, the average velocity of the wind is determined by:

$$v_m(z) = c_r(z) \times c_0(z) \times v_b = 0{,}634575 \times 1 \times 27 = 17{,}13\ m/s \tag{23}$$

7. Now, the turbulence intensity is calculated by:

$$I_v(z) = \frac{\sigma_v}{v_m(z)} \tag{24}$$

8. Replacing σ_v, comes:

$$I_v(z) = \frac{k_r \times v_b \times k_I}{v_m(z)} = \frac{0{,}234329 \times 27 \times 1}{17{,}13} = 0{,}369345 \tag{25}$$

9. Finally, the dynamic peak pressure can be calculated as shown in equation (26):

$$q_p(z) = [1 + 7 \times I_v(z)] \times \frac{1}{2} \times \rho \times v_m^2(z)$$
$$= [1 + 7 \times 0{,}369345] \times \frac{1}{2} \times 1{,}25 \times 17{,}13 \quad (26)$$
$$= 657{,}558\ N/m^2 = 0{,}66\ kN/m^2$$

According to Forster and Mollaert (2004), the local C_p values for both internal and external surfaces can be derived using appropriate codes and papers. Eurocode 1 is one of these papers. Therefore, the C_p values are obtained from En (1991). Thus, this procedure may not be very accurate.

Considering that the structure has only two inclination planes, and that the membrane is securely fixed to the skeleton, it can be considered that each of the faces represent the H and I face represented in the section 7.2.5 of the En (1991). Thus, since the angle $\alpha = 20°$, the values of the pressure coefficients can be obtained by consulting the tables in chart $7.4a$ and chart $7.4b$. The values obtained are represented in Table 20.

Table 20 – External coefficients for wind pressure.

Zone	**Wind Direction**			
	$\theta = 0°$		$\theta = 90°$	
H	0,263	-0,267	0	-0,667
I	0	-0,4	0	-0,5

These values are then combined with the values presented in Table 21. The values must be combined with the ones of different sign since, for example, internal positive pressures attenuate external positive pressures, thus internal positive pressures must be combined with external negative pressures and vice-versa. The highest and lowest coefficients obtained are then multiplied by the dynamic peak pressure obtained in equation (37). These values are shown in Table 22.

Table 21 - Internal coefficients for wind pressure.

Negative Pressure	**Positive Pressure**
-0,3	0,2

Table 22 - Final maximum and minimum coefficients and loads

	Downwards Action	**Upwards Action**
Coefficient	0,463	-0,967
Load (kN/m^2)	0,306	-0,638

From this approach it is clear that the structure can withstand higher loads than those deduced with this Eurocode approach. Although this method of finding the wind load can be unreliable when applied to membrane structures. For a complex structure like this one, where the geometry can be updated, wind tunnel tests should be carried out in order to find the real pressure coefficient for the wind load.

Although, it is also obvious that the structure has some potential to withstand these magnitude loads, without instabilities. Yet, plasticization of the membrane may occur for higher loads. This was not the main objective of this primeval analysis. Thus, optimization of the process for analysing wind and also the plasticization of the membrane should be tackled in the future case studies of this project.

4.5.4.3. Other actions

For the purpose of this work, other actions were not analysed. Wind is the most complex action for membrane structure, therefore this action was slightly addressed. Although other actions like snow are also important ones, depending on the zone the structure shall be applied to.

5. CONCLUSIONS AND FURTHER IMPROVEMENTS

5.1. Conclusions

In this work, an exploratory structural approach to hybrid adaptive structures has been made. The building blocks of textile hybrid structures were studied, namely membrane structures and bending-active structures. These structures are considered rather complex due their inherent nonlinearities, both material and geometric. Thus, the structural aspects of these structures were discussed and presented. Also, routines for solving this type of problem are proposed, presented and validated, through interaction with the FEM software Sofistik®.

In general, the results of these validations (either against existing experiments or calculations) turned out to be satisfactory. Firstly, the membrane results have slightly deviations, but this can easily be explained by the difference of approach, as well as the use of a different mesh type. Then, the results from the spring experiment were also satisfactory, in spite of the difficulties felt during the experimental procedure: it is a very small-scale experiment and some difficulties also appeared when tracing the exact position of curves. Also, considering that satisfactory results were obtained in the validation through the tabled results based on the work of Adriaenssens and Barnes (2001), it can be considered that author's use of Sofistik®, together with the above defined routines, is a viable option for simulating bending as well as analysing membrane structures.

After the positive validation of these routines, they are applied to the hybrid concept and the kinetic adaptive principle is simulated by applying very small deformations through an interactive loop. The project suggested by Costa (2017) was selected, and it was found to be of great complexity. The adaptation principle and the improvements to the skeleton should be further studied with structurally and kinetically accurate physical models to understand all the principles of this movement. However, the results obtained through the structural adaptive principle by the effective pre-stressing of the bending-active elements are suitable, fitting in the previously defined scope of this work. Also, it has been proved that is possible to accurately simulate the interaction between bending-active elements and membranes through the Sofistik® suggested routines, as well as the kinetic adaptive principle. As well, the importance of an earlier study of the geometry and its impact in the overall structural function and performance is clearly exposed during the development of the work. The changes performed to the geometry and weave orientation by analysing the membrane-skeleton system revealed a major importance in the achievement of favourable results during the structural analysis. The definition of form through the application of

prestress to the membrane structure represents, in the same way, an accordance with the usual design approaches, defining a correct path the further developments of this work.

Finally, it is possible to conclude that through the application of the routines herein defined, the concept of adaptive textile hybrid structures is possible to be analysed. Through these developments, a strong foundation is set to possible further developments of these principles, thus opening a window to a concept that shows great importance in the future of structural engineering.

5.2. Further improvements

Considering the further development of this project, a wider study about the material properties should be done, specifically by developing laboratory test in GFRP and membrane materials, in order to acquire precise properties to simulate in the software. Also, fatigue tests are also very important to the further developments of this project, due to the kinetic principle of the structure. The possibility of developing this project with a group composed by architects and engineers should likewise be considered.

Additions to the method of calculation are also possible. The integration of the calculation power of Sofistik® with the manipulation supremacy of Rhinoceros 3D® and Grasshopper can also be studied in order to generate a more interactive and fluid process. Ideally, an automatic system would be set to optimize the structure geometry. Doing this would require an advanced interaction between Sofistik® and Rhinoceros 3D®. Using Grasshopper's optimization algorithms to find the perfect geometry and, then, using Sofistik® to proceed with the FEM form finding. However, this means that a way of outputting the stress results should be available, as well as an integration with an advanced software, like Rhinoceros 3D® Grasshopper. This way one could change the geometry by means of a smart optimization algorithm.

Also, the membrane positioning should be further studied. A way of simulating the interaction of the veins with the membrane could be found. Likewise, considerations should be made about the position of the membrane within the spines. Concerning the external actions, the influence of the wind dynamic effects on the structure overall geometry could be further developed. In this field, prototypes in conjunction with wind tunnels may provide a better understanding of the C_p values. Finally, the construction of a complete adaptive structure is a possible scenario, by paring each load case should with every stage of the structure, creating an adaptation matrix relating every load case to its adaptive stage. This could then be introduced in an algorithm that reacts to different load circumstances.

6. BIBLIOGRAPHY

Adriaenssens, S. and Barnes, M.R. (2001), "Tensegrity spline beam and grid shell structures", *Engineering structures*, **23**(1), 29-36.

Aziz, M.S. (2016), "Biomimicry as an approach for bio-inspired structure with the aid of computation", *Alexandria Engineering Journal*, **55**(1), 707-714.

Beccarelli, P. (2015), *The design, analysis and construction of tensile fabric structures*, Springer

Brancart, S., De Laet, L. and De Temmerman, N. (2016), "Deployable Textile Hybrid Structures: Design and Modelling of Kinetic Membrane-restrained Bending-active Structures", *Procedia Engineering*, **155**, 195-204.

Campbell, D.M. (1991). "The unique role of computing in the design and construction of tensile membrane structures", *American Society of Civil Engineers Second Civil Engineering Automation Conference*.

Costa, L.M. (2017), *Desenvolvimento de Estrutura Arquitetónica Têxtil Inteligente e Ativa em Flexão*, University of Minho

En, B. (1991), *1-4: 2005 Eurocode 1: Actions on structures—General actions—Wind actions*, NA to BS EN

Forster, B. and Mollaert, M. (2004), *European design guide for tensile surface structures: TensiNet*, TensiNet

Galilei, G. (1914), *Dialogues concerning two new sciences*, Dover

Galliot, C. and Luchsinger, R. (2009). "Non-Linear properties of PVC-coated fabrics used in Tensairity structures", *17th International Conference on Composite Materials*.

GARTI, F., Tutor, I., UdK, C.T. and Gengnagel, I. "Active-Bending Hybrid Structures".

Gengnagel, C., Alpermann, H. and Lafuente, E. (2013), "Active bending in hybrid structures", *Form—Rule/ Rule—Form*, **2013**, 12-27.

Gomes, C.A.F. (2014), *Use of generative algorithms and shape optimization strategies in structural design*

Henrysson, E. (2012), "Conceptual design and analysis of membrane structures".

Houtman, R. and Orpana, M. (2000), "Materials for membrane structures", *Bauen mit Textilien*, **4**, 27-32.

Keller, T., Tirelli, T. and Zhou, A. (2005), "Tensile fatigue performance of pultruded glass fiber reinforced polymer profiles", *Composite structures*, **68**(2), 235-245.

Knippers, J., Cremers, J., Gabler, M. and Lienhard, J. (2011), *Construction manual for polymers+ membranes: materials, semi-finished products, form finding, design*, Walter de Gruyter

Knippers, J. and Speck, T. (2012), "Design and construction principles in nature and architecture", *Bioinspiration & biomimetics*, **7**(1), 015002.

Levien, R. (2008), "The elastica: a mathematical history", *University of California, Berkeley, Technical Report No. UCB/EECS-2008-103*.

Lewis, W.J. (2003), *Tension structures: form and behaviour*, Thomas Telford

Lienhard, J. (2014), *Bending-active structures: form-finding strategies using elastic deformation in static and kinetic systems and the structural potentials therein*

Lienhard, J., Ahlquist, S., Knippers, J. and Menges, A. (2013). "Extending the Functional and Formal vocabulary of tensile membrane structures through the interaction with bending-active elements", *Re] Thinking lightweight structures, Proceedings of Tensinet Symposium, Istanbul*.

Lienhard, J., La Magna, R. and Knippers, J. (2014), "Form-finding bending-active structures with temporary ultra-elastic contraction elements", *Mob Rapidly Assem Struct IV*, **136**, 107.

Linkwitz, K. and Schek, H. (1972). "A new method of analysis of prestressed cable networks and its use to the roofs of the olympic games facilities in munich", *9th Congress of IABSE*.

Marques, D.F.C. (2015), *Análise estrutural e dimensionamento de estruturas de membrana*

Melville, S., Brandt-Olsen, C. and Harding, J. (2017). "Calibrated modelling of form-active structures", *IABSE Symposium Report*.

Philipp, B., Wüchner, R. and Bletzinger, K.-U. (2016), "Advances in the Form-finding of Structural Membranes", *Procedia Engineering*, **155**, 332-341.

Pyl, L., Wang, X., De Smedt, E., Colliers, J., Mollaert, M. and De Laet, L. (2016), "Existing Eurocodes applied to a membrane structure", *Procedia Engineering*, **155**, 142-151.

Rao, R. (2014), "Biomimicry in Architecture", *International Journal of Advanced research in Civil, Structural, Environmental and Infrastucture Engineering and Developing*, **1**(3), 101-107.

Seidel, M. (2009), *Tensile surface structures: A practical guide to cable and membrane construction*, John Wiley & Sons

Siev, A. (1963), "A general analysis of prestressed nets", *International Association for Bridge and Structural Engineering Publications*, **23**, 283-292.

SOFiSTiK, A. (2011), *SOFiSTiK Basics*, Oberschleißheim

SOFiSTiK, A. (2014), "Manual book–program ASE", *Oberschleissheim, Germany*.

Stimpfle, B. and Günther, D. (2016), "A project oriented approach to determine membrane properties", *Procedia Engineering*, **155**, 81-88.

Bibliography

Timoshenko, S.P. and Gere, J.M. (1961), "Theory of elastic stability. 1961", *McGrawHill-Kogakusha Ltd, Tokyo*, **109**.

Uhlemann, J. (2016), *Elastic constants of architectural fabrics for design purposes*, Shaker Verlag

Van Asselt, P. (2007), "Analysis of stressed membrane structures: Implementation of non-linear material behaviour in structural analysis".

Veenendaal, D. and Block, P. (2012), "An overview and comparison of structural form finding methods for general networks", *International Journal of Solids and Structures*, **49**(26), 3741-3753.

7. APPENDIX

TEDDY routines:

```
+PROG ASE urs:16.4
HEAD Form Finding
CTRL cabl 0
CTRL iter 3 v2 1
$ Grupo 1 membrana / Grupo 2 cabos
SYST prob th3 iter 50 $nmat yes
        GRP no all facs 1
        GRP no 1 facs 1e-10 prex 2 prey 2
        GRP no 2 facs 1 prex 0
        LC no 101 dlz 1 titl 'Formfinding'
END

+PROG ASE urs:16.5
HEAD Form Finding Compensation for Residual Forces Facs=1
CTRL cabl 0
SYST prob th3 iter 50 plc 101 $nmat yes
        GRP all facs 1
        LC 102 dlz 1 titl 'Last Formfinding facs 1'
END
```

Appendix Figure 1 - Routine implemented in Sofistik® to form find the membranes.

```
+PROG ASE urs:5
HEAD Form Finding
let#i 0
let#n 10
let#plc 1
let#key 1

loop
        let#i #i+1
        let#lc #lc+1

        SYST prob th3 tol -0.05 plc #plc
                CTRL opt iter val 3 v2 1
                CTRL opt beam val 5
                LC #lc DLZ 1 titl 'Iteration_#i'
                LCC no 902 fact #n
        END
         let#plc #lc
         let#n #n+10
endloop #n<=400

END
```

Appendix Figure 2 - Linear increment method routine implemented in Sofistik®.

```
+PROG ASE urs:5
HEAD Form Finding
let#i 0
let#n 10
let#plc 1
let#key 1

loop
        let#i #i+1
        let#lc #lc+1

        SYST prob th3 tol -0.01 plc #plc
                CTRL opt iter val 3 v2 1
                CTRL opt beam val 5
                LC #lc DLZ 1 titl 'Iteration #i'
                LCC no 902 fact #n
        END
         let#plc #lc
         let#n #n*1.4[-]
         let#gate #n*#key[-]
          if (#gate > 6000)
                  let#n 6000
                  let#key 0
          endif
endloop #n<=6000

END
```

Appendix Figure 3 - Adaptive increment method routine implemented in Sofistik®.

Appendix

VBA routine:

```
Sub MultiXY_Chart1()

    Dim rngDataSource As Range
    Dim iDataRowsCt As Long
    Dim iDataColsCt As Integer
    Dim iSrsIx As Integer
    Dim chtChart As Chart
    Dim srsNew As Series

    If Not TypeName(Selection) = "Range" Then
        '' Doesn't work if no range is selected
        MsgBox "Please select a data range and try again.", _
            vbExclamation, "No Range Selected"
    Else
        Set rngDataSource = Selection
        With rngDataSource
            iDataRowsCt = .Rows.Count
            iDataColsCt = .Columns.Count
        End With
        If iDataColsCt Mod 2 > 0 Then
            MsgBox "Select a range with an EVEN number of columns.", _
                vbExclamation, "Select Even Number of Columns"
            Exit Sub
        End If

        '' Create the chart
        Set chtChart = ActiveSheet.ChartObjects.Add( _
            Left:=ActiveSheet.Columns(ActiveWindow.ScrollColumn).Left + _
                ActiveWindow.Width / 4, _
            Width:=ActiveWindow.Width / 2, _
            Top:=ActiveSheet.Rows(ActiveWindow.ScrollRow).Top + _
                ActiveWindow.Height / 4, _
            Height:=ActiveWindow.Height / 2).Chart

        With chtChart
            .ChartType = xlXYScatterSmooth

            '' Remove any series created with the chart
            Do Until .SeriesCollection.Count = 0
                .SeriesCollection(1).Delete
            Loop

            For iSrsIx = 1 To (CLng(iDataRowsCt) - 9) Step 9
                '' Add each series
                Set srsNew = .SeriesCollection.NewSeries
                With srsNew
                    .Name = iSrsIx
                    .Values = rngDataSource.Cells(iSrsIx + 1, 2) _
                        .Resize(9, 1)
                    .XValues = rngDataSource.Cells(iSrsIx + 1, 1) _
                        .Resize(9, 1)
                End With
            Next
        End With
    End If

End Sub
```

Appendix Figure 4 - Adaptive increment method routine implemented in Sofistik®.

Form finding results:

Membrane related results

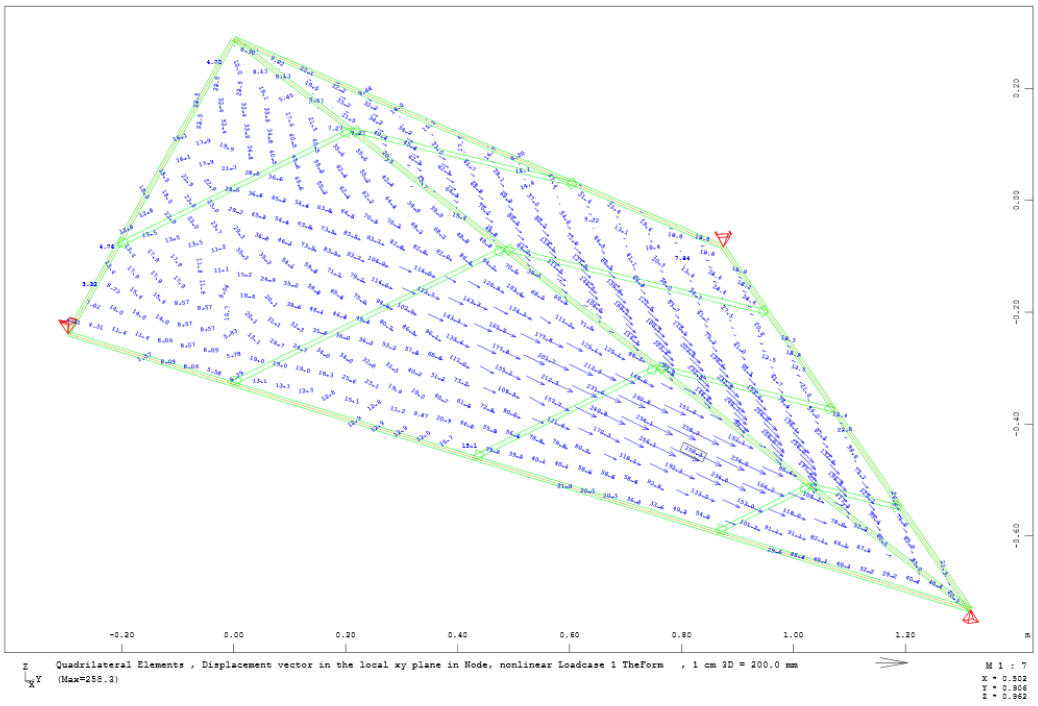

Appendix Figure 5 - Displacements in the local xy plane (mm).

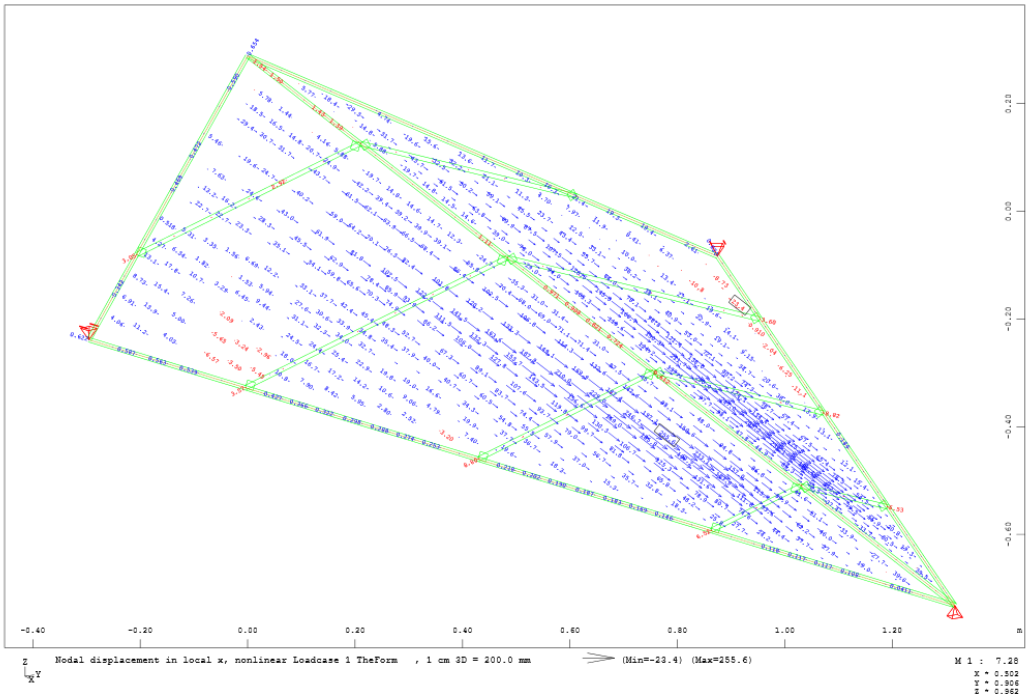

Appendix Figure 6 - Nodal displacements in local x direction (mm).

Appendix

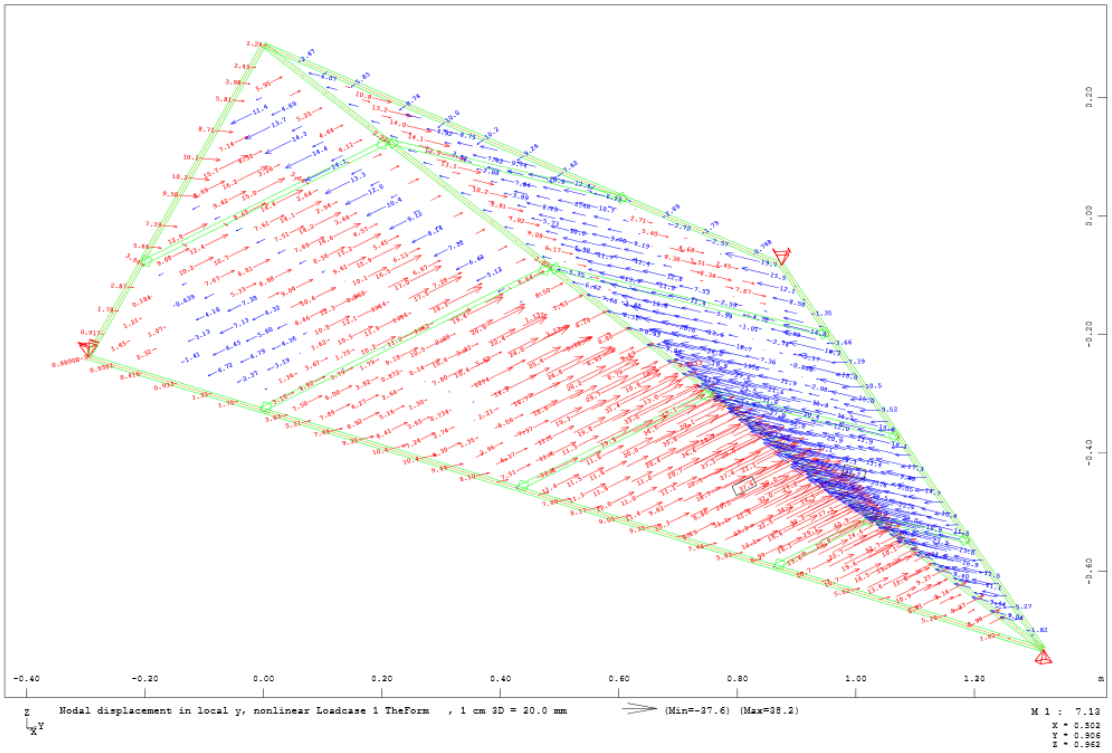

Appendix Figure 7 - Nodal displacements in local y direction (mm).

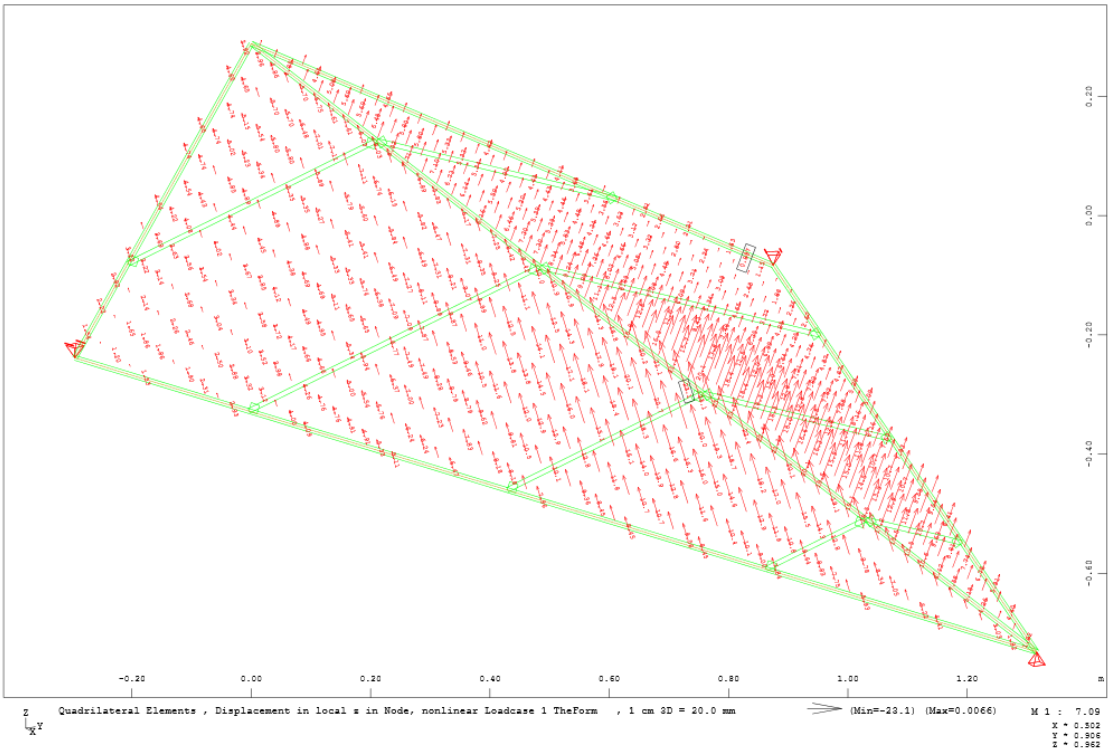

Appendix Figure 8 - Nodal displacements in local z (mm).

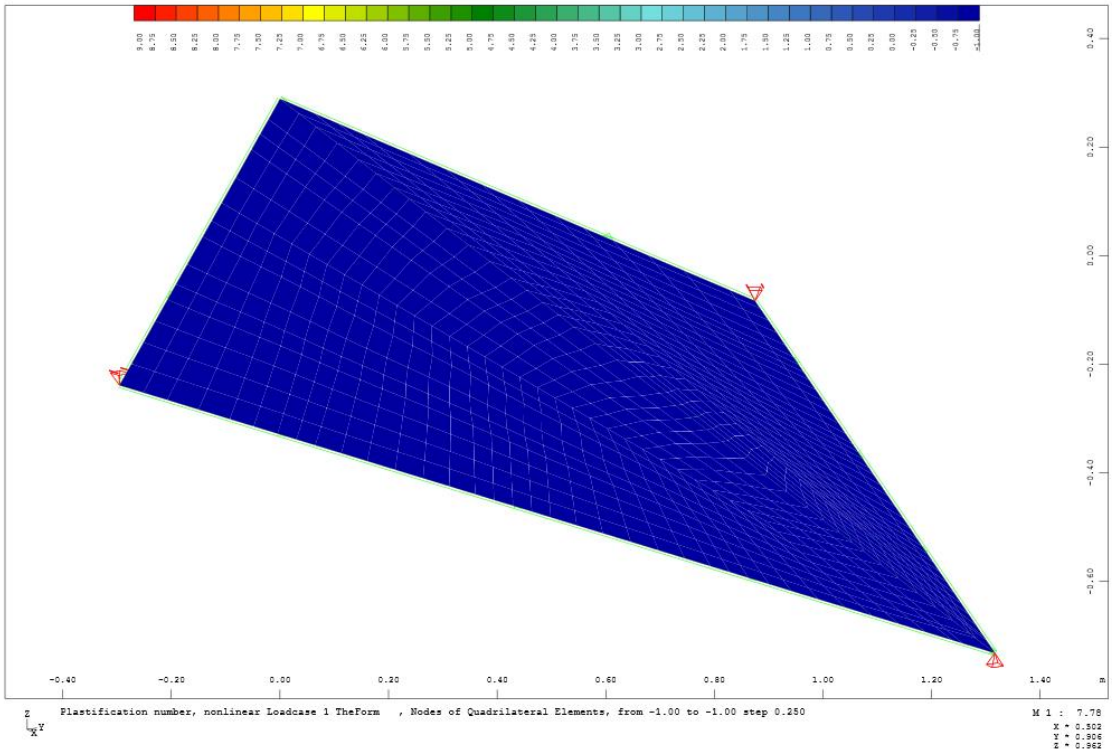

Appendix Figure 9 - Plasticization number, blue meaning no plasticization occurred.

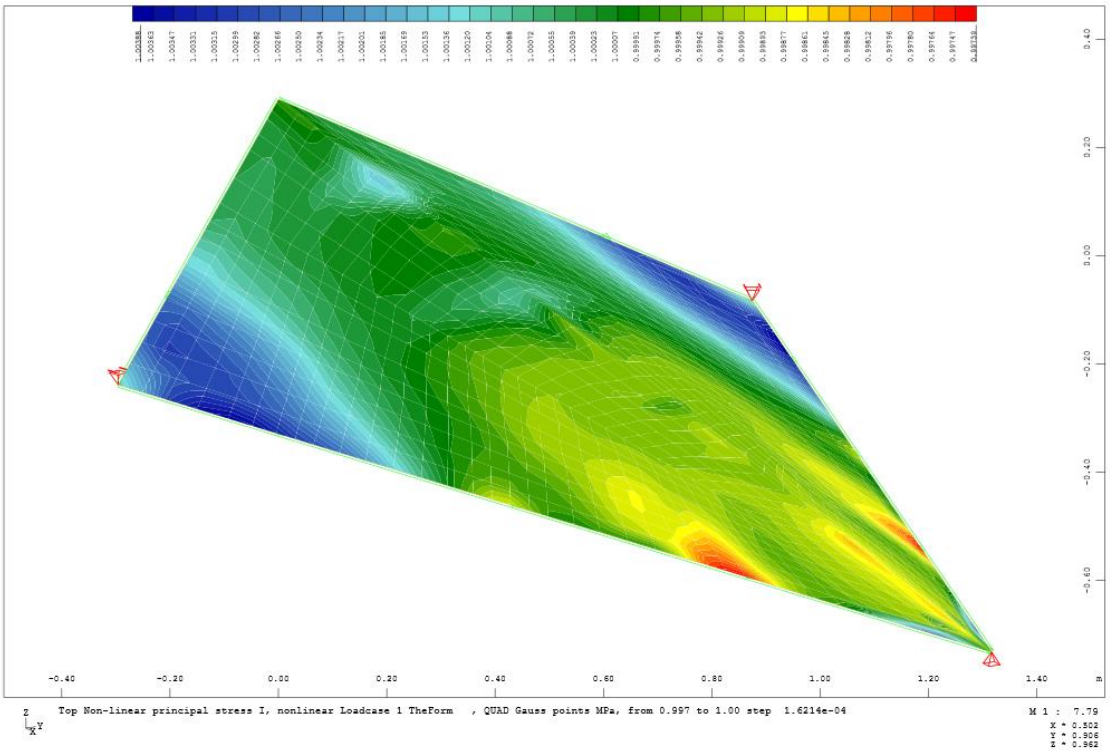

Appendix Figure 10 - Nonlinear principal stress I (MPa).

Appendix

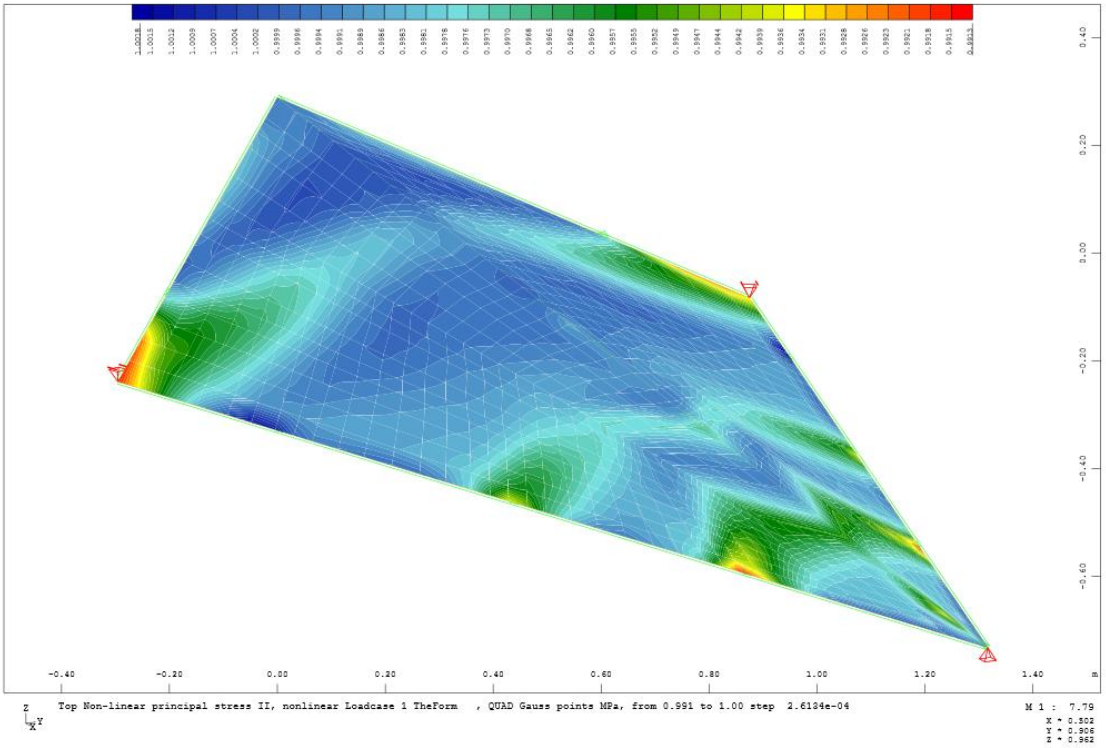

Appendix Figure 11 - Nonlinear principal stress II (MPa).

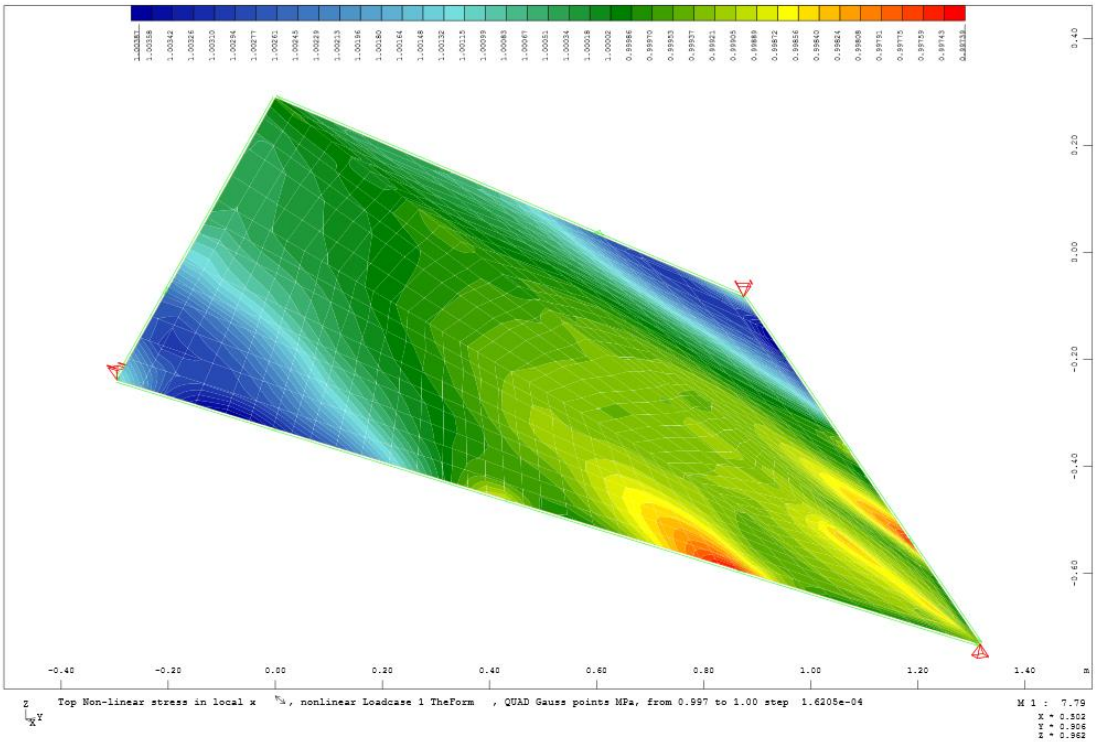

Appendix Figure 12 - Nonlinear stress in local x (MPa).

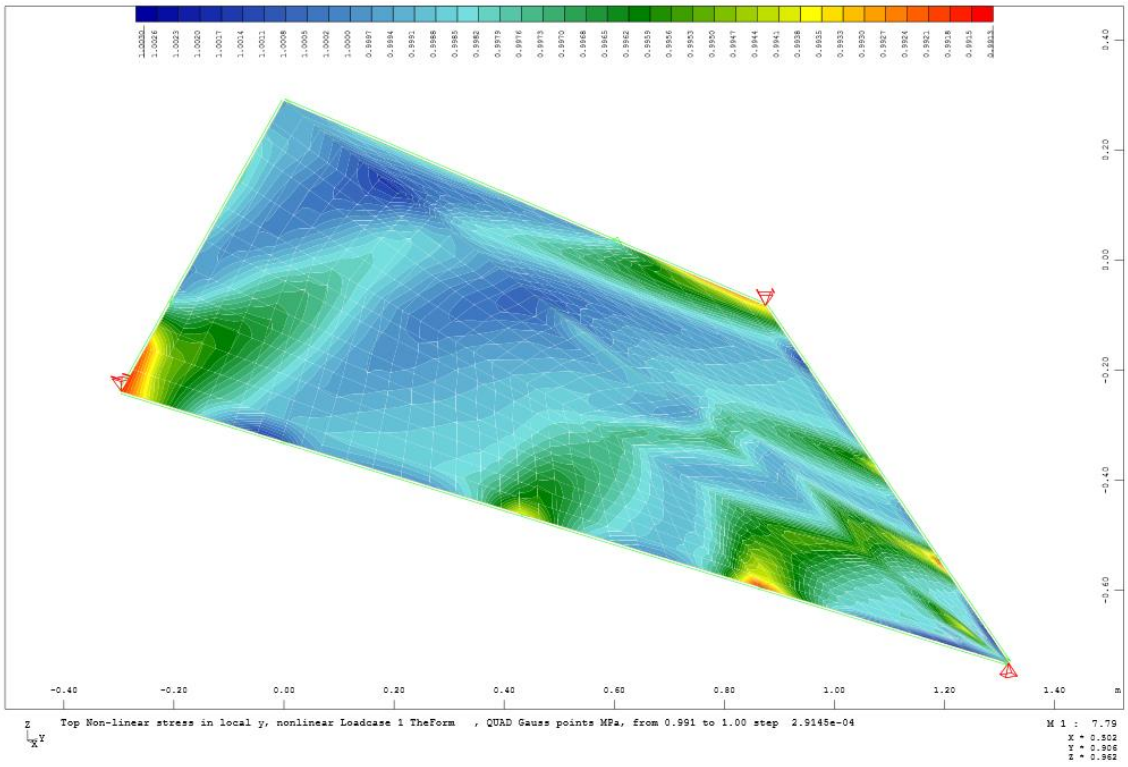

Appendix Figure 13 - Nonlinear stress in local y (MPa).

Skeleton related results

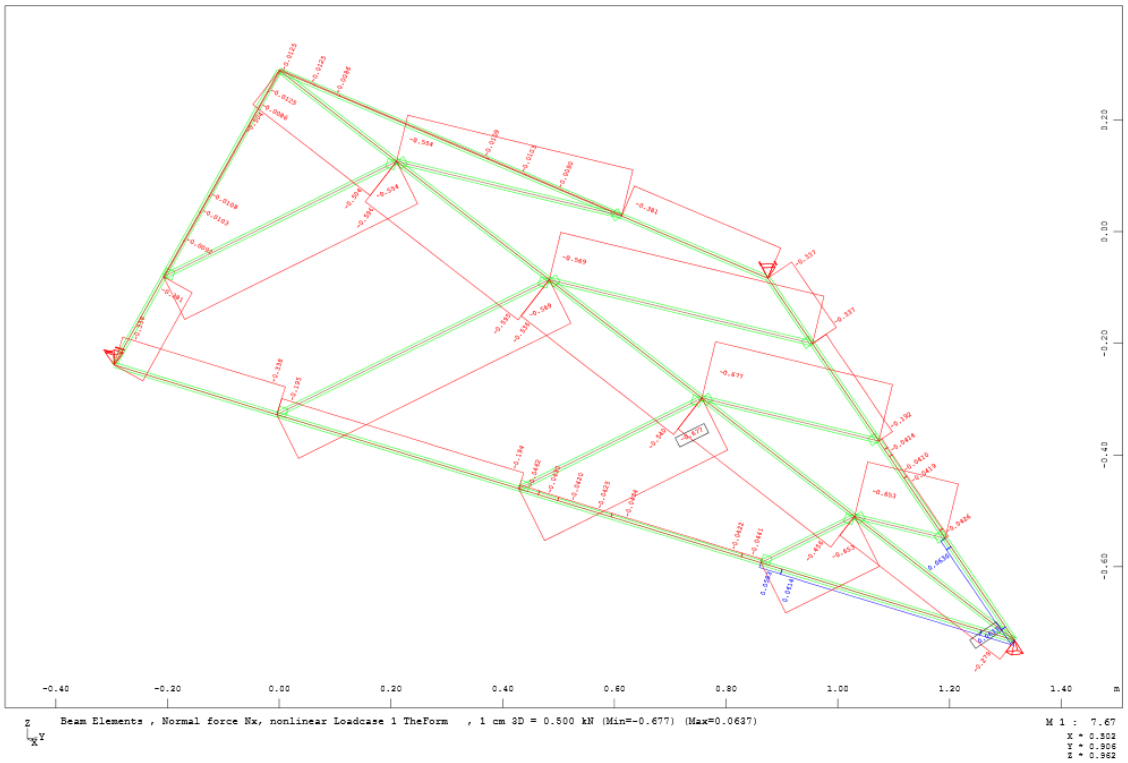

Appendix Figure 14 - Normal force (Nx) diagram (kN).

Appendix

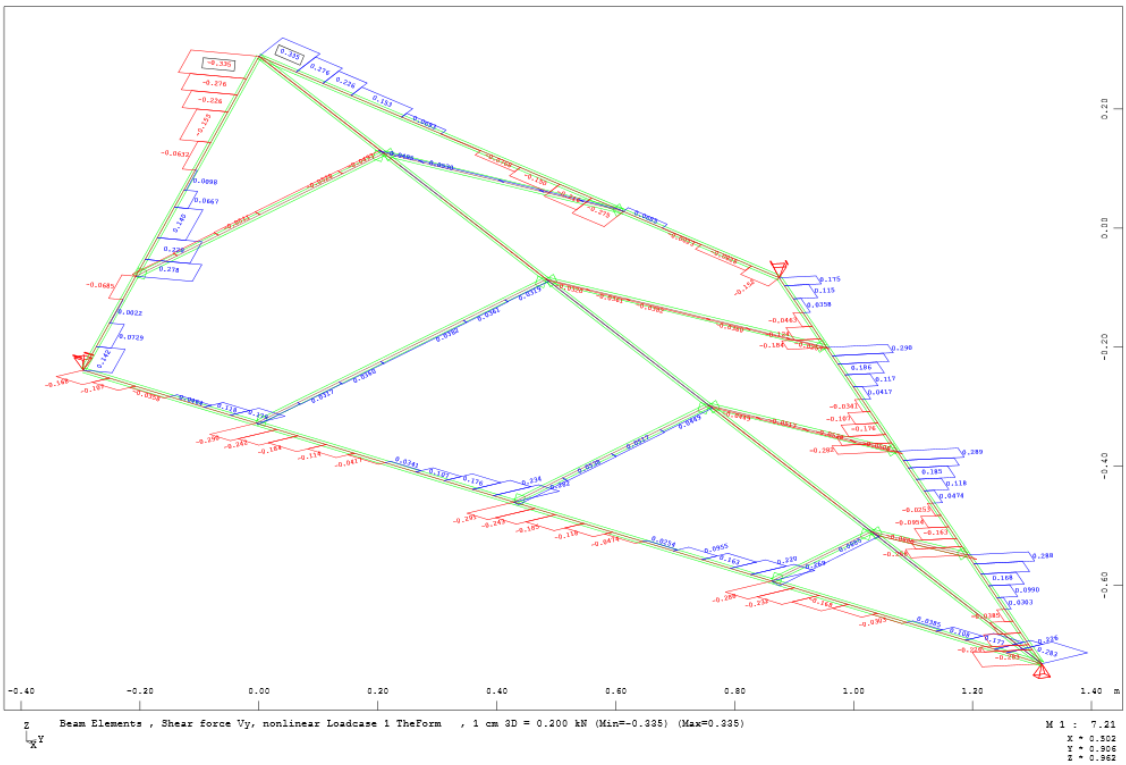

Appendix Figure 15 - Shear force (Vy) diagram (kN).

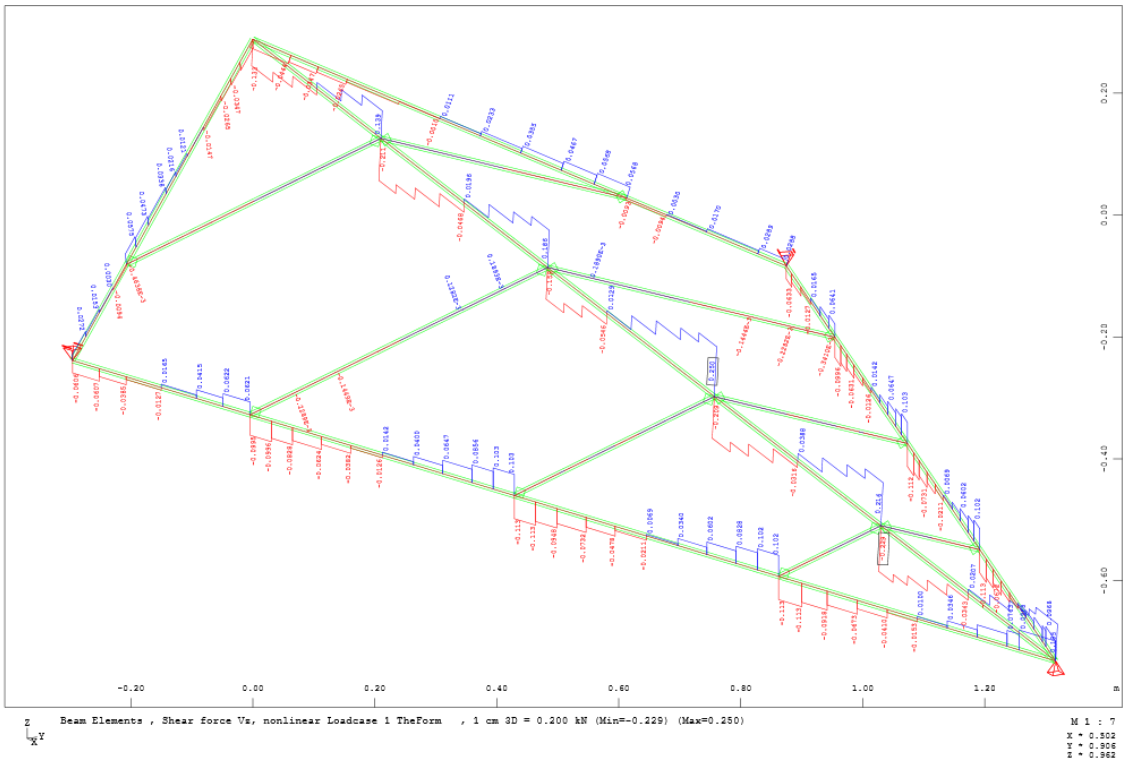

Appendix Figure 16 - Shear force (Vz) diagram (kN).

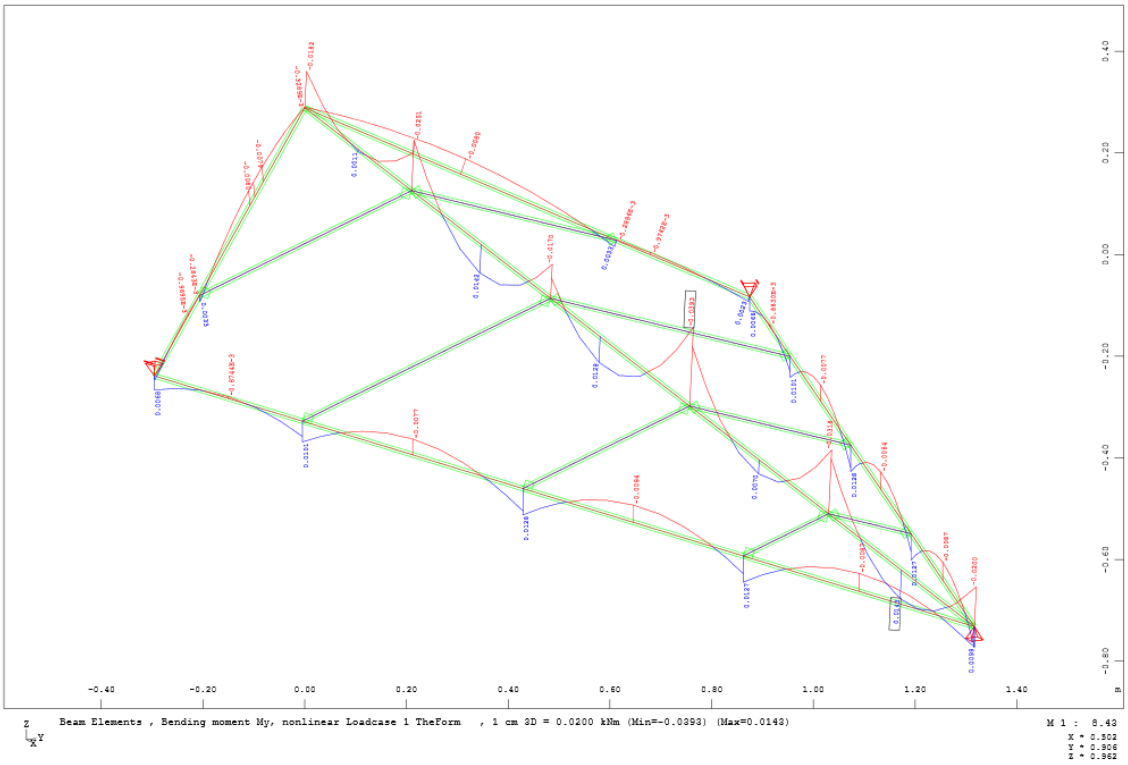

Appendix Figure 17 - Bending moment (My) diagram (kNm).

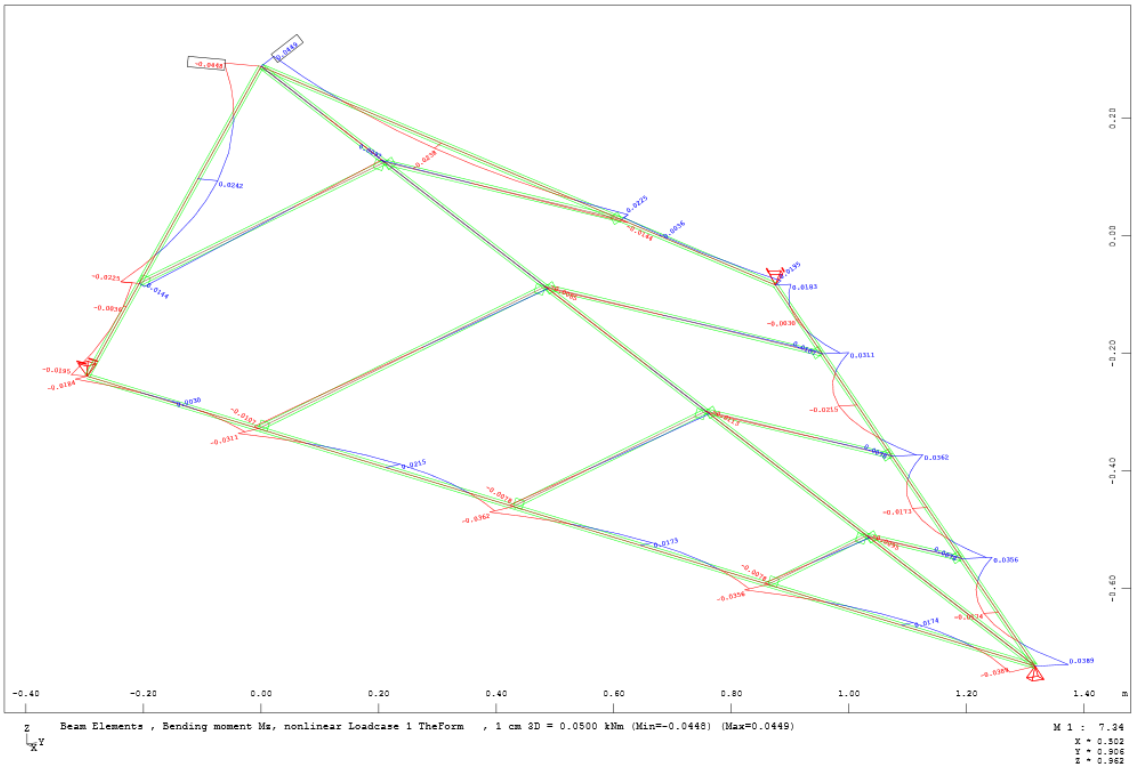

Appendix Figure 18 - Bending moment (Mz) diagram (kNm).

Appendix

Cross-sections stress

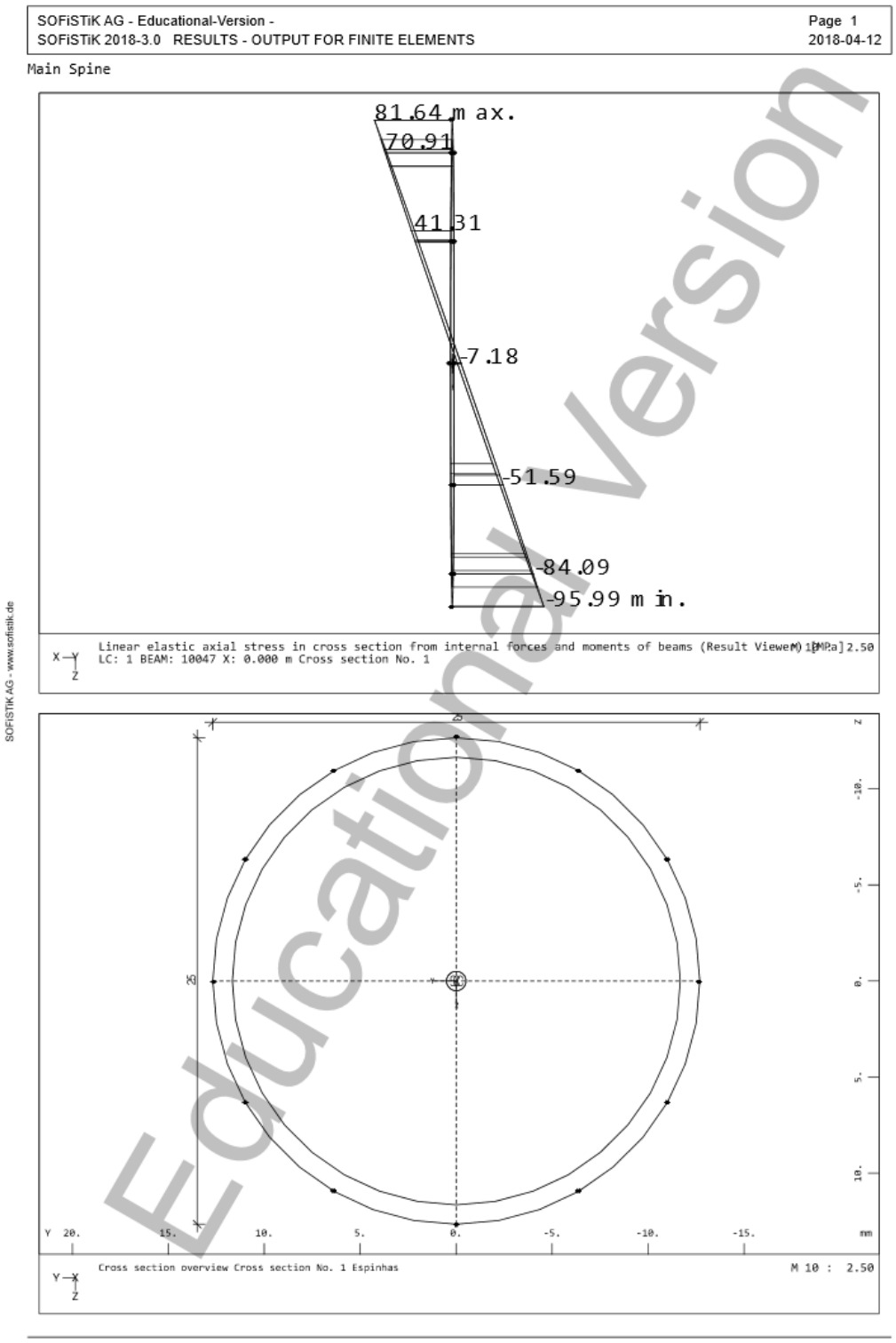

Appendix Figure 19 - Main spine, highest stressed section.

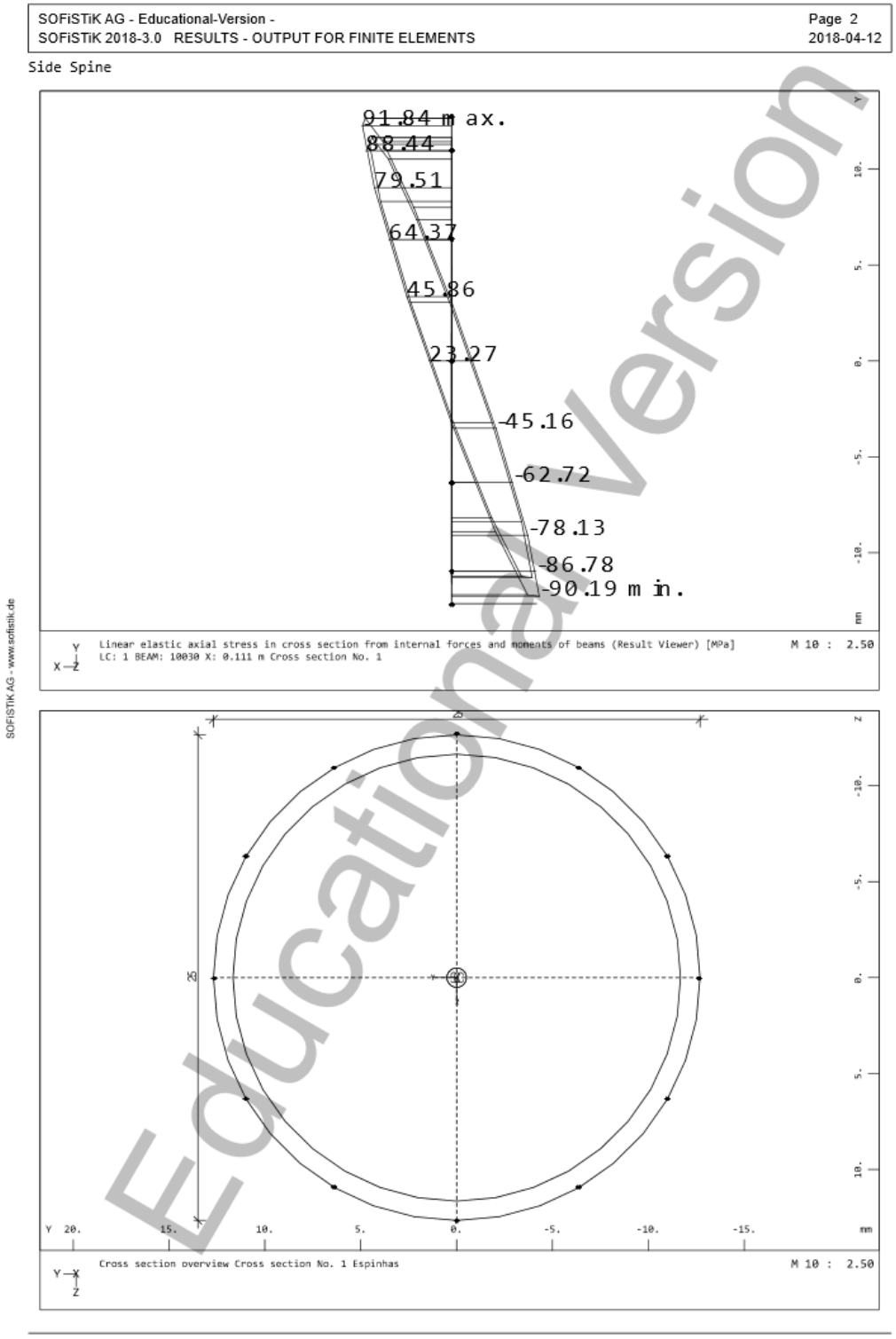

Appendix Figure 20 - Side spine, highest stressed section.

Appendix

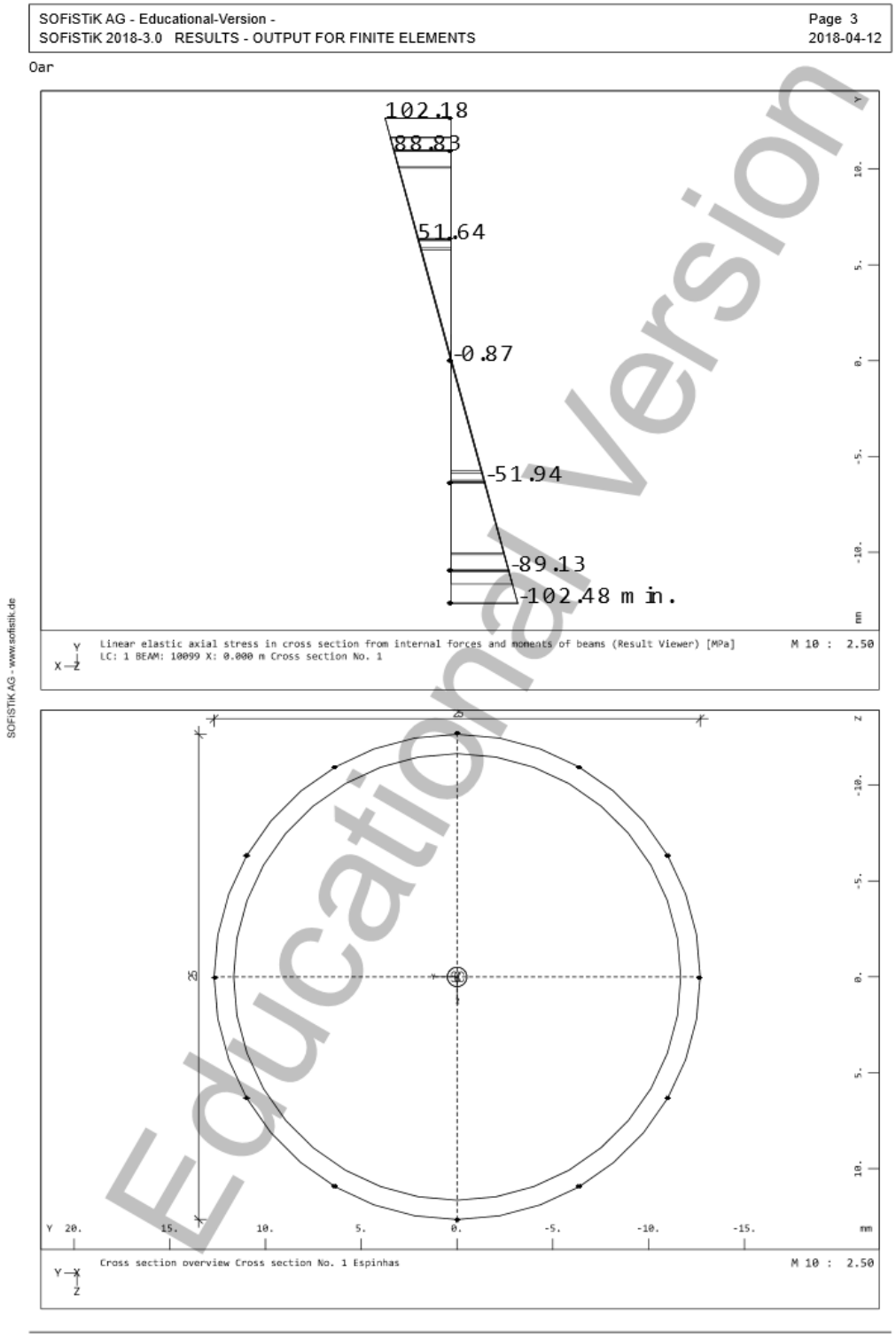

Appendix Figure 21 - Oar, highest stressed section.

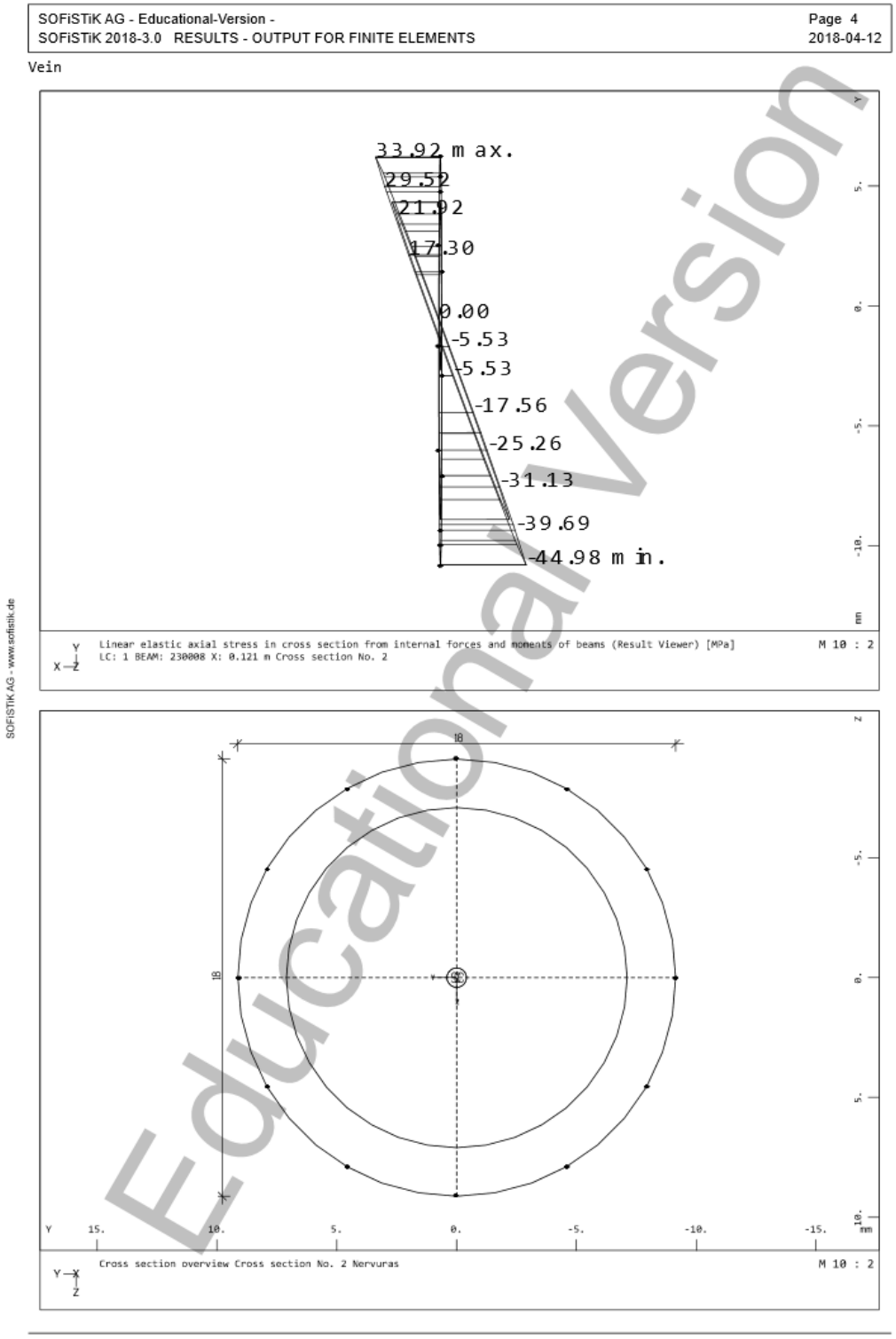

Appendix Figure 22 - Vein, highest stressed section.

Displacement of the structure (last stage):

Membrane related results

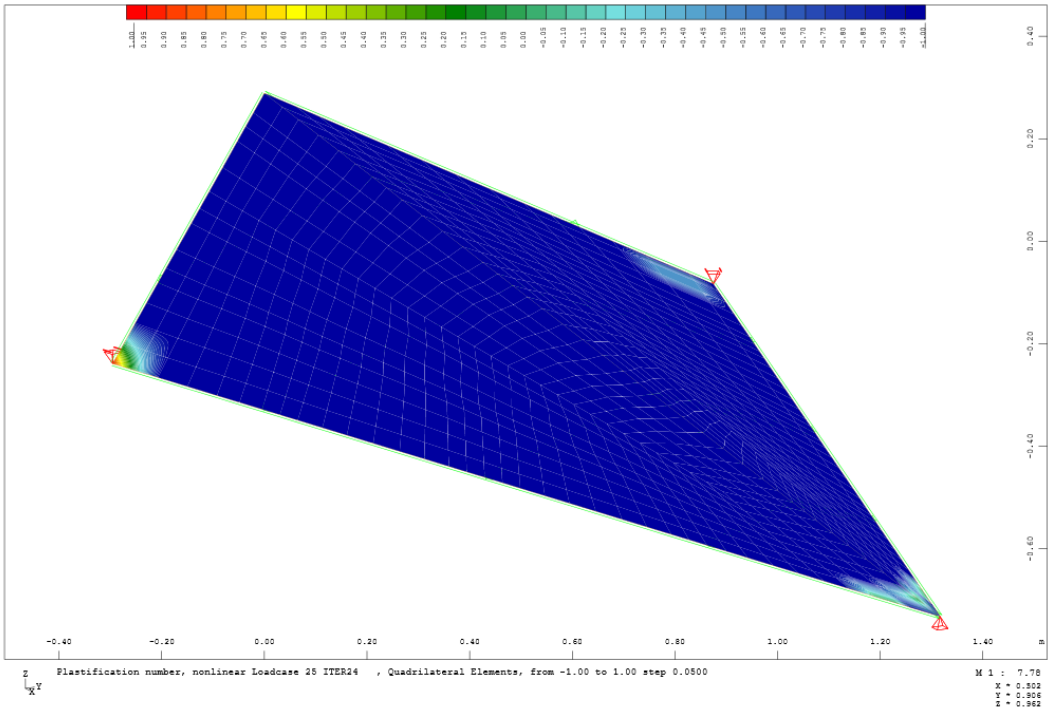

Appendix Figure 23 - Plasticization number, blue meaning no plasticization occurred.

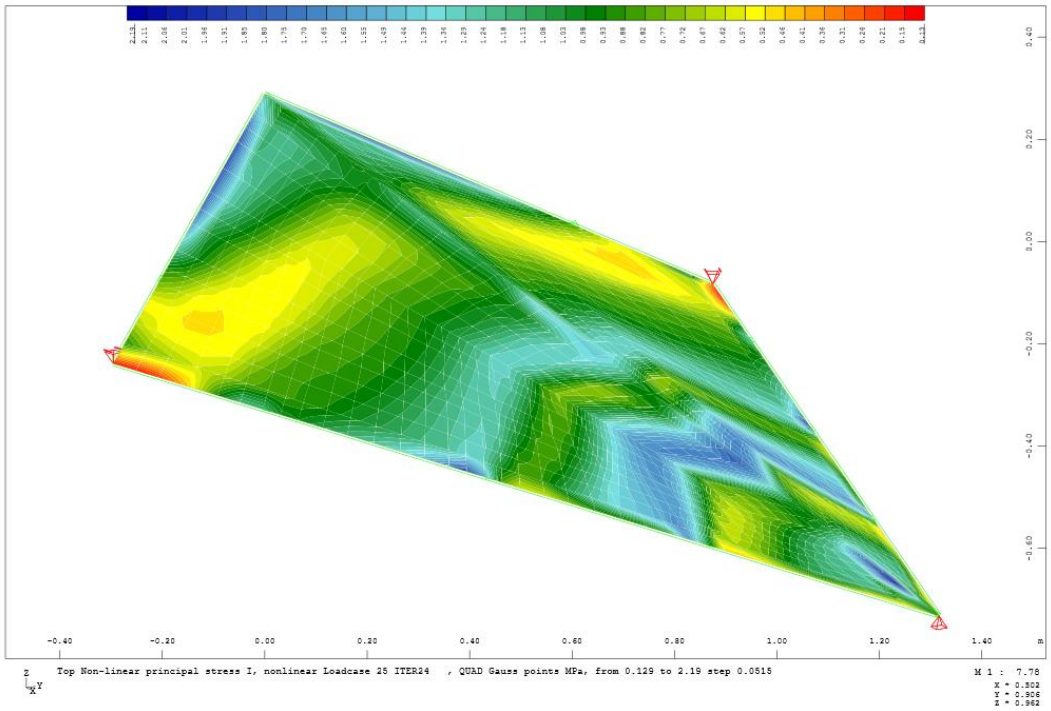

Appendix Figure 24 - Nonlinear principal stress I (MPa).

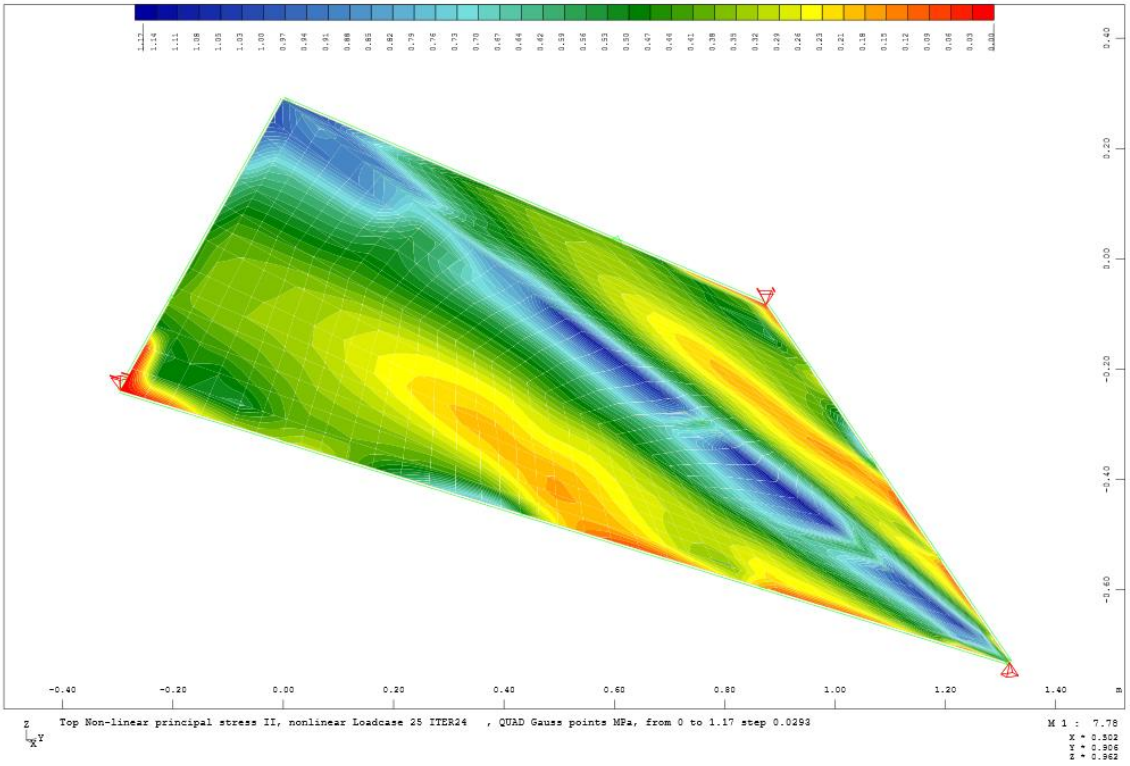

Appendix Figure 25 - Nonlinear principal stress II (MPa).

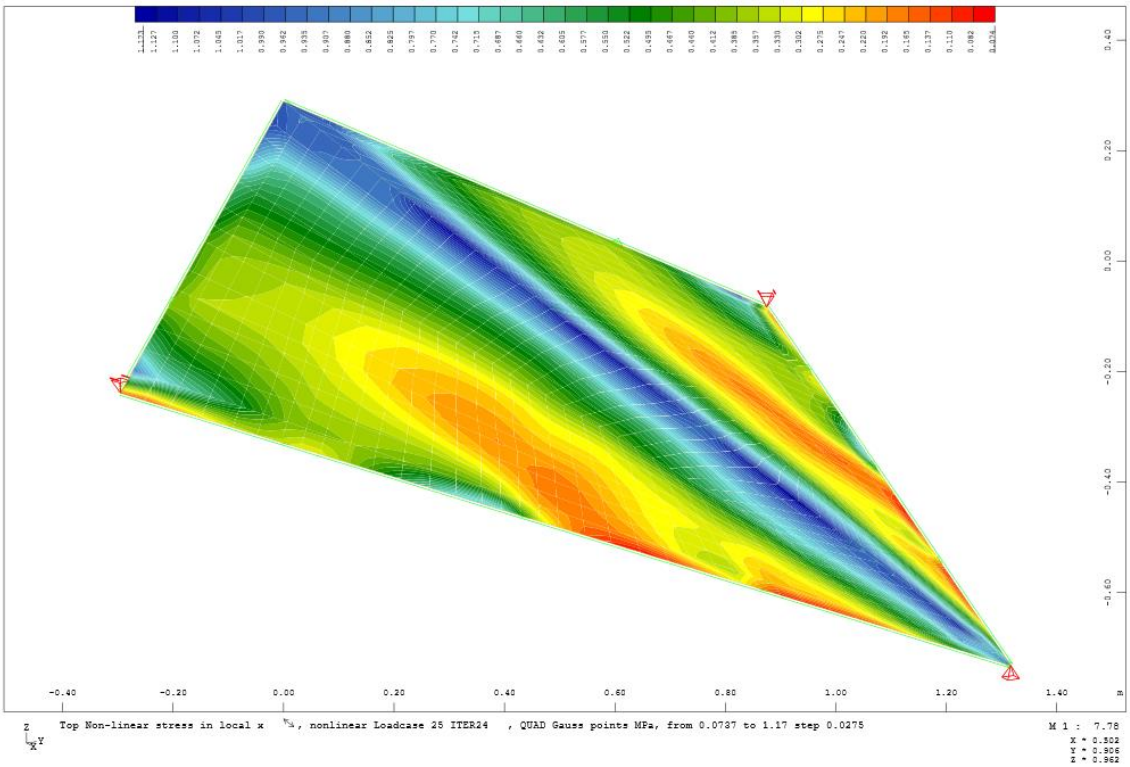

Appendix Figure 26 - Nonlinear stress in local x direction (MPa).

Appendix

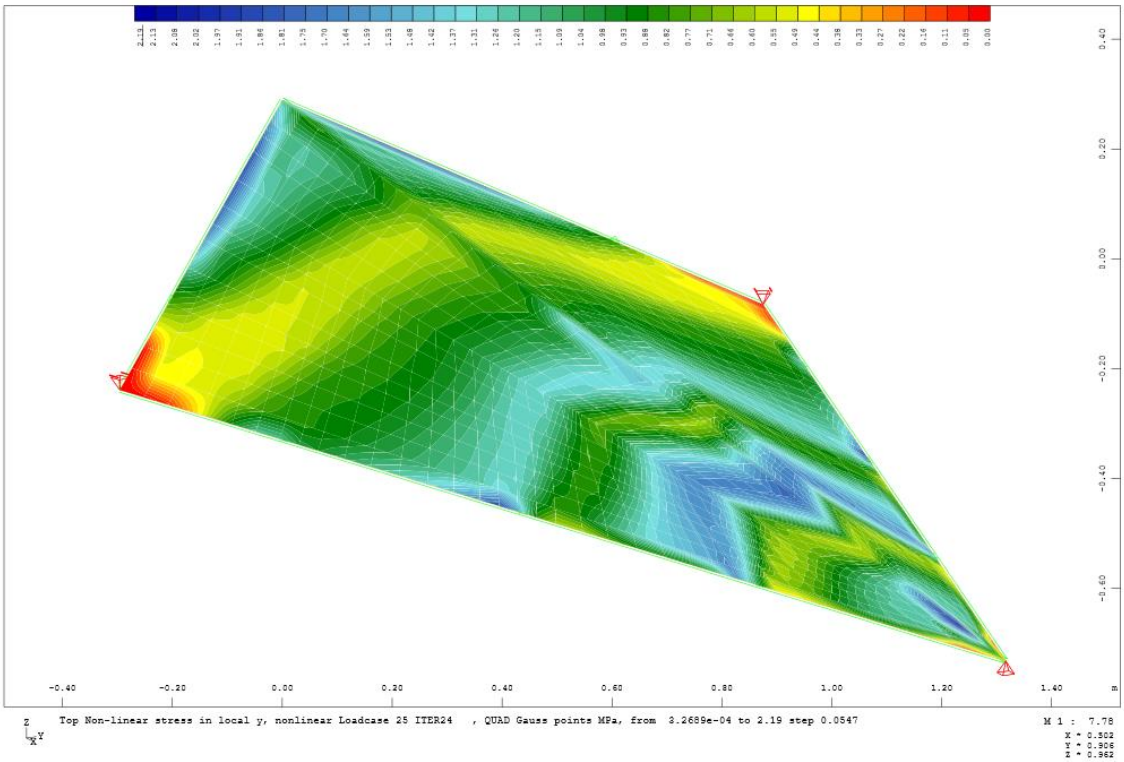

Appendix Figure 27 - Nonlinear stress in local y direction (MPa).

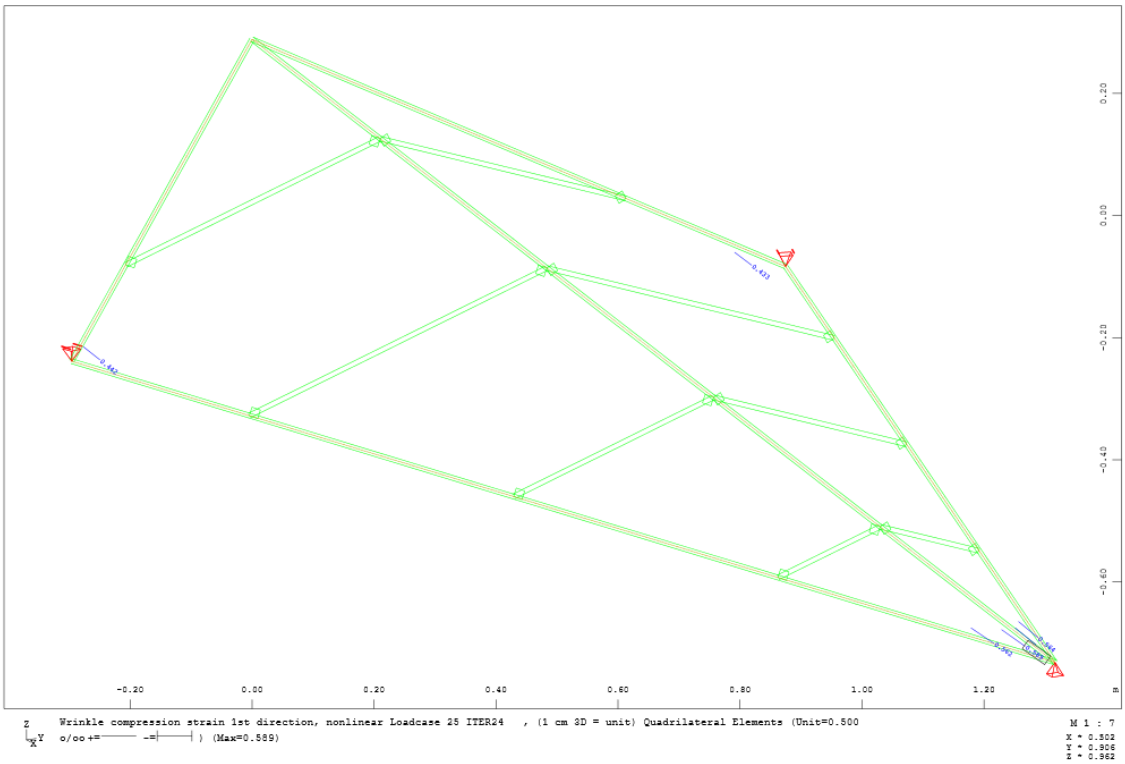

Appendix Figure 28 - Wrinkling compression strains, x direction.

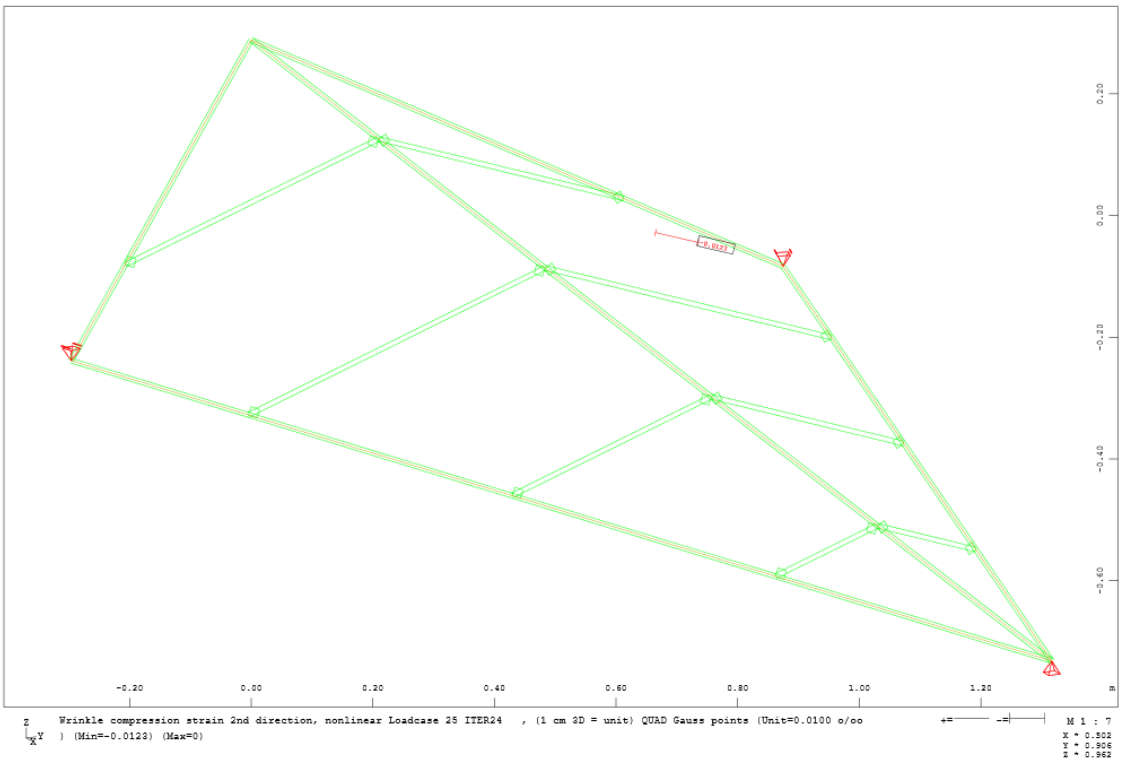

Appendix Figure 29 - Wrinkling compression strains, y direction.

Skeleton related results

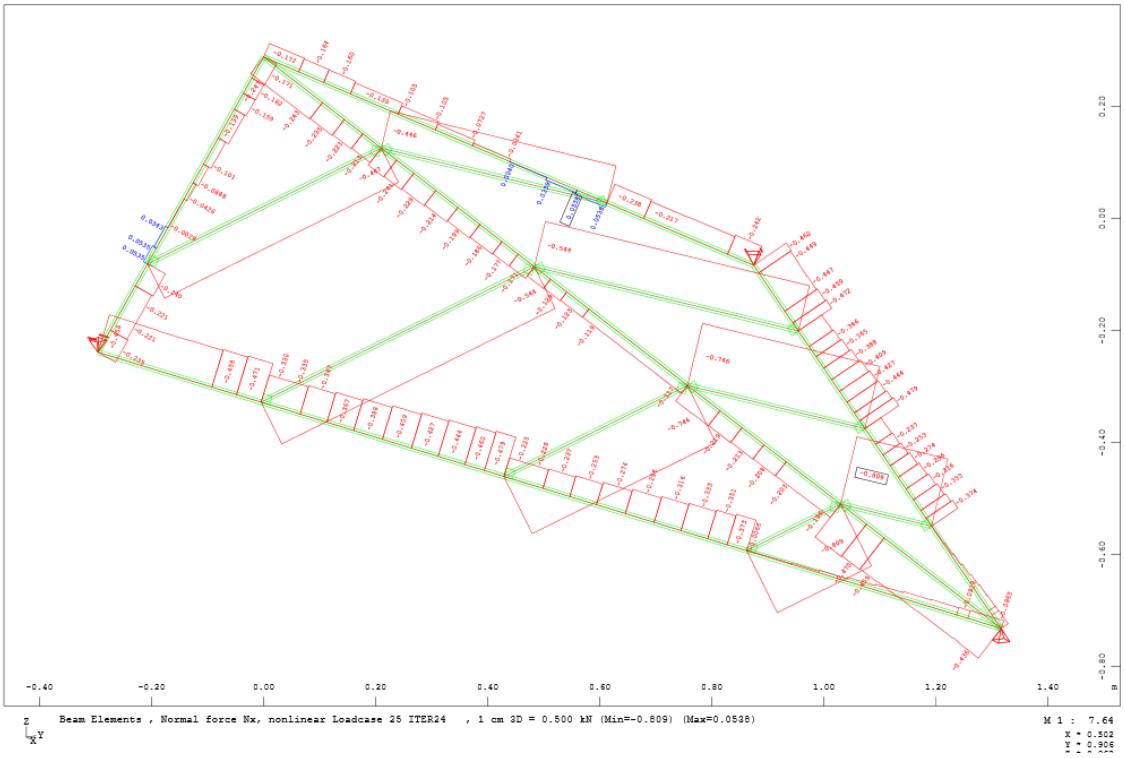

Appendix Figure 30 - Normal force (Nx) diagram (kN).

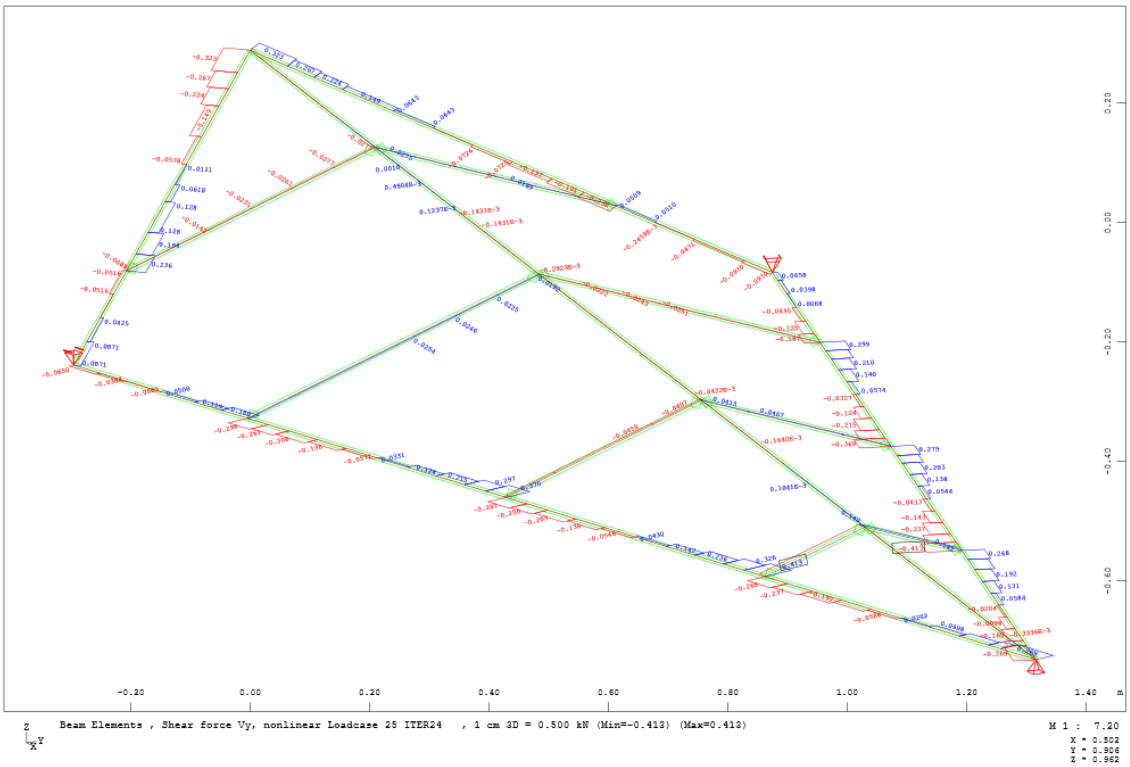

Appendix Figure 31 - Shear force (Vy) diagram (kN).

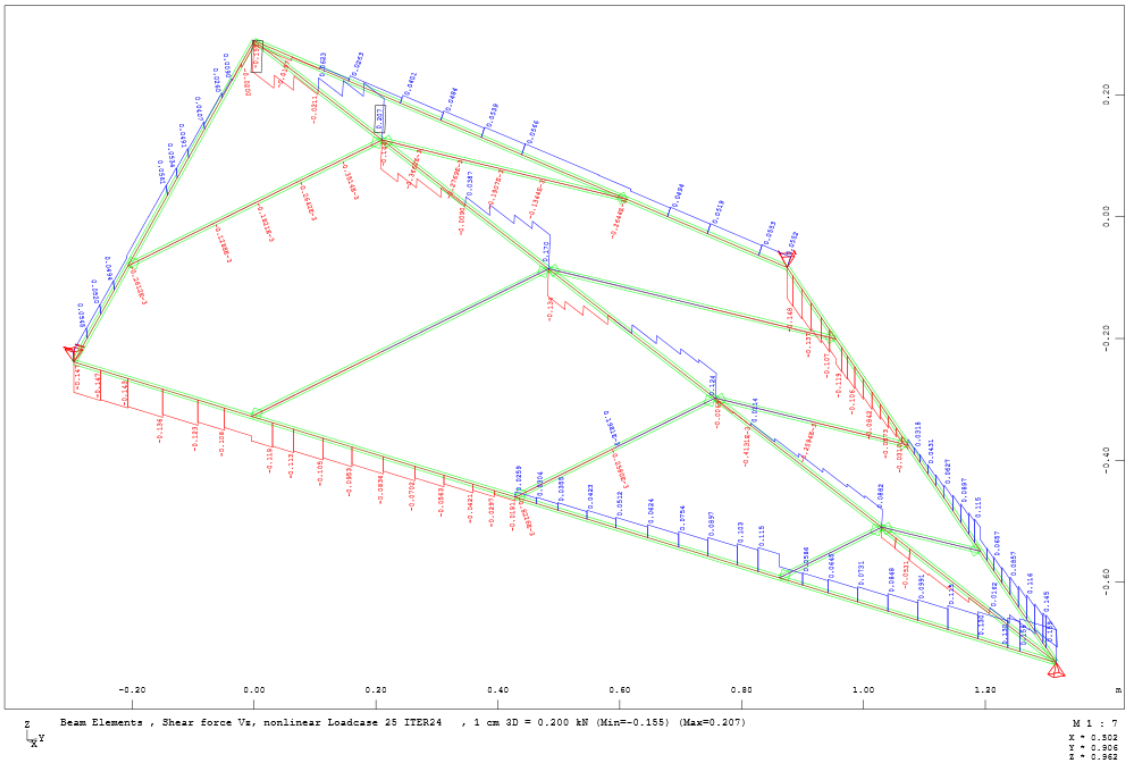

Appendix Figure 32 - Shear force (Vz) diagram (kN).

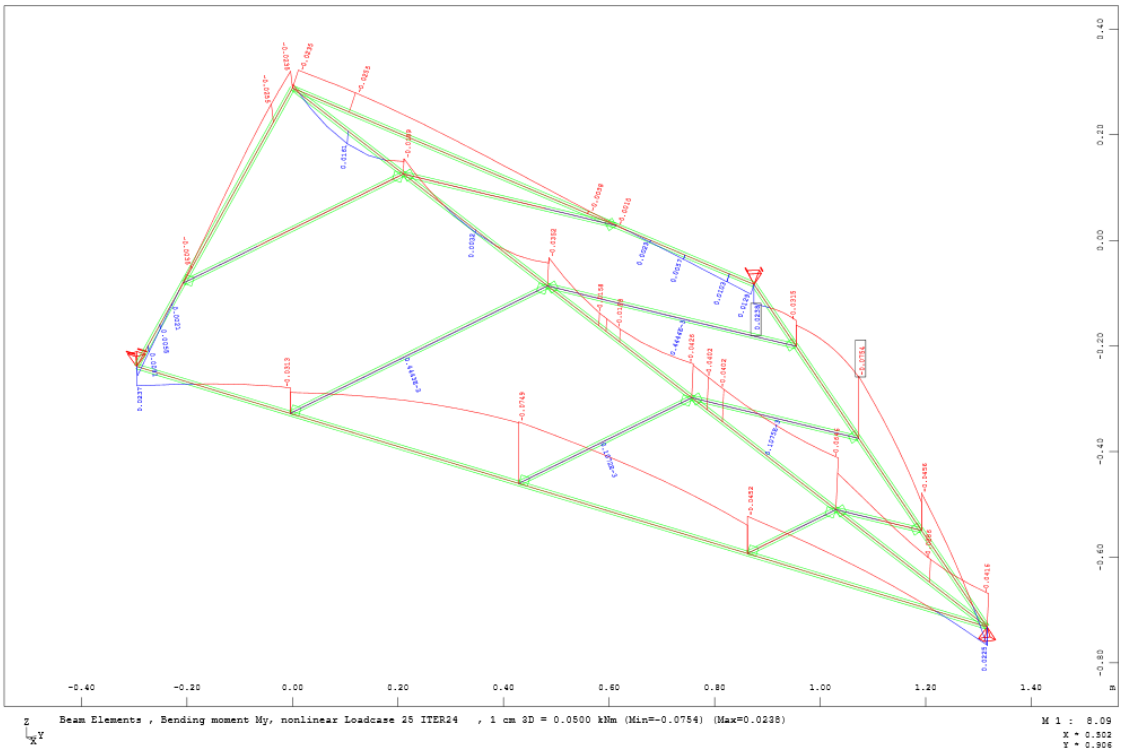

Appendix Figure 33 - Bending moment (My) diagram (kNm).

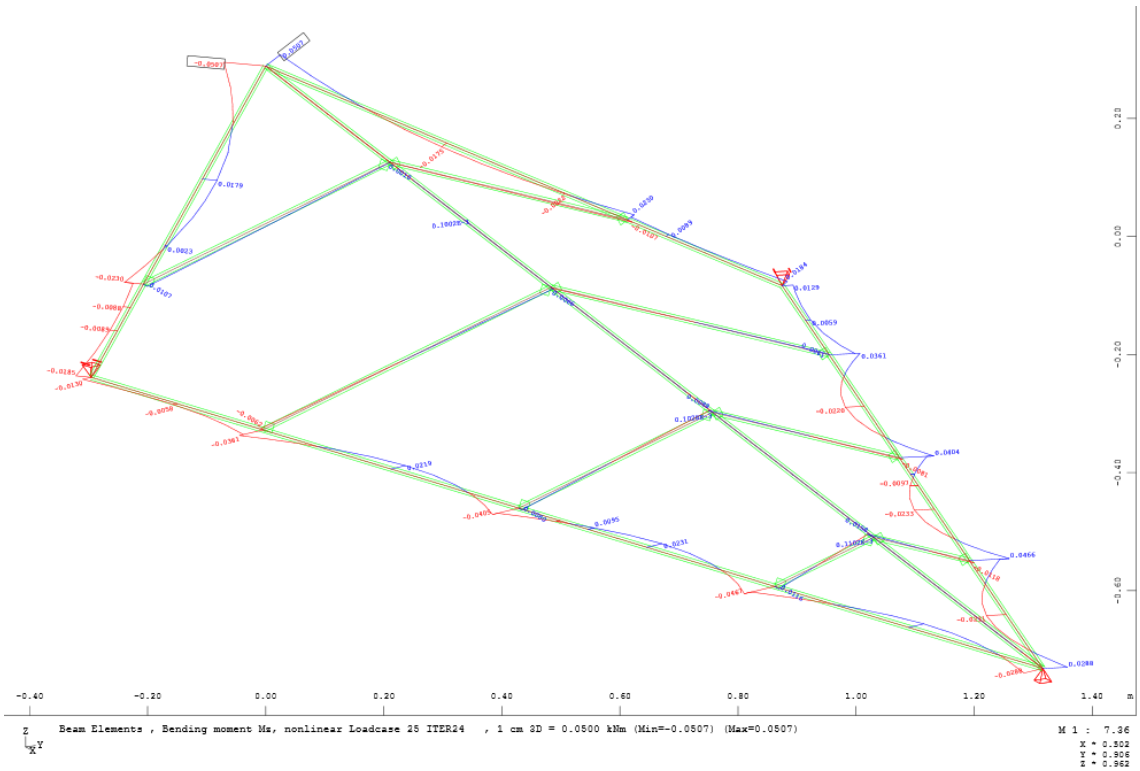

Appendix Figure 34 - Bending moment (Mz) diagram (kNm).

Appendix

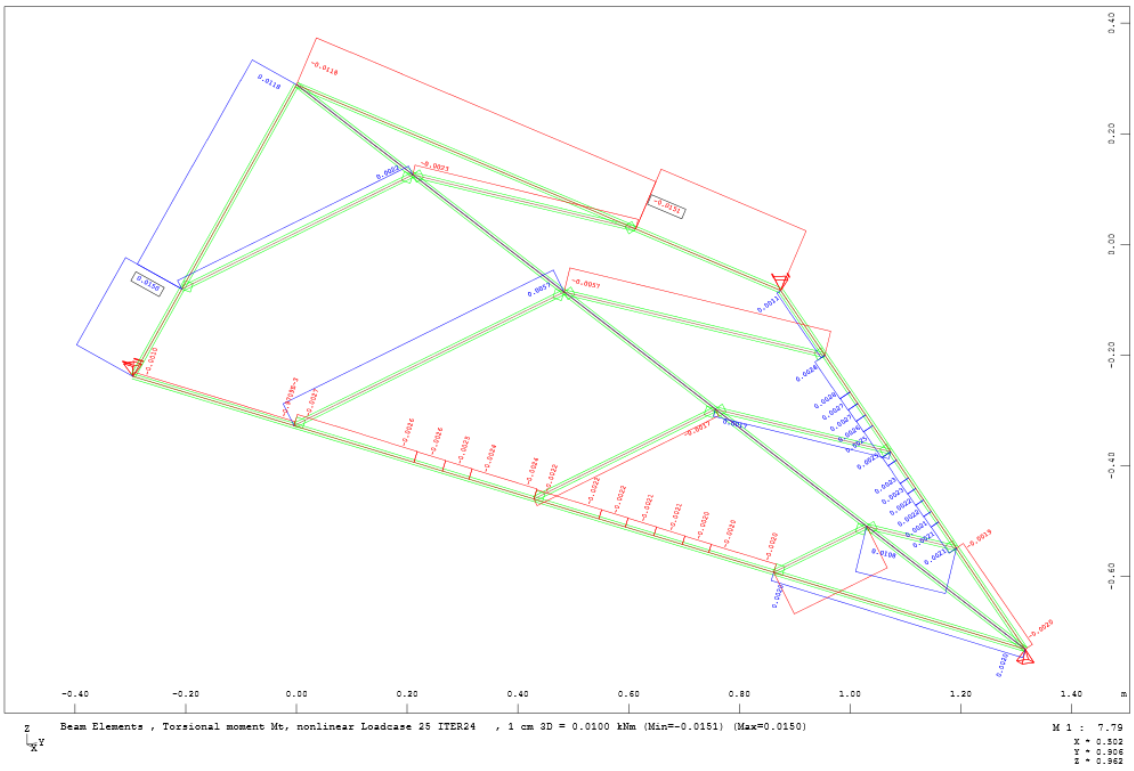

Appendix Figure 35 - Torsional moment (Mt) diagram (kNm).

Elastic Cable Approach – Last stage

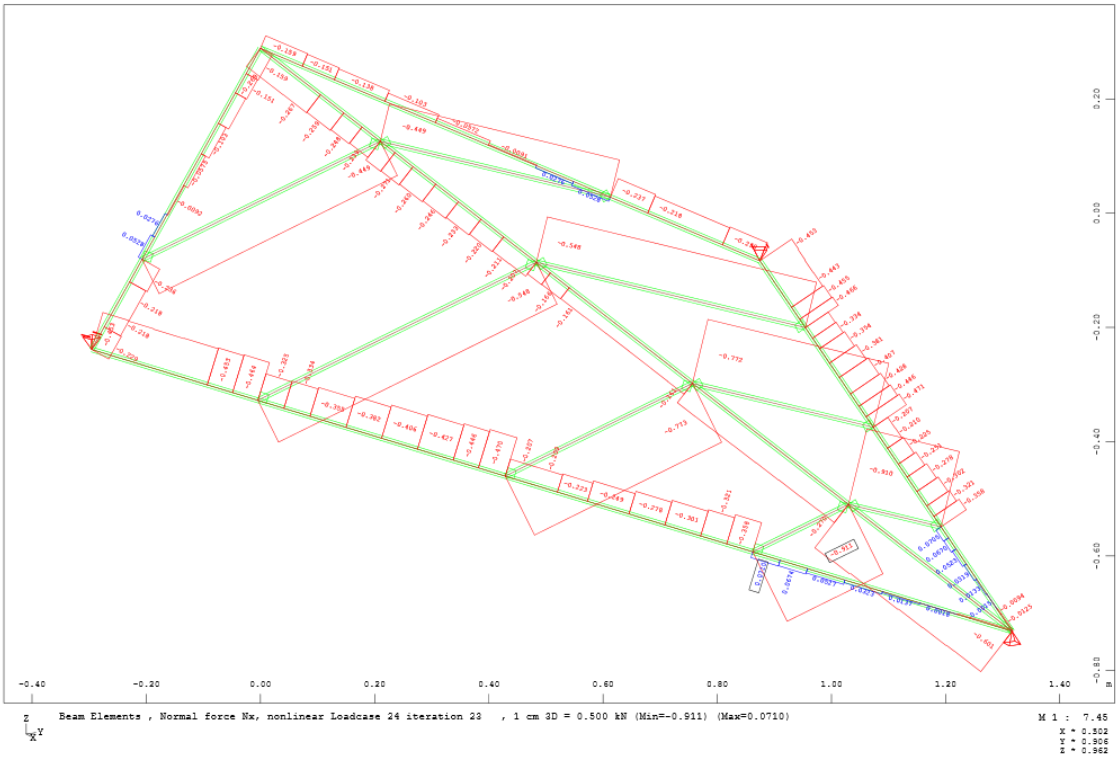

Appendix Figure 36 - Normal force (Nx) diagram (kN).

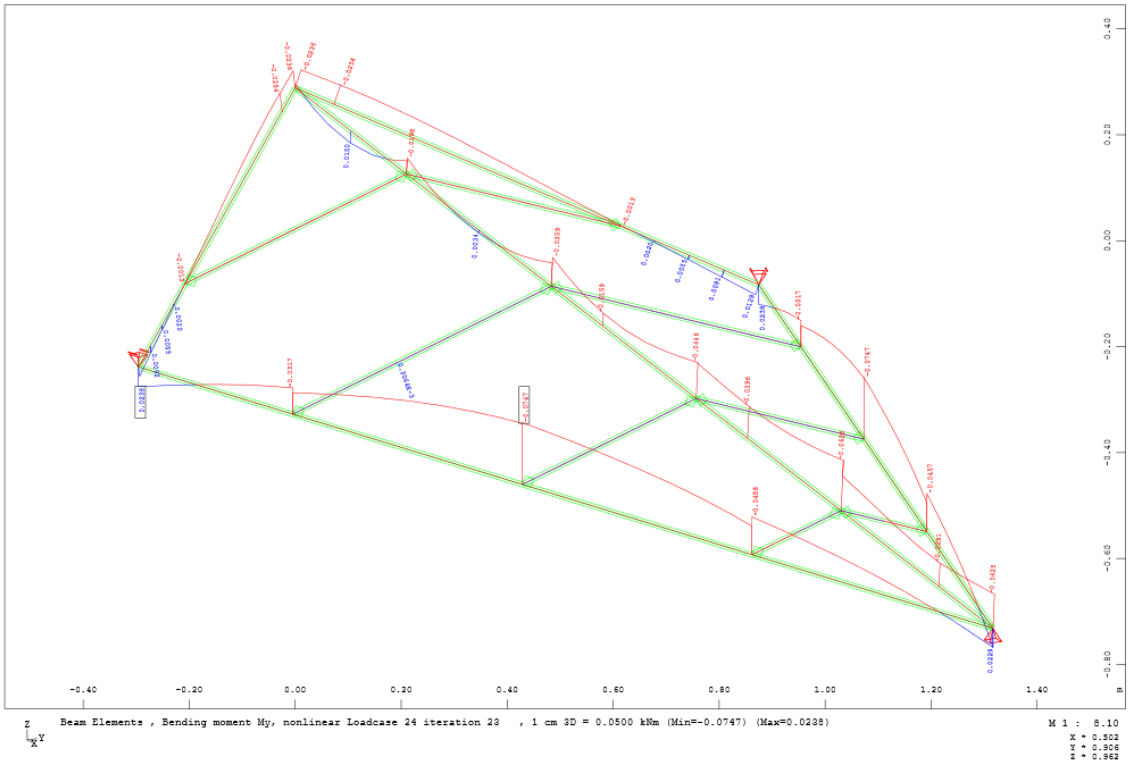

Appendix Figure 37 - Bending moment (My) diagram (kNm).

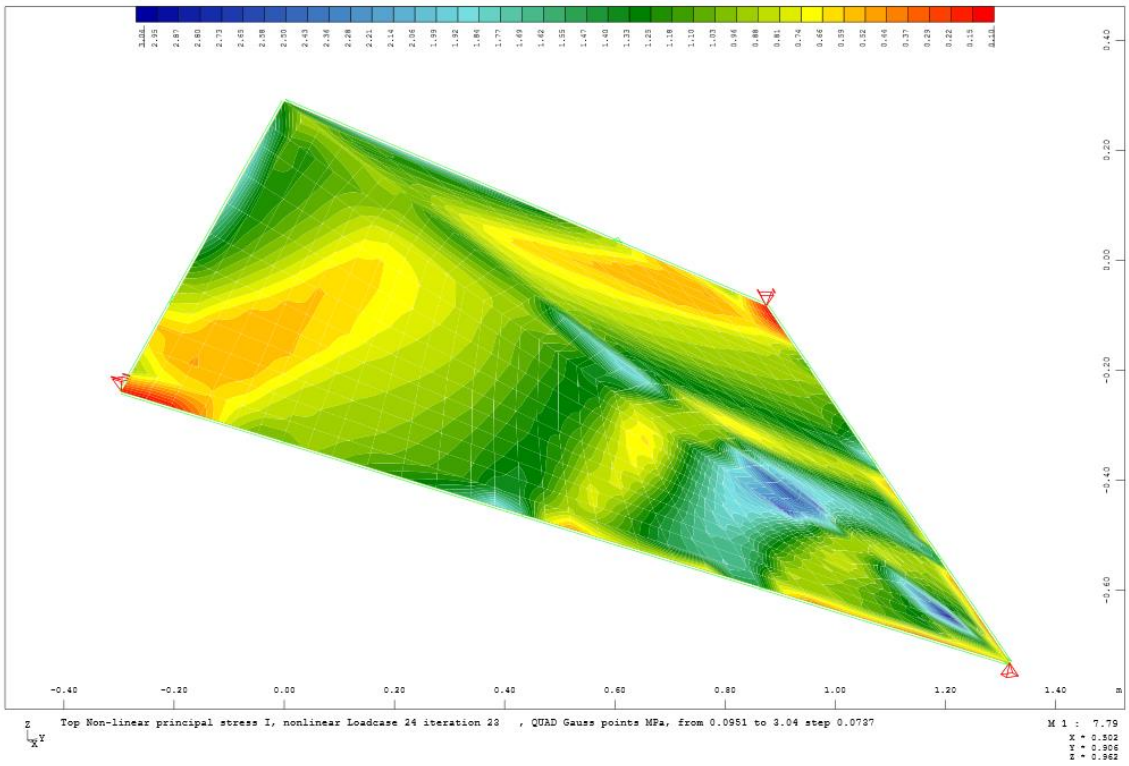

Appendix Figure 38 - Nonlinear principal stress I (MPa).

Appendix

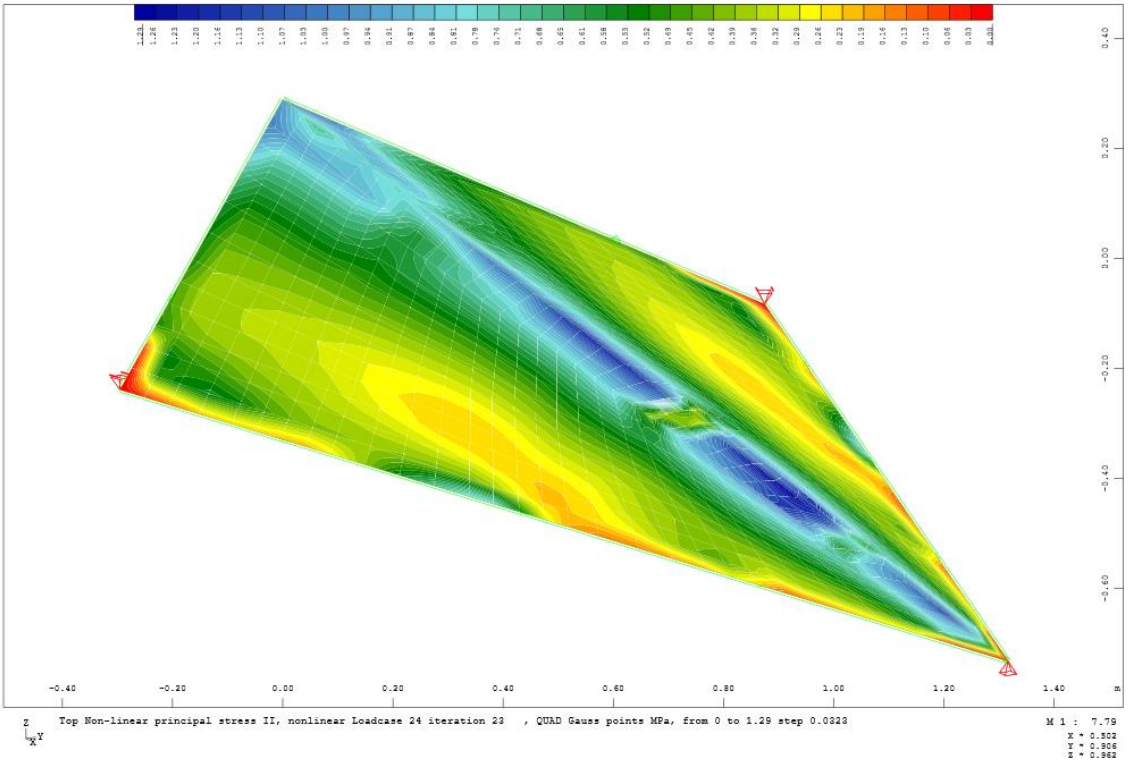

Appendix Figure 39 - Nonlinear principal stress II (MPa).

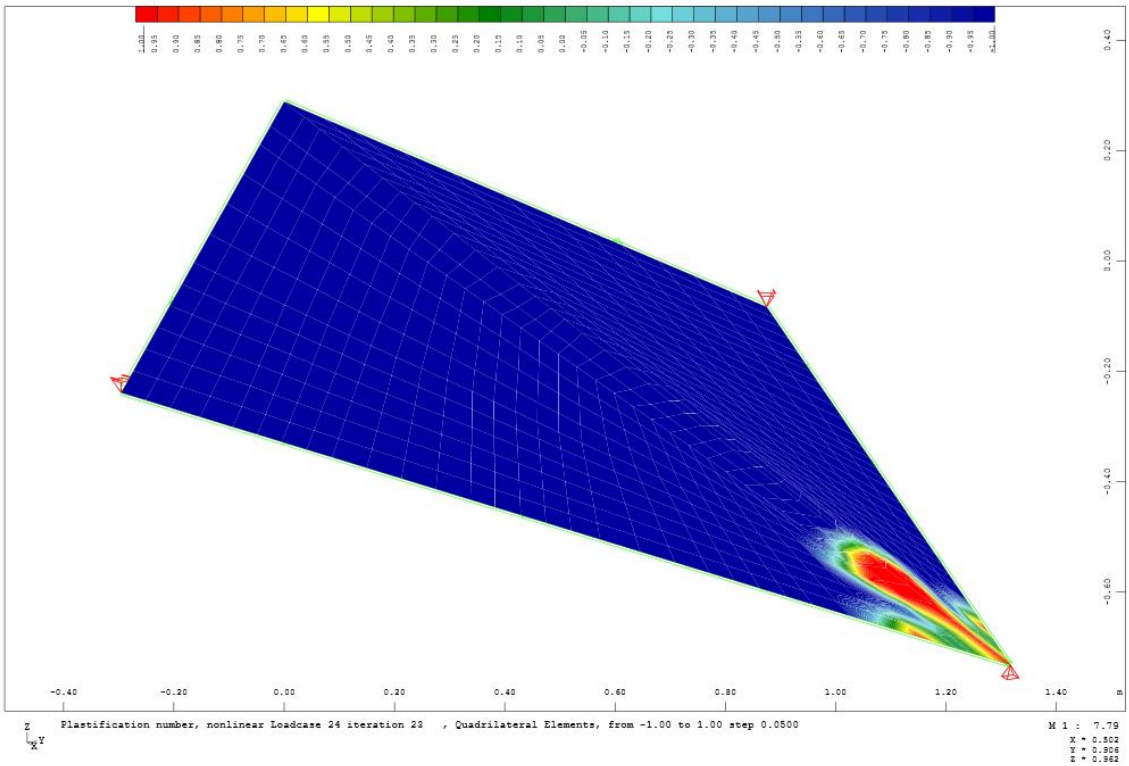

Appendix Figure 40 - Plasticization number.

Cross-section stresses

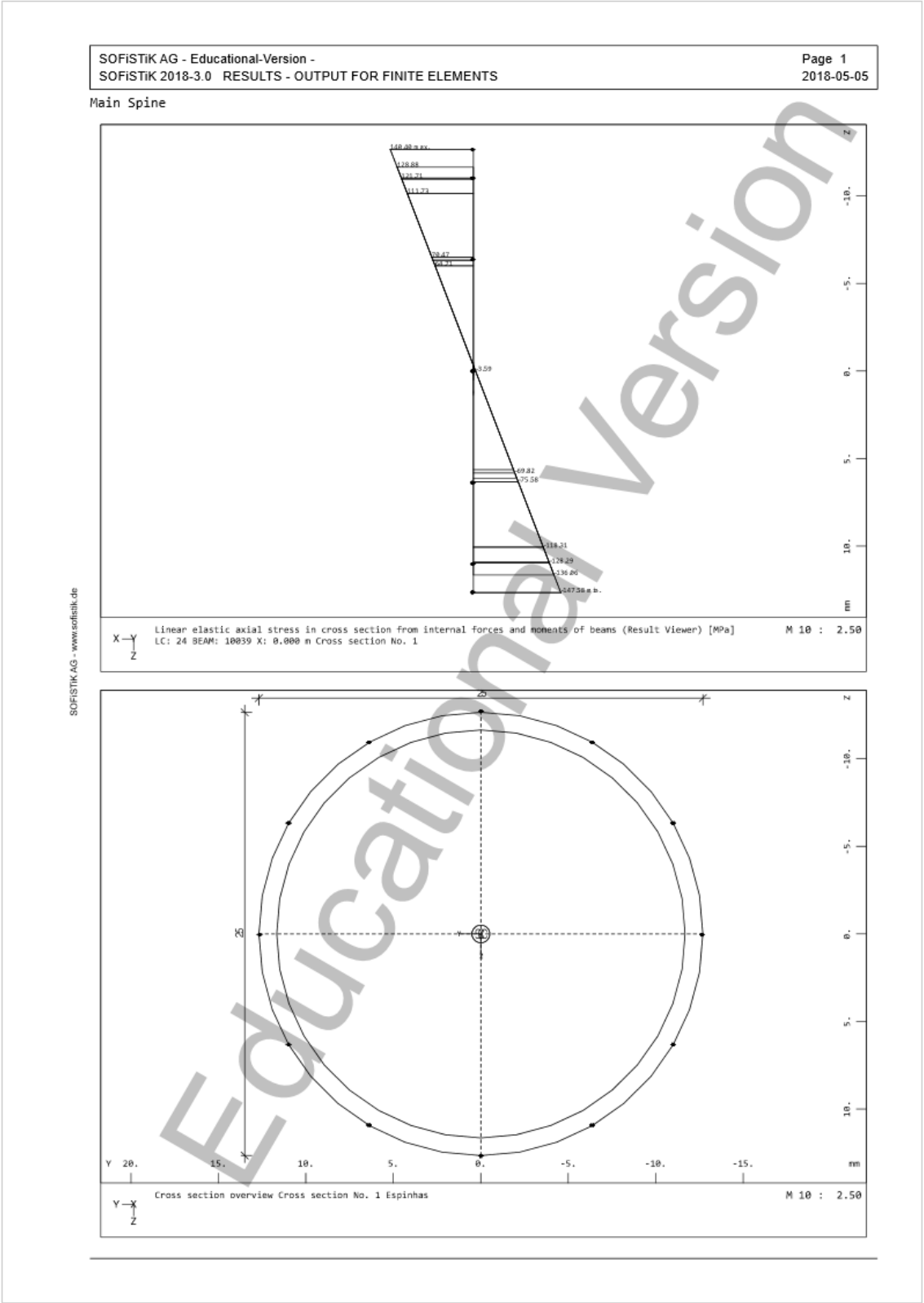

Appendix Figure 41 - Main spine, highest stressed section, elastic cable approach.

Appendix

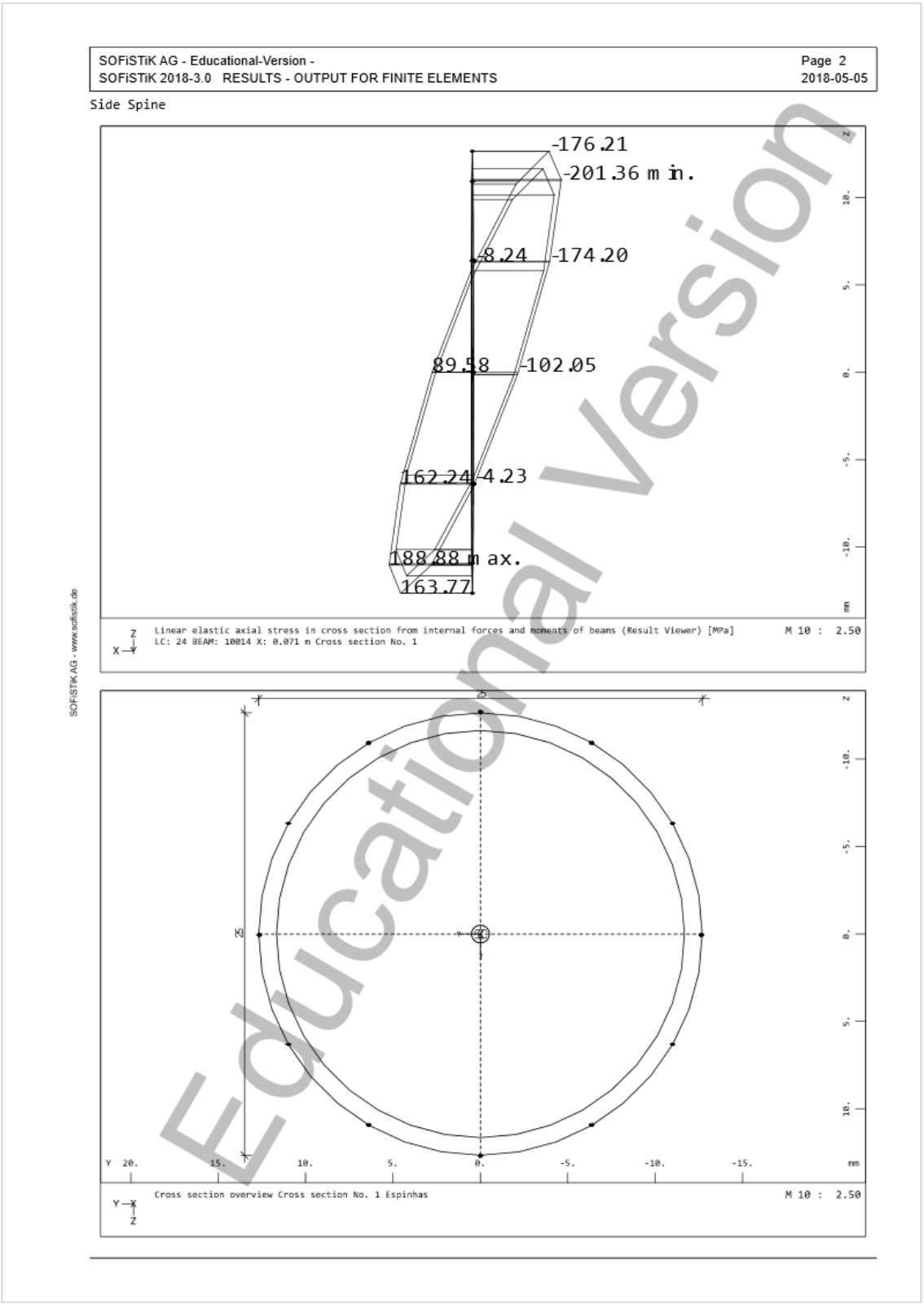

Appendix Figure 42 – Side spine, highest stressed section, elastic cable approach.

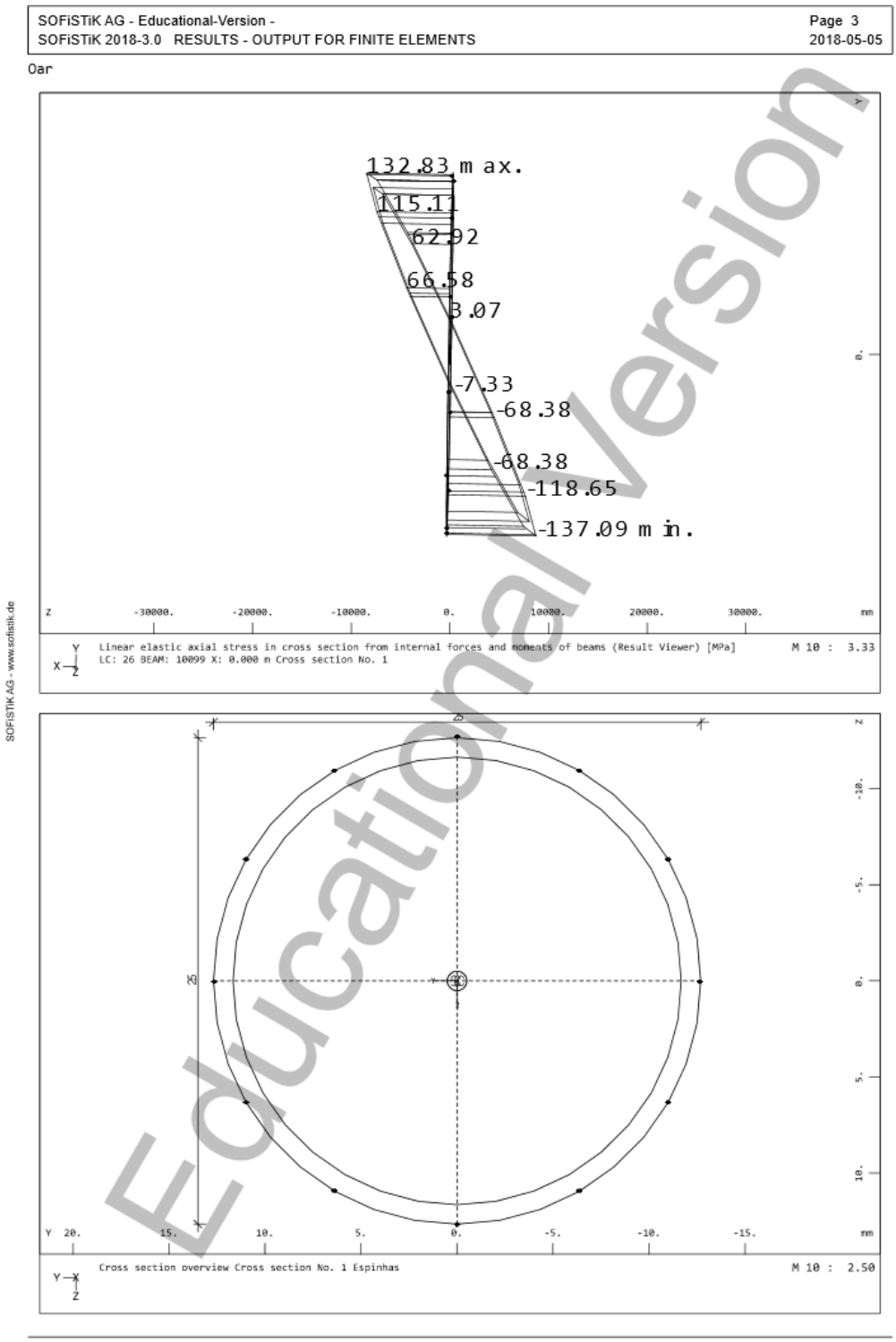

Appendix Figure 43 - Oar, highest stressed section, elastic cable approach.

Appendix

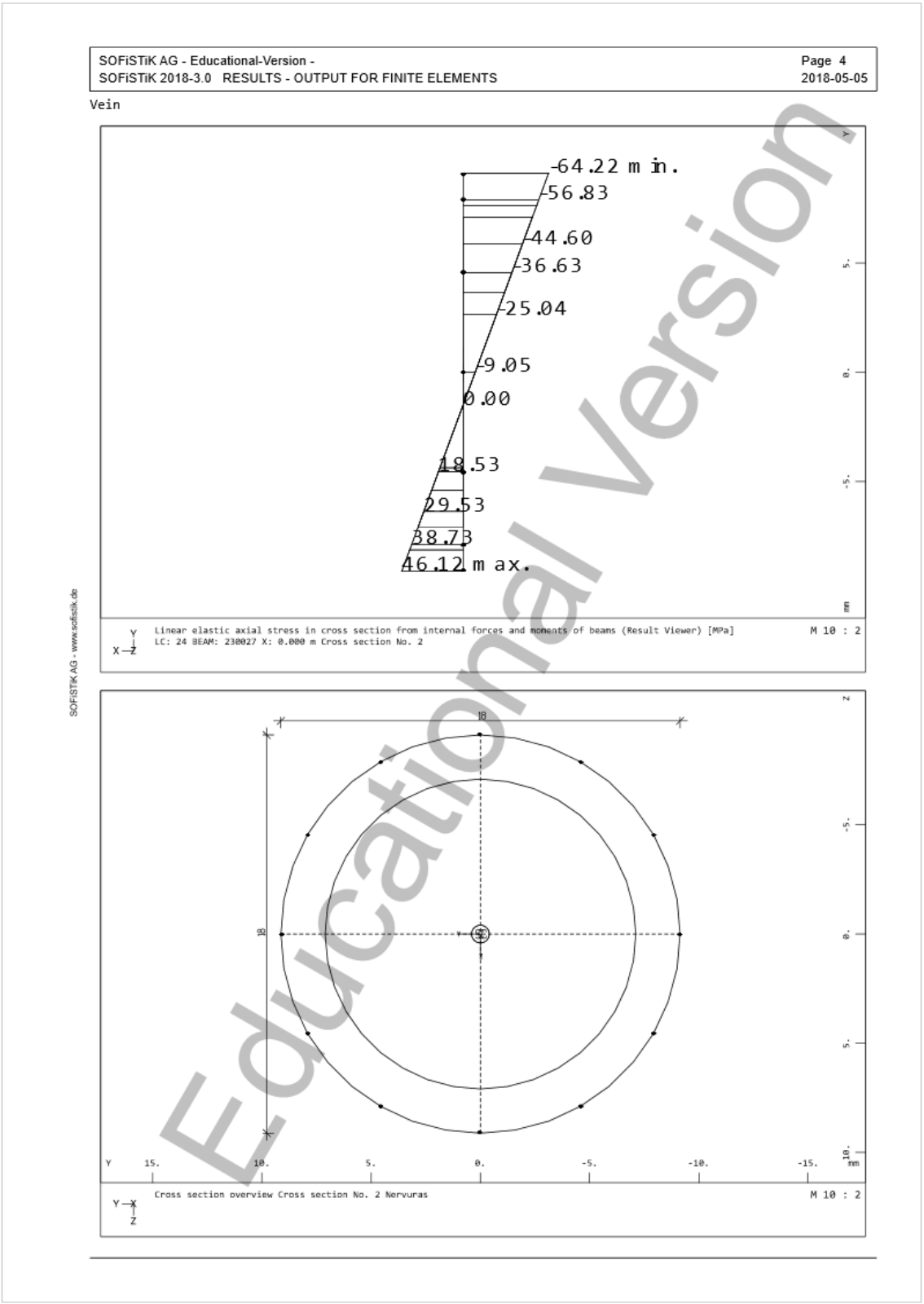

Appendix Figure 44 - Vein, highest stressed section, elastic cable approach.